

# **Environmental Stress Proteomics - Investigating the Effects of Heavy Metal Pollution and Ocean Acidification in Agriculturally Important Marine Species**

by

**Sridevi Muralidharan**

**Master of Agriculture, University of Sydney**

This thesis is submitted in partial fulfilment of the requirements for the  
award of the degree of  
**Doctor of Philosophy**

Department of Chemistry and Biomolecular Sciences

Macquarie University, Sydney, Australia

June 2014





## **Declaration**

I certify that this thesis titled “Environmental stress proteomics – investigating the effects of heavy metal pollution and ocean acidification in agriculturally important marine species” is an original work conducted by the author. Any form of assistance received for this work has been appropriately acknowledged. I also certify that this research material has not been submitted for any other degree to any other institution and to the best of my knowledge contains no information that has been previously written or published by any other person except where due reference is made in the text.

**Sridevi Muralidharan**

**June 2014**

## Abstract

This thesis is aimed at furthering our understanding of the biological impacts in important marine species of two environmental issues facing Australia - heavy metal pollution from anthropogenic activities and ocean acidification from increasing carbon dioxide levels. The effects of these stressors were explored by investigating the stress responses in agriculturally important aquatic marine animals, such as oysters and amphipods, using quantitative proteomics. We demonstrated the usefulness of labeled as well as label-free proteomics approaches in gaining insight of such environmental stresses in these animals at the cellular and molecular level.

Potential protein biomarkers were identified for stress responses arising from high metal toxicities of lead, copper and zinc in Sydney rock oysters. This study was among the first to apply shotgun proteomics and iTRAQ quantitation in Sydney rock oysters. The label-free and labeled analyses complemented each other, and in both analyses many unique proteins expressed at different metal stress conditions were identified. Differential metabolic response of these oysters under metal stress revealed their need to generate greater energy from all possible sugar resources, and their necessity to repair and replace damaged muscle proteins in order to maintain cytoskeletal integrity and shell structure at all times. Further, cellular stress responses due to zinc toxicity in conjunction with the presence or absence of sediment substrate were also studied in the amphipod *Melita plumulosa*. When stressed, amphipods seemed to decrease most physical activities, including fecundity, and modulate many cellular processes. Reproduction specific protein biomarkers for metal toxicity in Sydney rock oysters and *M. plumulosa* would certainly be useful for field evaluation by breeders.

This was followed by another study aimed at understanding hypercapnia – stress caused by excess carbon dioxide levels - among wild type and QX disease resistant Sydney rock oysters. Their metabolic responses were examined using label free shotgun proteomics. The quantitative data revealed that cytoskeletal proteins, nucleosome assembly, and sugar and lipid metabolic proteins showed some of the greatest expression changes, and may be associated with carbon dioxide stress tolerance. Altogether, we identified numerous stress-response proteins whilst adding a wealth of information to the existing knowledge of metal stress responses and hypercapnia in marine organisms.

## Acknowledgments

I would like to express my sincere gratitude to my supervisor, Professor Paul A. Haynes for granting me this opportunity to undertake a PhD in his laboratory, for introducing me to this amazing field of proteomics and mass spectrometry, his invaluable time, support and guidance over the period of my PhD and especially during my thesis writing.

Before coming to Macquarie University, I studied M. AGR at University of Sydney for two years and conducted research at PBI, Cobbitty under the supervision of Dr. Chong Mei Dong. I also spent four years of B. Tech undergraduate study at Anna University and conducted research projects at NBPGR, New Delhi for over a year under the supervision of DR. Kalyani Srinivasan, New Delhi. I am grateful to all who helped me at these institutions, in particular, to Dr. Chong Mei Dong and DR. Kalyani Srinivasan, who provided the references for my PhD application, I would like to thank Prof. David Raftos and Dr. Emma Thomposon for all their help in generating the oyster samples and guidance that I have received during the course of my PhD. I would also like to express my thanks to Dr. Ross Hyne for his guidance, timely and expert inputs during the amphipods growth experiments. I thank Dr. Mark Molloy and Dr. Alamgir Khan for their assistance in letting me access APAF instrumentation and resources. I would like to acknowledge Dr. Alamgir Khan for his expert advice during my 2DE experiments. I would like to thank Dylan Xavier, Matthew Fitzhenry, Thiri Zaw and Veronika for their useful advice on operating MS instrumentation. I was awarded the MQ Faculty of Science Post Graduate Research Fund to facilitate my visit to the state of art Mass Spectrometry laboratory at the University of Washington in late 2012. I was able to learn new MS techniques and also try some of their alternate data analysis methods there, and so I would like to thank Dr. David Goodlett, Dr. Brooke Nunn, Scott Heron, Yvonne Wu, and the other Goodlett lab members for their help and advice. I would also like

to express my acknowledgements to Prof. Helena Nevelainen and A/Prof. Patricia Fanning and Prof. Paul Haynes for their help in sustaining my candidature and scholarship during the course of my PhD. Thanks to all those co-authors who contributed to producing my first three publications during the course of my PhD.

I would also like to acknowledge past and present HDR students of the Dept. of CBMS including Naveid, Albert, Siba, Katherine, Garinè, Kunaal, Sarah, Crystal, Steve, Mehdi, Gayani, Iniga, Samantha, Arun, Rajeev, Vignesh, Chandrika, Nandan, Sock-Hwee, Prasanth, Jenny and Clara for making my PhD study a very enjoyable journey. I would like to thank Rajeev for not only being a good friend but also for his moral support during difficult times. I am also grateful to Dr. Robyn Peterson for being such an inspiration and for her advice in putting a tough fight until completion. I would like to thank Catherine Wong and Michelle Kang for all their assistance in purchase orders and budget substantiation during the course of my PhD.

Above all and most importantly, I am deeply grateful to my sister Lavanya to whom I dedicate this thesis, for all her encouragement, care and love which brought the best out of me. Thanks to my maternal aunt and uncle and my dad for all their support and motivation throughout the period of my research. Completion of this thesis would have not been possible without all of this. In addition to Prof. Paul Haynes, Prof. David Raftos, Dr. Ross Hyne, I would also like to thank Dr. Gavin Birch, for help in generating financial support for my PhD projects. Financial assistance was obtained from Macquarie University Research excellence scholarship and the Australian Research council.

# Table of Contents

Declaration .....	iii
Abstract .....	iv
Acknowledgements .....	vi
Table of Contents .....	viii
Table of Figures .....	xvi
List of Tables .....	xix
Abbreviations .....	xx
List of Publications .....	xxii
 <b>Chapter 1 Introduction.....</b>	<b>1</b>
1.1 Heavy metal pollution globally and in Australian waterways .....	1
1.1.1 Use of proteomics in environmental pollution studies .....	2
1.1.2 Proteomics as a tool to study ecotoxicological issues .....	4
1.1.3 Cross-species protein identification in non-model organisms .....	6
1.2 Copper contamination aquatic species.....	8
1.3 Zinc contamination and effects on aquatic species.....	15
1.3.1 Zinc contamination in combination with other contaminants .....	16
1.3.2 Zinc contamination in marine arthropods .....	17
1.3.3 Zinc contamination in non-mammals and mammals, including humans ..	21
1.4 Lead contamination in aquatic species .....	23
1.5 Proteomics as tool to understand changes caused by heavy metal pollution on marine biota, in response to heavy metal stress .....	25
1.5.1 Evaluation of Zn, Cu and Pb metal pollution using proteomics as tool in oysters and other bivalves .....	27
1.5.2 Evaluation of Zn metal pollution in amphipods using proteomics .....	28
1.6 Why address Ocean Acidification?.....	34
1.7 Effects of carbondioxide acidification on marine biota .....	39
1.7.1 Effects of ocean acidification and CO <sub>2</sub> fixation in oysters and other calcifying organisms, highlighting recent proteomics studies .....	46

1.8	Concluding remarks .....	51
<b>Chapter 2</b>	<b>Materials and Methods .....</b>	<b>53</b>
2.1	Protein extraction.....	53
2.1.1	Proteins extraction from oyster hemolymph performed using TCA-acetone precipitation .....	53
2.1.2	Proteins extraction from tissues homogenates of amphipods or oyster gill tissues using Tri-reagent.....	54
2.2	Trypsin digestion .....	55
2.2.1	In-gel trypsin digestion.....	55
2.2.2	In-solution trypsin digestion.....	56
2.3	Gas Phase Fractionation.....	56
2.4	nano LC-MS/MS mass spectrometry .....	57
2.5	Data processing and portioning .....	57
2.6	Protein ontology classification .....	59
2.7	Analysis of proteins expressed at all exposure conditions.....	60
2.8	Analysis of biological processes or metabolic pathways.....	60
2.9	Identification of unknown proteins .....	60
<b>Chapter 3</b>	<b>Quantitative proteomics of heavy metal stress responses in Sydney Rock oysters, before the release of the genome sequence .....</b>	<b>61</b>
3.1	Introduction .....	61
3.2	Materials and Methods .....	62
3.2.1	Oysters and heavy metal exposure .....	62
3.2.2	Protein fractionation by SDS-PAGE, in gel digestion and nano LC-MS/MS .....	63
3.2.3	Database searching for peptide identification .....	63
3.2.4	Quantitation of identified proteins .....	64
3.3	Results .....	66
3.3.1	Summary of protein identifications using different approaches .....	66
3.3.2	Quantitative analysis of differentially expressed proteins .....	69

3.3.2.1	Proteins differentially expressed in response to Lead, Zinc and Copper metal exposures .....	75
3.3.2.2	Presence or absence of proteins in controls vs. metal exposures ..	79
3.3.2.3	Proteins present at all 3 metal treatments and controls .....	79
3.3.3	Biological significance of 56 differentially expressed proteins in response to heavy metal stress.....	82
3.4	Discussion .....	85
3.4.1	Protein identification and quantitation using SDS-PAGE and GPF.....	85
3.4.2	Biological significance of metals in bivalves .....	86
3.4.3	Differentially expressed proteins with respect to functional categories found in this study .....	87
3.4.3.1	Cytoskeletal activity .....	87
3.4.3.2	Translation .....	89
3.4.3.3	Carbohydrate metabolism .....	89
3.4.3.4	Oxidative phosphorylation and ATP biosynthesis/ hydrolysis coupled transport .....	90
3.4.3.5	Protein degradation or stabilization.....	91
3.4.4	Potential biomarkers .....	91
3.5	Concluding Remarks .....	92

## **Chapter 4 Quantitative proteomics and biomarker discovery in Sydney rock oysters on heavy metal stress, elucidated using the recently released oyster genome sequence .....95**

4.1	Introduction .....	95
4.2	Materials and Methods.....	97
4.2.1	Summary of database searching and statistical analysis of MS/MS data obtained using the shotgun proteomics approach and the newly released Oyster genome database .....	98
4.2.2	Summary of 8plex iTRAQ approach .....	99
4.3	Results and Discussion .....	103
4.3.1	Protein extraction and proteomic analysis.....	103
4.3.2	Presence or absence of proteins at different metal treatments.....	107
4.3.3	Proteins found in all metal exposed as well as non-exposed oysters.....	107

4.3.4	Proteins found only in oysters exposed to Zn toxicity .....	110
4.3.5	Proteins found only in control oysters .....	114
4.3.6	Proteins found only in oysters exposed to Pb toxicity .....	116
4.3.7	Proteins found only in oysters exposed to Cu toxicity.....	120
4.3.8	Statistically significant differentially expressed proteins identified from quantitative label-free shotgun proteomics .....	126
4.3.8.1	Proteins differentially expressed in at least two out of three metal exposures .....	128
4.3.8.2	Proteins differentially expressed in response to Pb exposure .....	133
4.3.8.3	Proteins differentially expressed in response to Zn exposure.....	134
4.3.8.4	Proteins differentially expressed in response to Cu exposure.....	137
4.3.8.5	Novel proteins as potential biomarkers of stress exposure.....	141
4.3.9	Metabolic pathways .....	141
4.3.9.1	Cytoskeleton and protein polymerization .....	142
4.3.9.2	Translation .....	143
4.3.9.3	Carbohydrate metabolism .....	146
4.3.9.4	Gluconeogenesis.....	150
4.3.9.5	Pentose phosphate pathway .....	151
4.3.9.6	Glycogenesis .....	153
4.3.9.7	Glycogenolysis – Glycogen degradation .....	154
4.3.9.8	Citric acid cycle and electron transport chain .....	155
4.3.10	Identification and quantitation of proteins in Sydney rock oysters by iTRAQ .....	156
4.3.11	Significantly differentially expressed proteins in heavy metal exposed Sydney rock oysters relative to controls, identified using iTRAQ .....	158
4.3.12	Complementarity of label-free and iTRAQ analyses.....	162
4.4	Concluding Remarks .....	165

## **Chapter 5 Quantitative proteomics and biomarker discovery in response to Zn metal stress in epibenthic amphipod, *M.plumulosa* .....169**

5.1	Introduction .....	169
5.2	Materials and Methods.....	176
5.2.1	Materials and analytical chemistry .....	176

5.2.2	Test organism .....	177
5.2.3	Feeding .....	179
5.2.4	Test water .....	179
5.2.5	Artificial sediment substrate .....	180
5.2.6	Preparation of aqueous and sediment bound Zinc .....	180
5.2.7	Generation of survival data .....	183
5.2.8	Protein extraction .....	183
5.2.9	Two dimensional poly-acrylamide gel electrophoresis (2DE) .....	184
5.2.10	Progenesis 2DE Image Analysis .....	186
5.2.10.1	Image Quality check .....	186
5.2.10.2	Experimental design and masking spots of disinterest .....	186
5.2.10.3	Alignment .....	187
5.2.10.4	Filtering and refining detected spots .....	187
5.2.10.5	Progenesis stats .....	188
5.2.10.6	Viewing results .....	188
5.2.10.7	pI and M.Wt. calibration .....	189
5.2.10.8	Spot picking and report generation .....	189
5.2.11	Identification of proteins from 2DE spots using MALDI TOF/TOF and nanoLC-MS/MS .....	189
5.3.	Results and discussion .....	191
5.3.1	Background .....	191
5.3.2	Amphipod behavioural response to Zn exposure, when maintained either in seawater-only or in addition with silica-substrate. ....	192
5.3.3	Proteomics analysis of Zn toxicity responsive proteins using 2DE and mass spectrometric identification of differential proteins .....	194
5.3.4	Differentially expressed proteins in response to zinc stress from amphipods maintained in 25‰ seawater only .....	204
5.3.5	Differentially expressed proteins in response to zinc stress from amphipods maintained on silica substrate in 25‰ seawater .....	207
5.3.6	Biological relevance of some of the 41 Zn toxicity responsive differential proteins expressed in amphipods found in this study .....	209
5.3.6.1	Proteins involved in RNA metabolism .....	209
5.3.6.1.1	Serine-Threonine kinase Receptor-Associated	

Protein.....	209
5.3.6.1.2 Arm-like folded protein.....	209
5.3.6.1.3 DEAD box RNA helicases .....	210
5.3.6.2 Zn toxicity responsive proteins that are involved in cytoskeleton and protein polymerization.....	211
5.3.6.2.1 Tropomyosin .....	211
5.3.6.2.2 Actin .....	214
5.3.6.2.3 Myosin heavy chain .....	214
5.3.6.2.4 Catchin.....	215
5.3.6.3 Zn toxicity responsive proteins that are involved in DNA replication and repair .....	216
5.3.6.3.1 DNA polymerase.....	216
5.3.6.3.2 DNA-damage-inducible protein.....	216
5.3.6.4 Zn toxicity responsive proteins that are involved in carbohydrate metabolisms .....	217
5.3.6.4.1 Glyceraldehyde-3-phosphate dehydrogenase .....	217
5.3.6.4.2 Glycogen phosphorylase .....	218
5.3.6.4.3 Malate dehydrogenase .....	219
5.3.6.4.4 Phosphatidylinositol:UDP-GlcNAc transferase .....	220
5.3.6.4.5 Fructose biphosphate aldolase.....	220
5.3.6.5 Zn toxicity responsive proteins that are involved lipid metabolism .....	221
5.3.6.5.1 Glycerophosphodiester phosphodiesterase .....	221
5.3.6.5.2 Extracellular triacylglycerol lipase .....	221
5.3.6.5.3 DHHC palmitoyltransferase .....	222
5.3.6.6 Zn toxicity responsive proteins that are involved in cell cycle...223	
5.3.6.6.1 Cell morphogenesis protein Las 1 .....	223
5.3.6.6.2 Lon protease homolog .....	223
5.3.6.7 Zn toxicity responsive proteins that are involved in signal transduction .....	224
5.3.6.7.1 Guanine nucleotide binding proteins .....	224
5.3.6.8 Zn toxicity responsive proteins that are involved in transport / energy metabolism.....	225
5.3.6.8.1 ATP synthase beta subunit and GRP-78 .....	225

5.3.6.8.2	EmrB/ QaCA subfamily drug resistance transporter. ...	225
5.3.6.8.3	ABC transporter permease .....	226
5.4	Concluding Remarks .....	228

## **Chapter 6 Quantitative proteomics investigating ocean acidification effects on two breeds of Sydney rock oysters: Wildtype and QX disease resistant, and their metabolic responses toward increased levels of carbon dioxide .....231**

6.1	Introduction .....	231
6.2	Materials and Methods.....	234
6.2.1	Oyster breeds and CO <sub>2</sub> exposure conditions .....	234
6.2.2	Sample preparation for protein extraction.....	235
6.2.3	Filter Aided Sample Preparation method to digest proteins extracted from oyster gill tissues .....	235
6.2.4	Proteomic analysis .....	237
6.3	Results and Discussion .....	239
6.3.1	Protein identification and shotgun proteomic analysis .....	239
6.3.2	Presence and absence of proteins in different oyster groups.....	240
6.3.2.1	Proteins found only in QX disease resistant oysters .....	242
6.3.2.2	Proteins unique only to WT oysters .....	249
6.3.2.3	Proteins found in all groups of oysters .....	250
6.3.2.4	Proteins unique to all CO <sub>2</sub> exposed oysters from both WT and QXR breeds .....	252
6.3.2.5	Proteins found uniquely in WT oysters exposed to hypercapnia .....	253
6.3.2.6	Proteins found only in QXR oysters exposed to hypercapnia ....	257
6.3.3	Statistically significant differentially expressed proteins among CO <sub>2</sub> exposed oysters .....	260
6.3.4	Differentially expressed proteins among QXR <sub>CO2</sub> oysters relative to QXR <sub>controls</sub> .....	262
6.3.5	Differentially expressed proteins among WT <sub>CO2</sub> oysters relative to WT <sub>controls</sub> .....	268
6.3.6	Metabolic pathway analysis .....	273
6.3.6.1	Cytoskeleton and protein polymerization .....	273

6.3.6.2	Translation .....	276
6.3.6.3	Transcription .....	279
6.3.6.4	Protein metabolic processes .....	282
6.4	Concluding Remarks .....	284
<b>Chapter 7</b>	<b>Conclusions and future directions .....</b>	<b>287</b>
<b>References</b>	<b>.....</b>	<b>397</b>

## Table of Figures

Figure 1.1 A typical food web in marine ecosystems, with bivalves and amphipods at the base .....	29
Figure 1.2 The ocean carbon feedback cycle.....	36
Figure 3.1 Diagrammatic representation of protein identification data from both SDS-PAGE and GPF approaches for Sydney rock oysters .....	68
Figure 3.2 Distribution of differentially expressed proteins identified in oysters in response to heavy metal exposures.....	69
Figure 3.3 Log NSAF plots of differential and unchanged proteins in the 3 metal treatments relative to controls (a) GPF datasets (b) SDS-PAGE datasets.....	70
Figure 3.4 Fold changes (up or down regulation) for 56 proteins in response to heavy metal stress relative to controls.....	76
Figure 3.5 Qualitative distributions of proteins present across all treatments.....	81
Figure 3.6 Distribution of the 56 differentially expressed proteins based on their functional categories.....	83
Figure 4.1 Distribution of proteins in Sydney rock oysters upon exposure to different heavy metals and controls .....	106
Figure 4.2 Qualitative and quantitative distribution of proteins found at all exposed and non-exposed oysters.....	109
Figure 4.3 Qualitative and quantitative distribution of proteins found only in oysters exposed to Zn.....	112
Figure 4.4 Qualitative and quantitative distribution of proteins found only in non-exposed oysters (controls) .....	115
Figure 4.5 Qualitative and quantitative distribution of proteins found only in oysters exposed to Pb.....	117
Figure 4.6 Qualitative and quantitative distribution of proteins found only in oysters exposed to Cu .....	123
Figure 4.7 Log NSAF plots of differential and unchanged proteins in the three metal	

treatments relative to controls, (a) GPF datasets (b) SDS-PAGE datasets .....	127
Figure 4.8 Number of differentially expressed proteins in response to heavy metal exposures in Sydney Rock oysters.....	129
Figure 4.9 Fold changes (up or down-regulation) for 50 proteins that showed highest protein expression changes in response to heavy metal stress .....	144
Figure 4.10 Abundance of carbohydrate metabolism related proteins, that showed statistically significant differential protein expressions in response to metal stresses .....	148
Figure 4.11 Protein identification data from the 1DE, GPF and iTRAQ approaches in Sydney rock oysters.. .....	157
Figure 5.1 Different development stages in the amphipod's life cycle beginning from an embryo through to a young amphipod .....	178
Figure 5.2 Experimental groups setup used for the Zn exposure study on <i>M. Plumulosa</i> in 25‰ seawater .....	181
Figure 5.3 Fluorescent images of 2DE gels acquired for amphipods exposed to Zn (A) when maintained in 25‰ seawater-only, and (B) when maintained on silica substrate in 25‰ seawater .....	197
Figure 5.4 Qualitative and quantitative distribution of proteins differentially expressed in amphipods in response to Zn exposure when (a) maintained in 25‰ seawater-only, and (B) in addition with silica substrate .....	206
Figure 5.5 Fold changes (up- or down-regulation) for all proteins differentially expressed in response to Zn exposure relative to controls .....	212
Figure 6.1 Distribution of proteins across the two different oyster cultures that were either non-exposed controls or CO <sub>2</sub> exposed groups of oysters .....	241
Figure 6.2 Qualitative and quantitative distribution of proteins found only in QXR oysters.	246
Figure 6.3 Qualitative and quantitative distribution of proteins in all groups of oysters .....	251
Figure 6.4 Qualitative and quantitative distribution of proteins unique to CO <sub>2</sub> exposed WT oysters .....	256
Figure 6.5 Qualitative and quantitative distribution of proteins unique to CO <sub>2</sub> exposed QXR oysters.....	259
Figure 6.6 Log NSAF plots of differential and unchanged proteins in each CO <sub>2</sub> treatment relative to controls (A) QXR oysters, (B) WT oysters .....	261

Figure 6.7 Quantitative and qualitative distribution of differentially expressed proteins in QXR oysters in response to CO <sub>2</sub> exposures .....	267
Figure 6.8 Quantitative and qualitative distribution of differentially expressed proteins in WT oysters in response to CO <sub>2</sub> exposures.....	272
Figure 6.9 Abundance of statistically significant differentially expressed proteins involved in cytoskeleton and protein polymerization in WT <sub>CO<sub>2</sub></sub> / WT <sub>controls</sub> oysters.....	274
Figure 6.10 Abundance of statistically significant differentially expressed proteins involved in cytoskeleton and protein polymerization in QXR <sub>controls</sub> / QXR <sub>CO<sub>2</sub></sub> oysters .....	275
Figure 6.11 Abundance of statistically significant differentially expressed proteins involved in translation in WT oysters.....	277
Figure 6.12 Abundance of statistically significant differentially expressed proteins involved in translation in in QXR oysters .....	278
Figure 6.13 Abundance of statistically significant differentially expressed proteins involved in transcription in WT oysters.....	280
Figure 6.14 Abundance of statistically significant differentially expressed proteins involved in transcription in QXR oysters .....	281
Figure 6.15 Abundance of statistically significant differentially expressed proteins involved in protein metabolic processes in QXR oysters .....	283

## List of Tables

Table 1.1 Effects of zinc on representative aquatic oysters.....	19
Table 1.2 Effects of zinc on representative benthic amphipods. ....	32
Table 1.3 Changes in Ocean pH levels .....	35
Table 3.1 Protein identification summary of Sydney rock oysters after heavy metal treatments (Pb, Cu, Zn and control), using SDS-PAGE and GPF approaches ....	67
Table 3.2 Differentially expressed proteins after heavy metal stress in Sydney rock oysters, relative to non-exposed controls based on their Log NSAF ratios.....	72
Table 3.3 Biological process characterization of proteins present across all metal treatments and controls .....	80
Table 4.1 iTRAQ labels added to samples .....	101
Table 4.2 Proteins identifications summary for Sydney rock oysters .....	104
Table 4.3 Abundance changes of 50 most differentially expressed proteins after heavy metal stress imposition in Sydney rock oysters, identified by label-free shotgun proteomics	130
Table 4.4 Statistically differentially expressed proteins in response to heavy metal stress in Sydney rock oysters, identified by iTRAQ analysis .....	159
Table 5.1 Summary of protein identifications .....	196
Table 5.2 Spot data for a total of 36 differentially expressed 2DE protein spots in response to Zn toxicity from amphipods (a) maintained in 25‰ seawater-only, (b) maintained on silica substrate in 25‰ seawater .....	198
Table 5.3 List of proteins identified for each of the 36 differentially expressed spots in amphipods, in response to Zn stress when compared to controls maintained in (a) 25‰ seawater-only (b) silica substrate in 25‰ seawater .....	201
Table 6.1 Statistically differentially expressed proteins among QXR oysters exposed to CO <sub>2</sub> relative to their respective controls .....	263
Table 6.2 Statistically differentially expressed proteins among WT oysters exposed to CO <sub>2</sub> relative to their respective controls .....	269

## Abbreviations

1DE	One Dimensional Gel Electrophoresis
2DE	Two dimensional Gel electrophoresis
ABI	Applied Biosystems Incorporated
ACN	Acetonitrile
ACTH	Adrenocorticotrophic hormone
ADP	Adenosine diphosphate
ANOVA	Analysis of Variance
ANZECC	The Australian and New Zealand Environment Conservation Council
APAF	Australian Proteomics Analysis Facility
ARMCANZ	Agriculture and Resource Management Council of Australia and NZ
ATP	Adenosine triphosphate
AUC	Area Under the Curve / Peak Area
BCA	bicinchoninic acid
C <sup>18</sup>	Reverse Phase C <sup>18</sup> column
CaCO <sub>3</sub>	Calcium carbonate
CHCA	$\alpha$ -cyano-4-hydroxy-cinnamic acid
CID	Collision Induced Dissociation (collision activated dissociation)
CO <sub>2</sub>	Carbon dioxide
CO <sub>3</sub> <sup>2-</sup>	carbonate ion
Cu	Copper metal
CuCl <sub>2</sub>	Copper Chloride
Cy/P	Cytoskeleton and Protein polymerization processes
DDA	Data Dependant Acquisition
DNA	Deoxyribonucleic Acid
DTT	dithiothreitol
ESI	Electrospray Ionisation
FASP	Filter-Aided Sample Preparation
FDR	false discovery rate
GAPDH	Glyceraldehyde 3-Phosphate Dehydrogenase
GO	gene ontology
GPF	Gas Phase Fractionation
GPM	Global Proteome Machine
HCO <sub>3</sub> <sup>-</sup>	bicarbonate ion
HPLC	High-Pressure Liquid Chromatography
IAC	iodoacetamide
ICAT	Isotope-coded Affinity Tags
IEF	Isoelectric Focusing
IPG-IEF	Immobilised pH Gradient Isoelectric Focusing
iTRAQ	isobaric Tags for Relative and Absolute Quantification
LC	Liquid Chromatography
LC-MS/MS	Liquid Chromatography coupled MS/MS
LTQ-XL	Linear Ion Trap XL Mass Spectrometer
M	Reported Region for iTRAQ
M/A	Matrix to Analyte ratio
m/z	Mass to Charge ratio (mass divided by charge ratio)
MALDI TOF/TOF	MALDI coupled tandem TOF analyser
MALDI	Matrix Assisted Laser Desorption Ionisation
MASCOT	Proteomics search engine of peptide MS data by Matrix Sciences

mM	milli molar
$M_r$	Molecular Weight
mRNA	messenger Ribonucleic Acid
MS	mass spectrometry
MS/MS	tandem mass spectrometry ( $MS^2$ )
$MS^n$	Mass Spectrometry to the $n^{th}$ degree of times
MudPIT	Multidimensional Protein Identification Technology
N	Normalisation Region for iTRAQ
$NAD^+$	Nicotinamide adenine dinucleotide
nano-ESI	nano-litre ESI
nanoLC-MS/MS	nano-litre flow rate Liquid Chromatography MS/MS
Nd:YAG	Neodymium-doped yttrium aluminium garnet; Nd:Y <sub>3</sub> Al <sub>5</sub> O <sub>12</sub>
NH <sub>4</sub> HCO <sub>3</sub>	Ammonium bicarbonate
NSAF	Normalised Spectral Abundance Factors
OMSSA	Open Mass Spectrometry Search Algorithm
Pb	Lead
PbCl <sub>2</sub>	Lead Chloride
pCO <sub>2</sub>	Partial Pressure of Carbon Dioxide
PCR	Polymerase Chain Reaction
pH	measure of acidity (negative log of hydronium ion)
pI	Isoelectric Point
PMF	Peptide Mass Fingerprint
ppt	parts per trillion
pre-mRNA	precursor-messenger RiboNucleic Acid
QXR	QX disease resistant Sydney rock oysters
QXR <sub>CO2</sub>	QX disease resistant Sydney rock oysters exposed to hypercapnia
QXR <sub>controls</sub>	QX disease resistant Sydney rock oysters not exposed to hypercapnia
RNA	Ribonucleic Acid
ROS	reactive oxygen species
RT	retention time
SCX	Strong Cation Exchange
SDS-PAGE	Sodium Dodecyl Sulfate Polyacrylamide Gel Electrophoresis
SELDI	Surface Enhanced Laser Desorption Ionisation
SEQUEST	Proteomics search algorithm for tandem MS data
SILAC	Stable Isotope Labels with Amino Acids
SpC	Spectral Counts
TCA	Tri Chloro Acetic acid
TFA	Trifluoroacetic Acid
TFE	Trifluoroethanol
TMT	tandem mass tag
TOF	Time of Flight
WT	Widtype Sydney rock oysters
WT <sub>CO2</sub>	Widtype Sydney rock oysters exposed to hypercapnia
WT <sub>controls</sub>	Widtype Sydney rock oysters not exposed to hypercapnia
X!Tandem	Proteomics search algorithm for tandem MS data
Yki	transcriptional co-factor Yorkie
Zn	Zinc
ZnCl <sub>2</sub>	Zinc Chloride

## List of Publications

The following peer-reviewed publications arose from work presented in this thesis and are presented in Appendix A. The publications are referred to in-text by roman numerals as follows:

### Publication I

Less label, more free: approaches in label-free quantitative mass spectrometry. Karlie A. Neilson, Naveid A. Ali, **Sridevi Muralidharan**, Mehdi Mirzaei, Michael Mariani, Garinè Assadourian, Albert Lee, Steven C. Van Sluyter, and Paul A. Haynes. *Proteomics*, (2011), 11(4):535-53.

### Publication II

Quantitative proteomics of heavy metal stress responses in Sydney rock oysters. **Sridevi Muralidharan**, Emma Thompson, David Raftos, Gavin Birch and Paul A. Haynes. *Proteomics*, (2012), 12: 906–921. doi: 10.1002/pmic.201100417.

### Publication III

Analysis of rice proteins using SDS-PAGE shotgun proteomics. Karlie A. Neilson, Iniga S. George, Samantha J. Emery, **Sridevi Muralidharan**, and Paul A. Haynes. *Methods in Molecular Biology*, (2014), 1072:289-302. doi: 10.1007/978-1-62703-631-3\_21.

### Publication IV & V

**Chapter 5 - Quantitative proteomics and biomarker discovery in response to Zn metal stress in epibenthic amphipod, *M. plumulosa*** is in the process of being prepared as a manuscript for publication and is expected to be submitted to *Proteomics* by early 2014.

**Chapter 6 - Quantitative proteomics investigating ocean acidification effects on two breeds of Sydney rock oysters: Wildtype and QX disease resistant, and their metabolic responses toward increased levels of carbon dioxide** is also in the process of being prepared as a manuscript for publication and is expected to be submitted to *Aquatic Toxicology* by early 2014.

---

## **Chapter 1      Introduction**

---

Research on environmental stress proteomics is focussed on two main issues that pose definitive threats to the marine environment; anthropogenic heavy metal pollution and ocean acidification. Heavy metal pollution and ocean acidification are permanent changes in the waterways that not only affect the survival, growth and development of marine life and their ecosystems, but also impact other species of animals upstream in the food web, including humans.

### **1.1 Heavy metal pollution globally and in Australian waterways**

In marine waters, anthropogenic pollutants occur in the form of chemical compounds, heavy metals, petrochemical products, industrial effluents and sewage [1, 2]. All of these inputs have led to deterioration of water quality in many coastal and estuarine marine ecosystems. As a result, effective monitoring of the consequences of pollution on the biota in these areas is becoming increasingly important [3].

Heavy metal pollutants are of particular concern due to their wide prevalence, their potential to cause illness in humans, their ability to spread throughout the food chain, and their long half lives in the environment. Heavy metals such as lead, copper and zinc occur naturally in coastal marine systems, leaching from rocks and sediments. Sources of heavy metal pollution include storm water drains, surface runoffs, industrial effluent discharges, agricultural drains, mining industry and marine traffic. Heavy metal pollution is a problem not just in Australia but around the world. For example, in China, economic development has resulted in discharge of enormous amounts of heavy metals into the Pearl River

Estuary. It is estimated that  $3 \times 10^3$  tons of lead,  $15 \times 10^3$  tons of zinc,  $0.3 \times 10^3$  tons of cadmium and  $1 \times 10^3$  tons of arsenic run down the Pearl River into the sea every year [4], primarily coming from industries, mines, corrosion of materials, and agriculture.

Heavy metal pollution in Sydney Harbor and other Australian estuaries is a major concern for Australian state and federal governments, with geochemical studies identifying large amounts of heavy metals polluting ultrascopic fine estuarine grade sediments. It has been estimated that between 3000 to 7000 tonnes of copper, zinc and lead reside in the soft sediments of Sydney Harbor alone [5-8]. It is widely known that marine animals, as well as seabirds, are able to accumulate significant amounts of toxic heavy metals like lead, cadmium and mercury in their body tissues through feeding, and pass this upwards along their food web [9, 10]. Although vast numbers of these animals may not be directly exposed to industrial pollution, a significant proportion of marine biota is affected by bioaccumulation of toxic metals in their body. Up until now, the majority of scientific research in understanding various physiological and biological phenomena has been performed mainly using model vertebrates to be able to reflect biological advances and benefits also applicable to humans.

### **1.1.1 Use of proteomics in environmental pollution studies**

Although invertebrates account for 95% of all animal species, research on invertebrates using modern techniques such as genomics and proteomics still remains in an incipient stage when compared to the amount of work done on vertebrates, in spite of the key structural and functional roles they play in ecosystems. When compared to that vast pool, studies focusing on using invertebrates as subject species, in this case addressing heavy metal pollution, are certainly outnumbered. This may be a major contributing factor to our poor understanding of some underlying concepts in this area.

These include the behavior and response mechanisms of invertebrate organisms that are exposed to important global ecological effects including heavy metal pollution, carbon-dioxide acidification from global warming, and drought and temperature fluctuations.

Another valid reason for slow progress in eco-toxicoproteomics studies is the lack of available genome sequence information for most invertebrates. Despite the slow progress in obtaining genome sequence information for many invertebrates and aquatic animals, and even with the drawbacks of using non-model organisms in their studies, there is increasing evidence of proteomics studies involving the analysis of the effects of specific toxins on non-model species such as oysters [11], fish [12], crabs [13], mussels [14-16], snails [17], and clams [18, 19]. This shows increasing awareness, and will inspire researchers to commit more resources and time to applying these powerful proteomics techniques in ecotoxicology studies, thereby filling in gaps in our understanding at the molecular level [20].

Heavy metal pollution is one stress which has a great impact on gene and protein expression, thus it is the subject of considerable study which is necessary to further our understanding of all the pathways and mechanisms involved. Previous studies have proven that fish, bivalves and amphipods act as a better medium than flowing seawater for the detection of contamination levels of heavy metals and their toxic effects on aquatic animals and humans. The use of animal-based biological responses as biomarkers is becoming the most efficient mode of assessing heavy metal contamination. Therefore, bio-monitoring of sentinel organisms such as oysters or amphipods, using measured cellular changes as biomarkers, should be a more effective approach to investigate metal pollution than just monitoring the whole ecosystem for direct pollutant analysis [21].

### **1.1.2 Proteomics as a tool to study ecotoxicological issues**

The field of proteomics has moved beyond simple protein identification and is now driven to accurately and reliably quantitate the differences in protein abundance in an organism, cell, or tissue, at given times or under particular conditions [22-24]. Quantitative proteomics can be separated into two major approaches; the use of stable isotope labelling and label-free techniques. Common labelling techniques include modifying peptides with isobaric tags for relative and absolute quantitation (iTRAQ) [25] or tandem mass tags (TMT) [26], labelling proteins with isotope-coded affinity tags (ICAT) [27], or metabolically labelling proteins by incorporation of stable isotope labels with amino acids in cell culture (SILAC) [22]. Labelling strategies are often considered to be more accurate in quantitating protein abundances; however, these techniques require expensive isotope labels, specific software, and expertise to analyze data. Additionally, the number of samples that can be analyzed in a single experiment is limited and some labelling strategies cannot easily be applied to all types of samples. Traditionally, quantitation has been focused on using a comparative 2D gel approach whereby differences in protein abundances were determined by comparing stained protein spot volumes followed by identification of proteins by mass spectrometry (MS).

In recent years, the observation of a correlation between protein abundance and peak areas [28, 29] or number of MS/MS spectra [30] has widened the choice of analytical procedure in the field of quantitative proteomics. With the development of gel-free shotgun techniques such as multidimensional protein identification technology (MudPIT), proteomics has seen rapid growth in quantitating proteins at the MS level rather than by laborious visual comparisons. This shift has been encouraged by changes in MS instrumentation and the need to quantitate many more proteins at a time. Biomarker

discovery will benefit from this form of global-view quantitation as biomarkers are likely to be not one specific protein, but rather a set of proteins that have a unique expression pattern in response to a particular stimulus or condition.

Spectral counting is based on the observation that peptides from more abundant proteins will be selected for fragmentation more often and will produce a higher abundance of MS/MS spectra, and so the number of spectra acquired is therefore proportional to protein amount in data-dependent acquisition [30]. Many spectral counting strategies and statistical tools for analyzing spectral count data have emerged in the recent years, and have recently been extensively reviewed [31]. Spectral counting has also been used to analyze labeled samples. Spectral counting has been modified to take into consideration that the length of a protein will affect the number of spectral counts (SpC) such that a longer protein will generate more peptides and MS/MS fragments. A normalised spectral abundance factor (NSAF) provides an improved measure for relative abundance by taking into account the length of the protein, which is calculated by dividing the SpC for a protein by its length (L) [32-34]. This value is then normalised by dividing by the sum of all SpC/L for all proteins in an experiment. The dynamic range for NSAF values is approximately four orders of magnitude, and abundance changes as low as 1.4-fold can be detected [33]. NSAF values have been used in a study that showed spectral count data share substantially similar statistical properties with transcript abundance values [35]. NSAF values have been used extensively in recent applications and have been applied in a broad range of projects to represent relative abundance of identified proteins. Such projects include peptide immobilised pH gradient isoelectric focusing (IPG-IEF) analysis of rat liver membrane proteins [36], the subcellular analysis of nuclear proteins in *Saccharomyces cerevisiae* [37], temperature stress responses in rice [38], comparison of evolutionary adaptation of *Pachycladon* species through differential protein expression

[39], and the analysis of a wide range of mouse renal cortex proteins [40]. This method of normalising SpC relies on the notion that the size of a protein will bias the amount of peptides or fragment spectra collected; however, it has recently been suggested that normalizing SpC for size does not significantly improve the accuracy of spectral count quantitation [31].

The data processing workflow for a label-free quantitative shotgun proteomics experiment begins with matching spectra to peptides by database searching for protein identification. Database searching involves the use of scoring algorithms including those that employ spectral correlation functions, such as SEQUEST [41], and those which use probability-based scoring-related concepts such as MASCOT [41], X!TANDEM [42], and OMSSA [43]. Although these algorithms aim to be as specific as possible, they cannot eliminate the possibility of false positives in the output data set so further analysis is required to minimise false discovery rates [44]. Rigorous statistical assessment of data generated by both labeled and label-free proteomics studies is essential for accurately reporting results. Statistical tests generally used in data analysis software and stand-alone data analysis protocols include t-test (triplicates or more), local pooled error test (two or more replicates), G-test (one replicate), Fisher's exact test (one replicate), AC test (one replicate), and one-way ANOVA (one or more replicates and often for data within a time course analysis) [45, 31, 46, 47].

### **1.1.3 Cross-species protein identification in non-model organisms**

The oyster genome sequence has only recently become publicly available, and amphipods do not have a representative genome sequence available yet, nor does any closely related species. A traditional two dimensional gel electrophoresis (2DE) approach has long been considered the best choice for proteomics studies on unsequenced

organisms. Proteomics studies on such organisms often rely on protein sequence information from related, completely sequenced organisms. Since shotgun proteomics is a less expensive and more efficiently robust methodology for looking at the entire pool of proteins, and the oyster genome sequencing project was well underway when this work started, we chose to employ a shotgun proteomics approach for the work in this thesis involving oysters, but opted for traditional 2DE methodology for studies with amphipods. Fortunately, previous studies have shown that the use of protein sequences from several closely related species provides adequate protein identification [48]. Shotgun proteomics has previously reported to be successful in using cross-species databases for proteomic analysis of unsequenced organisms of flora and fauna such as *Leptospirillum spp.* [49], *Pachycladon spp.* [50], spinach [48], pea aphids [51], bananas [52], bacteria (*Mannheimia haemolytica*) [53], and barley [54]. Hence, we opted to use cross species database identifications for our initial heavy metal stress study with oysters, which was completed before the oyster genome sequence was available.

Two major challenges in using shotgun proteomics methodologies for studying non-model organisms are (a) peptide identification using a composite cross-species database, and (b) the need to address quantitation bias in spectral counting arising from shared peptides and protein matches of multiple entries of the same peptide for the given protein matching each of the related species present.

Friso *et al.* have shown that, in spite of using a well-established maize protein library for their study, they had to adopt a modified quantitation workflow to account for shared peptides, and duplicate protein identifications or grouping of similar proteins [55]. This further demonstrates the need to balance such bias in peptide quantitation for proteins, especially when working with unsequenced organisms, in order to conduct high

throughput proteomics. In light of this issue, we developed a quantitation strategy that adjusts the spectral counts for every oyster protein that shares peptide sequences from closely related species. This strategy not only corrects the bias in peptide quantitation of proteins, but also accommodates all peptide sequences that belong within the framework of each protein. This work represents a valuable addition to previous research efforts [56-58] because it circumvents the limitations mentioned above, and helps to evaluate the usefulness of shotgun proteomics data in this context. Other recent techniques such as the MultiTag approach [58] may appear to be more suitable to work with unsequenced organisms in general. However, MultiTag is unsuitable for amphipods, which contain large numbers of single amino acid polymorphisms, because this technology uses short (2-4 amino acid) peptide sequences for homology (sequence similarity) searches, rather than full tryptic peptides. Similarly, *de novo* sequencing might also appear to be suitable to work with unsequenced organisms, but time constraints, coupled with the fact that it is far better suited to single proteins rather than to complex mixtures, render it less suitable for our purposes [59].

## **1.2 Copper contamination in aquatic species**

Copper may exist in nature in the form of either minerals or uncombined metal. Copper content in aquatic ecosystems is mainly contributed by mining, automobile transiting, leaching of antifouling paints from marine ships, and industrial and waste water discharges into marine or fresh waters during the past century [60]. Although the atmosphere is the primary recipient of Cu pollution, anthropogenic inputs of copper in aquatic environments have grown to two to five times higher than natural loadings [61]. Cu is essential for the successful growth and development of many species of aquatic organisms, but when levels exceed beyond necessity, the rate and extent of accumulation

and retention has a direct impact on the life of the organism. In Michigan, due to increasing numbers of copper mines, several lakes found with elevated levels of copper (34 µg/L) showed low densities of fish populations [62]. Similarly in the Elizabeth river estuary of southern Chesapeake Bay, copper and other metals have risen to concentrations unfavourable for growth and survival of the copepod *Acartia tonsa* [63].

A study that used microarray technology to study metal metabolism and toxicity effects of 8-15 µg/L of Cu on zebrafish, found 573 genes to be significantly differentially expressed in response to copper exposure [64]. The study reported a decrease in sodium-potassium ATPase levels in Cu treated animals compared to controls, which indicates that Cu may be competing with Na<sup>+</sup> at the gradient channel. The authors also observed increasing cortisol levels in body of metal exposed fish; increasing levels of cortisol could cause alteration of many enzymatic activities and protein metabolism events. The study also reported changes in expression of genes involved in apoptosis indicating cellular damage, overexpression of genes involved in transcription indicating a jump in gene regulation processes, and changes in glutathione transferase and peroxidase and nucleotide binding.

In Norway, freshwater fish thrive only when copper levels are less than 60 µg/L [65]. The major route of copper accumulation in aquatic animals is through diet. Among marine organisms, the highest copper accumulations occur in molluscs such as cephalopods and oysters, especially in body tissues and soft parts. Over consumption of oysters as food by humans over a period of time could thus pose the threat of acute metal toxicity. Bivalve and benthic communities in the vicinity of chromated copper arsenate treated materials or effluents showed increased concentrations of these elements, reduced

total count of organisms, reduced species richness, discolouration of tissues, and low survival and diversity when compared to reference sites [66, 67].

Alternatively, excessive exposure to copper ions can cause oxidative damage by catalyzing reactions that generate oxyradicals [68, 69]. Recent studies on the oxidative damage caused by free hydroxyl radicals and other reactive oxygen species have shown them to be major contributing factors for the development of certain diseases [70, 71], bone defects and gastrointestinal damage [72], cancer [73, 74], diseases of the nervous system [75] and aging [76]. For instance, soluble copper ions can increase oxidative stress by substituting for iron in the Fenton reaction which catalyzes the conversion of hydrogen peroxide and superoxide into the highly cytotoxic hydroxyl radical [70, 77]. This may be because the two most common oxidation states for copper, Cu (I) and Cu (II), are easily interchangeable, which bestows copper with redox properties that can function as either an essential feature or a deleterious issue in biological systems.

It is widely known that mitochondria in cells are particularly sensitive to oxidative damage and rely upon various antioxidants and anti-oxidizing systems for protection and defense against oxidative stress. Since mitochondria are major sites for oxygen utilization facilitating respiration, they become a source of free radical generation as well as an important recipient of oxidative damage due to the same free radicals. Cellular defense mechanisms can become overwhelmed by the presence of excessive copper and oxyradicals, thus compromising respiratory function and further impairing cellular health and survival. Hence, many field studies have aimed at using gill tissues of aquatic organisms for understanding the effects of high copper concentrations present in water bodies that are in close proximity to pollution sources such as smelters. It is now established that bivalves and benthic organisms bioaccumulate some of the highest levels

of heavy metals, but most crop plants do not bioaccumulate copper in spite of prolonged exposure to copper rich soils, suggesting the possibility of a soil-plant/root barrier mechanism being present that protects the plants [78, 79]. Thus for example, a study showed that corn (*Zea mays*) did not accumulate copper from soils treated with 365kg of copper per surface hectare over a 13-year period; corn yield was also not affected under such conditions [80]. However, more studies are needed to verify this and confirm the possibility of any resistance offered by crops such as corn to copper phytotoxicity. On the other hand, a recent study on maize crops demonstrated growth and survival impairment due to excessive Pb exposure in soil [81].

Copper toxicity showed induction of DNA strand breakage in rats and a similar study conducted on mice showed chromosomal aberrations and sperm abnormalities which means that copper in excess could have the potential to act as a human mutagen [82, 83]. Excessive levels of copper or zinc can cause both functional and structural damage of enzymes or other biomolecules by displacement of ions at metal binding sites [84-86], or by non-specific binding to DNA causing DNA damage [73, 87]. This can progress further to embryotoxic and genotoxic effects causing neurodegenerative disorders and severe impairment in the growth and development of the organism [88, 71, 89]. Copper also aids as sites for oxygen coupling in haemocyanin in many molluscs and other invertebrates. In a recent in vitro study on effects of Cu toxicity on lysosomal activity, the authors found that copper played a part in the proton pump and chlorine selective channels. They reported that copper acted by inhibiting certain enzymes, ion channels and ATP-driven pumps leading to disrupted cell homeostasis, membrane potential and osmosis [90].

Fish eggs treated with 500µg Cu/L for four days resulted in a significant number of malformed fish larvae [91]. In an *in vitro* study, copper salts in the presence of hydrogen peroxide and ascorbic acid affected chromosomes and enhanced the rate of non-complementary nucleotides in synthesized DNA double helices. Another study where young sheep were administered 10.7mg Cu/Kg body weight as part of daily diet until death at 65-85 days, showed significant increase in sister chromatid exchanges in bone marrow due to toxicity [92], but the specific role of copper on mutagenicity and survival decline is unclear and needs further studies for verification. Toxic effects of copper on mussels (*Mytilus spp.*) showed valve closure and reduced filtration rates; these responses could be to slow down the uptake of Cu through lessening mussel contact with the ambient environment and by reducing blood flow within the animal [80]. The structure and function of cellular membranes in mussels were impaired by Cu toxicity and this was evidenced by the stimulation of membrane lipid peroxidation and the resulting formation of lipofuscins as a result of the end products from lipid peroxidation [93].

Copper exposure in mussels showed toxic effects on the mantle tissues, where heat shock protein 60 exhibited an increase in expression level in a dose-dependent manner; based on this response the authors concluded that heat shock protein 60 could be a potential biomarker for copper stress [94]. In another study, cross breeding of mussels from copper contaminated sites showed results that suggest that female mussels play a significant role in transferring copper tolerance traits to juveniles; thus copper tolerance is mostly maternally determined [95]. In another study looking at the bioconcentration factors (ratio of milligrams of copper per kilogram fresh weight soft parts to milligrams of copper per liter of seawater) in marine bivalves, the highest bioconcentration factor for copper was found in American oysters after exposure for 140 days, and the lowest was in bay scallops (*Argopecten irradians*) [96].

Soria *et al.* studied copper toxicity effects in embryos of certain species from temperate (bivalves) and tropical (clams) regions, and found that excessive copper was more toxic to the embryos of giant clams than embryos of bivalves. They also showed that copper concentrations in molluscs were 12-32 times higher than that found in other benthic organisms [97, 98]. This was an interesting result and the difference in response between these two species could be because most tropical bivalves live under already high thermal limits and Cu exposure was acting as an additional stressor, leaving the bivalves poorly equipped to combat the additional stress.

When *Busycon canaliculatum* (marine gastropods) were exposed to lethal concentrations of copper, gills and osphradium showed progressive histopathology revealing swelling of the gill filaments, amoebocytic infiltration of the connective tissue, and necrosis and sloughing of the mucosa [99]. There is preliminary evidence of genetic adaptation by some freshwater gastropods to become copper-resistant strains as the study observed certain gastropods survived prolonged exposure in media containing elevated concentrations of 35 µg Cu /L [100]. A study using freshwater gastropods found that ionic copper causes up-regulation of lysosomal enzymes, acid and alkaline phosphatases; immature gastropods were also seen to be more sensitive than adults [101]. Crustaceans demonstrated seasonal fluctuations in the rate of bioaccumulation of metals, for example field studies on isopods showed greatest concentrations of Cu accumulated during summer when temperatures become naturally slightly elevated compared to cooler climates [102], and also increased bioaccumulation of Cu occurred at the time of molting [103].

Fish exposed to 15µg Cu/L (sublethal) and 150µg Cu/L (lethal) showed changes in whole-body sodium levels and lipid peroxidation, Na/K-ATPase activity, metallothionein levels, and catalase activity [104]. A recent study investigated levels of selenium, copper,

cadmium, zinc, arsenic and lead in Lake Macquarie (Australia) to determine if any threshold limits have been surpassed, and whether these levels posed a threat to resident species or human consumers. From the body concentrations of metals accumulated in fish tissues, they reported biomagnification of selenium occurred at the highest levels, surpassing human consumption threshold limits, whereas copper, cadmium, zinc or lead showed no threat. Interestingly, upon testing crustaceans as part of the same study, crustaceans showed Cu accumulation that exceeded maximum permitted concentrations for human consumption. This needs further study in a different manner to verify these findings [105].

Port Curtis was the site of toxicity assessment for a recent study to investigate levels of several anthropogenic contaminants, because it is one of Australia's leading ports. Positively, the study reported dissolved metal content in water to be well within safety standards set by ANZECC/ARMCANZ 2000 guidelines (Agriculture and Resources Management Council of Australia and New Zealand (ARMCANZ), and Australian and New Zealand Environment and Conservation Council (ANZECC)). However, biota showed evidence of bioaccumulation of metals, and mercury was identified as a potent human health risk factor [106]. A related study on human derived kidney cells has correlated increased Cu blood levels with increase in methemoglobin, decrease in glutathione levels, increase in glutamic oxaloacetate transaminase and lactic dehydrogenase, indicating possible liver necrosis, increase in creatine phosphokinase activities due to damaged muscle cell membranes, severe hemolysis and kidney damage, and greater chances of uremia or death [107].

### **1.3 Zinc contamination and effects on aquatic species**

Most of the zinc introduced into aquatic environments is absorbed onto hydrous iron and manganese oxides, clay minerals, and organic materials, and eventually is partitioned into the sediments. Zinc is present in sediments as precipitated zinc hydroxide, ferric and manganic oxyhydroxide precipitates, insoluble organic complexes, insoluble sulfides, and other forms. As the sediments change from a reduced to an oxidized state, soluble zinc is mobilized and released; however, the bioavailability of different forms of sediment zinc varies substantially and the mechanisms of transfer are poorly understood [108]. Zinc metal is used primarily in the galvanization of iron and steel products; production of noncorrosive alloys, brass, and white pigments; as fungicide in agriculture; and as therapeutics. Major sources of anthropogenic zinc in the environment include mining industry drainage, electroplaters, smelting and ore processors, domestic and industrial sewage, road surface runoffs, and corrosion of zinc alloys and galvanized surfaces.

Although zinc is an essential metal to biota and has its primary effect on zinc-dependent enzymes that regulate RNA and DNA, the pancreas and bone are primary sites for excess zinc deposits in birds and mammals [109]; the gill epithelium is a primary target site in fish [110]. Fish when exposed to high sublethal concentrations of zinc showed significant changes in blood and serum chemistry. They also showed significant changes in liver enzyme activity [111], muscle glycogen, total lipids, phospholipids, RNA, proteins and cholesterol [112]. Dietary zinc absorption is highly variable in animals; in general, it increases with low body weight and decreases with excess calcium or phytate and with deficiency of pyridoxine or tryptophan [108].

### 1.3.1 Zinc contamination in combination with other contaminants

The mechanism of bioaccumulation of Zn and Cd in organisms is more efficient at high salinity values [113]. Mixtures of zinc and copper are generally acknowledged to be more-than-additive in toxicity to a wide variety of aquatic organisms, including oysters [11], fish [108, 110, 114] and amphipods. A study exploring species behavior and effects on bioaccumulation levels as a consequence of exposures to multiple metals showed that when zinc was added to the ambient water it decreased copper accumulations in tissues of juvenile African catfish (*Clarias Lazera*), but copper added to the medium decreased zinc uptake. However, the survival rate of the fish was greatly reduced in mixtures of the two metals, indicating that they potentiate each other's lethal effects [115]. Another study on barnacles showed a similar situation, where simultaneous exposure to copper and zinc metals resulted in enhanced uptake and toxicity of both metals [116].

Under sublethal exposure to 500 µg Zn/L, freshwater killifishes (*Fundulus heteroclitus*) demonstrated changes in expression levels of many enzymes associated with oxidative stress including superoxide dismutase, glutathione-S-transferase and catalase. From this the authors concluded that Zn in water behaved as an oxidative stressor. They also investigated the role of salinity on Zn stress experienced by the animals by assessing damage to protein carbonyls and lipid peroxidation using a step wise increase in salinity while maintaining the same Zn levels. They found that salinity had an ameliorating effect on Zn toxicity based on results which showed that maximum damage of protein carbonyls and lipid peroxidation activities occurred at zero ppt (0% salinity), while the least damage occurred at 35 ppt (100% seawater salinity) [117]. Zinc demonstrated antioxidant properties against reactive oxygen species as evidenced when gill cells showed no cytotoxic effects from hydrogen peroxide when the cells were exposed to 100 µM zinc

sulphate solution first, followed by hydrogen peroxide exposure (up to 200 $\mu$ M). Co-exposures of Zn and hydrogen peroxide together showed evidence of cytotoxicity. This suggests that anti-oxidant gene expression to fight off free radicals induced by hydrogen peroxide is indirectly mediated by Zn; in contrast, Zn behaves as an additional stressor when co-exposed in seawater [118].

In higher organisms, zinc behaves as an antagonist to copper and potentiates the effects of deficiency of dietary copper in rats and chicks. However, this effect only occurs at significantly high dietary ratios of zinc to copper. Copper has usually been positively correlated with zinc, with their joint effects seen in a study where mixtures of Cu and Zn salts acted superadditively in worsening the toxicity of gills of several marine species [91, 108, 119]. The two metals also behave complementarily in certain enzymatic reactions where they can swap between charge states for metal binding sites in cellular systems.

### **1.3.2 Zinc contamination in marine arthropods**

Crustaceans, among other marine arthropods, are able to not only bioaccumulate Zn but also regulate body concentrations against fluctuations, but the ways in which regulation is achieved can vary among different species. Adult freshwater snails, *Melanoides tuberculata* were exposed to a range of metals including Pb, Cu and Zn over a period of 4 days, and maximum bioaccumulation of Zn occurred in the shells. The authors reported that the shells evidenced at least 35% higher bioaccumulation than other soft parts. Among all metals tested on snails, Cu was found to pose the highest toxicity effects on the animal and showed highest bioaccumulation in soft tissues [120]. Metallothioneins play an important role in zinc homeostasis and in protection against zinc toxicity; zinc is a potent inducer of metallothioneins [121-123]. Zinc interacts with many bio-chemicals to produce altered patterns of bioaccumulation, metabolism, and toxicity;

some interactions are beneficial to the organism and others are not, depending on the organism, its nutritional status, and other variables. For instance, different species of fish have responded differently to different ingestion routes for Zn, and Zn routed via diet has been effectively absorbed in most species. Knowledge of these interactions is essential to the understanding of zinc toxicokinetics.

Reproductive impairment was the main effect in response to Zn stress in freshwater teleosts when they were exposed at the 50-340 µg Zn/L range [124]. Reproductive decline occurred even at concentrations that were not expected to be stressful for the fishes survival, growth, or maturation [125]. This suggests that physiological evidence of Zn in an organism could take longer to become noticeable, even though slight cellular disturbances caused by metals could lead to genotoxicity and impair reproduction events of the organism. Total reproductive output was concluded as the most suitable assessing factor for evaluating effects of sediment toxicity among the four copepod species used in the study. *Nitocra spinipes* could be a suitable candidate for sediment-toxicity tests among few other copepod species [126]. Altered rate of development and increased numbers of deformed larvae, along with cellular disruptions in brain, muscle and epidermis were direct effects of stress caused due to Zn stress when Baltic herring (*Clupea harengus*) was exposed to >6 mg Zn/L [127].

Mussels, among other tested bivalves, showed significant decrease in their filtration rate when exposed to 470 – 860 µg Zn/L, as compared to controls. Filtration stopped completely when exposure was prolonged up to 7h; whereas other bivalves showed up to 50% decrease in filtration rate for the 7h, which continued even under higher exposure levels of 750-2,000 µg Zn/L. Therefore, not only is the amount of metal accumulation important, but also the rate of accumulation is vital. Since the data showed

similar metal concentrations in both dead and surviving mussels, it is possible that biovariability between individual mussels could affect their sensitivity to metals and the dead ones could have had lower lethal body limits than the surviving mussels [128].

**Table 1.1 Effects of zinc on representative aquatic oysters. Concentrations are in micrograms of zinc per liter of medium [80, 108].**

<b>Taxonomic group / organism</b>	<b>Concentration (ppb)</b>	<b>Effects</b>	<b>References</b>
<b>Pacific oyster, <i>Crassostrea gigas</i></b>			
Larvae	10-20	Reduced larval settlement in 20 days	[96]
Larvae	30-35	Reduced larval settlement in 6 days	[129]
Larvae	50	Normal growth and development inhibited after 5 days.	[130]
Larvae	70	Abnormal shell development in 48 h	[96]
Larvae	75	No deaths in 48 h	[96]
Larvae	80-95	Growth reduced 50% in 4 days	[129]
Larvae	119-310	LC50 (48 h)	[96]
Larvae	125	Substrate attachment inhibited in 5 days	[96, 129]
Larvae	200	No growth in 5 days	[130]
Embryo	233	LC50 (96 h)	[129]
Larvae	250	Increasing incidence of abnormal development and mortality	[130]
Sperm	444	Fertilization success reduced 50% in 1h	[129]
Larvae	500	Complete mortality at 48 h	[96]
<b>American oyster, <i>Crassostrea virginica</i></b>			
Adult	100	Whole body concentration were 2,560-2,708 mg Zn/kg fresh weight (FW) soft parts after 20-week exposure (1,036-1,708 mg Zn/kg FW soft parts in controls)	[131]
Adult	200	After exposure for 20 weeks, residues were 3,185-3,813 mg Zn/kg FW soft parts	[131]
Embryo	230	LC50 (96 h)	[129]
Larvae	340	LC50 (48 h)	[132]
<b>Red abalone, <i>Haliotis rufescens</i></b>			
larvae	19	No adverse effects after 9-day exposure	[80, 132]
Larvae	41	Normal development during 48-h	[132]
Larvae	50	50% abnormal development during exposure for 9 days	[132]
larvae	68	50% abnormal development in 48h exposure	[132]

Evaluation of chronic sublethal effects of Zn exposure in *Corophium spp.* has shown juveniles to be particularly sensitive to Zn stress. The juveniles showed reduced growth and survival when exposed to low Zn concentrations such as <1 mg/kg, whereas the adults responded to stress by reduced reproduction rates when exposures were conducted over a 100 day period [133]. Another study on *C. volutator* (length, 2.5–4.5 mm) exposed to slightly and moderately contaminated sediments showed reduced growth in comparison to controls [134]. In the Guacanayabo gulf region of Cuba, surface sediments were surveyed over a 20 year period and the data has shown that levels of Zn and Cu in oysters (*Crassostrea rhizophorae*) were above recommended limits for public health [135]. Zinc exposures on oysters at various developmental stages have shown that lethal effects mostly occur in larvae and embryos rather than adults, probably because adults have several well developed mechanisms to sequester toxic levels of metals. Unlike the younger animals (as shown in table 1.1), adults were able to bioaccumulate high Zn concentrations over prolonged periods, although they did suffer growth impairment and reduced reproduction rates.

Another study gradually exposed lobsters (*Homarus gammarus*) to zinc concentrations up to 505 µg Zn/L in seawater, and observed that the body concentrations of Zn were increased up to 100 fold compared to controls in blood, whole body tissues and organs such as hepatopancreas, excretory organs, and gills. Zinc concentrations in shells were 12 times more than in other body parts and this could largely be through adsorption [136].

Data from a recent study on understanding transport mechanisms used to sequester metals in lobsters suggest that Zn transport could be aided by the presence of an organic anion exchanger in lobster lysosomal membranes and two metal transporters on

hepatopancreatic membranes; a high affinity, low capacity cation antiporter and a low affinity, high capacity organic anion exchanger. The authors suggest that together these two systems could potentiate regulation of cytoplasmic metals over a wide concentration range [137]. Inside the cell, zinc is known to bind to a variety of existing ligands that maintain an inward diffusion gradient, preventing efflux of zinc. Recent findings indicate that metallothioneins I and II could play important roles in combating Zn toxicity [138]. Freshwater crayfish (*Orconectes virilis*) are able to easily endure high Zn toxicity (LC50 value is 84 mg) and are considered one among the more resistant crustaceans; that may be why they are found living in some streams containing 79-99 mg Zn/L in the Arkansas and Colorado river systems [139]. It is apparent that the lethal threshold body concentrations of Zn can significantly vary between species, therefore total body Zn concentration alone could not serve as a suitable toxicity indicator. Zn toxicity is probably governed by accumulation in certain metabolically relevant body parts, not just by total accumulated Zn concentration.

### **1.3.3 Zinc contamination in non-mammals and mammals, including humans**

A study on the potential effects of Zn nanoparticles in human embryonic kidney cells revealed that cytotoxicity, oxidative stress, associated damage to cell/tissues and DNA mutation are some of the major responses to zinc toxicity in human cells [140]. These findings are in line with some previous studies which also reported additional effects such as altered redox signaling, dysfunction in growth and development patterns and decreased reproduction rates. These responses occur after the organism's cell homeostasis mechanisms have become ineffective, because cell redox homeostasis is the natural way to sequester metals in most organisms to help them survive contaminated waters. Excessive Zn eventually results in cardiovascular diseases in humans; high zinc

intakes also decreases iron absorption, resulting in reduced bioavailability and thus leading to a reduction of erythrocyte life span by 67% [108]. Although not aquatic species, a study has shown that chickens demonstrate similar responses to Zn toxicity. In the study, when domestic chickens were exposed to 8000 mg Zn/kg through diet, they were quite resistant to Zn uptake, whereas chicks found the dose fatal. When fed to hens, it induced molting. Chicks when exposed to 2,000-3,000 mg Zn/kg via diet experienced growth inhibition and chicks that received lower dose such as 178 mg Zn/kg experienced immunosuppression; still lower doses such as 100 mg Zn/kg caused pancreas histopathology. Apart from these responses, chicks also showed zinc accumulations in tissues [141].

Although effects evidenced in pancreas could be a key in diagnosing Zn toxicity, it definitely may not be the first of signs of Zn toxicity in an organism. For example, in sheep and dogs it was found to take 4 weeks of continued ingestion of toxic amounts of zinc before the pancreas was affected [142, 143]. A recent genomics and proteomics study on Zn exposed rainbow trout, a non-model fish species, revealed 11 proteins that were differentially regulated in response to 3.5  $\mu$ M Zn in water, which included glutathione S-transferase, 6-phosphofructo-2-kinase, 40S ribosomal proteins, RNA binding protein, asparaginyl tRNA synthetase, and other proteins.

For the protection of marine species, the EPA recommends that total recoverable zinc concentration in seawater should be <58  $\mu$ g/L on an average and not beyond 170  $\mu$ g/L; for acid-soluble zinc the limits were <86 and 95  $\mu$ g/L; the same limits were applied to freshwater biota. Growing evidence from studies and surveys has shown that many species of marine animals including molluscs, crustaceans, fish and even plants are being adversely affected, even at lower than recommended limits such as 9 - 50  $\mu$ g/L, which are generally ambient zinc concentrations. There is clear evidence of significant effects at

metal concentrations below the current proposed thresholds for marine life protection, which indicates an update on these limits, or more specifically a lowering of the thresholds, should be undertaken by the EPA.

#### **1.4 Lead contamination in aquatic species**

Lead is known to possess complicated chemistry, in that Pb is soluble and bioavailable in conditions of low organic content, low pH, low concentrations of suspended sediments, and low concentrations of the salts of calcium, iron, manganese, zinc, and cadmium. Therefore, solubility of lead is low in water and in the presence of surface-films of organic materials, and Pb compounds tend to concentrate in the water surface micro-layer [144]. Lead containing compounds that are of anthropogenic origin are generally organo-lead compounds found mostly in the aquatic environment as contaminants; however, some organo-lead complexes form naturally. Most Pb that enters waterways occurs as precipitated carbonates or hydroxides in the sediment bed. Lead is easily precipitated by several common anions whereas desorption and replacement by other cations occur extremely slowly [144, 145]. In the presence of elevated Zn concentrations, Pb is accumulated up to 10 times more rapidly by marine fish in seawater [145].

Depending on the severity of toxicity of these heavy metals, arsenic (As), Pb and cadmium (Cd) are classified under the name priority pollutants, because they can pose toxicity even at low concentrations and they are non-essential for metabolic activity in biological systems. On the other hand, Cu and Zn are biologically essential metals needed for the survival of biota, but they can become detrimental when present at very high concentrations above threshold limits relative to the organism.

Lead toxicity leads to detrimental effects on the function and structure of kidney, bone, the central nervous system, and the hematopoietic system, and produces adverse biochemical, histopathological, neuropsychological, teratogenic and reproductive effects. Because of health concerns, Pb used in the manufacturing of gasoline, paints, ceramic products, and pipe solder has been dramatically reduced in recent years, thus slowly eradicating a major anthropogenic source of lead pollution. Previous studies in literature reveal that effects of Pb toxicosis may be shielded by zinc in terrestrial animals [146]. The toxic effect of Pb was shown to be reduced by the presence of dietary zinc in larvae of the house cricket. Zinc was also reported to protect against Pb toxicity in horses and against testicular injury induced by Pb in rats [145].

It is quite evident that the problem of heavy metal pollution primarily arose from unthoughtful activities by mankind during industrial and urban developments, contributing substantial heavy metal inputs into the marine environment. It is worth mentioning that once marine waters are polluted with heavy metals, they can never be fully recovered and the contaminants are capable of remaining undeteriorated for prolonged time periods. Although human contribution has reduced somewhat in developed countries in recent years, what have been already polluted still remains polluted – and will do so for a long time. Thus, marine waters and sediments have become open sinks for heavy metals due to their large capacity to retain metals for extensive time periods.

## **1.5 Proteomics as a tool to understand changes caused by heavy metal pollution in marine biota**

The proteome is highly dynamic because it alters in expression continuously in response to numerous intracellular and extracellular signaling, returning every subtle

external stimuli. This is in contrary to the nature of the genome, which is relatively stable throughout life. It is generally agreed that the ultimate objective of ecotoxicology is to identify and understand the effects of toxicants, for instance, in our case the effects of heavy metals (or other biotic or abiotic stressors such as CO<sub>2</sub> or temperature) on ecologically relevant species. Proteomic methodologies can be used not only to unravel new or missing links in partially known biological mechanisms underlying different metal stresses, but also to identify new candidate biomarkers. Hence, the main difference between a proteomic approach and the traditional experimental biology coupled with biochemical or enzymatic analysis is that the proteomics approach is not hypothesis-driven. In contrast, it is used to generate new hypotheses. With this approach, there is the possibility of identifying and quantifying thousands of proteins, without any assumptions on possible mode of action, as well as revealing links between proteins and metal exposure that have not been described earlier. This is unquestionably the major advantage of using proteomics. Thus, any breakthroughs from addressing such ecotoxicoproteomics studies will help find unexpected relationships and protein responses, leading to the development of new hypotheses.

Complexities due to post-translational modifications of proteins and degradation of proteins analyzed using proteomics more often reveal a different cellular phenotype when compared to those obtained using transcriptomics [20]. More than 350 different types of protein modifications are known, and it has been reported in literature that for every protein there is a possibility of up to ten post-translational modifications in eukaryotes [20].

All living organisms are capable of using several mechanisms to counter heavy metal toxicity. Among heavy metals, lead, cadmium and mercury are highly toxic metals

in both terrestrial and aquatic environments, but the mechanisms by which they pose a threat to living systems remain largely unclear. As a result of the few biologically relevant studies in this area, *in vivo* mechanisms that counteract toxicity and provide remediation to affected organisms remain unclear and poorly understood. Various metabolic pathways such as protein translocation, energy metabolism, stress response, cytoskeletal remodeling, and catalytic metabolic pathways have been recently shown to be involved in heavy metal stress response. However, the nature of interactions between these metabolic entities and proteins seem to be complex, and the programmed cellular and molecular events that lead to functional changes occurring in these metabolic pathways needs further research. In bacteria, efflux pumps are able to export toxic ions outside the cell. A previous study on yeast indicated glutathione and thioredoxin/thioredoxin reductase systems to be involved in cellular defense against cadmium toxicity [147]. Another study investigating zinc response in fish gill tissue of *Fugu rubripes* (puffer fish) by protein profiling used surface enhanced laser desorption ionization (SELDI) showed 7 proteins that were consistently present only in zinc-exposed gills, 4 proteins unique to non-exposed gills, and 11 proteins with different expression levels between tissues [110].

In higher eukaryotes, it is possible that  $\text{Cd}^{2+}$  can be sequestered by metallothioneins. Cadmium can also be detoxified by chelating to glutathione or phytochelatin. In *S. cerevisiae*, several proteins induced by cadmium have been separated by 2D-PAGE, providing a framework for the mechanism of  $\text{Cd}^{2+}$  toxicity and cellular protection against this toxic metal [147]. Another study by Kao *et al.* showed that the expression of 60 proteins was stimulated by copper ions, while 68 more proteins were down-regulated, suggesting that these suppressed proteins were mainly responsible for the cellular signaling process [77]. In a separate study, Zhu *et al.* described an investigation of *Paralichthys olivaceus* (olive flounder fish) brain tissue in an effort to discover available

biomarkers for monitoring levels of exposure to cadmium in continuously flowing seawater. They found that the expression levels of a group of proteins visible on 2D-PAGE gels, including transferrin-selected biomarkers, could be employed to continuously monitor the contamination level of cadmium in seawater, as well as halobios survival, and also to evaluate the risk of human fatalities [10]. In past years, a few toxicology studies [148-150] have been conducted on fish, mostly discussing effects on swimming behaviour affected by heavy metal stress, and most biomarkers identified seem to be involved in physiological processes, neurotransmission and energy metabolism.

#### **1.5.1 Evaluation of Zn, Cu and Pb metal pollution using proteomics as tool in oysters and other bivalves**

Numerous studies have shown that bivalve mollusks, particularly oysters [151-153] and mussels [154, 155], can act as biological indicators of environmental contamination, such as heavy metal pollution, in the marine environment. Bivalve mollusks have been used successfully for ecotoxicology studies of metal pollution in the past. Oysters have been utilized in toxicity studies of heavy metals [151, 156, 157] and polycyclic hydrocarbons [158], metal pollution on enzyme activities [159, 160], studying bioaccumulation of methylmercury and zinc [161], and investigating the effects of oil spills [162].

Oysters are an essential part of the marine food chain as shown in Figure 1.1. They also have a higher capacity than most bivalves for metal bioaccumulation via their filter feeding life history. This makes them useful biomonitors of heavy metal pollution in marine ecosystems. Sydney rock oysters (*S. glomerata*) are endemic to Australia where they are abundant in coastal waters, bays, inlets and sheltered estuaries. They are wide spread across Australia from Wingan Inlet in eastern Victoria, along the east coast of New

South Wales and up to Hervey Bay, Queensland, around northern Australia and down the west coast to Shark Bay in Western Australia. *S. glomerata* can bioaccumulate high levels of heavy metals and have a life span of up to 10 years, which is sufficient to investigate long term exposure. This combination of features led us to choose *S. glomerata* as subjects in the first project of our study which uses shotgun proteomics to investigate the effect of metal exposure on protein expression in oysters.

### **1.5.2 Evaluation of Zn metal pollution in amphipods using proteomics**

The pollution of estuarine sediments with chemical contaminants is an issue of major environmental concern. Contaminants including a variety of organic compounds and metals from agricultural, industrial and urban sources have been discharged into estuaries. These contaminants are adsorbed onto suspended particles in water and settle down eventually with sediments. The soft-bottom marine benthic community, which includes amphipods, is highly abundant, widely distributed and ecologically vital. Amphipods that live in sediments directly face toxic effects from contaminants, which indirectly affect human health as well (Figure 1.1).

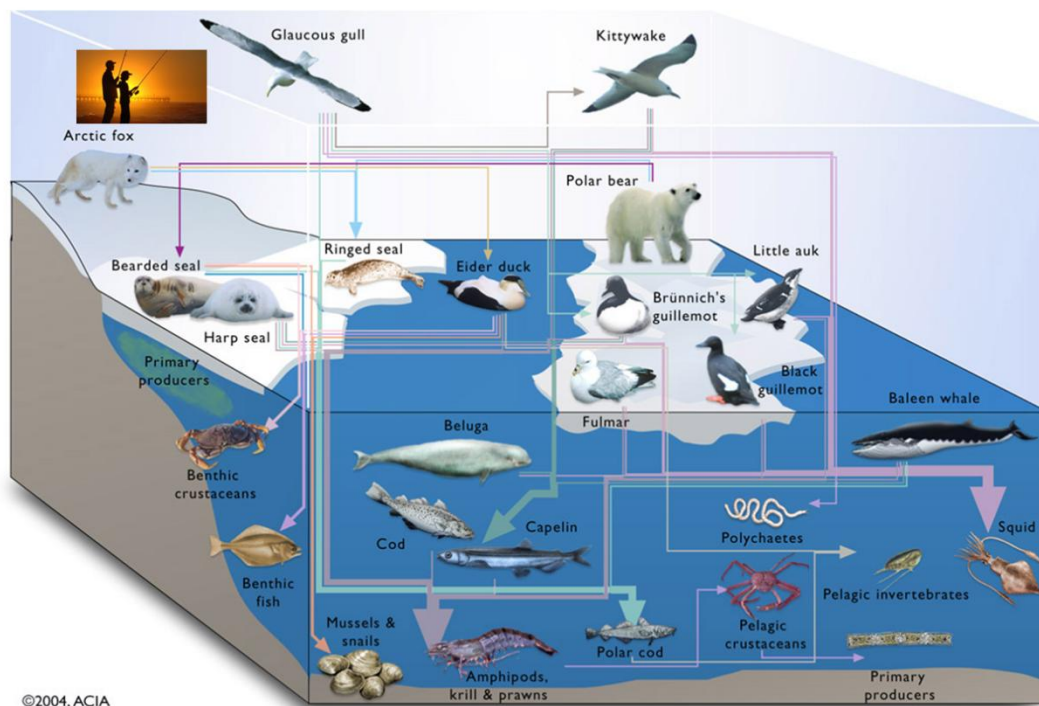


**Figure 1.1** A typical food web in marine ecosystems, with bivalves and amphipods at the base (Image adapted from ACIA overview report, 2004 [163]).

Silty mud carries the highest concentrations of metal contaminants, because contaminants tend to adsorb better to fine-grained sediments than coarse sediments. Such fine-grained sediments are more likely to be transported to regions far from origin as they are easily resuspended and transported by water currents. Sometimes toxicants that are strongly bound to sediments pose a severe threat to benthic communities.

Factors such as feeding strategies or burrowing behaviour also influence amphipods' sensitivity to metal stress [164]. Previous studies have shown amphipods to have increased sensitivity to metals and other toxicants compared to other benthic organisms, and to be capable of bioaccumulation of toxic metals and substances [165-167, 113]. Due to foraging behavior and benthic nature of the amphipods, soon after the amphipods ingest metal-rich particles, the toxicant metals enter the food web. A cascade of stages of bioaccumulation begins soon after the amphipods ingest the metals from

contaminated sediment particles (stage 1 in bioaccumulation of metals). When the amphipods become food to shellfish, fish and other organisms in the next order in the food chain, bulk accumulation of metals is achieved and this becomes stage II in bioaccumulation and so on, thus threatening larger consumers, including humans. Thus, benthic amphipods satisfy most criteria that render them highly suitable for marine monitoring and sediment ecotoxicology assessments. Different species of amphipods show different degrees of sensitivities to the same toxicant and recent studies have observed this sensitivity distribution [168, 169]. Amphipods of varying sizes also showed varying degrees of sensitivity when exposed to the same metal contaminant [168]. Therefore in order to perform well designed ecotoxicology tests, care should be taken, with species selection, breeding, assortment, and collection of amphipods all given utmost importance and priority because they are crucial starting inputs and are as vital as the exposure study itself.

The use of *Gammarus* species in sediment toxicology studies has long been established [170-177]. Amphipods show shifts in sensitivity distribution among individual subspecies that inhabit rocky environments owing to changes in degree of pollution [165, 178]. They are also known to be tolerant to varying physico-chemical characteristics of sediment and seawater. Over 6000 species of Gammaridea amphipods are known to exist and there is still lot to uncover about the ecology or behavioral responses of most species to various toxicants. This was apparent when the role of benthic amphipods in environmental disturbance was recently surveyed and not surprisingly, the researchers could only compile biological information for less than 3% of all the described species.

Environmental monitoring often involves forced curtailing of fishing and close shell-fisheries in heavily-contaminated regions, with significant economic expense. Metals

present at lower concentrations in estuarine sediments are generally not harmful to organisms. Some, like zinc, are essential for normal metabolism but are toxic above a critical threshold. Zinc that is released into the environment can be traced to a variety of industrial and domestic sources [108]. Although zinc is an essential metal to life, it can become a problematic environmental toxicant. Zinc exposure beyond nutritional levels could evoke a complex response involving a multitude of molecular and cellular entities. Some of these entities are known to be involved in physiological regulation of uptake and handling of zinc known as zinc metal sequestration, whereas other biochemical changes may be characterized as toxic effects due to excessive zinc metal stress.

The use of certain key benthic species as biomonitors for evaluating sediment toxicity in aquatic environments has become an increasingly important component of ecotoxicology research [179-182]. Similar to fish and oysters, gills of amphipods pose a critical target organ for zinc toxicity via sediments. At high concentrations, zinc elicits a response that is relatively stereotypical for most toxic metals. Amphipods exposed to a range of Zn levels have demonstrated distinct responses to toxicity. Zinc tolerant species (adults and juveniles) show tolerance to very high exposure levels in addition to lower incidences of mortality compared to other species (Table 1.2). A 14 days growth test assay has been recently developed for *Corophium colo* in Australia [134], for evaluating and monitoring of Zn effects by assessing growth of amphipods in contaminated sites. Field evaluation of this methodology would be beneficial and could set an example for developing more such diagnostic tools for early monitoring. In fish, induction of histological aberrations such as lifting of the epithelial cells away from the basement membrane, leukocyte infiltration, epithelial cell proliferation, necrosis, hypertrophy and increased mucus secretion have all been observed as effects of excessive zinc exposure [183].

**Table 1.2**      **Effects of zinc on representative benthic amphipods. Concentrations are in micrograms of zinc per liter of medium [80, 108].**

<b>Taxonomic group, organism</b>	<b>Concentration (ppb)</b>	<b>Effects</b>	<b>References</b>
Amphipod, <i>Allorchestes compressa</i> sp.	580-2,000	LC50 (96 h)	[184, 185, 130]
Brine shrimp, <i>Artemia prenauplii</i>	14-1,360	Egg hatching significantly reduced in dose-dependent manner; no effect on survival of larvae	[186]
Amphipod, <i>Gammarus duebeni</i> embryos	>100	Survival reduced in 7 days	[187]
Amphipods natural population	1,000	All dead in 7 days at 10 ppt salinity, 84% dead at 30 ppt	[187]
Zinc-tolerant population juveniles	1,000	50% dead in 14 days at 10 ppt salinity, 33% dead at 30 ppt	[187]
Zinc-tolerant adults	2,000	LC50 (96 h)	[184]

Other studies showed that as a result of zinc stress there was an increase in the diffusion distance between water and blood, which impairs O<sub>2</sub> uptake and CO<sub>2</sub> excretion and leads to hypoxemia, hypercapnia and acidosis [114, 188]. However, studies on lower concentrations of waterborne zinc (<12 µM) did not see these effects. Instead, there was a net loss of calcium across the gills, leading to potentially fatal hypocalcaemia [189]. These effects are more specific compared to the histopathological symptoms that were previously observed at higher concentrations of zinc.

In a series of studies, it was shown that zinc inhibits apical calcium entry, possibly through competition at an epithelial calcium channel. The basolateral transfer of calcium was also impaired, an effect that was caused by mixed inhibition of the high affinity Ca<sup>2+</sup>ATPase [190-194]. Results from such studies quite evidently indicate that in addition

to the above mentioned zinc-induced calcium inhibition mechanisms, zinc homeostatic mechanisms also seem to be simultaneously activated to prevent toxicity. This is evident from a reduced affinity for zinc influx [192] and increased production of the zinc-binding protein metallothionein in the gills [195, 190, 196]. Therefore, it is clear that both homeostatic and toxic metabolic events need protein replacement and this is best reflected by an increased protein turnover rate [190]. Hence, zinc exposure is likely to activate or deactivate many different systems in gill cells. These metabolic reactions in response to zinc stress could also be applicable to other organs and tissues indicative of similar effects due to excessive zinc exposures, but our knowledge of such systems is limited and to what extent these responses would be similar remains unknown and warrants further research.

A number of studies have investigated and reviewed individual genes and proteins in an attempt to explain effects observed at the organ and organismal levels in response to heavy metals [108, 197, 20, 181]. Functional genomics and proteomics technologies have allowed us to simultaneously study thousands of genes or proteins, and this ability to take a wider approach has enabled us to seek answers to biological questions faster than previously thought. So far, such techniques have primarily benefited research on well-characterized species such as human, mouse and yeast. Unfortunately, these species may be inappropriate from an ecotoxicological perspective. The wide distribution of oysters and amphipods in both marine and fresh waters, along with their high abundance in both benthic and pelagic environments, means that there is a need for more proteomics research on these two classes of species in order to further the knowledge regarding their specific sensitivity, response patterns, and mechanisms of dealing with heavy metal pollution. It is useful to have such studies in different species or at least in more abundant marine and freshwater species. In my opinion, the usage of these modern technologies, especially

proteomics, to study ecotoxicology in a relevant species demands more work for less information but is certainly not impossible.

## 1.6 Why address Ocean Acidification?

Global climate change is a definitive future phenomenon [198-201]. The impacts of ocean acidification is more severe for coral reefs and the southern oceans. A recent study published in *Nature* by Orr *et al.* in 2005 [202] has shown experimental evidence on increasing atmospheric carbondioxide ( $\text{CO}_2$ ) and reducing ocean pH, with paticular concern to Australia and neighbouring countries in the sourthern ocean. Experiments under scenarios of future levels of increased dissolved  $\text{CO}_2$  (hypercapnia) in seawater showed quite rapid dissolution of argonite shell structures (form of calcium carbonate and major constituent of many marine organisms including corals) and as a consequence of which compared to present levels the proposed undersaturation of the sourthern ocean with respect to argonite is newly estimated to occur by 2050, many decades sooner than previously estimated. Undersaturation occurs when there is simultaneous decline of calcification rates and increasing loss of calcium cabonate exoskeletons via dissolution by calcifying marine organisms due to drop in levels of seawater pH. Table 1.3 shows that surface ocean pH has dropped by more than 0.1 units of pH on log scale, where the change by 0.1 units represents 29% increase in  $\text{H}^+$  ion concentrations in seawater since industrial age.

As a result of this, some of the events predicted to occur by the end of this century in addition to hypercapnia situations include increases in ocean and ambient temperatures between 2–6 °C, a further reduction by 0.3-0.5 units in surface ocean pH (approximately triple the amount of current concentrations) and changes in sea level by 0.7–1.6 m due to oceanic ice melting.

**Table 1.3**      **Changes in Ocean pH levels.**

Time line	pH levels	Change in pH compared to pre-industrial levels	Test type	Percentage of H <sup>+</sup> ions
1700-1800s (Pre-industrial)	8.179		Field test	
1994 (recent past)	8.104	0.075↑	Field test	+ 18.9% ↑
Current levels	~8.069	0.11↑	Field test	+ 28.8% ↑
2050 ( predicted CO <sub>2</sub> levels = double that of present levels = 560 ppm)	7.949	0.230↑	Computer modelled	+ 69.8% ↑
2100 (IS92a)	7.824	0.355↑	Computer modelled	+ 126.5% ↑

Also quite likely are increased precipitation amounts (more during winter and spring), increased precipitation intensity, severely intense tropical and extratropical cyclones, and numerous other atmospheric phenomena. Over the last 200 years, levels of atmospheric CO<sub>2</sub> have gone up by 40%, from pre-industrial age levels of 280ppmv (parts per million volume) to 384ppmv measured in 2007 [203]. The acidification of our oceans is a result of significant increases in the rates of carbon emission collectively contributed by all humanity including combustion of fossil fuels, land use by urban and industrial developments, use of internal combustion engines, deforestation, and increased animal farming. Since that study was published, multiple other studies have revealed several issues that elevate ocean acidification as a threat to marine biota. Increasing CO<sub>2</sub> emissions and subsequent inputs into the atmosphere have led to a significant increase in the amount of total CO<sub>2</sub> absorbed by ocean waters globally through the ocean-carbon cycle, as illustrated in Figure 1.2.

At conditions of hypercapnia, excessive dissolving of  $\text{CO}_2$  in seawater increases the hydrogen ion ( $\text{H}^+$ ) concentration in the ocean, and thus decreases ocean pH. This reduction in pH induced by excess  $\text{CO}_2$  in marine waters has affected ocean acidity and impacts many different marine organisms. Anthropogenic  $\text{CO}_2$  inputs which decrease oceanic pH (acidification) also results in dissolution of calcium carbonate ( $\text{CaCO}_3$ ) from calcifying species like corals and shellfish; when  $\text{CaCO}_3$  starts to dissolve it releases  $\text{CO}_3^{2-}$  which would bind  $\text{H}^+$  ions and form  $\text{HCO}_3^-$  ions. The  $\text{HCO}_3^-$  ions further get protonated quickly and form carbonic acid which further decreases oceanic pH and increases the rate of dissolution of  $\text{CaCO}_3$ , thereby speeding up the whole ocean acidification phenomenon (Figure 1.2).

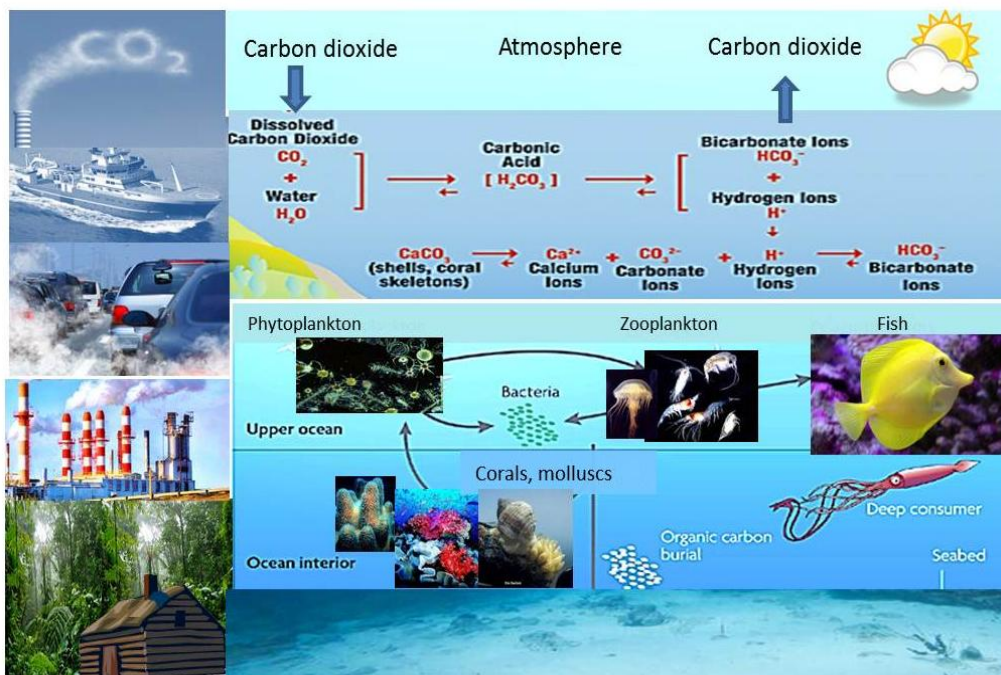


**Figure 1.2 The ocean carbon feedback cycle**

$\text{CaCO}_3$  commonly exists in two forms: calcite and aragonite, which is the more soluble form. Therefore, calcifying organisms such as corals, most oysters and molluscs, pteropods, and others that synthesize aragonite for building body structures, would be

more vulnerable to changes in ocean acidity than those that construct calcite structures (coccolithophores, echinoderms, some sponges and foraminifera, among others). That means, based on the projected range of future CO<sub>2</sub> emissions, any CaCO<sub>3</sub> aragonite structures produced by marine organisms could all vanish. This would also result in the extinction of many species including photosymbionts, plankton and algae that live on these CaCO<sub>3</sub> structural habitats.

Major repercussions of ocean acidity include: (a) the decreased calcification rates and increased dissolution rates of calcium carbonate, which are basic mineral components needed for corals, shells and other body structures in a wide variety of organisms in response to absorption of CO<sub>2</sub> by the ocean [204, 205]; (b) slowing growth rates of many marine calcifying corals which provide habitat for at least a quarter of all marine species; (c) species with aragonite and calcite structures may become undersaturated in the surface ocean within next 50 years [202] and (d) the biological effects of decreasing ocean pH could result in extinction of several marine species reaching far beyond limiting calcification [206]. All these responses could most probably be linked to the down regulation or up regulation of relevant genes responsible for each physiological symptom.

Ocean acidification occurs when the pH of the ocean waters decrease to acidic levels. The potential impacts of this have been quite well documented [203, 206, 202, 207]. In the recent past, the ocean was naturally saturated [202] with respect to CaCO<sub>3</sub> by the process of CaCO<sub>3</sub> compensation for demand, but recent anthropogenic inputs and concurrent increases in ocean acidity have affected the ocean-carbon cycle. It is possible that southern waters would begin to be understaturated by 2050 due to faster CaCO<sub>3</sub> dissolution due to the projected change in pH, and by end of this century the undersaturation of CaCO<sub>3</sub> could intensify and wipe out almost all carbonate habitats in the

Southern Ocean. Similar effects could also occur in other oceanic regions extending into the subarctic Pacific. The uptake from the atmosphere of huge amounts of anthropogenic carbon dioxide is making the world's oceans more acidic than they have ever been.

In light of this issue, Australian researchers have been proactive in monitoring acidification levels by repeatedly sampling water from specific regions of the Southern Ocean to examine physico-chemical properties, such as temperature, salinity, currents and vertical movement of water. Measuring the rate of transfer of water between the sea surface and the deep ocean can determine the amount of heat and CO<sub>2</sub> that the ocean can store; this was considered as a possible way to try regulate the rate and magnitude of climatic change effects [208].

Recent research has identified the major pathways involved in the movement of water around Antarctica and between the world's oceans. The work has contributed to improved climate change projections through new models that reproduce the mixing of water bodies and their effect on surface warming. There are a few well developed models, hydrographic surveys and time series data currently available that simulate stepwise ocean acidification processes. These are being used in efforts to help us understand the patterns of absorption of anthropogenic CO<sub>2</sub>, effects of reduced pH as a result of this absorption, and the rate of dissolution of CaCO<sub>3</sub> in surface waters leading to unsaturated CaCO<sub>3</sub> conditions [209, 210].

Ocean research has also shown that more than three quarters of all the CO<sub>2</sub> released by human activities is now found in the world's oceans and that about a third of this has been taken up in the Southern Ocean. As CO<sub>2</sub> continues to dissolve in the ocean it makes it continually harder for some marine organisms to form shells. These ecological changes in turn reduce the capacity of the ocean to absorb CO<sub>2</sub>.

## **1.7 Effects of carbondioxide acidification on marine biota**

Ocean chemistry is one of the most important factors in creating a balance between organisms and their habitats and any change in ocean chemistry (for example, changes in ocean acidity or carbonate chemistry) could have wide spread consequence on the stability of this balance. There has been an overwhelming response from the scientific community around the world to study the effects of ocean acidification and to understand the mechanisms behind those responses. The acidity of the oceans may be doubling in the next five decades which means it is happening 100 times faster than any change previously seen globally in the past 300 million years [206]. This could mean that marine biota may not be biologically fully equipped to adjust to these new levels of ocean acidity and other related changes, and therefore would mostly fail to withstand this threat. A recent survey examining geological records for historical data in connection with ocean acidification indicated that the current fossil fuel induced spike in ocean acidity is faster than what  $\text{CaCO}_3$  compensation can sustain, and hence the effects of this will be more intense than has ever been experienced before.

Ocean acidification is happening at such a fast pace that it is posing a serious threat to marine biota and biodiversity. Hence, an increasing number of studies are employing high throughput methodologies to study the effects of ocean acidification on some key marine organisms. The photosynthetic coral reefs around the globe are one of the main producers in the marine habitats, among other producers such as seaweeds, algae and other plants. Their primary productivity in the ocean is recycled to  $\text{CO}_2$  in the ocean-carbon cycle by many non-photosynthetic marine organisms including archaea, fungi, bacteria, protists, flagellates and ciliates and up across the food chain. Although non-synthetic microorganisms are dependent on these corals for nutrients, they are only directly affected

by lack of nutrients and seawater pH (acidification) and not by CO<sub>2</sub>. Corals and some other species are at greatest risk of becoming extinct, similar to what has happened for several other species within the early 21st century [211]. Ocean acidification affects several marine calcifiers such as coccolithophorid planktons [212, 213], crustaceans, oysters [214], other bivalves, coralline algae [215], planktonic foraminifera [216, 217] and corals [215, 202, 218]. One study investigated the effects of ocean acidification between two coral species and crustose coralline algae (their symbiotic dinoflagellates) in an effort to understand how these three species relate to each other, and also looked at how ocean acidification affects these species and correlates with warming temperatures [215]. For this study, they altered aquarium CO<sub>2</sub> conditions to twice (slight), three time (moderate) and four times (high) as that of present day levels under warm and cooler temperatures. The authors believed that these exposure levels simulated predicted CO<sub>2</sub> levels which are possible in the near future. Their results indicated that high CO<sub>2</sub> exposure caused a bleaching effect on the coral structure and enhanced dissolution rates of corals. Also, high CO<sub>2</sub> levels was reported to result in complete loss of productivity, measured as hourly rates of photosynthesis minus respiration integrated over the day, in both corals and algae. Coralline algae are sensitive reef-building species and are a critical component of marine reef systems. Coralline algae help establish carbonate for reef structures, extend reef growth by growing together, and act as a substrate for settlement for many invertebrates. Therefore, as a result of ocean acidification, substantial reduction in growth and survival of these algae would definitely threaten reef building activities and survival of many corals, and could also diminish large coral reef habitats.

A separate study on crustose coralline algae investigating whether ocean acidification impacted the ability of the algae to induce coral larval transformation observed reduced settlement of coral larvae and reduced transformation at pH 7.7 and

below[218]. Another major finding from this study upon direct exposure of algae to lower pH levels was, the likelihood of altered biochemistry of the algae which makes it associate to newer microbial flora that is unable to establish carbonate building on corals, thereby impacting coral growth.

From all the phytoplankton species that have been recently examined, it was found that rate of photosynthesis reduced by up to 10% when doubling the present CO<sub>2</sub> concentration and examining their photosynthetic response to changed CO<sub>2</sub> conditions. However an important exception was found in the case of *Emiliania huxleyi*, a globally abundant calcifying photoplankton. It showed an increase in the rate of photosynthesis in response to increased CO<sub>2</sub>, suggesting that this increase in CO<sub>2</sub> could perhaps be beneficial for the growth or viability of the organism; but it also showed a decrease in rate of calcification in response increased CO<sub>2</sub>, a deleterious effect thus offsetting any benefit derived from increased photosynthesis.

Since CO<sub>2</sub> and temperature are factors that play a vital role in achieving efficiency in important mechanisms such as photorespiration, carbohydrate metabolism, enzyme systems, and calcification, they are thought to play a significant role in maximizing the effects of ocean acidification. Acting as combined stressors, ocean acidification and warming cause alterations in the cell size and dimethyl sulfide production of the photosynthetic plankton, *E. huxleyi* [212]. Results indicate that the phytoplanktons experienced a significant decrease in cell diameter upon exposure to elevated CO<sub>2</sub> and temperature, along with an increase in the production of dimethyl sulphide, a trace gas of marine origin which is the source for 90% of marine biogenic sulphur that affects cloud formation and climate.

Ocean acidification itself has been known to cause serious issues, but a more complicated situation arises when there are multiple stressors occurring at the same time, leading to a situation where both global and local stressors pose a grave threat. From a global perspective, when natural marine ecosystems and marine biota face a combination of stressors along with ocean acidification, their interrelated impacts could be more severe, and cause broader ecological imbalance. Recent studies have started to touch on this possibility and results have shown impairment of mechanisms involved in calcium carbonate production and dissolution [217] along with non-linear amplification of CO<sub>2</sub> effects [219] under the influence of multiple stressors. These combined effects make the situation more difficult than expected. For instance, phytoplanktonic diatoms were found to be more sensitive to nitrogen limitation than ocean acidification in terms of growth, cell size, pigmentation and energy yield [213]. However, in terms of respiration rate and electron transfer rate, they were more sensitive to ocean acidification. Therefore, the combined effects of these two stressors on diatom species appear to be non-linear but synergistically amplified. A recent study investigated what happens when coral reefs experience additional short term CO<sub>2</sub> inputs in addition to elevated long term mean CO<sub>2</sub> conditions arising from ocean acidification by increasing anthropogenic CO<sub>2</sub> absorption. The results showed a three –fold nonlinear amplification of pCO<sub>2</sub> signal in response to the combined severe CO<sub>2</sub> stress [219], however the biological consequences of this situation remain unclear and need further research.

Ocean acidification also affects other important species involved in calcification such as foraminifers (belonging to the class of amoebid protists, size ranging between 1mm and 40µm), zooxanthellae or symbiodiniums (photosynthetic unicellular algae that supply nutrients and energy to most corals), and photosymbionts (obligate to reef animals and their environments). On this note, Reymond *et al.* looked at employing two stressors,

namely eutrophication and ocean acidification, in an effort to study their effects on the respiration, growth, survival and physiology of *Marginopora rossi*. This species is one of the benthic foraminifers that produce about 80% of global foraminifera carbonate for reef production, act as symbiotic habitat for several species of algae, and carry a large pool of photosymbionts inside the cytoplasm that aid in reef calcification. Inhibition of growth of *M. rossi*, and destabilization of its relationship with photosymbionts, was seen in response to the combined effect of stresses from ocean acidity and eutrophication [217]. Chlorophyll-a was observed to become more abundant in the foraminifers due to the increased rate of photosynthesis, however, there was no new growth. When ocean pH drops to 7.6 as a result of ocean acidification, either alone or in combination with other stressors, calcification in *M. rossi* and similar species will significantly decline.

Chemoautotrophic endosymbionts have recently been found to play a vital role in host nourishment through carbon fixation. They also produce and restore energy through the energy-generating sulphide oxidation pathway, and employ both the tricarboxylic acid cycle and the Calvin cycle to fix CO<sub>2</sub> to produce organic carbon. Proteomic studies have indicated that 12% of the cytosolic proteome of the endosymbiont is constituted by four major sulfide oxidation proteins, namely adenylylsulfate reductase  $\alpha$  subunit, dissimilatory sulfite reductase  $\alpha$  subunit, pyruvate:ferredoxin oxidoreductase, and fumarate reductase [220]. These are mainly involved in energy metabolism reactions, thus highlighting the importance of the role played by these three enzymes in meeting the symbiont-host metabolic needs. It is also possible that the endosymbiont is well equipped to adjust enzyme production for energy metabolism needs in response to changes in the prevailing environmental conditions. Most proteins of this symbiont have been identified to be involved in electron transfer, glycolysis, TCA cycle, sulfide oxidation based energy metabolism, cell signaling, transport and other cell membrane associated functions. Thus,

these symbionts could face ocean acidification risks equivalent to major coralline organisms.

Sea grasses are the most abundant autotrophic marine plants and are a major component of the ocean reef and water environments. They photosynthesize in submerged photic zones and are embedded in sediment or mud bottoms in shallow and sheltered coastal waters. The seagrass beds serve as a source of shelter and food for several hundred marine species including epiphytes, micro- and macroalgae, mollusks, nematodes, sea urchins, crabs, green turtles, fish and dugongs, among others. Thus they are critical to the oceanic food chain. Seagrasses are already declining due to anthropogenic activities, eutrophication and ocean acidification. Sea grasses decline in photosynthetic rates and growth, when faced with enhanced CO<sub>2</sub> levels. Macroalgae, however, are likely to show an increase in photosynthesis and growth under similar conditions [221]. This blooming effect in macroalgae could be from utilizing the newly available excess nutrients in the form of HCO<sub>3</sub><sup>-</sup> to aid their growth, but nutrient rich conditions are known to be directly toxic to most seagrasses causing them to decay. Also, excessive blooms of macroalgae could weaken the transmission of sunlight reaching the seagrass bed, thus hindering photosynthetic activities necessary for seagrass survival.

Antarctic krills demonstrated increased feeding rate and excretion rate upon exposure to elevated CO<sub>2</sub> levels when compared to ambient CO<sub>2</sub> conditions [222]. They also showed 17% decrease in urea excretion under elevated CO<sub>2</sub> conditions, but the mechanism of this remained unclear. Up-regulation of enzymes, namely malate dehydrogenase and lactate dehydrogenase, were also witnessed consistently among krills exposed to elevated CO<sub>2</sub> treatment.

In another extensive study, research experiments were conducted for a 60 day period under projected CO<sub>2</sub> levels to induce ocean acidification effects on calcified structures of 18 benthic marine organisms. Projected CO<sub>2</sub> levels used were selected with regard to levels predicted by impending global climate change [223]. Here, selection of species was done across a broad taxonomic range including crustacea, cnidaria, echinoidea, rhodophyta, chlorophyta, gastropoda, bivalvia, and annelida with organisms, and thus included organisms producing aragonite, low-Mg calcite, and high-Mg calcite forms of CaCO<sub>3</sub>. The results showed that 10 of the 18 species that were studied exhibited reduced rates of net calcification and, in some cases, net dissolution under elevated pCO<sub>2</sub>. However, in seven species, net calcification was found to increase under the intermediate and/or highest levels of pCO<sub>2</sub>, and one species showed no response at all. The authors concluded that these varied responses may be due to their inherent differences amongst species in regulating their response to environmental changes.

An organisms response can be thought of as stemming from the need to: (1) protect the outer shell layer by an organic covering; (2) slow down dissolving of their shell or skeletal mineral being unable to withstand lower pH; or, (3) utilize excess nutrients in the form of inorganic carbon and HCO<sub>3</sub><sup>-</sup> as part of an increase in photosynthesis. Although specific mechanisms involved in bring out these responses still remain unconfirmed, their results suggested that the impact of elevated atmospheric pCO<sub>2</sub> on marine calcification would be more varied than previously thought [223].

### **1.7.1 Effects of ocean acidification and CO<sub>2</sub> fixation in oysters and other calcifying organisms, highlighting recent proteomics studies**

Most molluscs, including oysters, have shells made out of calcium carbonate (aragonite or calcite) that are vital body structures developed for their survival. As mentioned before, ocean acidification makes it difficult for oysters, shellfish, molluscs and corals to survive and maintain shells or other calcium based structures. At pH 7.6 and below, the calcium structures are known to suffer dissolution due to acidic modifications in seawaters. These organisms are known to flourish between pH 7.6-8 as has been recorded in recent years is a substantial change.

Several hatcheries have reported incidents of oyster mortalities due to such acidic seawater conditions. In the U.S.A., the oyster industry is worth an estimated \$80 million annually. Regions including the Chesapeake bay, the west coast, the U.S.A.-Mexican border, and the Pacific Northwest have already started to sustain losses evidencing the effects of these devastating changes. There have been reports of significant decrease in developmental successes and reproduction rates in oyster larvae, when levels of carbonate ions fall below aragonite saturation levels [224]. Also acidic seawaters have caused reproduction failures in several wild oysters in several beds along the Puget Sound and east coast of Vancouver Island [225].

In Australia, oyster farming is carried out throughout most of the coastal waterline extending into south-east Asia. Sydney rock oysters and pacific oysters are major species grown by oyster farmers, valued about \$100 million annually. New South Wales accounts for 40% of Australian oyster production followed by 37% from South Australia and the remaining 20% is grown in Tasmania. Exports account for only 3% of total oyster production, of which 80% is sold to Hong Kong, Japan and Singapore. Botany Bay and

port Jackson experienced oyster mortalities recently and mitigation efforts have begun through scientific monitoring efforts to monitor changes in oyster larvae beds. However, ocean acidification still proceeds rapidly. On a global scale if not for a dedicated mission to prevent carbon dumping, it could soon become unfeasible to protect every organism in the ocean that builds corals or shells.

Proteomics studies on understanding ocean acidification effects are only beginning to gain momentum. At the moment only a few studies have used proteomics but they have provided a good starting point to provide insight as to how and what changes occur inside the oysters under altered CO<sub>2</sub> conditions. Tomanek *et al.* investigated mantle tissues of *C. virginica* for proteomic changes caused by exposure under elevated CO<sub>2</sub> levels (approximately 357 Pa pCO<sub>2</sub>) for 2 weeks. Mantle tissues are known to secrete calcium carbonate at the epidermis in many molluscs in an effort to build shells. Not only does the mantle offer a protective shell for the organism, it also aids in respiration and locomotion. Results from 2D gel electrophoresis coupled with mass spectrometry experiments showed 54 differentially expressed proteins, of which they were able to identify only 17 proteins [214]. Cytoskeletal proteins (many forms of actins) and proteins involved in oxidative stress (superoxide dismutase, peroxiredoxins) were the two main groups of proteins that were identified. The authors concluded that elevated CO<sub>2</sub> conditions caused extreme oxidative stress to cytoskeletons due to a possible increase in reactive oxygen species.

Hard shelled clams showed lower metabolic rates and higher antioxidant capacity than oysters in a study that exposed them to an increase in temperature (27°C) and elevated 800ppm CO<sub>2</sub> levels in discrete and combined conditions. Combined exposure from elevated temperature and CO<sub>2</sub> pushed clams to achieve very high metabolic rates that were not seen otherwise [226]. Although it has become clear that reduced growth and

survival, and poor juvenile development, are expected responses under combined conditions of thermal and high CO<sub>2</sub> stressors, the cellular mechanisms are only starting to become apparent.

The impact of several carbonate-system perturbations on the growth of Pacific oysters were tested on *C. gigas* and, interestingly, the oysters did not show any signs of stress in terms of reduced growth rate or developmental abnormalities under direct stress from low pH, alkalinity or aragonite saturation. However, *C. gigas* showed signs of stress when the availability of carbonate ions was reduced. It is plausible that increased concentration of free carbonate ions play a greater role in stressing the organisms (oysters) than pH or aragonite concentration or alkalinity. Hence, mechanisms used to regulate calcification or deal with CO<sub>2</sub> stress may in fact revolve more around dealing with availability of carbonate ions.

Biological variation among oyster species was once again apparent in a study comparing responses and sensitivities of two oyster species when exposed to different CO<sub>2</sub> levels. *C. virginica*, which lives predominantly in coastal habitats, was more sensitive to 800ppm high CO<sub>2</sub> exposures (projected CO<sub>2</sub> concentration for the end of the 21<sup>st</sup> century), and showed 16% decrease in shell size and 42% reduction in Ca content compared to controls [227]. On the other hand, although treatment conditions remained the same between the two oyster species, *Crassostrea ariakensis*, which lives predominantly in estuarine waters, was not stressed by the high CO<sub>2</sub> conditions and there were no significant changes in growth or calcification compared to controls [227]. From these findings it is apparent that differences in responses among oyster species are a fact, irrespective of the type of stressors. This also hints that species-specificity in oysters could be driven by the natural choice of habitat for each species. Here *C. virginica* was from

coastal seawaters whereas *C. ariakensis* was from natural estuarine bodies. Therefore, while assaying oysters and using them for monitoring environmental pollution, it is very important to factor in what natural habitat suits the species and what habitats are being tested. Choice of test species for any study is equally important. Not considering the species sensitivity or the habitats suited for the test organism when conducting environment monitoring could lead to incorrect inferences, and may not actually reflect real situations, as demonstrated in this study.

Analysis of protein pattern changes in oyster larvae that were exposed to high CO<sub>2</sub> conditions revealed 18% decrease in total proteins and identified some key signature proteins compared to those exposed to ambient CO<sub>2</sub> conditions [228]. Calcification processes may have been hindered between days 4-6 of exposure, as there was significant decrease in shell size during this period. Proteins that changed in expression include up-regulation of fascilin, annexin, nucleotide diphosphate kinase and vacuolar H<sup>+</sup>ATPase, and down-regulation of cytochrome C oxidase, troponin, tubulins and calmodulins. These protein expression changes were related to physiological changes such as reduced growth and metabolic rate, decreased calcification, and poor developmental success, all of which are responses previously seen in most calcifying species exposed to high CO<sub>2</sub>.

Barnacle species are sessile suspension feeders that permanently attach their bodies to hard surfaces such as rocks, and most commonly they grow their calcite shells directly onto the hard substrate. Barnacles are vulnerable to ocean acidification and this was evident when larvae of barnacle species showed changes in expression levels of proteins in response to elevated CO<sub>2</sub> conditions. From these findings, significant differential proteins that changed at least 2 fold compared to controls include down-regulation of heat

shock protein 83 and NMD3 family protein, and up-regulation of two glycoproteins, citrate synthase and transketolase [229].

There is still considerable uncertainty concerning the rates of change at which these threats are approaching, but it is clear that these changes will definitely be manifest in important and tangible ways. As the stability of a coral reef structure gets disturbed, the rates of dissolution would be exponentially proportional to rate of acidification. This will have a direct impact on the aquatic food web and many of these marine species face extinction if reefs disappear or are greatly diminished. As a result of this, about 500 million people face an uncertain livelihood as they are directly dependent on coral reefs for their daily food and income.

Australia will be one of the worst affected if it were to lose the Great Barrier Reef due to ocean acidification because it generates over 6.5 billion dollars annually in tourism revenue, and 63,000 jobs from business pertaining directly to these reefs. There will be more dramatic ecological changes in store for Australia apart from damages to coral reefs. Efforts to stabilize atmospheric CO<sub>2</sub> at 450 ppm will manage to save only 8% of existing tropical and subtropical coral reefs in waters of the right pH level needed to support growth. Within decades, ocean acidification will also start to have major impacts on temperate and polar water ecosystems. In fact, colder water absorbs higher levels of CO<sub>2</sub> than warmer water. Our polar seas are already so acidic that they are starting to dissolve shells of some marine organisms. If left unattended, ocean acidification could lead to global eradication of our coral reefs by the next three decades.

## **1.8 Concluding remarks**

The pursuit of biomarkers for environmental pollution, including heavy metal pollution and ocean acidification, includes efforts to identify single proteins that are consistently up- or down-regulated after toxicant exposure, and is also aimed at discerning a proteomic signature, or pattern of proteins, changing in response to each stressor. These signatures together would certainly give us more information specific to the biological status of the organism. One strategy certainly does not exclude the other and frequently both are used simultaneously. The identification of these diagnostic protein expression signatures may overcome the lack of genome information, characteristic of these “non-model but environmentally relevant” species such as oysters or amphipods. This will enable the detection and monitoring of pollutants such as heavy metals or anthropogenic CO<sub>2</sub>, in both experimental and field settings, and will hopefully be an important factor in mitigation efforts to protect and maintain these vital oceanic ecosystems.



---

## Chapter 2

## Materials and Methods

---

This chapter describes the materials and methods that were common to more than one proteomics project as part of this Ph.D. research thesis. These mainly include those associated with label free proteomic analysis such protein extractions, trypsin digestion, peptide analysis by nanoLC-MS/MS, protein ontology classification and statistical analysis.

### 2.1 Protein extraction

#### 2.1.1 Protein extraction from oyster hemolymph using TCA-acetone precipitation

Aliquots of 400  $\mu\text{L}$  of haemolymph per oyster described in Chapter 3, were used for protein precipitation in a 1:3 v/v ratio with 10% trichloroacetic acid (TCA) and 0.07%  $\beta$ -mercaptoethanol in cold acetone. Proteins were precipitated overnight at  $-20^{\circ}\text{C}$ . The precipitate was centrifuged at  $12,000 \times g$  and the pellet was retained. In order to remove any traces of TCA, protein pellets were resolubilized in ice cold acetone followed by centrifugation at  $12,000 \times g$  for 15 min. This process was repeated three times. The final protein pellets were air dried and then solubilized in 50  $\mu\text{L}$  of 3 M urea in 100 mM tris HCl (pH 8.5). Protein concentrations were then estimated by the Bradford assay (Sigma Aldrich, U.S.A.).

### **2.1.2 Protein extraction from tissues homogenates of amphipods or oyster gill tissues using Tri-reagent**

Proteins from tissue homogenates of amphipods described in Chapter 5, or oyster gills in Chapter 6, were extracted using Tri reagent (Sigma Aldrich, USA). To the tissue homogenates, 100 $\mu$ L of bromochloropropane was added (for every 1mL of Tri reagent used), mixed vigorously for 30 sec, incubated at room temperature for 15 min and centrifuged at 12,000  $\times g$  for 15 min at 4°C. Upon phase separation, the clear top phase containing RNA was discarded. To the remaining solution comprising of two phases containing DNA and protein, 300 $\mu$ L of ethanol (100% analytical grade) was added, mixed by inversion, and allowed to stand at room temperature for 3 min, followed by centrifugation at 2000  $\times g$  for 5 min. The top phase containing DNA was removed and to the remaining phase, 4 volumes of ice cold 100% acetone was added, mixed vigorously, allowed to stand at 20°C for 30 min and centrifuged at 12,000  $\times g$  for 10 min. Supernatants were discarded and the protein was obtained in the form of a pellet. The protein pellets were washed three times to remove traces of Tri reagent by resuspending the pellet in 2 mL of 0.3M guanidine hydrochloride in 95% ethanol for 20 min, centrifuging at 7,500  $\times g$  for 10 min at 4°C and discarding the supernatant. A final wash was performed by resuspending the protein pellets in 100% ethanol for 20 min then centrifuging at 7,500  $\times g$  for 30 min at 4°C. Protein pellets were air dried and protein concentrations were quantitated using Bradford assay before fractionation by two dimensional gel electrophoresis (2DE) or sodium dodecyl sulphate - polyacrylamide gel electrophoresis (SDS-PAGE).

## 2.2 Trypsin digestion

### 2.2.1 In-gel trypsin digestion

Each gel lane from the SDS-PAGE gel for every sample was cut into 16 equal sized fractions using a scalpel, and each fraction was further diced and transferred into a well of a 96-well microtitre plate. Similarly, each gel spot picked from a 2DE gel was diced into 4-6 pieces and transferred into a well of a 96-well microtitre plate. The gel pieces were destained by briefly washing with 100 mM  $\text{NH}_4\text{HCO}_3$ , then three times with 200  $\mu\text{L}$  of 50% v/v ACN/50% v/v 100 mM  $\text{NH}_4\text{HCO}_3$  for 10 min, and finally dehydrated with 100% ACN. The samples were air dried and reduced with 50  $\mu\text{L}$  of 10 mM dithiothreitol (DTT) in 50 mM  $\text{NH}_4\text{HCO}_3$  at 37°C for 1h before alkylating in the dark with 50 $\mu\text{L}$  of 50 mM iodoacetamide in 50mM  $\text{NH}_4\text{HCO}_3$  at room temperature for 1 h. They were washed with 100 mM  $\text{NH}_4\text{HCO}_3$ , then with 50% v/v ACN/50 % v/v 100mM  $\text{NH}_4\text{HCO}_3$  for 10 min, dehydrated with 100% ACN and air dried. Finally, dried SDS-PAGE gel bands were reconstituted with 25  $\mu\text{L}$  of trypsin (12.5ng/ $\mu\text{L}$  in 50mM  $\text{NH}_4\text{HCO}_3$ ) for 30 min at 4°C and then digested overnight at 37°C, whereas for the 2DE gel spot samples 10  $\mu\text{L}$  of 5ng/ $\mu\text{L}$  trypsin was used. Peptides corresponding to 16 fractions of SDS-PAGE gels fractions for each biological replicate of the four oyster metal exposure samples were recovered by three extractions with 30 $\mu\text{L}$  of 50% v/v ACN/2% v/v formic acid to each fraction, dried using a vacuum centrifuge and reconstituted in 10  $\mu\text{L}$  of 2% formic acid for nanoLC-MS/MS analysis. Peptides obtained from 2DE spots were extracted in the same manner, then desalted and concentrated using C18 zip tips (Varian) and eluted using either the matrix solution for MALDI-TOF/TOF mass spectrometry analysis; or 90% v/v ACN/0.1% v/v formic acid, dried using a vacuum centrifuge and reconstituted in 10  $\mu\text{L}$  of 2% formic acid for nanoLC-MS/MS analysis.

### 2.2.2 In-solution trypsin digestion

Twelve aliquots of protein extracts (75 µg), representing biological triplicates for controls plus treatments, were used for in-solution digestion prior to gas phase fractionation (GPF). In the oyster heavy metal stress study twelve aliquots represent biological triplicates from four metal treatment groups, namely PbCl<sub>2</sub>, ZnCl<sub>2</sub>, CuCl<sub>2</sub> and controls. In the oyster CO<sub>2</sub> seawater acidification project, twelve aliquots of protein samples represent biological triplicates of QXR and WT oysters that were either controls or CO<sub>2</sub> treated. Protein aliquots in 3M urea were briefly washed with 100 mM NH<sub>4</sub>HCO<sub>3</sub>, reduced with 10 µL of 55 mM DTT/NH<sub>4</sub>HCO<sub>3</sub> (100 mM) at 37°C for 1 h before alkylating in the dark with 10 µL of 50 mM iodoacetamide in NH<sub>4</sub>HCO<sub>3</sub> (100 mM) at room temperature for 1 h. They were then diluted with 100 mM NH<sub>4</sub>HCO<sub>3</sub> to reduce the urea concentration to 1 M and digested with trypsin at the ratio of 1:20, trypsin to protein, at 37°C for 16 h. Peptides were desalted using C18 Omix tips (Varian), and redissolved in 80 µL 2% v/v formic acid.

## 2.3 Gas Phase Fractionation

Aliquots of solution digested peptides obtained for each biological replicate oyster in (i) heavy metal stress study and (ii) oyster CO<sub>2</sub> acidification study, were analyzed by nano LC-MS/MS using a LTQ-XL linear ion trap mass spectrometer (Thermo, San Jose, CA); the method previously developed by Brexi *et al.* [230] was adopted. Each aliquot containing 80 µL of solution digested peptides was divided into eight equal volume amounts for eight successive injections into the nanoLC system for a gas phase fractionation (GPF) experiment. Survey spectra were scanned in m/z ranges of 400–510 amu, 500 – 610 amu , 600 – 710 amu, 700 – 810 amu, 800- 910 amu, 900- 1010amu, 1000 -1310amu, 1300-2000amu.

## 2.4 nanoLC-MS/MS mass spectrometry

Reversed-phase columns were packed in-house to approximately 7cm (100 $\mu$ m I.D.) using 100Å, 5 $\mu$ m Zorbax C18 resin (Agilent Technologies, CA, USA) in a fused silica capillary with an integrated electrospray tip. An electrospray voltage of 1.8kV was applied at a liquid junction upstream of the C18 column. Samples were injected onto the column using a Surveyor autosampler (Thermo), which was followed by an initial wash step with buffer A (5%v/v ACN, 0.1%v/v formic acid) for 10min at 1  $\mu$ L/min. Peptides were eluted from the column with 0–50% buffer B (95% v/v ACN, 0.1% v/v formic acid) over 30 min at 500 nL/min followed by 50–95 % buffer B over 5 min at 500 nL/min and a further 5 min with 95 % buffer B prior to column re-equilibration. The column eluate was directed into a nanospray ionization source of the mass spectrometer. Automated peak recognition, dynamic exclusion and MS/MS of the top six most intense precursor ions at 35% normalization collision-induced dissociation energy were performed using Xcalibur software (Version 2.0, Thermo). Survey scans of spectra were recorded in full mass range of m/z 400-1500 for peptides extracted from in-gel digestion, or in batches of 8 m/z ranges in case of in-solution digested protein samples used in GPF experiments as mentioned in section 2.3.

## 2.5 Data processing and portioning

Tandem MS spectrum files obtained for samples subjected to nanoLC-MS/MS were converted from .RAW format to .mZXML using ReAdW.exe (freely available to download from <http://sourceforge.net/projects/sashimi/files/ReAdW%20%28Xcalibur%20converter%29/>) prior to database search. The sets of .mZXML data files for a given sample (batch of 8

from GPF experiments or batch of 16 from SDS-PAGE experiments) were then placed into one directory and peptide-to-spectrum matching was performed using the Global Proteome Machine (GPM) software incorporating the X!Tandem algorithm [231]. Output excel files from GPM were exported to comma-separated value format, which was then input into the Scrappy program for statistical analysis [232]. The Scrappy program is series of R modules used for statistical analysis which was developed in our laboratory and made freely available for download from <http://www.proteomecommons.org>. Using the Scrappy program, Normalized Spectral Abundance Factors (NSAFs) for each protein were calculated with the inclusion of an additional spectral fraction of 0.5 to all counts to compensate for null values [233]. The NSAF for a protein was calculated from the number of spectral counts (SpC, the total number of MS/MS spectra) identifying the protein, divided by the length of the protein (L), divided by the sum of all SpC/L for a total of N proteins in the experiment [233].

Student's t-tests and a one way ANOVA were performed using Log NSAF values for each metal stress dataset against controls, implemented in the Scrappy package, to identify and categorize proteins with statistically significant differential abundance patterns [234, 232]. The Scrappy software package, which was developed in our laboratory, includes an adjusted p-value which uses a Bonferroni correction to adjust for multiple hypothesis testing, thus minimizing type I errors. Filtering of protein and peptide identification data were based on (i) a protein should have a minimum of 5 peptides among the three replicates (ii) the protein hit should be identified in all 3 replicates of the corresponding treatment (iii) the overall protein FDR was less than 1% and peptide FDR was less than 0.1 % in each of the final lists of reproducible proteins for each treatment. This filtering approach has been shown to be statistically valid in numerous studies published by our laboratory [38, 11, 234, 232, 235]. Proteins with p-values of less than

0.05 were selected as statistically significant and those found to be significantly different in abundance were further analyzed in order to identify changes in expression patterns. Up-regulation or down-regulation of a protein was determined based on the statistical significance of NSAF values when compared to controls. All proteins reproducibly expressed in any one of the treatments/exposures were partitioned into groups based on their presence or absence and protein lists were generated for each combination of groups.

Note that we use the terms ‘up-regulated’ and ‘down-regulated’ throughout this thesis to indicate changes in protein accumulation between two or more samples. While we may not have any formal evidence of protein regulation from the experiments described, it is a much easier and more intuitive terminology to use than any of the alternatives we considered.

## **2.6 Protein ontology classification**

In order to identify the biological processes associated with a particular protein, the protein ontology information was extracted from the UniProt database (<http://www.UniProt.org>) and KEGG (<http://www.genome.jp/kegg/>). Accession numbers were extracted using Refseq IDs from NCBI. These were then matched to Uni-Prot IDs to extract the corresponding gene ontology information from the UniProt database. This information was further supplemented with general biochemical pathway information from the KEGG database using reference KEGG identifiers. Proteins were then classified based on their biological processes and protein abundance.

## **2.7 Analysis of proteins expressed at all exposure conditions**

Proteins expressed at all metal stress or hypercapnia conditions in each section were analyzed by a one-way analysis of variance (ANOVA) of the log NSAF data. The natural log NSAF data of all samples were examined for normal distribution of data for each sample, by generating the overlapped kernel density plots for all samples. The ANOVA was performed to identify proteins that showed different abundance patterns between the different exposure conditions. For this, the Scrappy software which comprised the standard R implementation for linear models and ANOVA was used [232].

## **2.8 Analysis of biological processes or metabolic pathways**

The change of abundance of proteins or enzymes involved in selected metabolic pathways or processes were examined to determine the effect of metal stress or hypercapnia on those metabolic pathways or processes, which included cytoskeletal and protein polymerization, translation, protein metabolic process, carbohydrate metabolism, glycolysis, TCA cycle, energy metabolism, and lipid biosynthesis and breakdown.

## **2.9 Identification of unknown proteins**

Proteins which did not have any gene ontology annotation were further investigated. They were searched within NCBI, and those identified as hypothetical proteins that did not have a known function assigned were subjected to BLAST (Basic Local Alignment Search Tool [236]) search against the NCBI and SwissProt non redundant databases. If the results of the search did not match with a known protein with at least 80% identity, the protein was considered to be an unknown protein.

---

## **Chapter 3**

# **Quantitative proteomics of heavy metal stress responses in Sydney Rock oysters: before the release of the genome sequence**

---

### **3.1 Introduction**

In this chapter, we used non-2DE shotgun proteomics to elucidate the proteomic profiles of oysters exposed to heavy metals, in an effort to draw a broader picture of the dynamic changes caused by heavy metal stress. Shotgun proteomics were performed using two different approaches, SDS-PAGE gel slice fractionation of proteins and gas phase fractionation (GPF) of peptides. As this research was undertaken prior to the release of the Pacific Oyster genome sequence in 2012, we identified proteins using a composite Bivalvia sequence database that we assembled. For quantitative analysis, we devised an unbiased quantitation strategy suitable for proteomics studies for organisms lacking information from completely sequenced genomes. Our data revealed a panel of differentially expressed proteins that warrant further evaluation as molecular biomarkers of heavy metal stress responses in Sydney rock oysters.

## **3.2 Materials and Methods**

### **3.2.1 Oysters and heavy metal exposure**

Sydney rock oysters aged between 18 to 24 months were purchased from Aquaculture Enterprises (Eden, NSW), and were from the same tray-reared hatchery spat. Seawater used was pumped directly from Port Jackson, Sydney. Seawater samples were tested for a suite of metals, PCBs and PAHs at the start of the study. Following an initial 10 day period of acclimation to aquarium, oysters were exposed to  $\text{PbCl}_2$ ,  $\text{ZnCl}_2$  and  $\text{CuCl}_2$  (all at  $100\mu\text{g/L}$ ) for 96 h in 30L aquarium at Sydney Institute of Marine Sciences (Chowder Bay, Australia). Each metal exposure comprised 3 aquariums per metal with 10 oysters per aquarium. An additional set of 3 aquariums (10 oysters per aquarium) were used as controls with no added metals. Water temperature and salinity were tested daily. Oysters were fed every four days with M-1 bivalve feed (Aquasonic, Wauchope, NSW) and complete water changes were performed daily with the same concentrations of heavy metals. After 96 h metal exposure period, oysters were removed from aquarium, shucked, and approximately 0.5mL of exuding haemolymph per oyster was harvested from the pericardial cavity. Haemolymph was snap frozen and stored at  $-80^\circ\text{C}$  for further use. For ease of reference, these 4 metal exposure treatments are referred to in the text hereafter as Pb, Cu, Zn and controls.

All of the protein identification experiments described below were conducted with biological triplicates for each treatment (metals and controls), where each oyster was treated as one biological replicate. In spite of limited sample availability, use of biological triplicates in this fashion allowed us to not only perform statistical analysis on protein quantitation data in all datasets, but also to account for biological variation.

### **3.2.2 Protein fractionation by SDS-PAGE, in gel digestion and nano LC-MS/MS**

Twelve aliquots of protein extracts (75 µg) representing biological triplicates for controls plus three stress treatments (PbCl<sub>2</sub>, ZnCl<sub>2</sub>, CuCl<sub>2</sub> at 100µg/L), were fractionated by SDS-PAGE using Bio-Rad 10% Tris-HCl precast gels. Gels were electrophoresed at 70V for 5 min and 150V for 60 min, and then fixed for 1 h before staining with colloidal coomassie brilliant blue G-250 (Bio-Rad). After destaining, fractions from each gel lane were digested with trypsin as described in Chapter 2, section 2.2. Peptide digests were extracted and solubilized into 10 µL of 2% v/v formic acid. They were then subjected to mass spectrometric analysis using a nanoLC-MS/MS protocol as described in Chapter 2 section 2.4.

### **3.2.3 Database searching for peptide identification**

A customized Bivalvia database (14,002 proteins, Jan 2010) was constructed in-house from protein sequences of all organisms in the family Bivalvia available from the National Center for Biotechnology Information (NCBI). This composite database consisted of protein sequences in FASTA format corresponding to the Bivalvia class of marine and freshwater molluscs including mussels, oysters, clams, scallops, among others, that were submitted to NCBI and other public repositories including Swissprot, Protein Data Bank, and Protein Information Resource databases as of Jan 2010. As a first step to reduce redundancy, duplicate entries of proteins and proteins with different GI numbers but identical sequences across different species were removed upon retaining one representative for each protein, preferably that of an oyster. Raw files of nanoLC-MS/MS data were converted to .mzXML format prior to database search against this Bivalvia database. Searching was performed using the X!Tandem algorithm running under the Global Proteome Machine (GPM) software (version 2.1.1) [231]. Searches were processed

sequentially in sets of 8 GPF fractions per replicate or 16 gel based fractions per replicate and a merged non-redundant output file was generated for each set. Parent ion mass tolerance was set at 2 Da and fragment ion mass tolerance was set at 0.4 Da. Carbamidomethylation of cysteine was considered as a complete modification and oxidation of methionine was considered as a possible modification. Reverse database searching was used for estimating false discovery rates (FDR) at both peptide and protein levels. Output files were generated using peptide log (e) values less than -2 for GPF datasets and -3 for SDS-PAGE datasets.

### **3.2.4 Quantitation of identified proteins**

MS/MS data were searched against the composite Bivalvia database due to the lack of a complete genome sequence for oysters or any other closely related species. This resulted in a number of difficulties. Searching against the Bivalvia database often resulted in a subset of protein identifications that contained peptide matches to the same protein in a number of related bivalve species. This led to two main problems. First, multiple entries were present for the same protein from different species, each with a unique peptide(s) of its own. Second, quantitation of peptides was biased due to the presence of shared peptide sequences among different species for a single protein. Hence, we developed a quantitation strategy based on grouping multiple entries of a protein. We counted all the unique peptides from each species for a protein and considered one occurrence only for each shared peptide within the protein subset. Each group of identifiers for a protein was then allocated a single protein identifier based on the presence of the highest number of unique peptides.

All 24 lists of identified proteins, from both fractionation approaches for control plus the three stress treatments in triplicate, were subjected to strict filtering in order to create a final list of proteins for further analysis.

The first stage of filtering was based on 3 criteria. These 3 criteria were; (i) each peptide for a protein had to pass the threshold of peptide  $\log(e) < -2$  for GPF datasets and peptide  $\log(e) < -3$  for SDS-PAGE datasets, (ii) protein hits comprising entries from multiple species of bivalves were grouped under the nominated protein identifier (iii) the total peptide count of the corresponding protein hit having the highest count of unique peptides were summed with the respective unique peptide counts of all other entries for that particular protein subset. Thus, multiple entries of the same protein were manually removed by performing this modified quantification approach in the same manner for all protein lists in both datasets. After the first stage of filtering the resulting 24 lists (2 approaches x 3 replicates x 4 treatments) were further filtered using the following methodology.

The second stage of filtering included 2 criteria and a protein was retained only if it agreed with both criteria for at least one of the four treatments. They were, (i) it should have a minimum of 5 peptides among the three replicates (ii) the protein hit should be identified in all 3 replicates of the corresponding treatment in at least one of the two approaches. Peptide and protein FDRs were calculated after this filtering for each replicate across all treatments. Peptide FDR was calculated as: (twice the total number of peptides representing reversed protein hits in a list divided by the total number of peptides representing all proteins in that list)  $\times 100$  [237]. Protein FDR was calculated as the: (number of reversed proteins identified divided by the total number of proteins identified)  $\times 100$  [36]. Using the filtering parameters described, the overall protein FDR was less than

1% and peptide FDR was less than 0.1 % in each of the final lists of reproducible proteins for all four treatments.

Using the Scrappy program detailed in Chapter 2 section 2.5, protein identification data were partitioned as described previously [232]. NSAF values for all lists of proteins corresponding to each treatment and controls were generated and lists were further subjected to statistical analysis by (i) two sample comparisons using a students t-test, and (ii) one way ANOVA analysis of proteins found among all treatments. Differentially expressed proteins in response to stress for each of the three heavy metals were identified and analyzed for biological significance. Following this, six groups of proteins were selected for further analysis, including proteins unique to each of the three metal exposures; proteins expressed in all three metal exposures but not the control group; proteins expressed under all four exposure conditions; and proteins exclusive to control condition but absent in all 3 metal exposures. These groups were also investigated and characterized based on protein ontology information as described in Chapter 2 section 2.6.

### **3.3 Results**

#### **3.3.1 Summary of protein identifications using different approaches**

A numerical summary of the number of proteins reproducibly identified in oysters exposed to four different metal treatments (3 metal exposures plus controls) and two technical approaches (GPF and SDS-PAGE) is shown in Table 3.1 The individual replicate lists of proteins from the GPF approach for each metal treatment initially had an average of 367 proteins and 2766 peptides and also indicated high reproducibility of peptide counts with and among treatments; similarly, the protein lists from the SDS-PAGE approach showed an average of 695 proteins and 13189 peptides with high reproducibility between replicates. However, their protein FDR was high and this warranted further

filtering of the protein lists up to peptide  $\log(e)$  -3 at which the protein and peptide FDR values were less than 1% and peptide 0.3% respectively. Filtering with such high peptide thresholds is unusual for other experiments or species routinely investigated in many proteomics studies, which reaffirms one aspect of the degree of complexity of the oyster proteome. Previous genomic studies have shown that oyster genomic sequence contains an unusually high number of single nucleotide polymorphisms and repetitive sequences.

**Table 3.1 Protein identification summary of Sydney rock oysters in the context of heavy metal treatments (Pb, Cu, Zn and control), using SDS-PAGE and GPF approaches.**

Technical approach	Non-redundant count of proteins	No. reproducible proteins identified after each treatment				Differentially expressed proteins relative to control
		Pb	Cu	Zn	Control	
SDS-PAGE	84	49	43	52	38	49
GPF	49	27	28	27	25	29
Combined non-redundant count of proteins identified from both approaches: 93						
Combined non-redundant count of differential proteins from both approaches: 56						

A final non-redundant list of 84 proteins was identified from all four treatments using the SDS-PAGE approach, and 49 proteins were identified using GPF. Using the SDS-PAGE approach we reproducibly identified 49 proteins in Pb, 43 in Cu, 52 in Zn and 38 in controls. Using the GPF approach, we reproducibly identified 27 proteins in Pb, 28 in Cu, 27 in Zn and 25 in controls.

Combining the SDS-PAGE and GPF data, 93 unique reproducible proteins were identified in total. Of the 93 unique proteins identified, 44 proteins were exclusive to the SDS-PAGE dataset, whilst 9 proteins were identified only in the GPF dataset. There were 40 proteins that were common to both approaches. Figure 3.1 shows the distribution of the number of proteins identified from each treatment and those proteins common between both approaches. While these numbers may seem low compared to results of shotgun proteomics experiments in other species, they are a direct result of the relatively simple protein composition of oyster haemolymph, the lack of complete genome sequence information for oysters, and the biological variability previously observed between individual oysters [238].

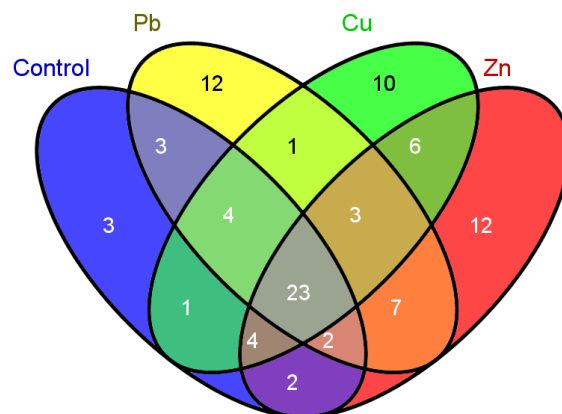


**Figure 3.1** Diagrammatic representation of protein identification data from both SDS-PAGE and GPF approaches for Sydney rock oysters. Numbers represent the total number of non-redundant proteins present in each heavy category.

Although the SDS-PAGE approach was more efficient in protein identification and quantitation, we found that using a combination of both SDS-PAGE and GPF produced significantly more useful data in terms of protein and peptide identifications than either

approach by itself. Supplementary information Tables S1 and S2 summarize proteins obtained from SDS-PAGE and GPF approaches respectively with peptide identification information including peptide sequences for all proteins in each replicate at four different metal treatments. Quantitation information in terms of NSAF values for 84 reproducible proteins identified by SDS-PAGE approach and 49 by GPF is shown in Supplementary information Tables S3.

### 3.3.2 Quantitative analysis of differentially expressed proteins

Considering the set of 93 reproducibly identified proteins, we found a total of 56 non-redundant proteins that were differentially expressed at statistically significant levels relative to controls after oysters were exposed to heavy metal stress, as shown in Figure 3.2. Of these 56 differentially expressed proteins, 9 were detected by both SDS-PAGE and GPF approaches whilst 34 were found exclusively in the SDS-PAGE dataset and 13 were exclusive to the GPF dataset.

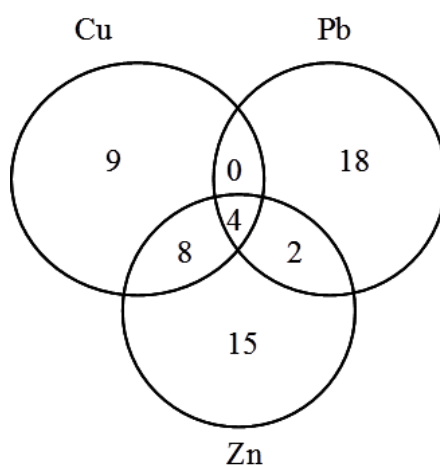


**Figure 3.2** Distribution of differentially expressed proteins, identified in oysters in response to heavy metal exposures. Numbers represent the total number of non-redundant differentially expressed proteins in response to either or all of the 3 metals. Differentially expressed proteins in response to each metal would be either up or down regulated relative to control.

All 56 proteins that changed significantly in their expression profiles in response to heavy metal stress were distinguishable from unchanged proteins using Log NSAF plots of protein abundance in each metal stress experiment relative to controls (Figure 3.3a and b).

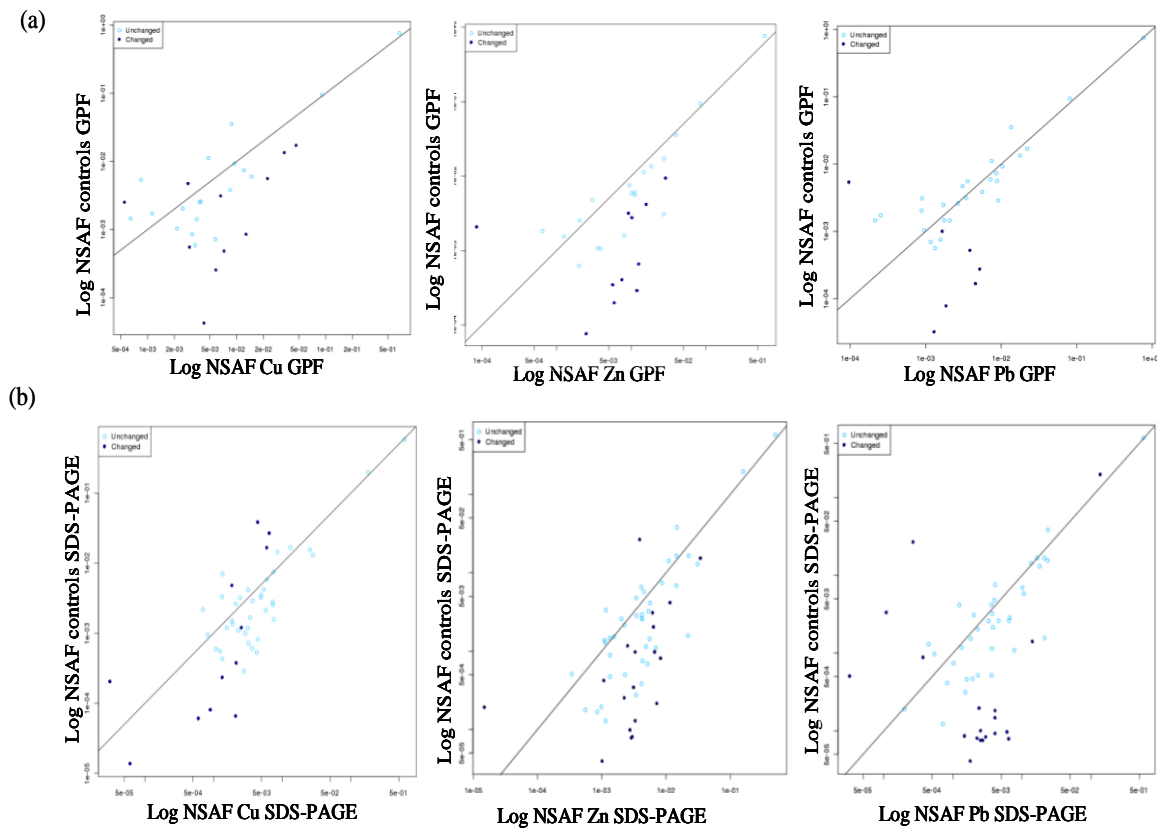


**Figure 3.3** Log NSAF plots of differential and unchanged proteins in the 3 metal treatments relative to controls (a) GPF datasets (b) SDS-PAGE datasets. Proteins with significant differential expression are shown as dark blue spots. Proteins with expression levels that did not differ significantly between metal exposures and controls are shown as lighter spots. Up and down regulated proteins are shown as darker spots below and above the diagonal respectively.

These plots show differentially expressed proteins as darker spots with those above the diagonal up-regulated in metal treatments relative to control, whilst those below the diagonal were down regulated. These plots provide an informative visual display of both the total number of significantly differentially expressed proteins and the overall trend of their differential expression.

A complete list of the 56 significantly differentially expressed proteins with quantitation information is included in Table 3.2. Appendix B1 gives a detailed account of protein identification and peptide sequence information for all of the 56 differentially expressed proteins found in this study, while a non-redundant list of all proteins identified as part of the protein profile of the oyster hemolymph from this study using Bivalvia database is given in Appendix B2.

Differential expression of 42 proteins was associated with single metals (15 for Zn, 9 for Cu and 18 for Pb), whereas 4 differential proteins were associated with all 3 metals. Another group of 8 proteins showed differential expression in response to both Cu and Zn but not Pb, whilst two proteins were differentially expressed in response to Pb and Zn but not Cu. According to Figure 3.4, significant responses to metal stress were shown by proteins involved in cytoskeletal and protein polymerization processes, translation and carbohydrate metabolism. From Figure 3.4, it is clear that 21 out of the 56 differentially expressed proteins were ribosomal proteins, which constitutes a striking 37.5%. All of the 21 ribosomal proteins followed the same trend in their differential protein expression in that they were all up regulated relative to controls.

**Table 3.2 Differentially expressed proteins after heavy metal stress in Sydney rock oysters, relative to non-exposed controls based on their Log NSAF ratios.**

No.	Identifier	Protein name	UniProt ID	Biological Process	Mr kDa	Fold change (a)(b)
<b>Elements in response to Pb stress only</b>						
1.	gi 78172537	NADH dehydrogenase subunit I	Q09X44	oxidative phosphorylation	33.6	↑44
2.	gi 27363140	ribosomal protein L12	Q8I9M1	translation	13.5	↑10.1
3.	gi 40642996	ribosomal protein L24	Q70MN8	translation	18.1	↑36
4.	gi 40642980	ribosomal protein S10	Q70MT4	translation	18.1	↑33.3
5.	gi 40642986	ribosomal protein S11	Q70MP3	translation	17.3	↑81.6
6.	gi 146336951	ribosomal protein S13	A5HIF0	translation	17	↑27.9
7.	gi 27363138	ribosomal protein S14	Q8I9M2	translation	7.5	↑22.5
8.	gi 82408382	ribosomal protein S15	Q2XSC2	translation	13.6	↑25.2
9.	gi 40643042	ribosomal protein S17	Q70ML5	translation	14.1	↑62.8
10.	gi 40643006	ribosomal protein S19	Q70MN3	translation	16.4	↑36
11.	gi 229891605	ribosomal protein S2	A3RLT6	translation	33.5	↑1.7
12.	gi 61619986	ribosomal protein S23	A1KYZ5	translation	15.9	↑17.2
13.	gi 22203724	ribosomal protein S27E	Q8MUE6	translation	9.3	↑27.9
14.	gi 40642988	ribosomal protein S3a	Q70MP2	translation	29.9	↑24
15.	gi 18565104	Actin	Q8TA69	Cy/P	41.7	↓1.4
16.	gi 14422379	calponin-like protein	Q966V3	Cy/P	44.5	+Control-Pb ↓15.8
17.	gi 73665577	myosin essential light chain	Q0ZVW7	Cy/P	17.9	+Control-Pb ↓55.3
18.	gi 118596568	cytochrome c oxidase subunit I	A0P9Z8	oxidative phosphorylation	33.6	↓2.4
<b>Elements in response to Zinc stress only</b>						
19.	gi 116008297	mitochondrial H <sup>+</sup> ATPase $\alpha$ subunit	Q000T7	ATP biosynthesis / hydrolysis coupled transport	59.6	↑5.4
20.	gi 46909221	fructose-bisphosphate aldolase	Q6PTH3	carbohydrate metabolism	21.5	↑3.2
21.	gi 46909451	triosephosphate isomerase	Q6PTL0	carbohydrate metabolism	16.2	↑6.9
22.	gi 194068375	beta-tubulin	B3XZN3	Cy/P	49.9	↑2.7
23.	gi 58219310	tubulin	Q5H7U8	Cy/P	50.1	↑2.6
24.	gi 51701479	histone H2A	Q8I0T3	nucleosome assembly	13.4	↑4
25.	gi 207008800	histone H2B	Q6WV85	nucleosome	13.8	↑15.1

No.	Identifier	Protein name	UniProt ID	Biological Process	Mr kDa	Fold change (a)/(b)
26.	gi 115501910	receptor of activated kinase C 1	Q08G56	assembly oxidative phosphorylation	35	↑8.9
27.	gi 148717307	calreticulin	A5LGG9	protein folding	48.2	↑26
28.	gi 46391574	G protein beta subunit	Q5GIS3	protein signal transduction	37.5	↑2.6
29.	gi 33337635	Rho-GDI related protein	Q5K6R5	protein signal transduction	15.6	↑9.2
30.	gi 22758856	ribosomal protein L19	Q8ITC1	translation	23.6	↑37.2
31.	gi 22758866	ribosomal protein L23a	Q8ITB8	translation	19.3	↑28.2
32.	gi 40643000	ribosomal protein S8	Q70MN6	translation	24.2	↑37.2
33.	gi 5817598	myosin heavy chain	Q9U7E3	Cy/P	223.1	↓4.5
<b>Elements in response to Cu stress only</b>						
34.	gi 152003987	sarco/endoplasmic reticulum calcium ATPase	B2KKR2	ATP biosynthesis /hydrolysis coupled transport	110.3	↑32.4
35.	gi 34484251	sodium/potassium ATPase $\alpha$ subunit	Q6W959	ATP biosynthesis /hydrolysis coupled transport	45.8	↑11.2
36.	gi 40642728	phosphoglucomutase	Q70X61	carbohydrate metabolism	60.9	↑10
37.	gi 220979902	cell division cycle 42	B8ZHK4	cell cycle / division	19.2	↑5.7
38.	gi 21388656	twitchin	Q7YT99	protein signal transduction	526.5	↑4.5
39.	gi 40642990	ribosomal protein L5	Q70MP1	translation	30.8	↑5.7
40.	gi 40642982	ribosomal protein S25	Q70MT3	translation	13.7	↑18.6
41.	gi 44885729	arginine kinase	Q760P6	amino acid metabolism	39.6	↓2.8
42.	gi 51315721	histone H4	Q7K8C0	nucleosome assembly	11.4	↓8.7
<b>Elements in response to both Copper and Zinc stress</b>						
43.	gi 28475277	glyceraldehyde 3-phosphate dehydrogenase	Q869H6	carbohydrate metabolism	33	Cu↑ 3.1; Zn↑ 2.3
44.	gi 18073531	heat shock protein 70	Q8WQ94	stress response	71.8	Cu↑ 2.9 ; Zn↑ 2.8
45.	gi 22758854	ribosomal protein L11	Q8ITC2	translation	19.2	Cu↑ 41.4 ; Zn↑ 10.2

No.	Identifier	Protein name	UniProt ID	Biological Process	Mr kDa	Fold change (a)(b)
46.	gi 32169292	ribosomal protein L7	Q7Z0P7	translation	28	Cu↑ 30 ; Zn↑102.9
47.	gi 73427346	mantle gene 2	Q3YL64	unknown	20.9	Cu↑ 3.7; Zn↑ 2
48.	gi 50512854	glycogen phosphorylase	Q596I0	carbohydrate metabolism	98.6	+Control-Cu ↓24.5; Zn↑ 3.5.
49.	gi 113207854	phosphoenolpyruvate carboxykinase	Q0KHB7	carbohydrate metabolism	71.4	Cu↓ 2.6 ; Zn↓ 1.7
50.	gi 146326704	DNA-directed RNA polymerase beta subunit	A5CW24	transcription	154.8	+Control-Cu ↓6.6 ; +Control-Zn↓12.8
<b>Elements in response to Lead, Copper and Zinc</b>						
51.	gi 86156234	ATP synthase beta subunit	Q2HZD8	ATP biosynthesis /hydrolysis coupled transport	46.2	Cu↑ 16.3 ; Pb↑ 19 ; Zn↑ 23.2
52.	gi 229485193	peroxiredoxin 6	C4NWI5	cell redox homeostasis	24.4	Cu↑ 19.3 ; Pb↑ 7.4 ; Zn↑ 15.1
53.	gi 46359618	78kDa glucose regulated protein	Q75W49	stress response	73	Cu↑ 32.8 ; Pb↑ 40.6 ; Zn↑ 2.1
54.	gi 219806594	tropomyosin	B7XC66	Cy/P	33	Cu↓ 4.1; Pb↓ 100.9; Zn↓ 6.7
<b>Elements in response to both Lead and Zinc</b>						
55.	gi 164510092	ubiquitin	B0B039	protein destruction	25	Pb↑ 12.3 ; Zn↑ 33.7
56.	gi 40643024	ribosomal protein L17A	Q70MM4	translation	14.7	Pb↑ 44 ; Zn↑ 26

a) Up and down regulation of proteins in response to metal stress relative to controls have been indicated by an upward arrow, '↑' and a downward arrow, '↓' respectively.

b) Presence and absence of proteins in response to metal stress relative to controls have been indicated by a plus, '+' and a minus, '-' sign respectively.

### **3.3.2.1 Proteins differentially expressed in response to Lead, Zinc and Copper metal exposures**

We identified 24 proteins (Table 3.2) that responded to Pb exposure, of which 18 were differentially expressed specifically due to Pb exposure. 14 of the 24 proteins that responded to Pb exposure (58%) were found to be up-regulated ribosomal proteins (S2, S3a, S10, S11, S13, S14, S15, S17, S19, S23, S27E, L12, L17A and L24). Their fold differences relative to controls varied widely from 1.7 for ribosomal protein S2 to 81 fold for S11. It is interesting to note that this substantial (14 out of 24) number of differentially expressed ribosomal proteins due to Pb exposure was not observed in any of the other metal exposures. We also found that cytoskeletal proteins, namely calponin-like protein and myosin essential light chain, were both absent only in Pb exposed oysters. Other proteins specifically affected due to Pb exposure included NADH dehydrogenase subunit I, cytochrome c oxidase subunit I and actin.

We identified a total of 29 differentially expressed proteins affected by Zn, of which 15 were differentially expressed specifically due to Zn exposure. These 15 proteins included tubulins, histones 2A and 2B, rho-GDI related protein, G protein  $\beta$  subunit, ribosomal proteins L19, L23a and S8, calreticulin, fructose-bisphosphate aldolase, triosephosphate isomerase and myosin heavy chain. Twenty one of the 29 proteins were up-regulated in expression. Two proteins, ubiquitin and ribosomal protein L17a were up-regulated in response to both Pb and Zn metal exposures. Ribosomal proteins such as L19, L23a and S8 showed the highest fold changes after Zn exposure, while glycogen phosphorylase, mantle gene-2 protein, glyceraldehyde 3- phosphate dehydrogenase and hsp70 also showed noticeable increases in expression (see Figure 3.4).

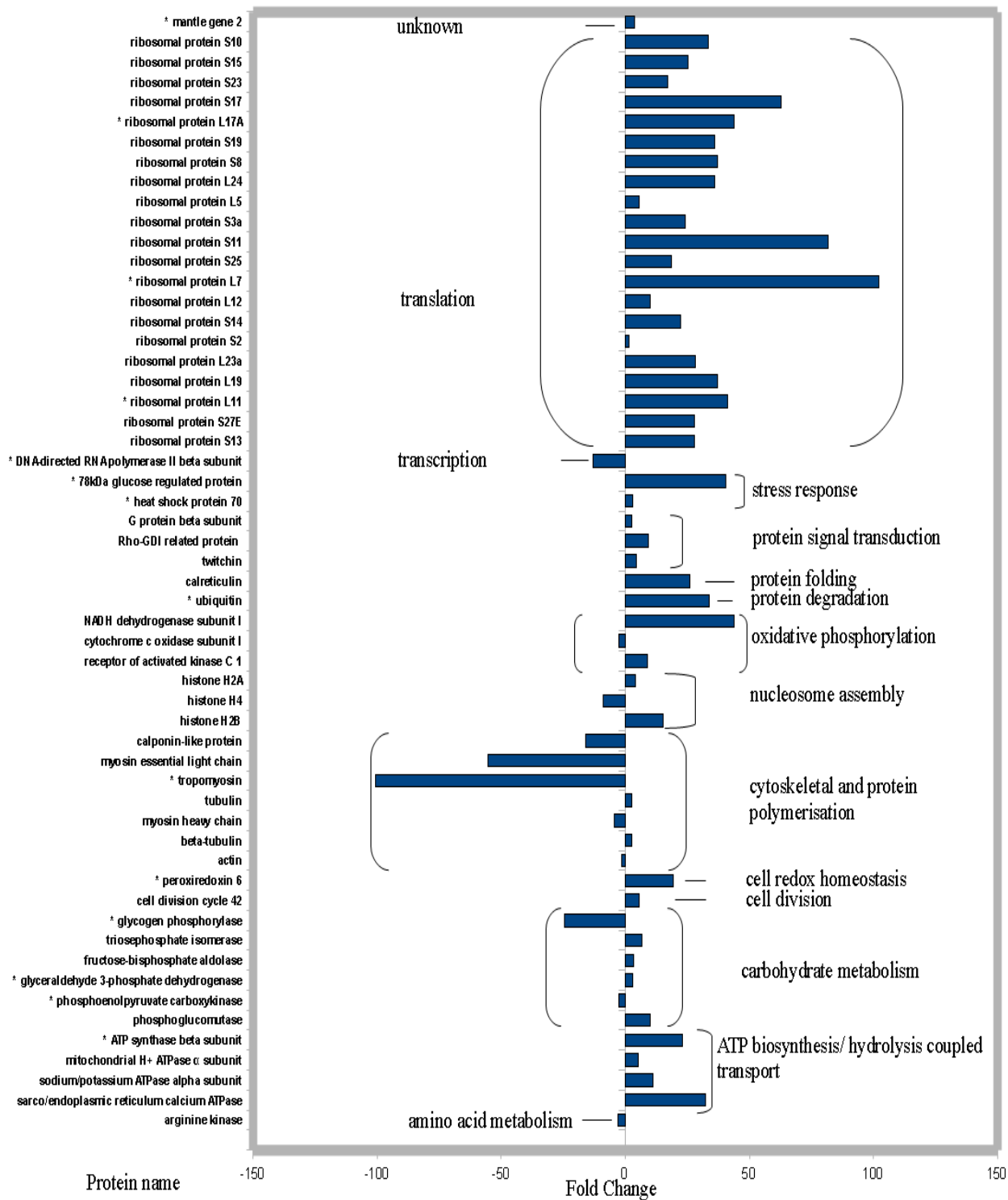


**Figure 3.4** Fold changes (up- or down-regulation) for 56 proteins in response to heavy metal stress relative to controls. Protein ontology information was obtained from UniProt and KEGG reference maps. Fold changes were calculated as the ratio of LogNSAF values in metal exposed oysters relative to non-exposed controls. Proteins have been grouped based on their association with distinct functional pathways. Differentially expressed proteins which responded to more than one metal exposure are indicated by an asterisk, “\*” (see Table 3.2 for specific information on the responses of these proteins with respect to each metal exposure).

The expressions of 21 proteins responded to Cu exposure, 5 were down-regulated and 16 up-regulated. Eight of these proteins were specific to Cu exposure only. The observed expression differences relative to controls ranged from an 8 fold down regulation for histone H4 protein to 41 fold up regulation for 78 KDa glucose regulated protein. Sarco/endoplasmic reticulum calcium ATPase isoform c, twitchin, sodium/potassium ATPase  $\alpha$  subunit, ribosomal protein L5 and phosphoglucomutase had some of the highest fold changes among the up regulated proteins after Cu exposure. Although glycogen phosphorylase was up regulated by 3 fold relative to controls after Zn exposure, it was absent in oysters exposed to Cu stress. Also, DNA directed RNA polymerase beta subunit protein was present in controls but absent in oysters exposed to Cu or Zn.

Among the 56 differentially expressed proteins, there were four proteins that were quantitatively changed in their protein expressions in response to all 3 metals. ATP synthase beta subunit, 78kDa glucose regulated protein and peroxiredoxin 6 were found to be up regulated in response to all 3 metals, whilst tropomyosin was down regulated in response to all 3 metals as shown in 3.3. It was intriguing to find that tropomyosin was down regulated a striking 100 fold less relative to control as a result of Pb exposure, while it only changed by 6 fold and 4 fold down regulation in response to Zn and Cu exposures respectively.

### **3.3.2.2 Presence or absence of proteins in controls vs. metal exposures**

Data analysis from both SDS-PAGE and GPF revealed 2 proteins that were present in triplicate analysis of all 3 metal exposure datasets but undetected in controls. These two proteins were voltage-dependent anion channel protein and ubiquitin.

### **3.3.2.3 Proteins present at all 3 metal treatments and controls**

ANOVA analysis of both SDS-PAGE and GPF datasets showed interesting expression patterns of proteins that were present in all 4 treatments (3 metals and controls). This group represents the proteins that were present at Pb, Zn, Cu metal treatments and controls and are listed in Table 3.3. Here, 19 proteins were identified to be present in all treatments, of these 15 proteins showed differential protein regulation in response to at least one of the 3 metals and is included in Figure 3.4, while 4 proteins remained unchanged. The four unchanged proteins were elongation factor-1 $\alpha$ , catalase, extracellular superoxide dismutase and paramyosin. Proteins that were present across all treatments were actin, arginine kinase, ATP synthase beta subunit, beta-tubulin, catalase, cytochrome c oxidase subunit, elongation factor 1 $\alpha$ , extracellular superoxide dismutase, fructose-bisphosphate aldolase, glyceraldehyde 3-phosphate dehydrogenase, glycogen phosphorylase, heat shock protein 70, histones H2A and H4, mitochondrial H<sup>+</sup> ATPase  $\alpha$  subunit, myosin heavy chain, paramyosin, phosphoenolpyruvate carboxykinase and tubulin. These proteins corresponded to 8 basic functional categories namely carbohydrate metabolism, plasma membrane ATP synthesis coupled proton transport, stress response, cytoskeleton and protein polymerization, amino acid metabolism, nucleosome assembly, oxidative phosphorylation and protein biosynthesis as shown in Figure 3.5.

**Table 3.3      Biological process characterization of proteins present across all metal treatments and controls**

<b>Protein GI number</b>	<b>Protein name</b>	<b>UniProt ID</b>	<b>Biological process category</b>
gi 44885729	arginine kinase	Q760P6	amino acid metabolism
gi 113207854	phosphoenolpyruvate carboxykinase	Q0KHB7	carbohydrate metabolism
gi 28475277	glyceraldehyde 3-phosphate dehydrogenase	Q869H6	carbohydrate metabolism
gi 46909221	fructose-bisphosphate aldolase	Q6PTH3	carbohydrate metabolism
gi 50512854	glycogen phosphorylase	Q596I0	carbohydrate metabolism
gi 18565104	Actin	Q8TA69	Cy/P
gi 194068375	beta-tubulin	B3XZN3	Cy/P
gi 5817598	myosin heavy chain	Q9U7E3	Cy/P
gi 58219310	tubulin	Q5H7U8	Cy/P
gi 42559342	paramyosin	O96064	Cy/P
gi 51315721	histone H4	Q7K8C0	nucleosome assembly
gi 51701479	histone H2A	Q8I0T3	nucleosome assembly
gi 118596568	cytochrome c oxidase subunit I	A0P9Z8	oxidative phosphorylation
gi 116008297	mitochondrial H <sup>+</sup> ATPase $\alpha$ subunit	Q000T7	plasma membrane ATP synthesis-coupled proton transport
gi 86156234	ATP synthase beta subunit	Q2HZD8	plasma membrane ATP synthesis coupled proton transport
gi 112144576	elongation factor-1 alpha	A6XIN5	protein biosynthesis
gi 18073531	heat shock protein 70	Q8WQ94	stress response
gi 151573941	Catalase	A7L9T8	stress response
gi 229485195	extracellular superoxide dismutase	C4NWI6	stress response

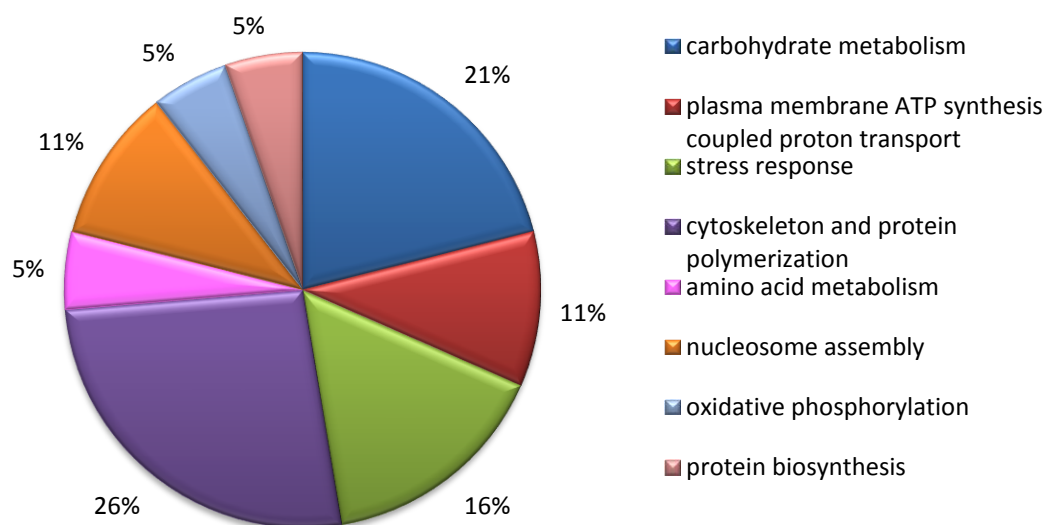


**Figure 3.5 Qualitative distributions of proteins present across all treatments. Proteins with known biological process were functionally categorized based on proteins as a percentage in each biological process category.**

The highest percentage of proteins was expressed in cytoskeleton and protein polymerization category with 26% of the 19 proteins, which was followed by carbohydrate metabolism at 21%. These two form the two major groups of proteins found consistent in both approaches. 16% of total proteins belonged to stress response while nucleosome assembly and ATP synthesis accounted for 11% of proteins each. The remaining three categories constitute 5% each. Therefore, these 19 proteins that represent this group are thought to be essential for the survival of the oysters. There are almost certainly more proteins present than those shown here, but our limited protein identification at this stage can be attributed to the high degree of biological variability between individual oysters, high frequency of polymorphisms which necessitates stricter

filtering of proteins, and also the paucity of genome sequence data when compared to well curated genomic and proteomic information for species such as mouse, human, rice, yeast and various bacteria.

### **3.3.3 Biological significance of 56 differentially expressed proteins in response to heavy metal stress**

Protein ontology analysis of the 56 differentially expressed proteins in response to each metal treatment, as reported in sections 3.3.2.1 and 3.3.2.2, revealed 15 major functional categories to be affected by heavy metal stress as shown previously in Figure 3.4. All except one could be assigned to a known functional category.

Figure 3.6 shows the quantitative distribution of each of the 56 differentially expressed proteins after metal treatment displayed in terms of their functional annotations. Differentially expressed proteins were first categorized based on their function as a percentage of the total number of proteins (Figure 3.6 a), and then recategorized as a percentage of protein abundance within each functional category based on sum NSAF values (Figure 3.6 b). Comparison of the two plots showed that the total number of proteins within a functional category often followed a different trend than when functional categories were quantified based on their overall protein abundance.

A considerable proportion of the 56 proteins that differed significantly between controls and metal exposed oysters were ribosomal proteins (37.5%, 21 out of 56) involved in translation. However, ribosomal proteins accounted for only 10% in terms of overall protein abundance. Figure 3.6a also shows that all of the 21 ribosomal proteins were up regulated after metal exposure and had amongst the highest fold differences in abundance relative to controls.

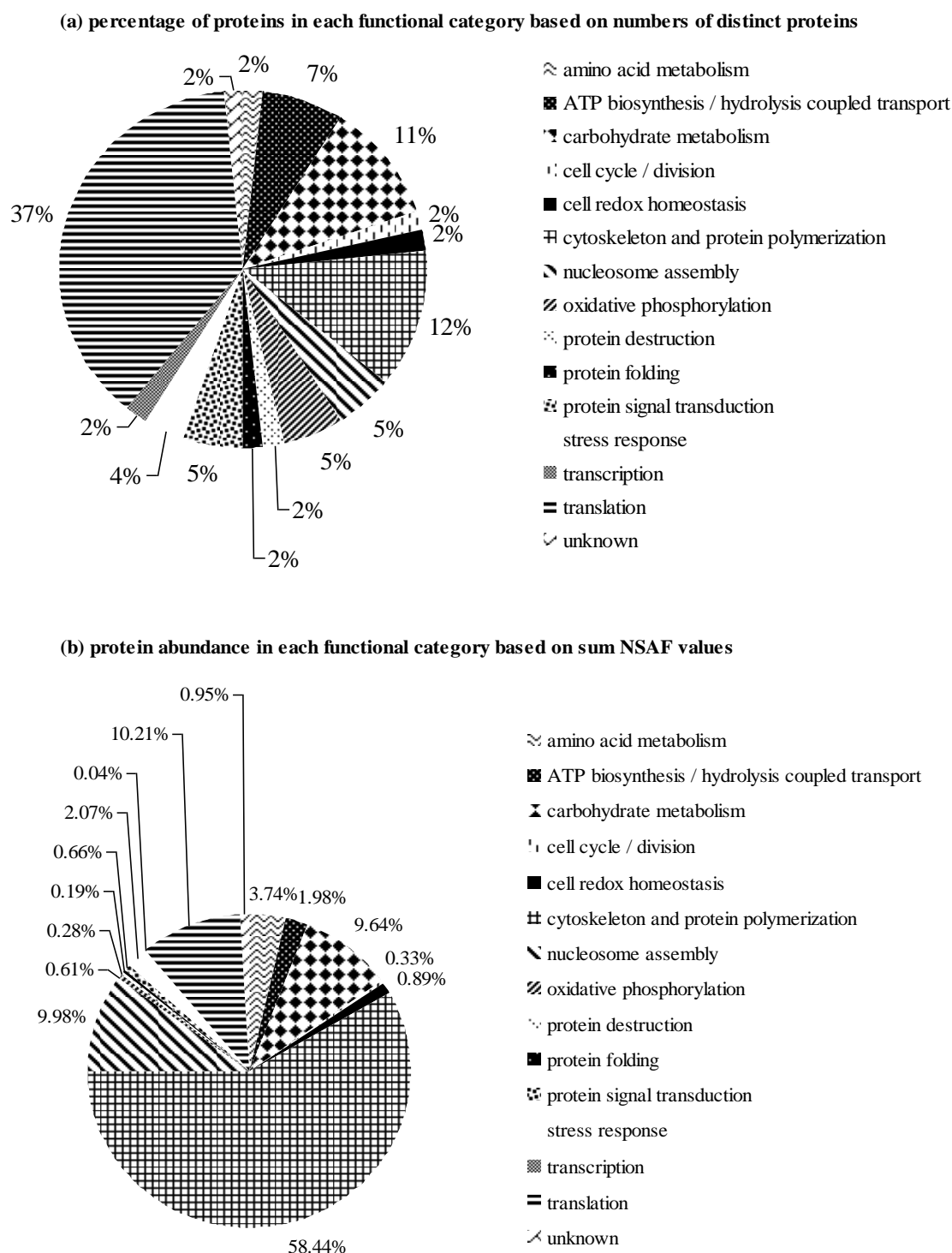


**Figure 3.6** Distribution of the 56 differentially expressed proteins based on their functional categories. Proteins were grouped with their known biological process information obtained from UniProt and KEGG databases. They have been classified into 15 different functional categories. They were resorted (a) as a percentage of protein number (b) as a percentage of protein abundance based on their sum NSAF values in each biological process category.

Proteins associated with cytoskeletal activity and protein polymerization, such as actins, calponin-like protein, myosin heavy and light chains, tropomyosin and tubulins comprised 12.5% of the total number of differentially expressed proteins, and contributed 58% in terms of protein abundance. Five out of seven proteins in this category were down regulated by metal exposure, and, with the exception of tropomyosin and myosin light chain, the fold changes of the remaining five proteins relative to controls were amongst the lowest detected (fold change ranged between  $3 \pm 1$  fold).

The next most abundant group of differential proteins is involved in carbohydrate metabolism. These included phosphoenolpyruvate carboxykinase, glyceraldehyde 3-phosphate dehydrogenase, fructose-bisphosphate aldolase, triosephosphate isomerase, phosphoglucomutase and glycogen phosphorylase. These proteins were associated with various metabolic pathways including glycolysis or gluconeogenesis, the pentose phosphate pathway, galactose metabolism, starch and sucrose metabolism, the citrate cycle, amino sugar and nucleotide sugar breakdown. The carbohydrate metabolism group of proteins constituted about 10% of both the number differentially expressed proteins and protein abundance (Figure 3.6). Although 5% of total differentially expressed proteins belonged to the oxidative phosphorylation category, they accounted for less than 1% of the protein abundance. For a complete overview of functional categorization of all 56 differentially expressed proteins, see Figures 3.4 and 3.6 A and B.

### **3.4 Discussion**

#### **3.4.1 Protein identification and quantitation using SDS-PAGE and GPF**

We identified and quantified a combined non-redundant total of 93 distinct proteins in the proteome of biological triplicates of Sydney rock oyster haemolymph, from an initial set of 451 distinct proteins identified in individual MS/MS analysis of at least one treatment. This came after manual quantitation and filtering of over 3000 proteins in all 24 lists of protein identification data.

Protein identification and quantitation were successful despite the lack of a complete oyster genome sequence, because we employed strict filtering criteria and manual curation at both the protein and peptide level. Proteins identified in this study provide two levels of information. First, they give an overview of the cellular machinery in normal and metal-stressed Sydney rock oysters. Second, they identify changes in protein abundance resulting from heavy metal stress.

To our knowledge, this is the first study of its kind to use two different proteomics approaches to produce protein identification and quantitation data in Sydney rock oysters, and to investigate differential protein expression in response to heavy metal stress. It is also the first study to develop a quantitation strategy that may be generally applicable to shotgun proteomics studies of organisms with no available genome sequence. Importantly, the label-free quantitative shotgun proteomics approaches that we used were able to detect proteins that were present or absent in a given treatment. The inability to do this reliably has been a drawback in many labeled approaches, which do not perform optimally when faced with missing channels of information.

Of the two techniques used in this study, the SDS-PAGE approach identified more proteins, and more differentially expressed proteins, than the GPF approach. However, GPF was able to reproducibly identify some low abundance proteins in terms of peptide counts that were not reproducibly found in SDS-PAGE datasets (probably masked by highly abundant peptides). The reproducible proteins exclusive to GPF datasets did not follow any particular trend in terms of physical parameters such as molecular weights or peptide length. GPF could therefore be used as an alternative technique for validation of SDS-PAGE approaches.

For both the SDS-PAGE and GPF approaches, our manual quantitation curation provided a new level of accuracy for protein quantitation, providing more effective pictures of cellular status. Shotgun proteomics studies of organisms with unsequenced genomes are feasible, but require modified quantitation strategies.

### **3.4.2 Biological significance of metals in bivalves**

Among the existing threats to the health of bivalves, heavy metal pollution is second only to pathogenic infection in terms of importance. Studies with proteomic biological relevance on bacterial infection are predominant in the literature [239-245]. However, similar studies of heavy metal stress in bivalve populations are rare.

Some metals are known for their beneficial involvement in several biological processes. These ‘essential’ metals include Cu, which plays an important role in electron transport chains and lipid peroxidation. Cu and Zn are redox in nature and so are also involved in Fenton-like reactions to counteract free radicals [246] via peroxidases and lysozymes. However, many metals at high concentrations pose health risks. For instance, Cu was traditionally used as an antifouling agent in ship paints and hence is known for

toxicity at high doses to the larvae, embryos and juveniles of bivalves including *C. gigas*, *Argopecten irradians* and *M. galloprovincialis* [247]. Wang *et al.* studied the toxicity effects of Pb, Cd and Hg on early developmental stages of *M. meretrix* and have noted the possible role of metal pollution in decreasing populations of some bivalves [247].

### **3.4.3 Differentially expressed proteins with respect to functional categories found in this study**

The proteomic methods used in this study provide an extensive view of the effects that high metal concentrations have on oysters by detailing the cascade of protein alterations triggered by metal exposures. This contrasts with many previous studies that have analyzed the effects of metals on individual molecules, such as heat shock protein 70, glyceraldehyde-3-phosphate dehydrogenase, glutathione S transferase, super-oxide dismutase and ATP synthase [248-252].

#### **3.4.3.1 Cytoskeletal activity**

In the current study, superoxide dismutase and actin were the two most abundant proteins identified. Even though superoxide dismutase was not affected by metal exposure, actin was down regulated in response to Pb. In addition to actin, calponin-like protein was also down regulated in response to Pb. Since calponin is known to be involved in the regulation and modulation of actin-mediated movement, the binding of calponin to actin has an inhibitory effect on actomyosin MgATPase activity which is  $\text{Ca}^{2+}$  independent. This binding causes a decrease in the enzymatic activity of myosin and this inhibitory effect can be reversed by calmodulin in the presence of  $\text{Ca}^{2+}$  [253]. In the current study, the down-regulation of major cytoskeletal proteins, namely actin, calponin-like protein, myosin heavy and myosin essential light chains, highlight the possible

relationship between metal stress and altered cellular plasticity and movement. Since the simultaneous down-regulation of calponin-like protein, actin and myosin essential light chain occurred in response to Pb stress, a hypothesis can be drawn where Pb could be capable of direct binding to cytoskeletal proteins. Other cytoskeletal proteins such as myosin heavy chain, tubulin and  $\beta$ -tubulin showed differential protein expression specific to Zn. Tropomyosin, which was down regulated in response to all 3 metals in this study, has been previously shown to bind to actin thereby causing stability and rigidity of actin microfilaments. Even though the roles of tropomyosin in muscle and non-muscle tissues remain unclear, structural information reveals that this protein forms a coiled-coil structure of 2 parallel helices containing 2 sets of 7 alternating actin binding sites [254-256]. A recent study has shown that in striated muscle, tropomyosin mediates the cross-talk between the troponin complex and actin in order to facilitate and further regulate contraction. This reflects one of the main findings of this study; metals have detrimental effects on cytoskeletal activity. These changes in cytoskeletal proteins collectively reinforce their potential as a valuable combination of protein biomarkers for Pb and/ or Zn stress in oysters. Differential expression of these cytoskeletal proteins is in agreement with several previous studies [162, 257-259, 246].

It is also clear that proteins from “housekeeping” genes (previously widely used as internal standards), such as actins and tubulins, can undergo considerable modulation. Therefore it may not be helpful to use them as internal protein standards for future studies. Their differential expression has also been previously reported in response to other toxicological agents [181].

### **3.4.3.2 Translation**

Ribosomal proteins are involved in translation of proteins and are the principal structural constituents of the ribosome. They are also known to play other important roles in cellular growth and regulation apart from their usual functions [260, 261]. High fold changes in 21 up regulated ribosomal proteins suggest a possible future direction in further understanding their involvement in metal stress.

Thirteen out of these 21 ribosomal proteins belong to the small ribosomal subunit indicating that the small ribosomal subunit could be more sensitive to excessive levels of metals than the large subunit. Up- regulation of these ribosomal proteins suggests that the oysters probably initiated an increase in the synthesis of other proteins in order to combat stress. For instance, RPS3a is known to play a significant role in initiating protein synthesis and its differential expression was previously reported in *A. purpuratus* in response to Cu stress [262, 246].

### **3.4.3.3 Carbohydrate metabolism**

Both glycogen phosphorylase and glyceraldehyde-3-phosphate dehydrogenase (GAPDH) were up regulated in response to Cu and Zn. Since GAPDH catalyses fatty acid beta oxidation in mitochondria, the up regulation of this enzyme could be associated with the utilization of fatty acids as an alternate source of sugar for energy replacement soon after the depletion of glycogen. In normal conditions, glycogen storage is essential for reproduction [263]. Forced utilization of glycogen reserves to disseminate the accumulated metal concentrations may cause depletion of glycogen thereby affecting reproduction and development of oysters. This could be an indication of possible increase in energy expenditure for survival under stress conditions and also the need for utilization

of reserve energy resources. The altered expression of glycogen phosphorylase has been previously reported in *Scrobicularia plana* exposed to high metal content [19].

#### **3.4.3.4 Oxidative phosphorylation and ATP biosynthesis/ hydrolysis coupled transport**

NADH subunit I, which is a respiratory chain enzyme found in mitochondria, was strongly up-regulated (44 fold) in response to Pb. This protein is a major source of reactive oxygen species [264] and can cycle between active and inactive forms that can be distinguished by their reactivity towards divalent cations and thiol-reactive agents [265]. It is possible that when Pb concentration due to bioaccumulation is not high, this enzyme protects the respiratory chain of oysters and, similarly to superoxide dismutase, influences the activities of other enzymes. Elevated levels of NADH subunit I, which is the largest multimeric respiratory enzyme in the mitochondria, could be attributed to damage caused to the inner mitochondrial membrane where this enzyme is located.

Among the four differentially expressed proteins that responded to all 3 metals, 3 were up regulated and 1 was down regulated. The three up regulated proteins were ATP synthase  $\beta$ -subunit, 78KDa glucose regulated protein and peroxiredoxin 6, and the down regulated protein was tropomyosin. Of these, ATP synthase  $\beta$ -subunit, which is known to be involved in ATP synthesis and hydrogen ion transport processes, was up-regulated by 16 fold. The 78KDa glucose regulated protein is a well-known stress response protein involved in ATP binding and was increased in expression up to 40-fold. The differential expression of these two proteins may indicate that when elevated levels of metal bioaccumulation occur there is an increase in demand for ATP for energy production.

#### **3.4.3.5 Protein degradation or stabilization**

Ubiquitin was found to be up regulated in response to both Zn and Pb by up to 12 fold and 33 fold respectively, indicating an increase in protein degradation pathways. Similarly, heat shock protein 70, which is a known stress related protein involved in protein stabilization, was up regulated in response to both Cu and Zn, in agreement with previous findings in literature [266, 18, 240, 246].

Even though Cu is known to bind to metallothioneins in the process of Cu detoxification our data did not show glutathione-S-transferase or metallothioneins to have statistically significant differential protein expression. This could be attributed to the fact that Cu is also known to be mostly bound to heat stable proteins associated with organelles. Oysters might also have the ability to protect some metal sensitive fractions by converting toxic forms of metals to non-toxic forms [123].

#### **3.4.4 Potential biomarkers**

Our shotgun proteomics approaches were able to identify more proteins than any other study in the literature pertaining to heavy metal stress responses in bivalves. Although changes in expression of any of the 56 proteins can be considered indicative of heavy metal stress response, we noted several combinations of these 56 differentially expressed proteins which warrant further investigation for use as protein biomarkers. Combinatorial biomarkers are thought to be more specific and reliable in indicating stresses when compared to a single protein biomarker. Up-regulation of ATP synthase  $\beta$ -subunit, 78KDa glucose regulated protein and peroxiredoxin 6 in conjunction with down-regulation of tropomyosin can be used to indicate high concentrations of Pb, Cu and Zn occurring simultaneously. A duplet up-regulation of ubiquitin and ribosomal L17A could

indicate high levels of Zn and Pb. A triplet combination of up regulation of glycogen phosphorylase and DNA directed RNA polymerase beta subunit, and down-regulation of ribosomal protein L11, could be used to indicate high levels of Cu and Zn stresses. Pb stress levels can also be exclusively monitored by up-regulation of four ribosomal proteins, namely RPS11, RPS13, RPS17 and RPS10, in addition to the down-regulation of both actin and calponin.

### **3.5 Concluding Remarks**

The lack of oyster genome sequence made this study challenging and so our results are of significance to researchers working with oysters. We successfully devised an approach to solve several complexities during the analysis of our spectral count data sets which include (a) using peptide (rather than protein) log(e) filtering to help minimize protein and peptide false discovery rates; (b) construction of an in house Bivalvia database to compensate for the unavailability of a complete oyster genome sequence; (c) development of a manual curation strategy for quantitation of spectral count data in order to account for shared and unique peptides between proteins from similar species.

This is the first study to use shotgun proteomics in oysters (or bivalves) to elucidate the identification of a significant number of proteins with biological relevance in response to heavy metal stress. With the availability of the complete genome sequence for oysters in future, these data may be supplemented with additional detailed protein information. Further validation of these heavy metal stress biomarkers by orthogonal techniques will be a valuable continuation of this work. These biomarkers when used in combination to develop bioassays have the potential to increase the detection rate of heavy metal stress in oysters in the field. The potential biomarkers identified here may be able to act as an early warning system to prevent heavy metal stress from affecting growth quality

and health of marine biota. Despite these indicative suites of proteins, it is acknowledged that complex mixtures of contaminants in the environment might limit their utility for field biomonitoring. Field work studies on the same suite of metals were subsequently carried out and many protein signatures identified using our previous laboratory experiments were reconfirmed. Therefore, further validation during development of these biomarkers as assays is vital for field use.

### **Supplementary information**

The following Supplementary information for this study is available in the enclosed DVD

**Supplementary Information Table S1** Proteins identified using SDS-PAGE approach along with peptide identification information including peptide sequences for all proteins in each replicate at four different metal treatments.

**Supplementary Information Table S2** Proteins identified using GPF approach along with peptide identification information including peptide sequences for all proteins in each replicate at four different metal treatments.

**Supplementary Information Table S3** Peptide quantitation information in terms of NSAF values for 84 reproducible proteins identified by SDS-PAGE approach and 49 by GPF.

## Notes

The work presented Chapter 3 was performed prior to the release of the oyster genome and was published in *Proteomics* in Mar 2012. The final version of the manuscript is presented as Publication II in Appendix A. In addition, a detailed description of the pipeline used for data analysis in this work is included here and in Chapter 2.

Supplementary tables, including protein identification and quantitation information, referred to in-text can be found on the DVD attached to this thesis.

Other supplementary data are included in Appendix B as indicated.

This project was performed in collaboration with a fellow PhD student, Emma Thompson and her supervisor Prof. David Raftos, of the Department of Biological Sciences, Macquarie University, Sydney. Emma was involved in the Oyster exposure experimental design, culturing of oysters and metal exposures. I performed the extraction and purification of proteins and peptides from the haemolymph of these oysters, all other proteomics experiments including MS/MS analysis using two different label-free experiments. I also performed all of the data analysis including the development of a manual quantitation strategy, data interpretation and quantitation of peptide data, which led to identifying the relevance of differential expression of several proteins toward metal stress response in Sydney rock oysters, and preparation of the manuscript (approximately 95%).

---

## Chapter 4

# **Quantitative proteomics and discovery of biomarkers for heavy metal stress response in Sydney rock oysters, elucidated using the recently released oyster genome sequence.**

---

### 4.1 Introduction

Since “Proteome” refers to all of the proteins expressed by the genome, it refers to all the proteins produced by an organism, and is of great relevance when studying protein response patterns in the organism in relation to a particular environmental stress. Unlike the genome, which is relatively static, the proteome changes constantly in response to thousands of intra- and extracellular environmental signals. Changes in the proteome occur with health or disease, the nature of the tissue, developmental stages, or from effects of environmental or other stressors. As such, the dynamic proteome studied in this chapter is defined as “the proteins present in hemolymph samples of Sydney rock oysters at each of the three metal toxicity conditions (Pb, Cu and Zn) relative to non-exposed controls oysters.

The Pacific oyster genome sequence (*Crassostrea gigas*) was recently completed and was found to encode more than 26,000 proteins. This species is a close relative of *Saccostrea glomerata*, the Sydney Rock oyster, so it can be used successfully in many proteomics approaches. This new genome information holds great promise for proteomic

applications in oysters, such as resolving oyster mortalities and diseases caused by various pathogens and anthropogenic pollutants, but also in bio-monitoring of environmental changes, hopefully driving better strategies and policy making in environmental conservation.

Therefore, with the aim of finding valuable and highly relevant proteomic information to supplement our previously acquired Sydney rock oyster metal stress MS/MS data, we re-interrogated the previously acquired mass spectrometric data using the *C. gigas* Oyster genome sequence. We aimed to study the effects of heavy metal pollution on *S. glomerata*, and the associated metal stress responses, and take advantage of the wealth of unexploited information present in the available oyster genome sequence. Therefore, this study was carried out as a successor to our previous study (Chapter 3), to reanalyze the effect of metal stress on *S. glomerata* and update the panel of protein biomarkers previously established. Through this effort we obtained a better peptide-to-spectrum matching rate and, obviously, reduced cross-species sequence variability. This helped in obtaining more accurate and reproducible peptide and protein identification information. In addition to re-analyzing the proteomics data with the newly available oyster genome, we discuss our results in comparison to those found using the *Bivalvia* protein database as described in Chapter 3.

Our main objectives in this study were to identify proteins expressed in oyster hemolymph when oysters were exposed to 96 h of high metal concentrations (Pb, Cu and Zn, compared to controls), by (a) re-analysing the shotgun proteomics MS/MS data obtained previously (Chapter 3) against the new Oyster genome sequence; (b) by performing an additional 8plex iTRAQ analysis experiment using fresh samples and investigating the MS/MS data using the Oyster genome sequence. We also aimed to

identify proteins that showed changes in expression in response to metal stress, especially to identify those that impact certain metabolic pathways and to further examine the effects of metal stress on those pathways. In addition to this, we also aimed to identify novel heavy metal stress proteins that have not been functionally characterized yet, as these are high value targets for further study.

## **4.2 Materials and Methods**

Detailed accounts of methodologies used for proteomics analysis have been described in Chapters 2 and 3. The materials and methods used in culturing of oysters and exposure to different heavy metals have been described in detail in Chapter 3. In this chapter, section 4.2.1 describes the specific methodologies used for the database searching of the mass spectrometric .RAW files against the oyster genome sequence and the subsequent generation of protein identification data. Section 4.2.2 provides the experimental strategy used to perform proteomic analysis using isobaric tags for relative and absolute quantitation (iTRAQ), for potentially finding a new set of differential proteins in response to heavy metal stress in oysters, as well as validating some of the protein biomarkers found in the previous study in Chapter 3.

#### **4.2.1 Summary of database searching and statistical analysis of MS/MS data obtained using the shotgun proteomics approach and the newly released Oyster genome database**

Raw files of MS data obtained from nanoLC-MS/MS analysis of two shotgun proteomics approaches, (1) SDS-PAGE and (2) GPF, were converted to mzXML format and searched against the National Center for Biotechnology Information (NCBI) *Crassostrea gigas* Reference Sequence (RefSeq) database (26,086 proteins, October 2012), using the X!Tandem algorithm incorporated into the GPM software (version cyclone 2011.12.01).

The 16 fractions of each replicate used in the SDS-PAGE approach were processed sequentially and a merged, non-redundant GPM output file with protein and peptide identifications was generated at peptide  $\log_e \leq -2$ . In the case of GPF data, 8 fractions from each replicate were processed sequentially and a merged, non-redundant output file with protein and peptide identifications were obtained with peptide  $\log_e \leq -1$ . MS/MS spectra were also searched against the reverse database to generate possible false positives and to estimate FDR rates. The 12 lists of proteins from each dataset (SDS-PAGE and GPF data) identified for three replicates in each of the four exposure conditions were filtered based on two criteria; a protein was retained if it was present reproducibly in all replicates of at least one treatment, and had a total spectral count of  $\geq 3$ . Peptide and protein FDRs were subsequently calculated. Peptide FDR of a list is  $2 \times (\text{total number of peptides identified for reversed protein hits} / \text{total number of peptides identified for all proteins in the list}) \times 100$ . Protein FDR was calculated using  $(\text{number of reversed protein hits} / \text{total number of proteins in the list}) \times 100$ . FDRs were calculated after combining replicate data and, if required proteins were further filtered to minimize

FDR to  $\leq 1\%$  at the protein level and  $\leq 0.5\%$  at the peptide level in the final list of reproducible proteins for each treatment.

NSAF values for each protein were calculated. Log(NSAF) values were calculated for proteins in each replicate list in each treatment group, and statistical analyses were performed using student's *t*-tests and ANOVA, implemented in the R stats package and incorporated within the SCRAPPY program [234, 232]. Data for all proteins expressed at four treatment groups were partitioned based on their presence or absence at a given treatment, similar to a Venn diagram. Proteins were categorized based on different abundance patterns and five groups were selected for further analysis; proteins found in all oysters at all treatments, proteins present only in non-exposed control oysters, proteins unique to Pb exposed oysters, proteins unique to Cu exposed oysters and proteins unique to Zn exposed oysters. In addition, we examined further those that were found to be statistically differentially expressed in response to heavy metal stress. Proteins were annotated using various protein databases, including InterPro, UniProt KB and KEGG. GO information was inferred in terms of biological processes and metabolic pathways.

#### **4.2.2 Summary of 8plex iTRAQ approach**

In addition to the GPF and SDS-PAGE label free quantitative shotgun proteomic approaches described above, an 8-plex iTRAQ experiment was carried out. The eight labelling reagents were divided into two sets of four. The Cu, Pb, Zn and control oyster samples were then prepared and labeled twice each, so duplicate analysis of each sample was performed. Each of the eight iTRAQ protein samples was pooled from 2 oysters to minimize biological variation. Since the Bradford assay used in Chapter 3 for protein quantitation was not compatible with TEAB buffer used in iTRAQ labelling, a gel based technique was used to quantitatively compare and measure samples of unknown

concentration with samples of known concentration of protein. Image-based measurements of area corresponding to the gel lane of samples with known protein concentrations (e.g. 10 $\mu$ g and 50 $\mu$ g) were graphed, and an equation describing the relationship between protein concentration and area was generated using Microsoft Excel. From this equation, the concentrations of the unknown protein samples were calculated. For each of the eight samples, approximately 75 $\mu$ g of protein was used for the iTRAQ labelling.

Proteins were reduced and alkylated with the iTRAQ reagent 8-plex kit according to instructions provided by the manufacturer (Applied Biosystems, Foster City, USA). Samples were reduced with 100mM tris (2-carboxyethyl) phosphine (TCEP) and 200mM methyl methane thiosulphonate (MMTS) in isopropanol for 10 min. Samples were digested with trypsin in a 1:20 trypsin to protein ratio, for 16 hours at 37 °C. Protein digests were dried and resuspended in 30  $\mu$ l of 0.5M TEAB (pH 8.5).

Samples were labeled with iTRAQ labelling reagents 8-plex kit following instructions provided by the manufacturer. Isopropanol (70 $\mu$ l) was added to each tube containing iTRAQ labelling reagents 113 – 121 and this mixture was added to samples as shown in Table 4.1. After 2 h of incubation, the labelling reaction was quenched by adding milli-Q water (70 $\mu$ l). The labelling efficiency was then tested for each of the eight samples in addition to duplicate control samples labeled by 115 first, followed by 119, by mixing 2  $\mu$ l of each sample with 1  $\mu$ l of MALDI matrix solution in a fresh tube and analyzing by MALDI-TOF/TOF. The duplicate control samples showed absence of label 119 in their spectra, suggesting complete labeling efficiency by 115. Labeled peptide samples were then mixed together and dried in a vacuum centrifuge prior to fractionation by SCX liquid chromatography.

**Table 4.1**      **iTRAQ labels added to samples**

<b>iTRAQ label</b>	<b>sample</b>
113	Pb exposed oysters replicate 1
114	Zn exposed oysters replicate 1
115	Control oysters replicate 1
116	Cu exposed oysters replicate 1
117	Pb exposed oysters replicate 2
118	Zn exposed oysters replicate 2
119	Control oysters replicate 2
121	Cu exposed oysters replicate 2

An Agilent quaternary HPLC pump with a polySulphoethyl A 200 mm x 2.1 mm, 5µm, 200Å column (PolyLC, Columbia, MD) was used for fractionating iTRAQ labeled peptides by SCX chromatography. Buffer A was 5 mM potassium phosphate, 25% (v/v) acetonitrile, pH 2.7 and buffer B was 5 mM potassium phosphate, 350 mM potassium chloride, 25% (v/v) acetonitrile, pH 2.7. The dried iTRAQ labeled sample was resuspended in buffer A, and loaded on the SCX column. After sample loading and washing with buffer A, buffer B concentration was increased from 10% to 45% over 70 min and then ramped up to 100% and maintained at 100% for 10 min at a flow rate of 300 µl/min. A total of 33 fractions were collected from the SCX chromatographic separation, resuspended in 100 µl of 0.1% (v/v) trifluoroacetic acid, 2% (v/v) acetonitrile, and 40 µl of each fraction was loaded on to a reverse phase peptide Captrap (Michrom Bioresources) and desalted at 10 µl per min for 15 min. The trap was then switched on line with a 150µm x 10cm C18, 3 µm, 300 Å ProteCol column (SGE). Peptides were eluted from the column by gradually increasing buffer B (90% (v/v) acetonitrile, 0.1% (v/v) formic acid) from 5% to 90% over 120 min in three linear gradient steps. After peptide elution, the column was cleaned with buffer B for 15 min and then equilibrated with 95% buffer A (0.1% (v/v) formic acid) for 30 min.

The reverse phase nanoLC eluent was subjected to positive ion nanoflow electrospray analysis in an information dependent acquisition mode. Mass spectra were acquired on a QStar XL hybrid quadrupole TOF mass spectrometer (Applied Biosystems). A TOF-MS survey scan was acquired ( $m/z$  380-1600, 0.5 second), and the three most intense multiply charged ions (counts >70) in the survey scan were sequentially subjected to MS/MS analysis. MS/MS spectra were accumulated for 2 seconds in the mass range  $m/z$  100-1600 with a modified enhanced all Q2 transition setting favouring low mass ions which enhanced the ion intensities of the reporting iTRAQ tag ions for quantitation. The nanoLC ESI MS/MS data were searched against the NCBI Oyster genome Refseq database (26,086 proteins, March 2013), with the aid of the Paragon algorithm of the ProteinPilot software (Applied Biosystems). The search was performed through protein ID search effort with biological modifications selected in ID focus. The data were analyzed for protein identification and relative quantitation, where detected protein confidence threshold cut-off was  $\text{ProtScore} \geq 1.3$  which corresponds to 95% confidence limit. The correction factors for the iTRAQ reagents provided by the manufacturer were considered to account for isotopic overlap. The ProGroup algorithm within the ProteinPilot software grouped proteins to determine a minimal non-redundant set of protein identifications, and also performed a quantitative analysis of relative ratio of the labeled proteins between samples, and associated p-value representing the probability of the observed ratio to be different to 1 by chance. In addition to this statistical analysis, a ratio > 1.2 fold change cut-off was applied to the reported iTRAQ ratios in order to consider a protein to be up-regulated, or corresponding ratio < 0.8 to be considered as down-regulated.

## **4.3 Results and Discussion**

### **4.3.1 Protein extraction and proteomic analysis**

Table 4.2 shows a summary of protein identifications from hemolymph of oysters exposed to metals, or controls, from each of the three approaches used in this study, namely SDS-PAGE gel fractionation, GPF and iTRAQ. The average number of redundant peptides and proteins identified in replicate oysters in each exposure group indicated acceptable reproducibility and correlated well with the standardized 75µg of protein analyzed in each experiment. A combined total of 356 non-redundant proteins were identified from the two label free shotgun proteomics plus iTRAQ labelling techniques. However, protein profiles of individual oysters revealed high level of biological variation between them, as previously reported, which resulted in reduced numbers of reproducibly identified proteins. In addition to inherent biological variability, several of the most abundant proteins including collagens, myosins and actins showed greater frequency of single nucleotide polymorphisms and sequence repeats in oysters. These are some of the main challenges faced in our previous study [11] and also during the sequencing of the oyster genome by BGI [267]. As a result of these, protein lists from GPM searches of SDS-PAGE and GPF datasets showed higher FDRs than most other shotgun proteomics studies. Therefore, to reduce the number of false positives, we applied stricter filtering criteria similar to that adopted in our previous study (see Chapter 3), We filtered peptides by peptide loge scores < -1 for GPF and < -2 for SDS-PAGE datasets to reduce protein and peptide FDRs to less than 1% and 0.5% respectively.

**Table 4.2 Protein identifications summary for Sydney rock oysters**

Technical Approach	Reproducible protein counts at protein FDR < 1%				Non-redundant count of protein identifications
	Pb	Cu	Zn	Controls	
1 DE	134	166	185	117	285
GPF	61	53	49	56	111
Differential proteins relative to controls from shotgun analysis	34	102	86		185
iTRAQ analysis					139
Number of differentially expressed proteins in response to any of the 3 metal exposures from iTRAQ analysis					12

The nanoLC-ESI-MS/MS data corresponding to the iTRAQ analysis were searched against the same NCBI Pacific oyster genome Refseq database (26,086 proteins, March 2013), as was done with the label-free shotgun proteomics data. Differentially expressed proteins in response to each of the three metal exposures, were identified separately. Proteins with a p-value < 0.05 and a ratio > 1.2 or < 0.8 were considered up or down regulated respectively. The ratios 113/115, 117/115, 113/119 and 117/119, representing (Pb exposed/controls), and the ratios 114/115, 118/115, 114/119 and 118/119, representing (Zn exposed/control), and the ratios 116/115, 121/115, 116/119 and 121/119, representing (Cu exposed/controls), were used for the analysis. Proteins that were up-regulated or down-regulated for each metal treatment were retained only if their differential expression was reproducibly identified relative to both controls (115 and 119) from the two replicate sets (see Table 4.1). Proteins identified in this study offer two levels of information. First, they provide an overview of the cellular machinery in control and

metal-stressed Sydney rock oysters. Second, they identify changes in protein expression following exposure to heavy metal stress.

Of the three proteomics approaches tested, the SDS-PAGE approach resulted in more protein identifications and more differentially expressed proteins. This is consistent with the findings of our previous study described in Chapter 3. The iTRAQ experiment resulted in identification of 52 proteins unique to the iTRAQ approach, while GPF was able to reproducibly identify some lower abundance proteins, in terms of peptide counts, that were not reproducibly found in SDS-PAGE datasets (probably because they were masked by highly abundant peptides). However, each approach identified unique proteins not identified reproducibly by the other two and this makes them useful and affordable alternatives that provide complementary information maximising the potential of this study. A total of 356 non-redundant proteins were identified from the three metal and one non-metal exposure groups upon combining results from the three proteomics approaches.

With respect to the label-free shotgun proteomics results, the number of non-redundant proteins in each exposure group as well as the combined total from all three exposures identified using the oyster genome protein database in this study is greater than that obtained when using the 'Bivalvia' cross-species protein database for this analysis in Chapter 3. This reaffirms the advantage of having a sequenced genome for the organism under study, as we were able to more efficiently match spectra to peptide sequence of proteins specific to the organism, minimize peptide sequence mismatches due to species variation, and reduce variation due to sequence polymorphisms (which is especially important when working with oysters). Figure 4.1 shows that the category representing the highest number of proteins (72) are those expressed at all exposure conditions, which presumably play an indispensable role in overall cell maintenance and metabolism.

However, Figure 4.1 also indicates that metal exposures at high concentrations caused significant changes in the proteome by the unique expression of 25, 46 and 49 proteins exclusive to Pb, Cu and Zn exposed oysters, respectively, as opposed to 8 in non-exposed oysters.

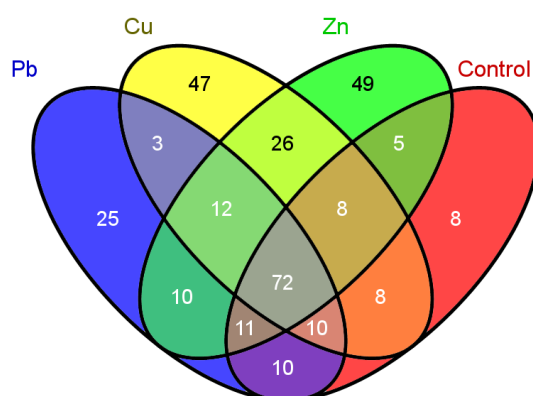


**Figure 4.1** Distribution of proteins in Sydney rock oysters upon exposure to different heavy metals and controls. Cu, Pb, Zn denote oysters exposed to 100  $\mu\text{g/L}$   $\text{CuCl}_2$ ,  $\text{PbCl}_2$ ,  $\text{ZnCl}_2$  in seawater respectively, and controls represent non-exposed oysters. Shades represent presence or absence of proteins in each combination across all treatments. The number of protein identifications included in each treatment represents a combined total from both SDS-PAGE and GPF approaches.

Supplementary information Table S4 summarizes proteins obtained from SDS-PAGE and GPF approaches with peptide identification information for all proteins in each replicate at four different metal treatments. Quantitation information in terms of NSAF values for all reproducible proteins identified in each heavy metal stress exposure condition and controls, from either SDS-PAGE or GPF approaches is shown in supplementary information S5.

#### **4.3.2 Presence or absence of proteins at different metal treatments**

Although considerable numbers of proteins were found in other categories, we chose to focus on those uniquely expressed at stress conditions, those unique to non-exposed oysters, and those that are expressed in all conditions (Figure 4.1). Proteins found in the categories referred above were further analyzed by extracting GO information from Uni-Prot, KEGG and InterPro databases. A biological process was assigned to over 95% of all proteins identified in this study; hypothetical proteins that did not match to any known protein via a BLAST search were termed as unknown proteins. Those proteins with known biological processes were classified into ontology categories qualitatively as well as quantitatively based on summed NSAF values.

#### **4.3.3 Proteins found in all metal exposed as well as non-exposed oysters**

ANOVA analysis of both SDS-PAGE and GPF datasets showed differences in expression patterns of proteins that were present in all four treatments. Proteins expressed at all exposure conditions including controls are listed in Appendix C1, with the biological process as found in Uni-Prot. The 72 proteins in this group were graphed as a percentage in each biological process category (Figure 4.2A). This group presumably includes many essential proteins. The largest group of these proteins was those involved in cytoskeleton and protein polymerization (40%), followed by those responsible for signal transduction (14%), and carbohydrate metabolism (12%). When re-graphed using the summed NSAF values in each biological process category as a measure of protein abundance, Figure 4.2B shows that the most abundant group was involved in cytoskeleton organisation (52%) followed by cell redox homeostasis proteins (31%). This included actins, calponins, myosin heavy chains, paramyosin, plastin, spectrin, severins,  $\beta$ -tubulin and  $\alpha$ -actinin. It is also clear that the abundance as well as count of proteins involved in cytoskeleton and

protein polymerization was high in all oysters in all exposure conditions. Since shell structure and muscle activity are critical for the survival, development and sustenance of oysters, it is not unexpected that the cytoskeletal related proteins are found in high abundance under all environmental conditions.

Spectrin is a cytoskeletal protein that lines the intracellular side of the plasma membrane in eukaryotic cells. Spectrin forms pentagonal or hexagonal arrangements, forming a scaffold and playing an important role in maintenance of plasma membrane integrity and cytoskeletal structure. In invertebrates, three forms of spectrins are known,  $\alpha$ ,  $\beta$  and  $\beta$ H. A mutation in  $\beta$  spectrin in *C. elegans* resulted in an uncoordinated phenotype in which the worms were paralysed and much shorter than wild-type [268]. In addition to the morphological effects, the Unc-70 mutation also produced defective neurons where neuron numbers were normal but neuronal outgrowth was defective. Similarly, spectrin apparently played a critical role in determining the health of *Drosophila* neurons. Gene knock-out experiments of  $\alpha$  or  $\beta$  spectrin in *D. melanogaster* resulted in neurons that were morphologically normal but showed reduced neurotransmission at the neuromuscular junction [8]. Severe metal toxicity also has the potential to cause paralysis in muscle tissues, and may result in genotoxicity from spasmodic neurological mutations which could give rise to developmental disorders in newly progressing juveniles.

The next most abundant group included proteins such as extracellular SOD and non-selenium glutathione peroxidase, which are involved in cell redox homeostasis. Although proteins involved in cell redox homeostasis were low in numbers, they were greater in abundance compared to other proteins. Therefore, the increased abundance of cell redox proteins reflects the importance of antioxidant systems in oysters and their roles

in protecting cells from the damaging effects of free radicals when living in constant flux in natural environments.

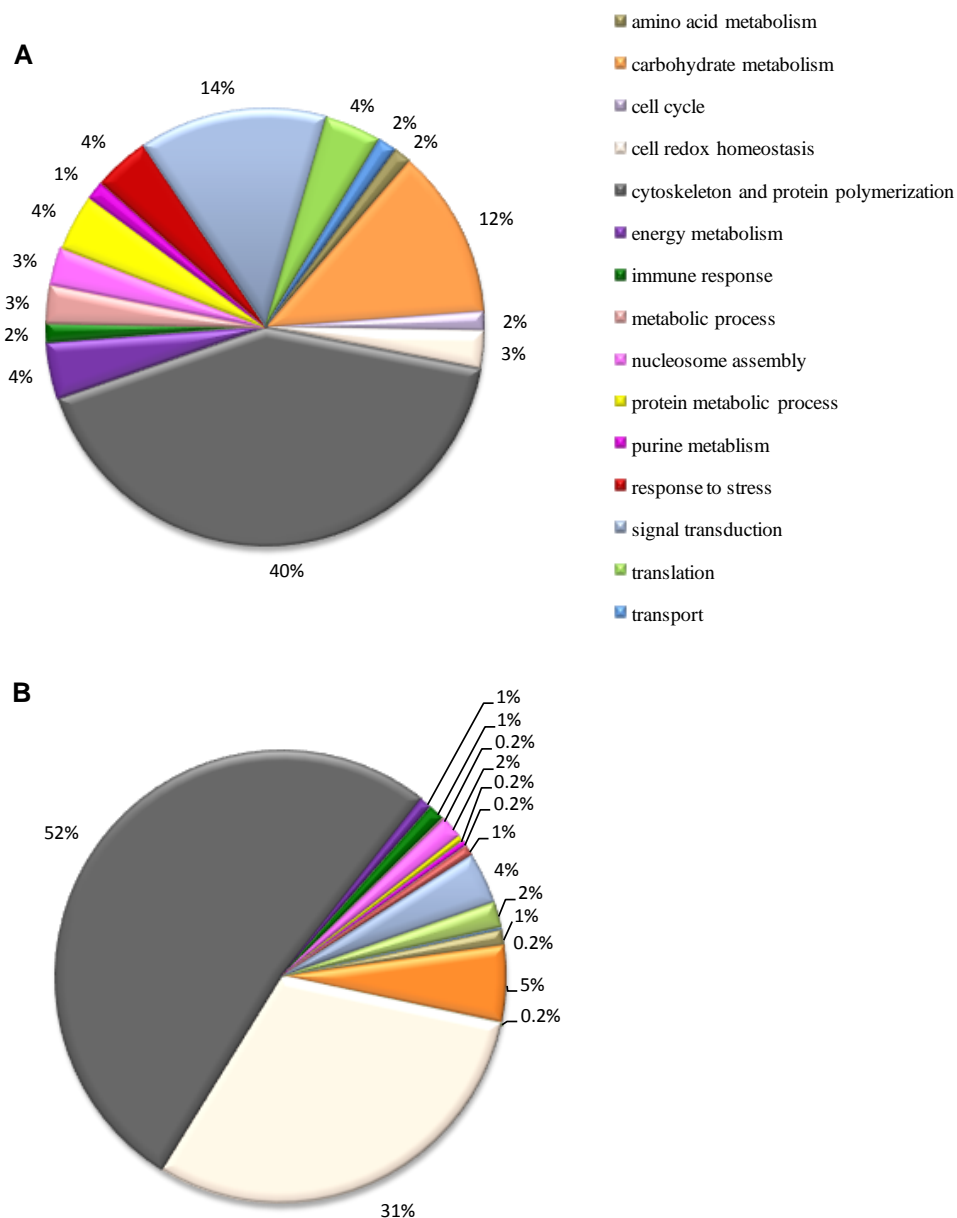


**Figure 4.2** Qualitative and quantitative distribution of proteins found in all metal-exposed and control oysters. Proteins with a known biological process were categorized as a (A) percentage of protein number in each biological process category and (B) percentage of protein abundance in each biological process category, represented by the summed NSAF of proteins. NSAF of each protein represents the average NSAF of the biological triplicate.

#### **4.3.4 Proteins found only in oysters exposed to Zn toxicity**

The 49 proteins expressed only in zinc exposed oysters are listed in Appendix C2, along with their biological processes as found in UniProt. Proteins with known biological processes were graphed as a percentage in each biological process category (Figure 4.3A), and regraphed using combined NSAF values for each category in order to represent their abundance (Figure 4.3B). Figure 4.3A shows that majority of these proteins were involved in signal transduction (19%), followed by those responsible for protein metabolic processes (17%), then by cytoskeleton and protein polymerization (15%). Figure 4.3A also shows equal distribution among the number of proteins involved in translation, transport and carbohydrate metabolism, each comprising 9% of the total proteins found only in oysters exposed to excessive levels of zinc. However, Figure 4.3B shows that the nucleosome assembly proteins (26%), and the cytoskeletal and protein polymerization proteins (25%) were the most abundant, followed by those involved in signal transduction (16%) and protein metabolic process (9%).

Proteins responsible for signal transduction include integrin beta, angiopoietin-4, ankyrin-2, guanine nucleotide-binding protein subunit beta-2-like 1, ras-related protein rab-7a, ras-related protein rab-18-B, ras-related C3 botulinum toxin substrate 1, protein phosphatase 1B, and flotillin-2. Proteins belonging to this category were mainly involved in small GTPase mediated signal transduction pathways such as the MAPK signalling pathway and the HIF-1 signaling pathway. Small GTPases include the superfamily of ras related GTPases, which also encompasses the rho GTPases family. These act as molecular switches, alternating between active and inactive GTP-bound states. This switching activity allows for the regulation of intracellular signal transduction pathways involved in transcriptional regulation of cell cycle control, cell trafficking, and cytoskeletal

organization. In oysters, GTPases mediate the intracellular formation and organization of actin stress fibres in making the cytoskeleton. Activation of these signalling molecules may lead to the assembly and recruitment of more contractile actin:myosin filaments, either to replace damaged cytoskeleton caused by Zn stress in oysters, or to polymerize new actin monomers (G-actin) and organise them into filamentous actin (F-actin) through filament bundling [269]. Cytoskeletal disruption is a known stress response in oysters exposed to greater levels of heavy metals [11, 270], and such disruptions are often facilitated by cellular changes affecting rho family GTPases involved in actin nucleation during stress fibre formation [269]. *Vibrio parahaemolyticus* is a bacterium that infects shellfish including oysters and is known to cause sea-food borne gastroenteritis. A recent study investigated the effects of such pathogenesis by *V. parahaemolyticus* and recorded evidence of cytoskeleton disruption mediated by changes in Rho GTPases expression levels. A similar effect in oysters may also be caused by excessive levels of zinc [271].

A majority of proteins uniquely expressed in response to zinc stress were mainly responsible for proteolysis and folding (Figure 4.3A). Proteins in this category include various proteasome subunits, ubiquitins and ubiquitin related proteins, and programmed cell death protein 6, among others. Other proteins such as T-complex protein 1 subunit delta and vacuolar protein sorting-associated protein 2 were also related to protein folding and sorting. Oysters have naturally evolved to withstand external stresses that often exist in harsh marine environments. Damage caused to the proteins by zinc exposures at higher levels may pose greater stress and create immunosuppressed conditions, and such proteins require removal by proteolysis. Protein turnover requirements or protein biosynthesis under such conditions may be met by utilizing the amino acids made available by protein degradation.

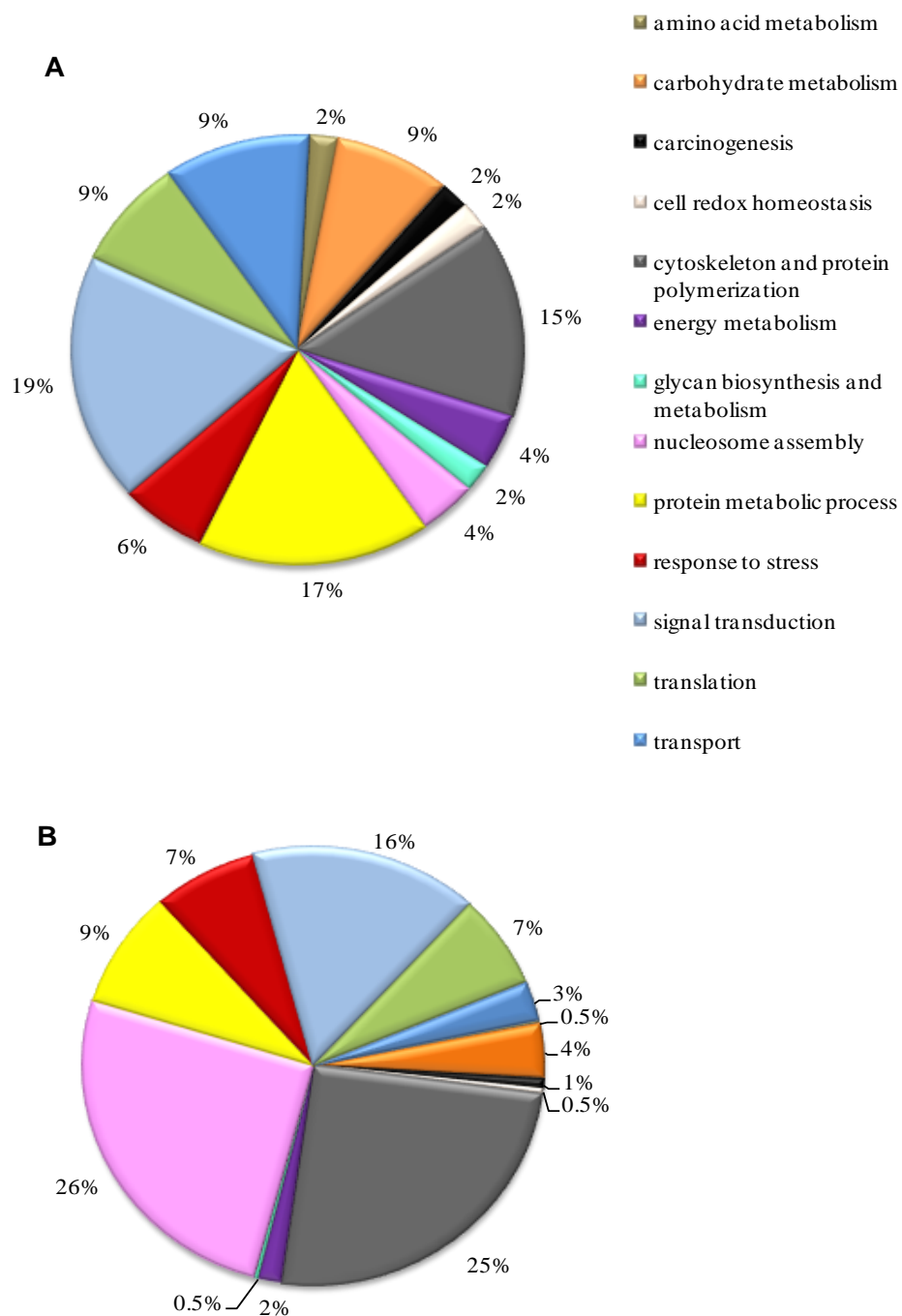


**Figure 4.3** Qualitative and quantitative distribution of proteins found only in oysters exposed to Zn. Proteins with a known biological process were categorized as a (A) percentage of protein number in each biological process category and (B) percentage of protein abundance in each biological process category represented by the summed NSAF of proteins. NSAF of each protein represents the average NSAF of the biological triplicate.

We also identified two proteins involved in nucleosome assembly, namely histone H2B and protein SET, which were the most abundant among those expressed uniquely only in Zn exposed oysters (Figure 4.3B). H2B forms a core component of the nucleosome which is important in chromosomal stability, and is known to play a vital role in DNA repair, replication and transcription regulation. Since histone H2B contributes to the formation of the eukaryotic nucleosome octamer core, an altered abundance of this protein could be associated with chromatin related mechanisms of metal stress tolerance. Methylation and demethylation of histones has been suggested to be strongly associated with gene regulation, by antagonising and enhancing the effects of other histone modifications, including those involving other proteins that bind to histones [272]. The up-regulation of histone H2B may be associated with the Zn metal tolerance characteristic of oysters, and may indicate the recruitment of repair or compensatory mechanisms involving histone pathways to mitigate effects of metal stress.

In a recent study on American oysters, *C. virginica*, histone H2B was found to possess a potent antimicrobial function against human pathogens, *V. parahaemolyticus* and *V. vulnificus*, that usually reside in oysters [273]. It may be possible that this protein has other novel functions such as anti-stress properties against metal toxicity in addition to antimicrobial properties that protect oysters from stressors. Protein SET which shows histone methyltransferase activity, has been recently established to be an essential gene that plays a central role in the assembly of transcriptionally activating or repressing protein complexes. It has been found to be ubiquitously expressed at early developmental stages, as studied in *C. elegans*, and more restricted as development progresses [274]. In oysters, the role of protein SET in the context of metal toxicity remains unclear and needs further research.

#### **4.3.5 Proteins found only in control oysters**

The eight proteins expressed only in non-metal exposed oysters are summarized in Appendix C3 with their biological processes as found in UniProt. Of these, those with known biological processes were graphed as a percentage in each biological process category (Figure 4.4A), and regraphed using combined NSAF values for each category to represent their abundance (Figure 4.4B). Figure 4.4A shows that majority of proteins were involved in protein metabolic processes (37%), followed by cytoskeleton and protein polymerization (25%) and transport (25%). Although the number of proteins involved in protein metabolic processes was greater, Figure 4.4B shows that the most abundant category were the cytoskeleton and protein polymerization proteins (81%). The abundance of proteins involved in protein metabolic process and transport were found to be equally distributed at 9% each, also shown in Figure 4.4B.

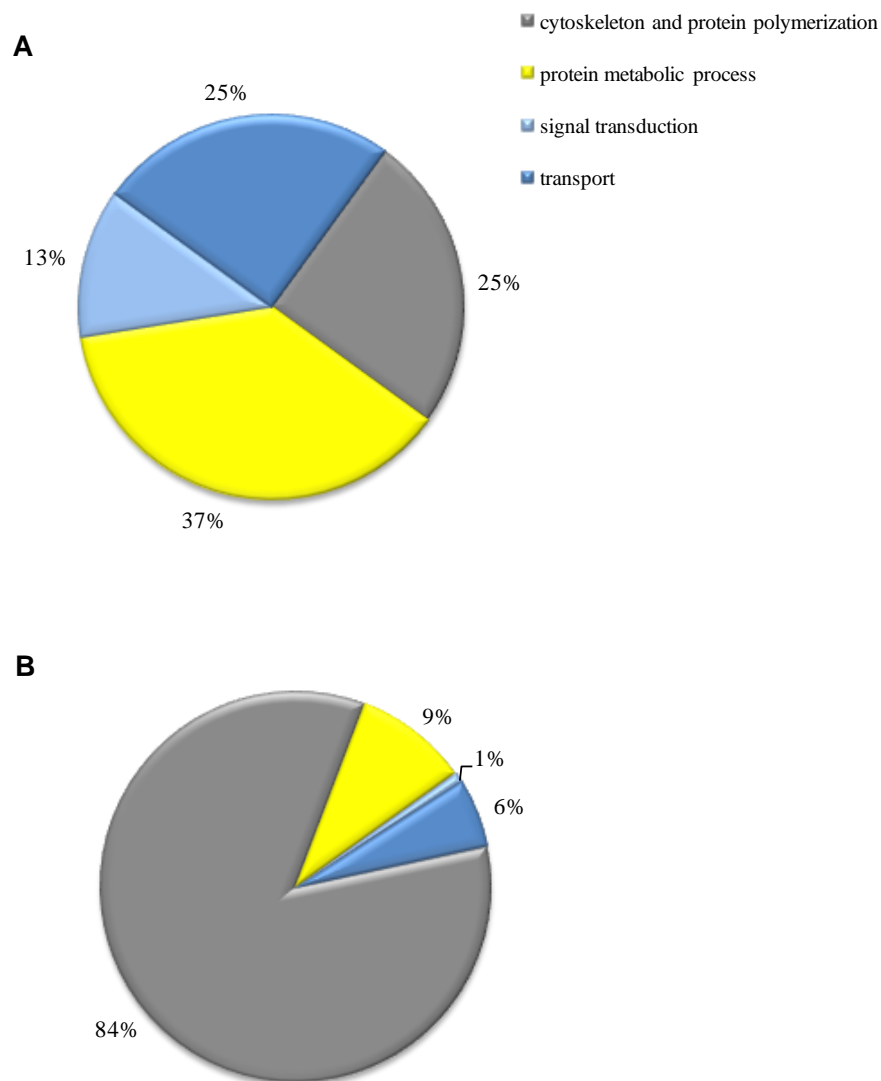


**Figure 4.4** Qualitative and quantitative distribution of proteins found only in non-exposed oysters (controls). Proteins with a known biological process were categorized as a (A) percentage of protein number in each biological process category and (B) percentage of protein abundance in each biological process category represented by the summed NSAF of proteins. NSAF of each protein represents the average NSAF of the biological triplicate.

#### **4.3.6 Proteins found only in oysters exposed to Pb toxicity**

Proteins expressed only in Pb exposed oysters are summarized in Appendix C4 with their biological processes as found in Uni-Prot. Proteins with known biological processes were graphed as a percentage in each biological process category (Figure 4.5A), and regraphed using combined NSAF values for each category in order to represent their abundance (Figure 4.5B). Figure 4.5A shows that majority of proteins were involved in translation (50%) followed by those responsible for signal transduction (10%). In reference to their abundance distribution, Figure 4.5B shows that each of these groups of proteins is also high in relative abundance, where the most abundant category was translation (50%), followed by those involved in signal transduction (16%) and cytoskeleton organization (14%).

Most proteins were involved in translation, consistent with our previous oyster heavy metal stress study [11]. Unique proteins expressed in response to Pb stress which were responsible for translation include several 40S ribosomal proteins such as RP S10, S11, S12, S13, S15, S16, S17, S23, S24, S27, S4 X isoform, and saccin. They also included 60S ribosomal proteins, namely L23 and L27a. Several 40S ribosomal proteins including some of those identified in our study were also reported to be up-regulated in adult oysters exposed to pesticides typically measured in the Vilaine and Arcouest estuaries in France [275]. Of these, RP S10, S11, S13, S15, S17, S23 and S27 were also up-regulated and expressed uniquely in response to Pb stress in Sydney rock oysters, which again is consistent with results shown in Chapter 3 [11].

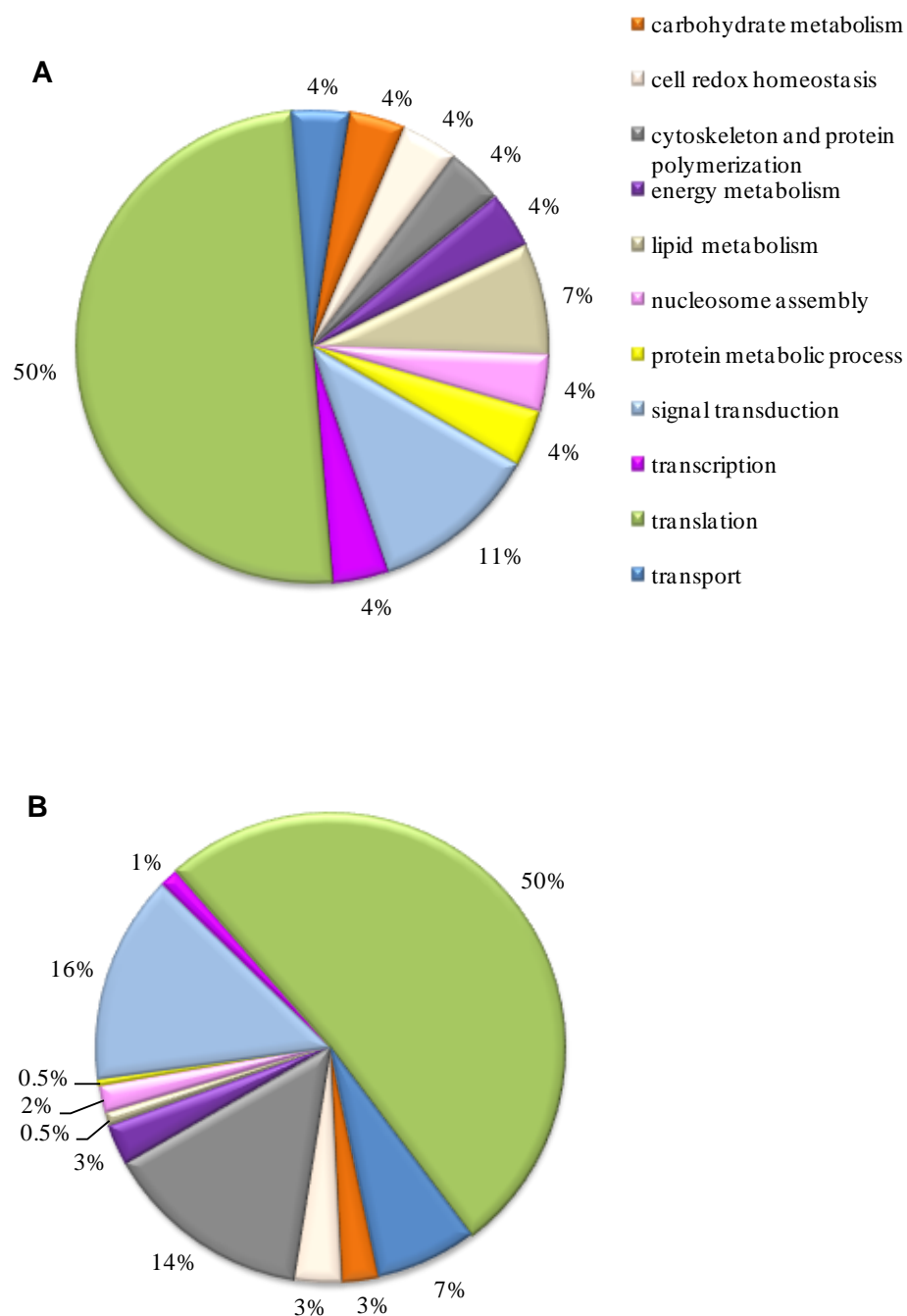


**Figure 4.5 Qualitative and quantitative distribution of proteins found only in oysters exposed to Pb.** Proteins with a known biological process were categorized as a (A) percentage of protein number in each biological process category and (B) as a percentage of protein abundance in each biological process category represented by the sum of NSAF of proteins in each biological process category. NSAF of each protein represent the average NSAF of the biological triplicate.

Of the unique proteins expressed in response to Pb stress, those involved in signal transduction included 14-3-3 protein  $\gamma$ , ras-related protein Rap-1b and a ras family like protein. These proteins are widely involved in Hippo signalling and MAPK signalling pathways. The Hippo signalling pathway is known to be involved in restricting cell proliferation and stimulating apoptosis, for example in regulating organ size control and tumour suppression [276, 277]. In this pathway, protein kinase Hpo activates protein kinase Warts (Wts) by phosphorylation. Wts in turn inactivates the transcriptional co-factor Yorkie (Yki) by phosphorylating it at three sites, thus preventing Yki from initiating DNA transcription of genes associated with cell proliferation. Phosphorylation of Yki at serine-168 by Wts associates the Yki protein with 14-3-3 proteins which anchors Yki in the cytoplasm [278]. This prevents Yki from entering the nucleus, reinforces inhibition of gene expression of growth associated genes, stops reactivation of Yki and further represses cell proliferation.

Identifying unique expression of 14-3-3 protein- $\gamma$  in Pb exposed oysters in this study is interesting because 14-3-3 proteins are known to regulate the cell cycle as well as prevent apoptosis by controlling the nuclear and cytoplasmic distribution of signalling molecules with which they interact. 14-3-3 proteins are also known to perform crucial functions during undisturbed cell divisions, and regulation mechanisms involving 14-3-3 ligand association ensure that mitosis is not prematurely activated prior to the completion of DNA replication. Our results suggest that in order to prevent metal stress from triggering this situation, and to restrain cell proliferation, oysters may be co-opting a Hpo signalling cascade like the one described above, by overexpressing 14-3-3 proteins to sufficiently bind to Yki proteins, localise them in the cytoplasm and thus prevent transcription of growth promoting genes and oncogenes. Therefore, Hpo signalling pathway and 14-3-3 protein- $\gamma$  could act as vital biomarkers for Pb stress at critical

concentrations in oysters and other related species. Further validation by phosphoproteomics studies may allow for such biomarkers to be used in biomonitoring of metal contamination levels, and environmental site evaluations. The 14-3-3 protein  $\gamma$  has been previously identified as a potential biomarker for cytotoxicity effects stemming from exposure to higher concentrations (5nM) of 2,3,4,7,8-pentachlorodibenzofuran (2,3,4,7,8-PCDF) in HepG2 cells in rats [279]. In our study, in response to metal toxicity at higher concentrations it appears that oysters are also using the Hpo signalling pathway in regulating stress from cytotoxicity.

Proteins involved in Mitogen-activated protein kinase signalling pathway (MAPKs) include ras-related protein rap-1b and ras family like protein. The MAPK signalling pathway is integral to the mechanisms by which cells and organisms respond to biological stimuli, including a wide variety of environmental stressors. Mizuno *et al.* characterized the *Caenorhabditis elegans* vhp-1 gene, encoding an MAPK. Their results indicated that loss-of-function mutations in each component in the pathway resulted in hypersensitivity of *C. elegans* to heavy metals, and this kind of hypersensitivity is also quite possible in oysters. Their results suggest that VHP-1 could play a pivotal role in the integration and fine-tuning of stress responses regulated by the MAPK pathway [280]. Therefore, both the Hpo signalling pathway and MAPK signalling pathways are stress responsive and could act as key indicators of the effects of Pb metal stress response in oysters.

Annexin is involved in transport as well as in the calcium dependent phospholipid binding of apoptotic cells to the outer phospholipid plasma membrane for removal via phagocytosis. This occurs through the translocation of phosphatidylserine onto the plasma membrane. A study on oyster hemocytes revealed the predominance of annexin associated

removal of damaged hemocytes due to high cadmium cytotoxicity when subjected to 200-1000  $\mu\text{mol.l}^{-1}$  Cd, and in addition to this they observed necrosis of oyster hemocytes when exposed to such high concentrations of cadmium [281]. Annexins have been successfully used to assay apoptotic cells both *in vitro* and *in vivo* [282]. Since our study involves hemolymph samples that contain hemocytes, unique expression of annexin in oysters exposed to Pb stress suggests the presence of severe cytotoxic conditions causing a weakened immune system, where a similar mechanism involving annexin associated removal of damaged apoptotic hemocytes could take place. Therefore, this protein can be a useful biomarker of the cytotoxicity levels of metals in the environment. Quantitative measurement of annexin in oysters could not only reveal their biological status but also reflect the degree of impact caused by metal contamination of the site.

#### **4.3.7 Proteins found only in oysters exposed to Cu toxicity**

Proteins expressed uniquely in Cu exposed oysters are summarized in Appendix C5 with their biological processes as found in Uni-Prot. Proteins with known biological processes were graphed as a percentage in each biological process category (Figure 4.6A), and regraphed using combined NSAF values for each category in order to represent their abundance (Figure 4.6B). Figure 4.3A shows that majority of proteins were involved in translation (21%) followed by those responsible for protein metabolic processes (19%) and then by proteins involved in signal transduction (13%). However, Figure 4.3B shows that the most abundant group of proteins belong to translation (35%), followed by protein metabolic process (29%), cytoskeleton and protein polymerization (8%). Although there were many proteins that belonged in the signal transduction category (11%), their overall abundance was low (4%).

Proteins involved in translation included ribosomal proteins from the 40S small ribosomal subunit such as 40S RP S3 and S3a, and ribosomal proteins from the 60S large subunit such as 60S acidic RP P0, RP L4, RP L5, RP L7a and RP L19. Ribosomal proteins RP L4, RP L5 and RP L7a were also found to be differentially expressed in 24 h post hatch larvae of fathead minnow, *Pimephales promelas*, after copper exposure up to 200µg/L in 48 h toxicity tests [283]. Other uniquely expressed proteins include glycyl-tRNA synthetase, importin subunit beta, and polyadenylate-binding protein 4. In *S. cerevisiae*, glycyl-tRNA synthetase is known to be expressed by two genes, GRS1 and GRS2 and under normal conditions GRS1 is known to take part in cytoplasmic and mitochondrial activities, whereas GRS2 remains silent. However, under the influence of stress such as high pH or heat shock conditions, GRS2 was found to be up-regulated, more heat stable at higher temperatures, and restored growth defects under stress when compared to GRS1 [284]. This kind of dual functional activity may also help oysters in stress management when exposed to excess heavy metal content. Acute Cu surface stress in *E. coli* revealed numerous differentially expressed proteins including over expression of those mainly involved in transport and protein catabolism, and reduced expression of those involved in translation and protein synthesis [285]. General stress response, signal transduction, carbohydrate metabolism, energy production, cell envelope maintenance, and DNA-replication and repair were also highly represented functions, along with many efflux proteins and multidrug resistance proteins.

Most of the proteins responsible for protein metabolic processes that were unique to Cu exposed oysters were involved in protein folding, sorting and proteolysis, consistent with our results in Chapter 3. They include T-complex protein 1 subunit gamma, tyrosyl-tRNA synthetase, sorting nexin-2, cystatin-A2, 26S proteasome non-ATPase regulatory subunit 2, proteasome subunit beta subunit type 2, putative leucine aminopeptidase,

ubiquitin precursor protein and kyphoscoliosis peptidase. The latter four proteins of this list are clearly involved in proteolysis.

T-complex protein 1 subunit gamma was up-regulated and intensely s-nitrosylated in neuroblastoma cells in response to mitochondrial complex I inhibitor exposures. This treatment could potentially cause neurodegenerative diseases compromising neuronal survival, for instance S-nitrosylation of GAPDH triggers apoptotic cell death in many cell types [286]. T-complex protein gamma, a chaperonin, has been shown to be involved in biogenesis, cilia assembly and structure maintenance, and in the proper folding of cytoskeleton associated proteins [287]. S-nitrosylation of cysteine residues is a post-translational modification that is involved in protein regulation and changes in the s-nitrosylation rates can lead to neurodegeneration. In oysters, heavy metal stress could trigger excess s-nitrosylation, and an imbalance of s-nitrosylation could further cause mitochondrial dysfunction leading to loss of function of several pro-survival proteins and altered signal transduction pathways. As a result of such metal stress, up-regulation of T-complex protein 1 subunit gamma could occur in order to counteract these effects, prevent protein dysfunctions, maintain cytoskeleton integrity and positively regulate other important biological functions such as tumour suppression and cell cycle regulation.

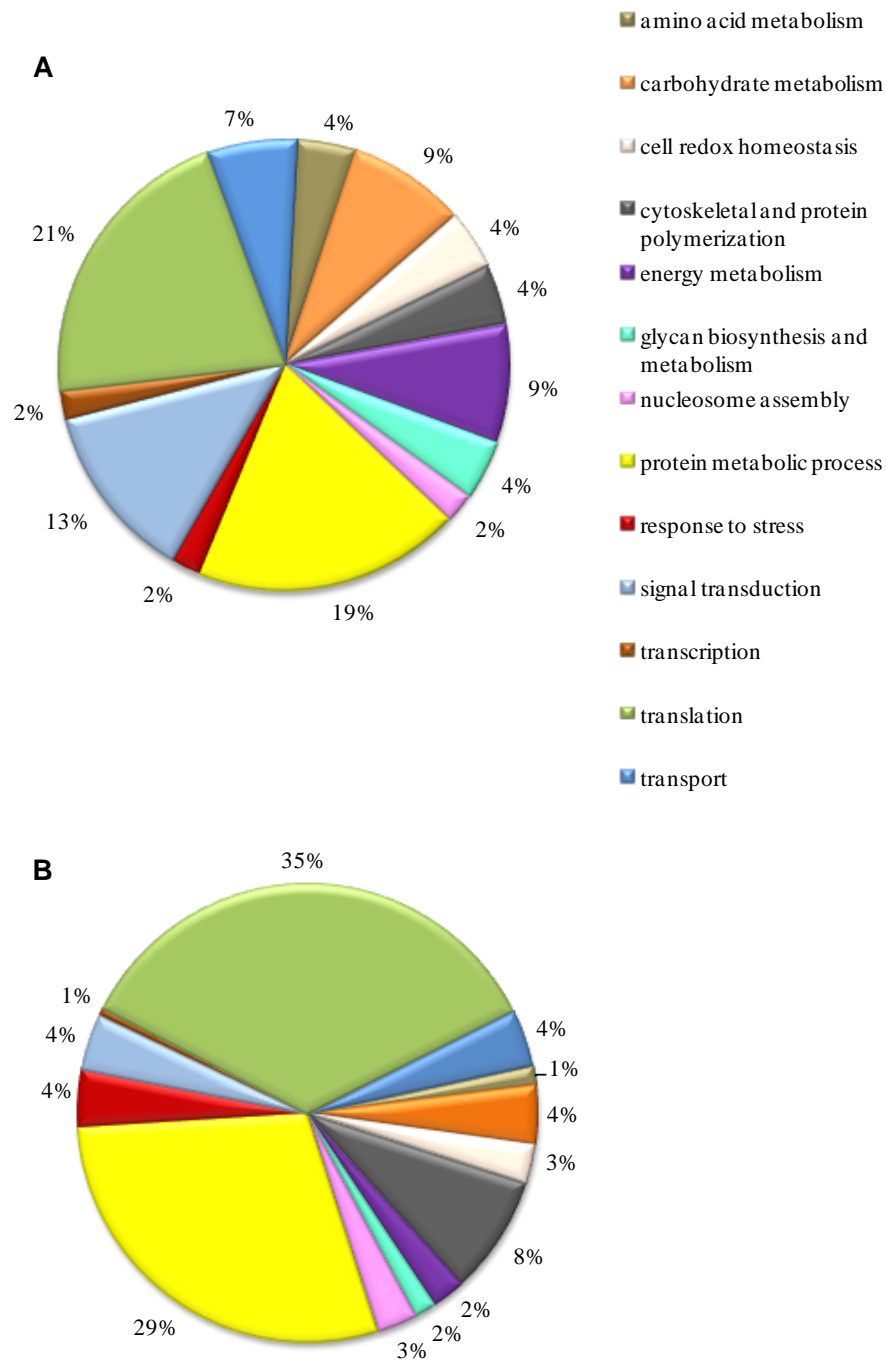


**Figure 4.6 Qualitative and quantitative distribution of proteins found only in oysters exposed to copper. Proteins with a known biological process were categorized as (A) percentage of protein number in each biological process category and (B) percentage of protein abundance in each biological process category represented by the summed NSAF of proteins. NSAF of each protein represent the average NSAF of the biological triplicate.**

In our study, we found tyrosyl-tRNA synthetase was uniquely expressed in oysters exposed to high concentration Cu stress. A recent study has indicated that intravenous exposure of Indium, a metal commonly used in the electronics industry, caused embryotoxicity and external, skeletal and visceral malformations in the fetuses of pregnant rats [288]. Protein expression changes were observed in the embryo and yolk sac membrane of cultured rat embryos exposed to indium, which included increased expression of tyrosyl-tRNA synthetase. In their study, in addition to observing over-expression of tyrosyl-tRNA synthetase, changes in expression levels were also seen in stress proteins, glycolytic pathway and cytoskeletal proteins, indicating yolk sac dysfunction. These biological changes were consistent with our results in oysters, which suggests these proteomic effects are indicative of Cu stress and may be useful targets for metal pollution mitigation and Cu stress therapeutic purposes.

We also identified proteins involved in proteolysis, ubiquitin conjugation pathway and protein catabolic processes. These included kyphoscoliosis peptidase, cystatin-A2, putative leucine aminopeptidase, 26S proteasome non-ATPase regulatory subunit 2, proteasome subunit beta subtype 2, and ubiquitin precursor protein. Metal toxicity affects protein functions commonly by altered protein folding which renders proteins non-functional. Protein degradation is needed for the removal of such damaged, mis-folded and unwanted proteins. This is critical to all cellular organisms, but particularly important in sessile organisms like oysters, which are frequently exposed to several environmental stresses. Hence, cells may regularly scan for proteolytic targets as a means of maintaining protein homeostasis. Previous transcriptomics studies in *C. virginica*, American oysters, revealed several genes vital to the apoptosis system, suggesting *C. virginica* possess advanced apoptosis regulating systems.

From *in vitro* studies, kyphoscoliosis peptidase has been found to play a central role in skeletal muscle disease and muscular dystrophy. A previous study showed degradation of filamin C due to its proteolytic activity, and upon kyphoscoliosis peptidase deficiency, subcellular localization of filamin C was observed in muscle fibres [289]. From *in vivo* studies in mice, this was elucidated by the interaction with several sarcomeric cytoskeletal proteins, namely filamin-c and myosin binding protein C [290]. However, as far as we know, neither kyphoscoliosis peptidase or cystatin-A2 have been previously reported to be differentially expressed in response to metal stress, so our study is the first to report such a finding. Cystatin-A2 shows cysteine type endopeptidase inhibitor activity and belongs to type 1 of the cysteine protease inhibitors. They do not have any disulphide bonds or carbohydrate side chains and exist as single chain polypeptide sequences of around 100 amino acid residues.

Proteins which are targeted to the 26S proteasome are conjugated with a polyubiquitin chain through an enzymatic cascade prior to being sent to the 26S proteasome for degradation into peptides. Although many ubiquitination processes occur as ATP-dependent cycles, the non-ATPase dependent nature of this subunit may involve an altered pathway for energy requirements which remains unclear and needs further research. In plants, this subunit is known to play important roles in diverse processes that include shoot and root apical meristem maintenance, cell size regulation, trichome branching, and stress responses [291]. This subunit was found to have specific roles in the yeast and mammalian proteasomes where it promoted the assembly of the regulatory particle with the 20S core protease of the 26S proteasome [291]. Hence, the regulatory subunit of the 26S proteasome may protect and prevent the core 20S protease from indiscriminate degradation of cytoplasmic or nuclear proteins. Similar to our previous findings, Cu metal stress may result in oxidative damage to proteins due to increase in

abundance of reactive oxygen species in the cells [11]. Over-expression of the proteases, peptidases and proteolytic activities associated with the proteasome proteolytic pathway identified in this study may be indicative of the measures adopted by oysters to facilitate degradation of these damaged proteins, and thus prevent cytotoxicity and maintain homeostasis. Therefore, increased protein expression of the proteasome and proteases in response to Cu stress, as observed in this study, can act as key proteomic signatures indicative of high Cu toxicity. Similar cellular responses involving the proteasome and proteases have previously been reported in *Arabidopsis* in response to Cd stress [291], in *Mytilus trossulus* (bay mussel) in response to heat stress [292] and in rats in response to oxidative stress [293].

#### **4.3.8 Statistically significant differentially expressed proteins identified from quantitative label-free shotgun proteomics**

Proteins that showed a significant change in relative abundance in each treatment group in response to metal stress were identified by performing a t-test using log(NSAF) values, where Log (NSAF) values of proteins in each metal treatment in biological triplicates were compared with those of control samples. Of the 381 reproducibly identified proteins, we found a non-redundant total of 185 proteins that were differentially expressed at statistically significant levels relative to controls based on log(NSAF) ratios. Of these 185 differentially expressed proteins, 14 were detected by both SDS-PAGE and GPF approaches while 146 were found exclusively in the SDS-PAGE dataset and 25 were exclusive to the GPF dataset. All 185 proteins that changed significantly in their expression profiles in response to heavy metal stress were distinguishable from unchanged proteins using Log (NSAF) plots of protein abundance in each metal stress experiment relative to controls (Figure 4.7A and B).

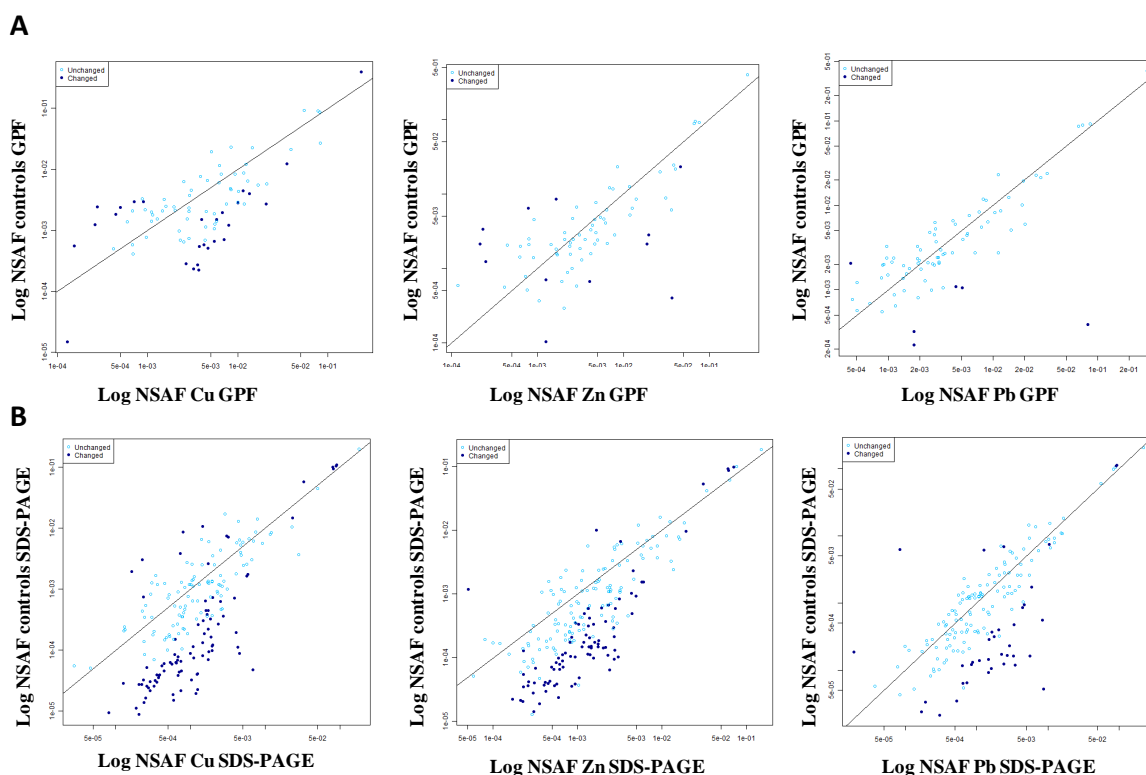


**Figure 4.7** Log NSAF plots of differential and unchanged proteins in the three metal treatments relative to controls (a) GPF datasets (b) SDS-PAGE datasets. Proteins with significant differential expression are shown as darker spots. Proteins with expression levels that did not differ significantly between metal exposures and controls are shown as lighter spots. Up and down regulated proteins are shown as darker spots below and above the diagonal respectively.

These plots provide an informative visual display of both the total number of significantly differentially expressed proteins and the overall trend of their differential expression. A list of the top 50 significantly differentially expressed proteins, as sorted by expression ratios, in response to metal exposures, along with annotation and quantitation information, is shown in Table 4.3 (see Appendix C6 for complete list of 185 differentially expressed proteins in response to metal stresses along with biological process and quantitation information).

#### **4.3.8.1 Proteins differentially expressed in at least two out of three metal exposures**

Differential expression of 143 proteins was associated with single metals (51 for Zn, 71 for Cu, and 21 for Pb), whereas three differential proteins were associated with all three metals (Figure 4.8). The three differential proteins that changed in protein expression levels in response to each of the three metals were phosphoglycerate kinase, muscle lim protein and 78 kDa glucose-regulated protein; they were up-regulated by an average of 24-, 3- and 4-fold respectively. Identification of phosphoglycerate kinase and muscle Lim protein as differentially expressed proteins in response to metal stresses were possible only upon the availability of the Oyster genome sequence, as these proteins were not identified previously when oyster metal stress data were analyzed with our *Bivalvia* cross species database [11].

Another group of 25 proteins showed differential expression in response to both Cu and Zn but not Pb, while seven proteins were differentially expressed in response to Pb and Zn but not Cu. Three proteins were differentially expressed in response to both Cu and Pb but not Zn (Figure 4.8). Of the 185 differentially expressed proteins, those involved in cytoskeleton and protein polymerization constituted 16%, followed by those involved in carbohydrate metabolism, protein metabolic process, signal transduction, translation and transport proteins, with each biological process category constituting 13% of the total.

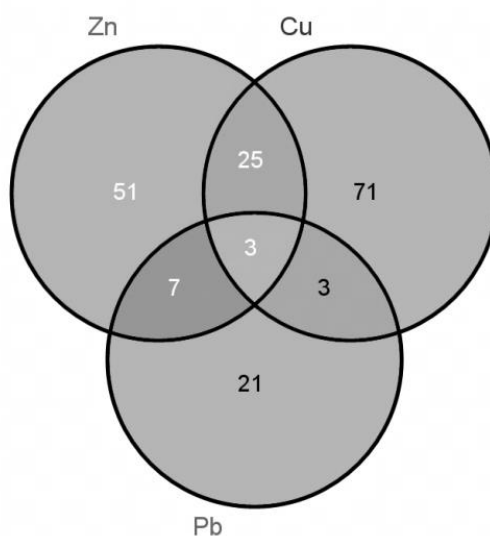


**Figure 4.8** Number of differentially expressed proteins in response to heavy metal exposures in Sydney Rock oysters. Numbers represent the total number of non-redundant differentially expressed proteins in response to metal stress in either or all of the metal exposures. Differentially expressed proteins in response to each metal may be either up- or down-regulated relative to controls.

We also found that signal transduction proteins were increased in response to different metal stresses. For example, 14-3-3 protein gamma was increased in expression by 51 fold in response to Cu and 16 fold in response to Pb, while ADP-ribosylation factor protein was increased in expression by 14 fold in response to Pb and 18 fold in response to Zn. Investigation of spatial memory disturbances in mice after traumatic brain injury revealed that ADP ribosylation of 14-3-3 gamma protein was associated with the impairment of spatial memory [294]. ADP ribosylation of 14-3-3 gamma protein occurred through the depletion of  $\text{NAD}^+$  levels in brain cells by the poly ADP-Ribose polymerase-I protein. Further, the percentage of impairment of spatial memory was indirectly proportional to  $\text{NAD}^+$  levels existing in cells after stress imposition and directly proportional to the degree of inhibition of ADP ribosylation of 14-3-3 gamma protein. This intriguing observation in oysters requires further research.

**Table 4.3 Abundance changes of 50 most differentially expressed proteins after heavy metal stress imposition in Sydney rock oysters, identified and quantified by label-free shotgun proteomics.**

Identifier	Protein name	UniProt ID	Biological process category*	Mr KDa	Ratio of differential expression <sup>a,b</sup>
<b>Proteins in response to Pb stress only</b>					
gi 405967637	Tropomyosin	K1QNV6	Cy/P	39	+Control-Pb↓75.5
gi 405964878	40S ribosomal protein S11	K1QN79	translation	22.1	-Control+Pb↑29.2
gi 405952804	40S ribosomal protein S17	K1QGB4	translation	16.2	-Control+Pb↑20.2
gi 405955817	40S ribosomal protein S24	K1PUV4	translation	21.1	-Control+Pb↑19.3
<b>Proteins in response to Cu stress only</b>					
gi 405966815	Uncharacterized protein	K1Q620	unknown	12.8	-Control+Cu↑60.7
gi 405969654	Sodium/potassium-transporting ATPase- $\alpha$	K1R0L4	energy metabolism	11.6	-Control+Cu↑34.3
gi 405965244	Dolichyl-diphosphooligosaccharide--protein glycosyltransferase subunit 2	K1QHM2	glycan biosynthesis and metabolism	77.1	-Control+Cu↑31.8
gi 405954873	Uncharacterized protein	K1QKD6	unknown	13.5	-Control+Cu↑31.2
gi 405959695	Clathrin heavy chain 1	K1PNR3	transport	191.8	-Control+Cu↑30.6
gi 405952567	$\beta$ -1,3-glucan-binding protein	K1PFG1	carbohydrate metabolism	284.7	-Control+Cu↑23.3
gi 405946057	Talin-2	K1PFH4	Cy/P	27.4	-Control+Cu↑20.8
gi 405953294	Kyphoscoliosis peptidase	K1PQ64	PMP	25.6	-Control+Cu↑20.0
gi 405962799	Tyrosine-protein kinase transforming protein Src	K1PVR8	signal transduction	51.2	-Control+Cu↑18.5
gi 405971478	S-formylglutathione hydrolase	K1QRD4	carbohydrate metabolic process	31.2	-Control+Cu↑18.0
gi 405953394	Dynein heavy chain, cytoplasmic	K1QHK9	Cy/P	561.2	-Control+Cu↑17.3
gi 405973144	Importin subunit beta-1	K1R2V1	translation	224.1	-Control +Cu↑16.6
gi 405964118	Talin-3	K1Q6W3	Cy/P	61.8	Cu↑16.1
gi 405978156	Plasma membrane calcium-transporting ATPase 3	K1QZU8	energy metabolism	151.3	-Control+Cu↑15.1
gi 405970598	Citrate synthase	K1RM80	carbohydrate metabolism	49.4	-Control+Cu↑14.7

Identifier	Protein name	UniProt ID	Biological process category*	Mr KDa	Ratio of differential expression <sup>a,b</sup>
gi 405964548	Heat shock protein 70 B2	K1QG22	response to stress	69.7	-Control+Cu↑13.6
gi 405961702	Myosin regulatory light chain A, smooth adductor muscle	K1Q801	Cy/P	14.6	+Control-Cu↓13.4
gi 405957027	Heterogeneous nuclear ribonucleoprotein K	K1Q324	transcription	60.4	-Control+Cu↑13.1
<b>Proteins in response to Zn stress only</b>					
gi 405965393	Actin, cytoplasmic	K1QPJ1	Cy/P	41.6	-Control+Zn↑92.0
gi 405961865	Ubiquitin-like modifier-activating enzyme 1	K1R1M7	PMP	97.9	-Control+Zn↑24.7
gi 405965171	Uncharacterized protein	K1Q2H5	unknown	65.2	-Control+Zn↑23.8
gi 405966532	Tripartite motif-containing protein 2	K1Q5A6	PMP	56.2	+Control-Zn↓23.2
gi 405959640	Transitional endoplasmic reticulum ATPase	K1PVA1	PMP	88.6	-Control+Zn↑21.7
gi 405976041	Ras-related C3 botulinum toxin substrate 1	K1RGQ0	signal transduction	34.0	-Control+Zn↑21.1
gi 405970591	Universal stress protein A-like protein	K1QWC6	response to stress	16.2	-Control+Zn↑14.8
gi 405975785	Filamin-A	K1RZ99	Cy/P	90.7	+Control-Zn↓14.6
<b>Proteins in response to lead and copper</b>					
gi 405965638	Tubulin alpha-1C chain	K1QQ68	Cy/P	50.1	-Control+Pb↑166; -Control+Cu↑143
gi 405968450	Calcium-transporting sarcoplasmic ATPase	K1QA13	energy metabolism	11.00	-Control+Pb↑7.1; -Control+Cu↑55
gi 405950430	14-3-3 protein gamma	K1PPQ1	signal transduction	28.5	-Control+Cu↑51.2; -Control+Pb↑16
<b>Proteins in response to lead and zinc</b>					
gi 405974492	40S ribosomal protein S14	K1QQB6	translation	16.3	-Control+Pb↑35.1; -Control+Zn↑14.1
gi 405961012	Superoxide dismutase [Cu-Zn]	K1QDI4	oxidation-reduction processes	15.9	-Control+Pb↑16.2; -Control+Zn↑9.3
gi 405965232	60S ribosomal protein L12	K1Q2L2	translation	18.7	Pb↑15.0; Zn↑9.0
gi 405961802	ADP-ribosylation factor	K1PTH4	signal transduction	124.2	-Control+Pb↑14.3; -Control+Zn↑18.8
<b>Proteins in response to lead, copper and zinc</b>					
gi 405963233	Phosphoglycerate kinase	K1QCC1	carbohydrate metabolic process	43.0	-Control+Pb↑7.0; -Control+Cu↑37.8; -Control+Zn↑29.3

Identifier	Protein name	UniProt ID	Biological process category*	Mr KDa	Ratio of differential expression <sup>a,b</sup>
<b>Proteins in response to copper and zinc</b>					
gi 405961963	Spectrin beta chain	K1QFR9	Cy/P	280.0	-Control+Cu↑39.4; -Control+Zn↑21.0
gi 405959469	Talin-1	K1Q2B5	Cy/P	60.9	-Control+Cu↑30.1; -Control+Zn↑24.3
gi 405972993	Ras-like GTP-binding protein Rho1	K1QVS0	signal transduction	36.1	-Control+Cu↑24.7; -Control+Zn↑37.2
gi 405957030	Ras GTPase-activating-like protein IQGAP1	K1PNK5	signal transduction	186.5	-Control+Cu↑17.6; -Control+Zn↑6.5
gi 405962453	Cdc42-like protein	K1PJ53	signal transduction	21.3	-Control+Cu↑16.5; -Control+Zn↑20.8
gi 405960427	PDZ and LIM domain protein 5	K1PQ23	unknown	55.2	-Control+Cu↑16.5; -Control+Zn↑6.2
gi 405959086	UTP--glucose-1-phosphate uridylyltransferase	K1Q1D1	carbohydrate metabolism	57.2	-Control+Cu↑16.1; -Control+Zn↑10.2
gi 405951708	Ribosomal protein L19	K1PDL3	translation	23.5	-Control+Zn↑15.4; -Control+Cu↑9.9
gi 405964355	Calpain-A	K1Q056	PMP	114.7	-Control+Cu↑13.0; -Control+Zn↑10.9
gi 405965075	Aldehyde dehydrogenase, mitochondrial	K1QNT7	amino acid metabolism	56.9	-Control+Cu↑11.4; -Control+Zn↑11.7
gi 405977633	1,4-alpha-glucan-branching enzyme	K1QYM7	carbohydrate metabolism	79.2	-Control+Cu↑10.5; -Control+Zn↑14.2
gi 405950592	Phosphoglucosyltransferase-1	K1PQD4	carbohydrate metabolism	64.8	-Control+Cu↑9.7; - Control+Zn↑14.7

<sup>c)</sup> Up- and down-regulation of proteins in response to metal stress relative to controls have been indicated by an upward arrow, '↑' and a downward arrow, '↓' respectively.

<sup>d)</sup> Presence and absence of proteins in response to metal stress relative to controls have been indicated by a plus, '+' and a minus, '-' sign respectively.

\* Cy/P and PMP refers to the biological process categories namely, cytoskeleton and protein polymerization and protein metabolic process.

Comparison of protein identification data using the Bivalvia database versus the *C. gigas* Oyster protein sequence database revealed that use of a complete genome resulted in greater protein count (by 226%) and differential proteins (by 230%). Further, this enhanced the biological relevance of the peptide quantitation data and differential proteins, and enabled a more accurate picture of the molecular cascade of events that occur inside the particular organism, as opposed to a related species. Therefore the ability to identify proteins is dependent on the content of protein database employed.

#### 4.3.8.2 Proteins differentially expressed in response to Pb exposure

We identified 34 proteins (listed in Appendix C6) that responded to Pb exposure showing noticeable increases in expression, of which 21 proteins changed specifically due to Pb exposure and 12 proteins were among the top 50 differentially expressed proteins in response to heavy metal stress in this study (Table 4.3). Tropomyosin was down-regulated by 75 fold in Pb exposed oysters compared to controls. The remaining eleven of the 12 proteins that responded to Pb exposure were found to be up-regulated, which included several ribosomal proteins (S11, S14, S24, S17 and L12), tubulin alpha-1C chain, calcium-transporting sarcoplasmic ATPase, 14-3-3 protein gamma, superoxide dismutase [Cu-Zn], phosphoglycerate kinase and ADP-ribosylation factor. Their expression level differences relative to controls varied widely, from 7-fold for phosphoglycerate kinase to 166.1 fold for tubulin alpha 1C-chain. It is interesting to note that of all the ribosomal proteins differentially expressed in response to metal stress, 55% were differentially expressed in response to Pb exposure, and such a substantial number was not observed in any other metal exposures. This result was consistent with our previous findings obtained in Chapter 3. Tubulin alpha-1C chain has been identified as a potential biomarker for periodontitis which is an inflammatory disease that affects the connective tissues and bone mineral reabsorption, and is caused by *Porphyromonas gingivalis* [295].

Further to this, paramyosin, and myosin heavy and light chains, were also down-regulated in Pb stress conditions relative to controls, thus causing maximum cytoskeletal damage. Tubulin alpha-1C has been reported as one of few molecular signatures for cardiac ion channel regulation affected by murine P19 embryonal carcinoma cells [296]. It has also been reported as a potent biomarker for both early stages of regeneration in cerebellum of the brain in the central nervous system in fish [297], and toxicity response

to 2,3,7,8-tetrachlorodibenzo-p-dioxin which is a potent environmental toxin for humans [298].

Other proteins specifically affected due to Pb exposure included phosphoglycerate kinase and calcium-transporting sarcoplasmic ATPase. The ATP-producing glycolytic enzyme phosphoglycerate kinase has been shown to be associated with the sarcoplasmic reticulum in cardiac and skeletal muscle [299]. They may function together to provide energy in the form of ATP for driving the  $\text{Ca}^{2+}$  transport pump, which is vital in maintaining cellular  $\text{Ca}^{2+}$  homeostasis. Cell signalling appears to be closely connected to maintaining redox balance in oysters and this is another opportunity where further enquiry will lead to a better understanding.

Metal toxicity in Sydney rock oysters likely causes significant oxidative damage and potent inflammatory response in vital organs and tissue components. This may further compromise survival capabilities and may also be extended to other organisms when exposed to metal toxicity.

#### **4.3.8.3 Proteins differentially expressed in response to Zn exposure**

In this study, we also identified a total of 86 differentially expressed proteins affected by Zn, of which 51 showed differential protein expression specific to Zn stress (Figure 4.8) and 25 proteins were among the top 50 differentially expressed proteins in response to heavy metal stress in this study (Table 4.3). These 25 proteins included spectrin- $\beta$ , talin-1, tubulins, filamins, actins, ras-like GTP-binding protein Rho, ras GTPase-activating-like protein, ribosomal proteins L19 and S14, ubiquitin-like modifier-activating enzyme 1, UTP-glucose-1-phosphate uridylyltransferase, calpain-A protein and aldehyde dehydrogenase. Twenty-three of the 25 proteins were up-regulated in expression,

where fold differences relative to controls varied widely from 6.5 for ras GTPase-activating-like protein to 92 fold for cytoplasmic actin. Among the first 50 differentially expressed proteins, tripartite motif-containing protein-2 (TRIM2) and filamin-A were the only two proteins that was down-regulated in response to Zn stress. Spectrins, talin-1, tubulins, filamins and actins are major constituents of the cytoskeletal and protein polymerization network. Each of these proteins maintain a dynamic equilibrium in cytosol and membrane fractions, and collectively they are known to exhibit specific patterns of association with focal contacts between cell and substrates, indicative of a vital role in cytomatrix architecture, microfilament association and movement [300].

Two proteins related to these, severin and plastin, were found in all metal stress conditions as well as controls (see section 4.3.3). Severin shows an evolutionary relationship with villin, fragmin and gelsolin, and is known to have large repeating sequence segments. However, these multiple repeats within the actin-severing proteins have yet to be related to any known function. Plastin, which is an actin binding protein, has been found to be involved in bundling of actin in the absence of calcium and is known to be conserved and expressed in most tissues of eukaryotes. Increased expression of these proteins may collectively indicate an increase in activities involving actin polymerization and cytoskeletal organisation. Such efforts in activities concerning cytoskeletal organisation and recruitment of new proteins to replace damaged ones reflect the importance of cytoskeletal maintenance in oysters.

A recent study has shown in mice that spectrin-2 may target other proteins that are critical to structural and regulatory aspects of the cell to membranes in the heart and brain. It was also found to regulate a sodium ion transport mechanism, in which phosphorylation of Ca/calmodulin-dependent kinase was targeted by spectrin [301].

TRIM2 is known for being involved in tumorigenesis and viral infections but the function of the protein remains largely unclear. In humans, it has been shown to function as a ubiquitin ligase that binds and regulates the neurofilament light subunit through ubiquitination, and when deregulated it triggers neurodegeneration [302]. PDZ and Lim domain proteins help to scaffold cytoskeletal elements that form muscle fibres and provide a link to signalling by connecting certain kinases and other transcription factors with mechanical stress-strain sensors. In addition to this, they are known to play an important role in heart development and in the regulation of cardiomyocyte cell expansion in mice, where over-expression was reported to promote progression of heart hypertrophy [303]. Based on sequence similarity for Lim and PDZ domains of mouse, these proteins in oysters may also be involved in causing hypertrophy as a result of severe metal toxicity.

Taken together, these protein expression changes suggest that, as a result of Zn toxicity, addressing the damages caused to the cytoskeleton and initiating replacement of those damaged proteins may be a priority response for Sydney rock oysters in order to maintain cytoskeletal integrity which is indispensable for survival.

#### 4.3.8.4 Proteins differentially expressed in response to Cu exposure

The expression level of 102 proteins responded to Cu exposure; of these 71 showed differential protein expression specific to Cu (Figure 4.8) and 34 were among the top 50 differentially expressed proteins for Cu stress. Of these 34 differential proteins in the top 50, 18 proteins showed differential expression to Cu only, 12 showed significant protein expression changes to both Cu and Zn, and 3 proteins responded to both Cu and Pb. All of these proteins that responded to toxicity for more than one metal showed similar expression patterns, which could indicate common upstream signalling pathways leading to their transcriptional initiation.

Among the top 50 differential proteins, only two were down-regulated in response to Cu stress; myosin regulatory light chain A from the smooth adductor muscle, and alanopine dehydrogenase, which is involved in glycerol metabolism. The observed expression differences relative to controls ranged from a 13.4 fold down-regulation for myosin regulatory light chain A protein, to 143-fold up-regulation for tubulin  $\alpha$ -1C. An unknown uncharacterised protein (GI 405966815) was up-regulated by 60 fold and was the next highest after tubulin  $\alpha$ -1C to show differential regulation in response to Cu stress. The latter did not show any significant homology with any known protein upon a BLAST search and appears to be a novel metal stress response protein against Cu toxicity which is an obvious and interesting target for further research.

Some of the highest fold changes among the up-regulated proteins after Cu exposure included tubulin  $\alpha$ -1C chain, plasma membrane calcium-transporting ATPase 3, sodium/potassium-transporting ATPase  $\alpha$  subunit, calcium-transporting sarcoplasmic ATPase, dolichyl-diphosphooligosaccharide glycosyltransferase subunit 2, clathrin heavy chain 1, talins 1,2 and 3, tyrosine-protein kinase transforming protein S-formylglutathione

hydrolase, dynein heavy chain, importin  $\beta$  subunit 1, 14-3-3  $\gamma$  protein, citrate synthase, heat shock protein 70 B2, ras-like GTP-binding protein Rho1, ras GTPase-activating-like protein IQGAP1, cdc42-like protein, PDZ and Lim domain protein (Table 4.3). It was intriguing to find that tubulin alpha-1C chain was up-regulated a striking 143-fold relative to control as a result of Cu exposure, while it also changed by 166 fold in response to Pb but showed no expression changes in response to Zn. As previously mentioned in this study, tubulin alpha-1C chain, a cytoskeletal protein, has shown differential protein expression in inflammatory response towards periodontitis resulting in destruction of connective tissues [295], as a potent biomarker for early stages of regeneration in cerebellum of the brain in the central nervous system in fish [297], and in toxicity response to 2,3,7,8-tetrachlorodibenzo-p-dioxin (TCDD) which is a potent environmental toxin in humans [298]. Based on the results in this study, tubulin alpha-1C is also a potential biomarker for Pb and Cu metal toxicity in oysters, and further research is needed in developing this protein as a useful tool for field use in environmental biomonitoring for metal contamination.

Cu exposure caused significant increases in intracellular ATPase levels, indicating a severe demand and disturbance of the energy metabolism. It appears that the observed increase in protein expression levels of V-type proton ATPase A and ATPase E proteins, calcium-transporting sarcoplasmic ATPase, sodium/potassium-transporting ATPase subunit alpha, succinate dehydrogenase flavoprotein subunit B, and plasma membrane calcium-transporting ATPase 3 would result in significant ADP production from increased utilisation of ATP. These protein expression changes could be directed to address the damage caused to tissues by metal toxicity, and the subsequent need to retain structural integrity and defence of the oysters by replenishing vital proteins such as cytoskeletal proteins which are prone to such damage.

Dolichyl-diphosphooligosaccharide glycosyltransferase subunit 2 was the only differential protein from the top 50 most differential proteins that was involved in glycan metabolism, and was up-regulated by 31 fold after Cu stress. This enzyme belongs to the eukaryotic ribophorin II proteins and is associated with the biosynthetic pathway of protein N-linked glycosylation via asparagine. The mammalian oligosaccharyl glycosyltransferase protein complex affects N-glycosylation of newly synthesised polypeptides, and has previously been found differentially expressed in response to gastric cancers [304]. It is possible that this protein may play a role in protecting other proteins from being affected by Cu stress by post-translationally modifying them via glycosylation.

Interestingly, alanopine dehydrogenase involved in the glycerol catabolic process, and myosin regulatory light chain which is vital for regulation of both smooth muscle and non-muscle cell contractile activity were down-regulated in response to Cu metal toxicity by 11 and 13 fold respectively. This suggests that Cu stress may cause reduced myosin II motor function, which is known to be regulated by phosphorylation of the regulatory light chain. It may also indicate a link to the possible utilisation of glycerol to meet glucose and energy shortages. Glycerol catabolic processes involve the breakdown of glycerol-3-phosphate, a phosphoric monoester of glycerol. Within this process in oysters, alanopine dehydrogenase is known to catalyze the reductive imination between pyruvate and alanine, or glycine, while utilizing NADH to produce novel imino acids called 2,2'-iminodipropionic acid (alanopine), or 2-methyliminodiacetic acid (strombine) [305]. The physiological role of this enzyme was found to be in the maintenance of a redox balance during anaerobiosis in the adductor muscle and heart of the oyster [306].

In two bivalves, *R. Cuneata* and *M. edulis*, alanine and succinate were reported as being produced by glucose degradation [307, 308]. In their study, Simpson and Awapara [309] established that the pathway leading to the formation of succinate was mediated by phosphopyruvate carboxylase, and indicated the presence of competition for a common substrate such as phosphoenolpyruvate, which occurred between the enzymes NAD oxidoreductase and malate dehydrogenase. Such was also the case between the following enzymes: NAD oxidoreductase or octopine dehydrogenase; pyruvate phosphotransferase or pyruvate kinase; oxaloacetate carboxylase or phosphopyruvate carboxylase; and phosphopyruvate carboxylase or pyruvate kinase. Studies on the kinetic and regulatory properties of some of these enzymes in *M. edulis* and *C. gigas* [310-312] suggested that the regulation of these enzymes was dependent on intracellular pH and levels of alanine and fructose 1,6-bisphosphate. For example, phosphopyruvate carboxylase may be activated under anaerobic conditions, while the activity of pyruvate kinase may be reduced [305].

Recent studies on the isolated heart of the oyster are of particular interest because they clearly demonstrated that only a small fraction (4%) of the glucose converted to succinate during 1 hr of anoxia [305], contrasting with the studies on *R. cuneata* and *M. edulis* where as much as 50% of the glucose was converted to succinate [307, 308]. In the anoxic oyster heart, most of the glucose was converted to alanopine and an unidentified amino acid which is metabolically linked to alanine and pyruvate, while aspartate was the major metabolic source of succinate [313]. The enzyme alanopine dehydrogenase was predominantly found in the muscles of the oyster (adductor and heart). It was reported to comprise a single polypeptide, with an unusually low affinity for alanine or glycine, and strong inhibition from succinate at low pH. These properties of the enzyme may suggest a possible role in redox regulation.

#### **4.3.8.5 Novel proteins as potential biomarkers of stress exposure**

Of the total of 185 differentially expressed proteins identified in this study, three proteins were unknown, uncharacterised, novel proteins which did not match to any known protein upon a BLAST search. We have collectively termed these as ‘novel metal toxicity responsive proteins’. Of these three novel metal responsive proteins, two were specific to Cu toxicity, whereas the third protein was specific to Zn toxicity. Since these proteins showed increased expression levels of up to 60 fold, further research targeted to characterising these proteins could lead to a not only understanding their role in the cellular machinery but also in maximising their potential as useful protein signatures for metal toxicity tests.

#### **4.3.9 Metabolic pathways**

In addition to analysing protein expression information by categorisation on the basis of which stresses were involved, we also examined the impact of the whole range of metal stresses on specific metabolic pathways. The effect of heavy metal stress on important metabolic pathways or processes was determined by analysing the change in abundance of the proteins or enzymes involved in important metabolic pathways in response to heavy metal stress. The results of this analysis are summarized in Figure 4.9.

#### **4.3.9.1 Cytoskeleton and protein polymerization**

The abundance of cytoskeleton and protein polymerization related proteins such as tubulins, actins, talins, spectrin, filamins, myosins, vinculins, collagens, myophilins, dyenins and kinesins were considered. Twenty-nine of these were found to be statistically differentially expressed in our study, and of these 29, tubulin alpha-1C, actin, spectrin beta, talin-1, talin-2, talin-3 and dynein heavy chain subunit increased significantly in abundance at high metal toxicity, while tropomyosin, myosin regulatory light chain subunit and filamin-A decreased in abundance at high metal toxicity (Figure 4.9). Tubulin alpha-1C was up-regulated in both Cu and Pb stress conditions, spectrin beta and talin-1 were up-regulated at both Cu and Zn stress conditions, whereas the remaining proteins showed changes in relative abundance specific to single metals. Since oysters are adapted to dynamic changes in their natural marine environment, this is a good example where oysters regulate protein expressions in response to high metal stress, so that abundance of cytoskeletal proteins are increased.

The reduced abundance of paramyosin, tropomyosin, and myosin heavy and light chains due to high metal toxicity of Pb and Zn suggests that high metal stress compromises muscle activity and reduces muscle-energy demand. This implies that metal stress results in a strongly negative impact on the myosin motor protein content and therefore on muscle contraction and motility processes. It is likely that the increased abundances of most other cytoskeletal proteins in oysters keep protein expression at appropriate levels not only to repair metal induced oxidative damages in muscle tissue components, but also to enhance cytoskeleton protein turnover rates to sustain repair of cytoskeletal damage and thus maintain tissue integrity.

#### **4.3.9.2 Translation**

Of the translation associated proteins found in our study, 40S ribosomal protein S3, S3a, S10 to S17, S23, S24 and S27, and 60S ribosomal protein L5, L6, L7a, L12, L17, L19, L23, L23a and L27a, were statistically differentially expressed with increased abundance in at least one metal condition. Seven translation proteins were among the top 50 significantly differentially expressed proteins (Figure 4.9). In response to Pb stress, the 11 differentially expressed ribosomal proteins except L6, L12 and L23 belonged to the 40S subunit. In addition to that, they were all found to increase in protein abundance in response to Pb, similar to our previous findings in Chapter 3. In response to Cu stress, the abundance of 60S ribosomal protein L5, L7a and L23a, and importin beta subunit, increased in abundance, whereas 40S ribosomal protein S3a and 60S ribosomal protein L12, L17, L19, L23 and L23a increased in response to Zn stress. This suggests that among the three heavy metals, high Pb toxicity has a profound impact on protein biosynthesis by up to 35 fold up regulation of some of these ribosomal proteins, followed by Zn (15 fold) and Cu (10 fold) respectively. This impact on translation may also impact on other cellular resources due to greater need for protein turnover.

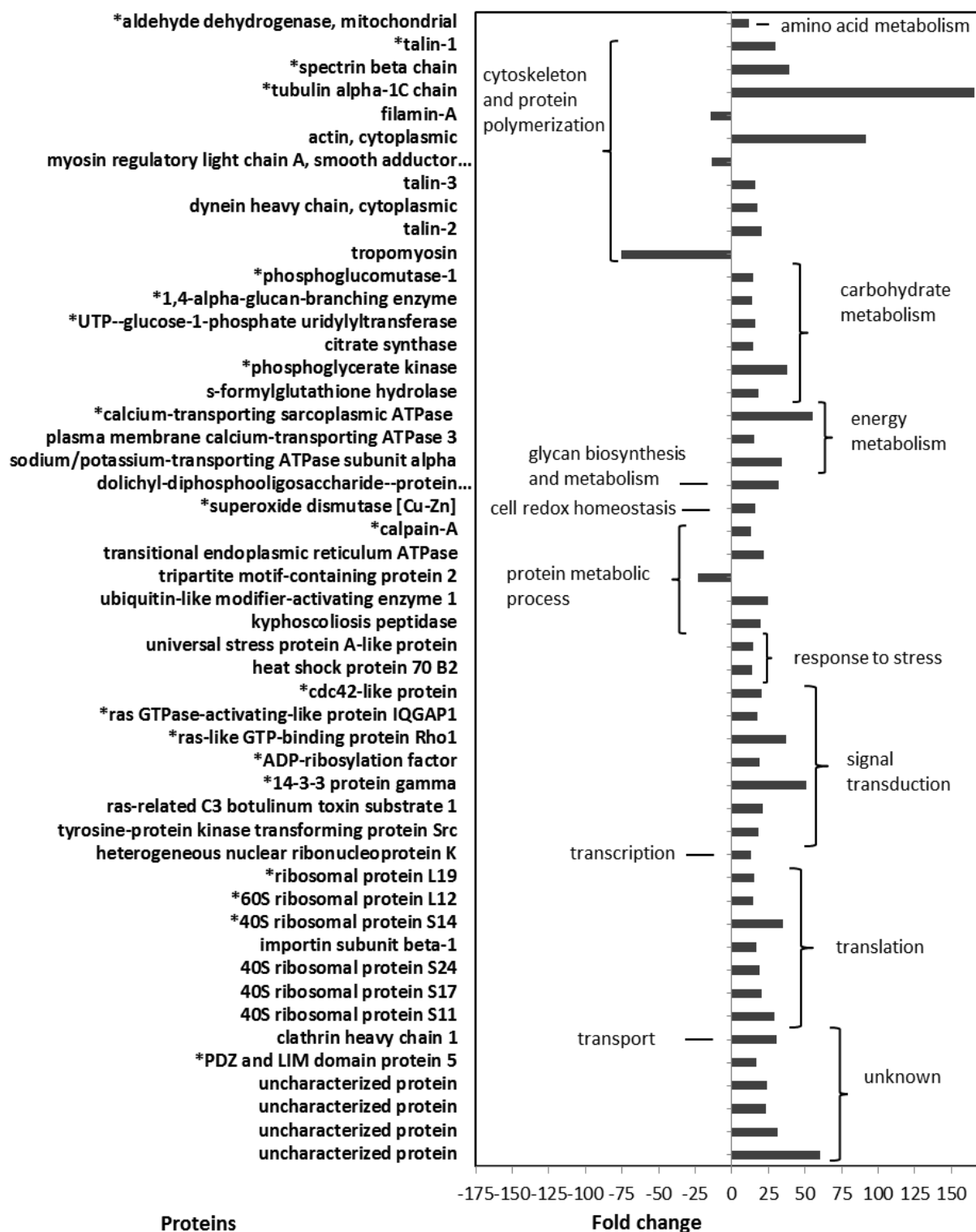


**Figure 4.9** Fold changes (up- or down-regulation) for 50 proteins that showed the highest protein expression changes in response to heavy metal stress relative to controls. Protein ontology information was obtained from UniProt and KEGG reference maps. Fold changes were calculated as the ratio of Log (NSAF) values in metal-exposed oysters relative to non-exposed controls. Proteins have been grouped based on their association with distinct functional pathways. Differentially expressed proteins that responded to more than one metal exposure are indicated by an asterisk, “\*” (see Table 4.3 for specific information on the responses of these proteins with respect to each metal exposure).

#### 4.3.9.3 Carbohydrate metabolism

Sugar metabolism is the primary source of energy and therefore we investigated the response of enzymes involved in important carbohydrate metabolic pathways such as glycogen metabolism, glycolysis, citrate cycle, pentose phosphate pathway, and sugar and starch metabolism. The carbohydrate metabolic proteins listed in Figure 4.9 showed increased expression in response to metal stress relative to controls. Many of these proteins showed protein expression changes in response to both Cu and Zn metal exposure treatments. Several proteins were differentially regulated in response to all three metals. Interestingly, when two or more exposures affected expression of the same protein, the expression was usually altered in the same direction, that is, increased or decreased, with each exposure.

Some enzymes involved in carbohydrate metabolic pathways have been previously reported to be responsive to stress in toxicological studies that involved oysters [11, 314] and mussels [315, 316]. However their responses vary among studies, suggesting that the differences in species, tissues (especially muscle tissues) and the type of stress conditions may have caused the variations. Moreover, it shows the complex nature of protein cellular responses to metal stress.

In our study we found several enzymes related to glucose metabolism showed differential protein expression: malate dehydrogenase, phosphoglycerate kinase, phosphoenolpyruvate carboxykinase, enolase, glyceraldehyde-3-phosphate dehydrogenase, triosephosphate isomerase, fructose-1,6-bisphosphatase and glucose-6-phosphate isomerase, all of which are involved in gluconeogenesis; and glycogen phosphorylase, phosphoglucomutase-1, glycogen debranching enzyme, and UTP-glucose-1-phosphate uridylyltransferase, which are responsible for glycogen breakdown. The

relative abundance of each of these in response to each metal stress is shown in Figure 4.10. The abundance of most of these enzymes clearly increased in metal stressed oysters compared to non-exposed oysters, suggesting that mechanisms involving glucose synthesis as well as glycogen degradation are enhanced in oysters exposed to significant Cu or Zn toxicity.

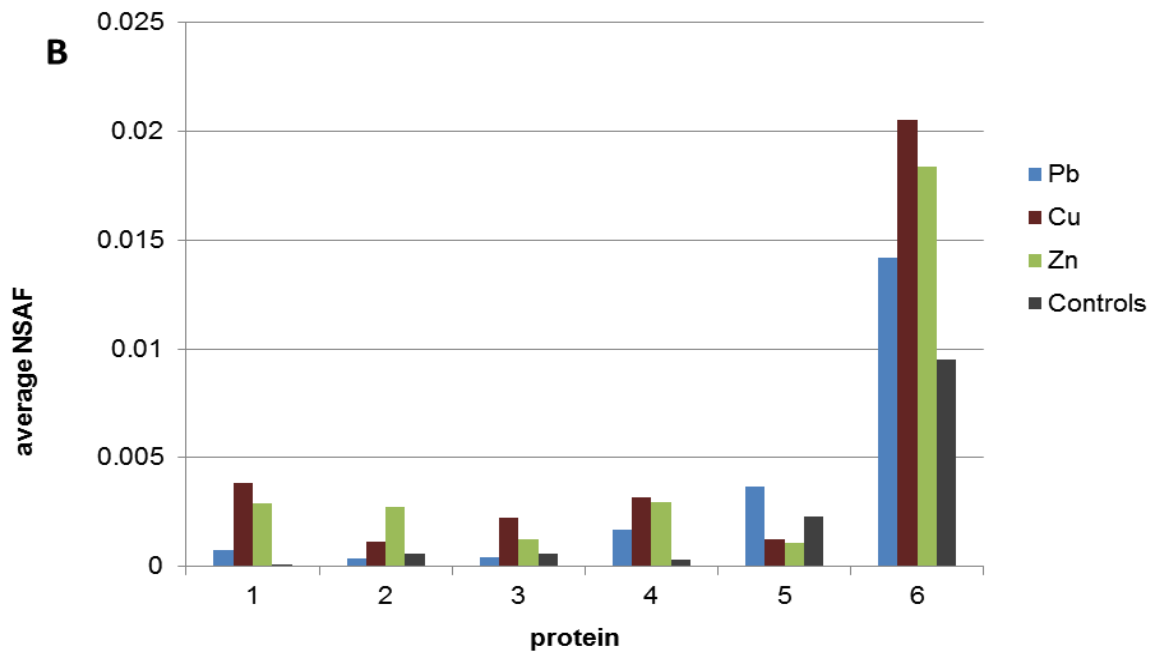
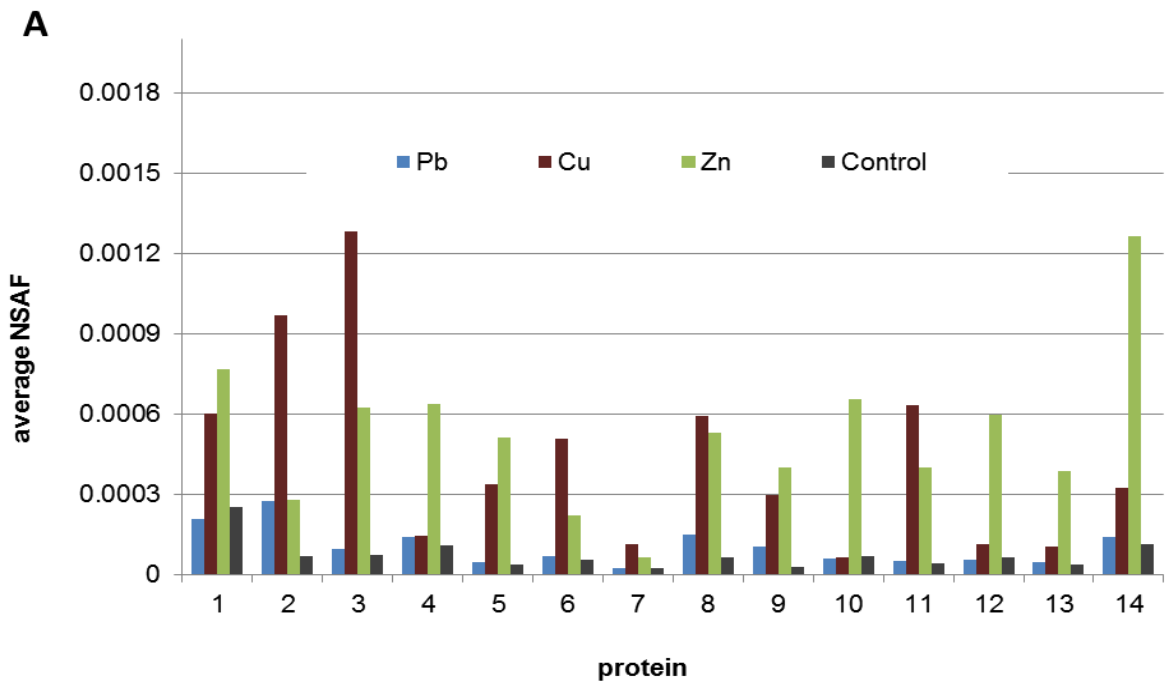


**Figure 4.10** Abundance of carbohydrate metabolism related proteins that showed statistically significant differential protein expression in response to metal stresses (p-value < 0.05; fold change > 2.0).

**(A)** Relatively low-abundance proteins. Numbers 1-14 on the horizontal axis refer to the following proteins; (1) transketolase, (2) citrate synthase, (3) S-formylglutathione hydrolase, (4) succinate dehydrogenase, (5) phosphoglucomutase-1, (6) glucose-6-phosphate isomerase, (7) glycogen debranching enzyme, (8) fructose-1,6-bisphosphatase, (9) 1,4-alpha-glucan-branching enzyme, (10) glucose-6-phosphate-1-dehydrogenase, (11) UTP-glucose-1-phosphate uridylyltransferase, (12) glycogen phosphorylase, (13) fumarate hydratase, (14) lactoylglutathione lyase.

**(B)** Relatively high-abundance proteins. Numbers 1-6 on the horizontal axis refer to the following proteins; (1) phosphoglycerate kinase, (2) triosephosphate isomerase, (3) malate dehydrogenase, (4) isocitrate dehydrogenase, (5) 6-phosphogluconate dehydrogenase, (6) glyceraldehyde-3-phosphate dehydrogenase.

#### 4.3.9.4 Gluconeogenesis

In oysters exposed to metal stress conditions, it appears from our results that glucose generation is facilitated by both glycogen degradation as well as gluconeogenesis. Increased levels of glycogen phosphorylase and phosphofructokinase relative to those of hexokinase indicate high activity of anaerobic degradation of glycogen for glucose and energy production, in addition to up-regulation of many gluconeogenic enzymes. Under metal stress, an altered gluconeogenesis pathway is adopted to generate glucose by a series of enzymatic chemical conversions beginning in the cytoplasm, starting from malate as the substrate via the malate to oxaloacetate reaction, instead of beginning with the usual pyruvate to oxaloacetate conversion in the mitochondria. High malate concentrations stimulate malate dehydrogenase activity, and, conversely, high oxaloacetate concentrations inhibit the enzyme. In mollusc muscles, the malate-aspartate cycle has been previously reported to be important in the reduction of  $\text{NAD}^+$  into NADH produced during glucose metabolism [317]. In the context of gluconeogenesis, malate is preferentially oxidised to oxaloacetate by the malate dehydrogenase enzyme through the reduction of  $\text{NAD}^+$  to NADH, which is further converted to phosphoenolpyruvate by the phosphoenolpyruvate carboxykinase. Following this reaction, phosphoglycerate kinase converts phosphoglycerate to 1,3-bisphosphoglycerate, which is further converted to glyceraldehyde 3-phosphate by the glyceraldehyde-3-phosphate dehydrogenase enzyme.

Triosephosphate isomerase is an enzyme that catalyzes the reversible reaction of glyceraldehyde 3-phosphate into dihydroxyacetone phosphate, which is then followed by the rate limiting step of gluconeogenesis, where dihydroxyacetone phosphate is converted by fructose-1,6 bisphosphate aldolase into fructose-1,6-bisphosphate. The next step in this pathway is dephosphorylation into fructose-6 phosphate by the enzyme fructose-1,6-

bisphosphatase. The resulting glucose-6-phosphate may then either be locked in the cell, maintaining intracellular glucose levels, or be acted upon by glucose-6-phosphatase to produce glucose molecules (further dephosphorylation), or enter glycolysis, or be cycled back into the pentose phosphate pathway producing more NADPH for antioxidation needs. Unused glucose-6-phosphate may also be stored in the form of glycogen via the glycogenesis pathway. Also in molluscs, lower carbohydrate utilisation and greater glycogen degradation for energy production may indicate a greater possibility of anaerobic activities of enzymes in muscles. Since most amino acids can be metabolized to pyruvate or oxaloacetates, damaged proteins and proteolytic products may also be repurposed via the gluconeogenesis pathway to derive glucose from their amino acids. Thus, in oysters experiencing metal stress, in addition to protecting from free radical damage under metal stress, the pentose phosphate pathway seems to be an important way to metabolise, shuttle and repurpose hexose or pentose sugars into gluconeogenesis, glycogenesis, or glycolysis intermediates.

#### **4.3.9.5 Pentose phosphate pathway**

We identified several proteins involved in the pentose phosphate pathway including glucose-6-phosphate isomerase, glucose-6-phosphate 1-dehydrogenase, transketolase, 6-phosphogluconate dehydrogenase, phosphoglucomutase, and fructose 1,6-bisphosphatase. Glucose 6-phosphate is primarily converted to ribulose 5-phosphate, and pentose sugars including those from the degradation of nucleic acids are then converted to glyceraldehyde-3-phosphate and fructose-6-phosphate through a series of enzymatic reactions. Firstly, glucose-6-phosphate dehydrogenase is stimulated by increased levels of its substrate glucose-6-phosphate, which in turn produces more NADPH while converting glucose-6-phosphate into 6-phosphoglucono- $\delta$ -lactone in the pentose phosphate pathway,

a rate limiting step in the metabolic pathway that supplies reducing energy to cells. The NADPH in turn maintains the level of glutathione in these cells to protect against oxidative damage. NADPH is known to reduce glutathione through glutathione reductase, during which it converts the reactive hydrogen peroxides into water molecules with the help of glutathione peroxidase. Unreduced hydrogen peroxides would be converted to free hydroxyl radicals by Fenton chemistry, which can cause severe oxidative damage in cells.

The isocitrate dehydrogenase mechanism appears to be the major source of NADPH in fat tissues. The enzyme 6-phosphogluconate dehydrogenase produces ribulose-5-phosphate which under the action of transketolase is converted to glyceraldehyde-3-phosphate and fructose-6-phosphate. Glyceraldehyde-3-phosphate may then enter into the gluconeogenesis pathway to be converted to fructose-6-phosphate, then to glucose-6-phosphate by glucose-6-phosphate isomerase. Upon isomerisation of fructose-6 phosphate into glucose 6-phosphate by glucose-6-phosphate-isomerase, glucose-6-phosphate products can have several fates such as the formation of glucose units to become absorbed by the cell, or contribution towards energy production in muscles as discussed earlier in this chapter.

Since all of the vital enzymes which belong to this pathway were identified to be statistically differentially expressed in response to metal stresses, it can be concluded that the protein expression patterns of some of these enzymes in this pathway could be used as biomarkers to evaluate metal toxicity.

#### 4.3.9.6 Glycogenesis

In our study we found several enzymes involved in glycogenesis, where glycogen is formed from highly branched glucans composed of chains of D-glucose, and several other enzymes related to glycogenolysis, which is breakdown of glycogen. Glycogen synthesis requires input energy, and in metal stress conditions oysters may avoid unwanted expenditure of energy. Glycogen is known to be synthesised from building blocks of UDP-glucose to form glycogen chains with ( $\alpha 1 \rightarrow 4$ ) bonds, lengthened by the action of glycogen synthase. Firstly, glycogen synthesis is initiated by the conversion of glucose to glucose-6 phosphate by the action of glucokinase, which is further converted to glucose 1-phosphate by the reaction of phosphoglucomutase-1. UDP-glucose monomers are formed from the enzymatic reaction of UTP-glucose-1-phosphate uridylyltransferase on the energy laden UTP and glucose-1-phosphate units. The activity of UTP-glucose-1-phosphate uridylyltransferase, also referred to as UDP-glucose pyrophosphorylase, is one of the vital steps in glycogenesis. Lastly, glycogen branches are made by the 1,4-alpha-glucan-branching enzyme (glycogen branching enzyme), which catalyzes the transfer of 7 glucose residues from the ( $\alpha 1 \rightarrow 4$ ) terminal residue to ( $\alpha 1 \rightarrow 6$ ) position on a glucose chain having at least 11 residues. All of these enzymes have been identified in this study, and protein expression levels of almost all of them were up-regulated due to metal stress in oysters exposed to Cu or Zn toxicity.

Glucose assimilation into glycogen was first studied by Fando *et al.* in the flat oyster *O. edulis*, in which gills and mantle tissues were reported to incorporate levels of glucose significantly higher than those seen in muscle tissue [318]. It was also reported that glycogen storage levels could act as a useful bioindicator of the current environmental status of an oyster and its ability to sustain further environmental stress [314]. A previous

study on mussels reported decreased oxygen consumption together with increased utilization of glycogen and carbohydrates during Cd exposure [319], and concluded that bivalves may adopt anaerobic metabolism when encountering heavy metal stress in the environment. However, many catalytic mechanisms concerning glycogen metabolism such as that of glycogen synthase are not well known. Further research on glycogen metabolism in oysters, especially at different subcellular localisations (gills, mantle and muscle tissues) may provide useful insights on the effects of metal stress and its impact on the reported reproduction impairments.

#### **4.3.9.7 Glycogenolysis – Glycogen degradation**

It is well known that under starvation or stress, glucose obtained from glycogen is utilised for energy. It is also known that glycogen phosphorylase and glycogen synthase, the two enzymes vital for the breakdown and synthesis of glycogen respectively, share structural similarities. In this study, we found over-expression of both glycogen synthase and glycogen phosphorylase in response to both Cu as well as Zn metal stress. In the context of glycogen degradation, glycogen is known to be cleaved by glycogen phosphorylase at the  $\alpha[1\rightarrow4]$  linkage of the non-reducing ends of the glycogen chain, producing monomers of glucose-1-phosphate. A glycogen debranching enzyme then removes the  $\alpha[1\rightarrow6]$  linkages of the branched glycogen and reshapes the chain into linear polymers. Glucose-1-phosphate units are then catalysed by phosphoglucomutase to be converted to glucose 6-phosphate by the transfer of the phosphate group from the 1' to the 6' position on each glucose monomer.

Glucose-6-phosphate monomers may be utilised differently depending on the requirements of the cells. They may be converted to free glucose to be absorbed as fuel for cells, in addition to that produced from gluconeogenesis. Under low cellular energy

conditions, they may enter the glycolytic pathway to produce ATP; and when the need for biosynthetic intermediates arises, glucose 6-phosphate monomers may enter the pentose phosphate pathway to yield pentose sugars (riboses) and/or NADPH. Lastly, due to the endergonic nature of the reactions, unused glucose-6-phosphates may be transformed back into glycogen.

It has been reported that proteins, which are the main components in muscle formation, do not contribute toward gametogenesis. However, gametogenesis appears to take place at the expense of glycogen reserves. An increase in reserves of glycogen and lipids that are stored in the digestive gland, gonad and surrounding mantle area was reported to be associated with reproductive efforts, and decreased below detectable levels after spawning [317]. Hence, in situations of stress arising from high metal toxicity, gametogenesis may not be preferred in oysters, and utilisation of glycogen and lipid reserves may probably be directed towards mitigating cellular damages from encountering such stress.

#### **4.3.9.8 Citric acid cycle and the electron transport chain**

All proteins involved in the citric acid cycle were found in our study and several were responsive to metal stress. Among them, citrate synthase and malate dehydrogenase showed significant increase in abundance in response to Cu metal stress (Figure 4.9). The enzymes isocitrate dehydrogenase, succinate dehydrogenase and fumarate hydratase increased in abundance in response to Zn stress. These proteins seem to be determining the initiation and generation of energy within cells in exposure to metal stress. Among the proteins involved in citric acid cycle which have been reported to be responsive to Cu stress include malate dehydrogenase and isocitrate dehydrogenase, both of which were reported to be stimulated in response to Cu stress in filamentous fungi [320]. Further,

enzymes involved in the citric acid cycle were suggested to augment the energy requirements of fresh water mussels subjected to chromium toxicity [321].

Of the proteins involved in electron transport chain, ATP synthase alpha and beta subunits increased in abundance in response to Zn metal stress (Table 4.3). ATPases such as V-type proton ATPase subunit A, V-type proton ATPase subunit E, calcium-transporting sarcoplasmic ATPase, and sodium/potassium-transporting ATPase subunit alpha also showed increased protein expressions in oysters in response to Cu toxicity. These results suggest that the TCA cycle and the electron transport chain are significantly affected and thus energy production is increased in the cell via this pathway, probably to drive activities focused on repairing damage to proteins and tissues from oxidative effects of metal toxicity. This is also in agreement with our previous study on oyster heavy metal stress as discussed in Chapter 3 [11].

#### **4.3.10 Identification and quantitation of proteins in Sydney rock oysters by iTRAQ**

Our stringent FDR thresholds in our studies with Sydney rock oysters demonstrate the statistical confidence requirements at the protein as well as peptide identification levels needed to address the issue of biological variation between oysters, caused by high frequency of SNPs and peptide sequence repeats. This is unlike results obtained for most other biological subjects used for proteomics experiments performed in our laboratory. A total of 285 reproducible proteins were identified from all four treatments using the 1DE approach, 111 proteins using GPF and 139 using 8-plex iTRAQ. This was after the removal of a large proportion of proteins from each group to meet our specified criteria of a protein FDR less than 1%. A combined non-redundant total of 356 proteins were found to be statistically reproducible protein identifications in at least one of the heavy metal treatments from all three proteomics approaches (Figure 4.11).

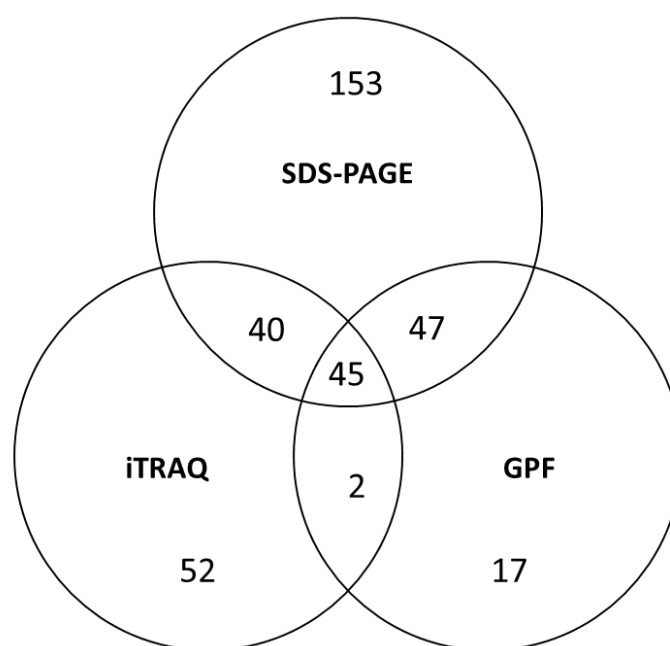


**Figure 4.11 Protein identification data from the 1DE, GPF and iTRAQ approaches in Sydney rock oysters. Numbers represent the total number of non-redundant proteins present uniquely or shared between each of the three approaches.**

The Paragon algorithm was used within ProteinPilot v3.0 software for statistical analysis of iTRAQ data. A total of 267 proteins were initially identified before grouping, and 139 proteins were found after grouping with 95% confidence, which represent 8056 spectra and 985 distinct peptides. Peptide and protein identification summary report generated by ProteinPilot from the 8-plex iTRAQ experiment has been provided in Supplementary information Tables S6 and S7 respectively.

Of the 356 distinct proteins identified from the three approaches, 153 proteins were exclusive to the 1DE dataset, whilst 52 and 17 were exclusive to the iTRAQ and GPF datasets respectively. There were 45 proteins reproducibly identified by all three approaches, 47 proteins were identified by both 1DE and GPF, 40 proteins were identified by both 1DE and iTRAQ, and 2 were common to iTRAQ and GPF, as shown in Figure

4.11. The iTRAQ experiments included identification of some new differential proteins in response to metal stress from each of the heavy metals. The identifications of these differentially expressed proteins from our iTRAQ experiments are highly reproducible, and are based on identifying each differentially expressed protein in at least four oysters, in each metal condition. In total, each of the protein identification was biologically reproducible among 16 individual oysters among two technical replicates. Further, the iTRAQ results were in agreement with some differential proteins already reported using the shotgun proteomics approach, as reported earlier in this study. Validation of certain differentially expressed proteins using iTRAQ was considered successful and complemented the list of protein biomarkers suitable for evaluating metal stress.

#### **4.3.11 Significantly differentially expressed proteins in heavy metal exposed Sydney rock oysters relative to controls, identified using iTRAQ**

From our iTRAQ analysis of Sydney rock oysters exposed to Pb, Cu or Zn stress, a total of 12 proteins shown in Table 4.4 were differentially expressed in response to metal stress; six proteins were associated with single metals and six proteins showed stress responses associated with two or more metals. Differential expression corresponding to each metal treatment group was considered statistically significant if proteins showed the same trend (either up-regulated or down-regulated) relative to both controls (115 and 119) from the two replicate sets (see Table 4.1), and this was in addition to having 95% confidence (ProtScore >1.3) and protein and peptide FDR  $\leq$  1%.

**Table 4.4** Statistically significant differentially expressed proteins in response to heavy metal stress in Sydney rock oysters, identified by iTRAQ analysis

Gene identifier	Protein description	Distinct Peptides	Fold Change	p-value
<b>Differentially expressed in response to Pb</b>				
gi 405962873	filamin-C	28	0.62↓	1.3E-05
gi 405971354	mitotic apparatus protein p62	3	5.82↑	0.015
<b>Differentially expressed in response to Zn</b>				
gi 405974805	muscle LIM protein Mlp84B	7	0.70↓	0.017
gi 405962295	radixin	6	0.76↓	0.039
<b>Differentially expressed in response to Cu</b>				
gi 405974166	titin	1	2.57↑	0.029
gi 405967288	40S ribosomal protein S4, X	3	2.26↑	0.011
<b>Differentially expressed in response to both Pb and Cu</b>				
gi 405975018	hemicentin	Cu 41; Pb 41	Cu 1.46↑; Pb 1.71↑	0.002
gi 405967949	elongation factor 1-alpha	Cu 12; Pb 12	Cu 2.19↑; Pb 1.50↑	0.012
gi 405961263	phosphoenolpyruvate carboxykinase	Cu 23; Pb 23	Cu 0.64↓; Pb 0.69↓	0.005
gi 405967652	hypothetical protein CGI_10017178	Cu 9; Pb 9	Cu 1.39↑; Pb 2.05↑	0.003
<b>Differentially expressed in response to both Cu and Zn</b>				
gi 405975056	myosin heavy chain, striated muscle	Cu 28; Zn 28	Cu 1.89↑; Zn 0.69↓	0.013
gi 405966986	paramyosin	Cu 6; Zn 6	Cu 0.66↓; Zn 0.51↓	0.006

Of the 12 differential proteins, five proteins were down-regulated in response to metal stress and seven proteins were up-regulated, except for myosin heavy chain from striated muscle, which showed opposing responses in Cu and Zn exposed oysters. Expression patterns for each of these proteins and the corresponding metal is given in Table 4.4. Most of the down-regulated proteins were involved in cytoskeletal protein polymerization and carbohydrate metabolism. These include a filamin-C, radixin, muscle lim protein Mlp84B, and paramyosin, all of which are involved in cytoskeleton organisation. The other protein in this category is phosphoenolpyruvate carboxykinase, which is involved in the conversion of oxaloacetate into pyruvate in the gluconeogenesis pathway.

Filamins are known to be involved in cross-linking actin filaments. Filamin protein structures contain conserved regions and tandem repeats of a 100-residue motif that is glycine and proline rich. These form the core of the repeats and are preserved across all filamin family members. Filamins were also recently found to aid in cell spreading and also be involved in calcium signalling by binding signalling components with cytoskeletal elements such as actins and collagens [322-324]. Over-expression of filamins was reported in the flat oyster *O. edulis*, as a response to bonamiosis disease affecting hemocytes [325].

Radixin is a barbed, end-capping actin-modulating protein which helps in crosslinking actin filaments with plasma membranes. Down-regulation of paramyosin, a major cytoskeletal protein, in response to Cu and Zn, was as expected, and indicates the possibility of severe muscle damage as a result of metal stress which may affect muscle strength and muscle growth. Further, this is also in agreement with results previously seen from our shotgun data in this chapter, and in previous studies involving analysis of mussels in response to silver toxicity [326].

Titins are also cytoskeletal proteins that play a role in muscle development and are known to control the assembly and elasticity of the sarcomeres in striated muscles and possibly play a role in controlling elasticity in chromosomes [327]. A recent study using myoblast cells reported impaired myofibrillogenesis upon mutation or deletion of the c-terminus or the kinase domain of titin, resulting in weaker muscle organisation, shorter myotubes and onset of symptoms similar to muscular dystrophy [328, 329].

The muscle lim protein is not well characterised but is known to act as a vital stress sensor. Down-regulation of muscle lim protein was observed in response to nitric oxide toxicity sufficient to cause muscle hypertrophy [330], whereas up-regulation was observed in a *Drosophila* model of parkinsons disease [331]. The protein is known to act as a vital regulator in myocyte function and has been shown to regulate F-actin dynamics in cardiac and skeletal muscles [332]. Therefore, in the context of metal stress responsive signature proteins, changes in protein expression levels of muscle lim protein could be associated with cardiac and skeletal myopathies, loss of F-actin depolymerisation functions, or impaired sarcomeres.

Myosin heavy chain was found to be down-regulated in response to Zn stress, which is in good agreement with our previous results for Zn toxicity studies in oysters in Chapter 3 [11]. However it was also found to be up-regulated in oysters after Cu toxicity in our iTRAQ study, and has been previously reported to be up-regulated in mussels in response to silver toxicity [326]. Such varied response patterns for some proteins among different studies are not unusual, and suggest that the differences in species, stress levels, type of toxicity, and tissues, may be responsible for the observed variation. Oysters exposed to Cu toxicity may experience loss of calcium ions and based on the findings from recent research on regulation of myosins [333], it can be suggested that in a Cu

stress-induced  $\text{Ca}_2^+$  deprived condition, the activity of myosin light chain may become reduced while myosin heavy chains may experience greater flexibility in promoting regulation.

From our iTRAQ analysis, we identified differential expression of hemicentin-1, elongation factor 1-alpha and phosphoenolpyruvate carboxykinase in response to both Pb and Cu metal toxicity (Table 4.4). The two cytoskeletal proteins, hemicentin-1 and elongation factor 1-alpha, were found to be up-regulated in oysters after Pb and Cu exposures. In contrast, changes in protein expressions for these two proteins were not reproducibly observed in our shotgun data. Hemicentin-1 has been reported to be involved in chitin metabolic processes and is known to contain thrombospondin multimeric domains with TSP1 repeats. This protein has been thought to be involved in facilitating cell to cell interactions, angiogenesis inhibition and apoptosis [334, 335].

#### **4.3.12 Complementarity of label-free and iTRAQ analyses**

The reason for using both label-free and iTRAQ quantitative techniques was because it has been shown on numerous occasions that different proteomic techniques complement each other [21, 235, 336]. A summary of the number of proteins identified from each technique in each metal exposure condition in our study is given in Table 4.2 and Figure 4.11. From label free analysis we identified 304 nonredundant proteins, and of these, 153 proteins were only found in 1DE shotgun data. In addition to these, 52 proteins were found exclusively from iTRAQ data. Further analysis of these groups showed that proteins involved in carbohydrate metabolism, energy metabolism, cell redox homeostasis, cytoskeletal proteins, protein metabolic processes, signal transduction and translation were expressed in response to metal stress in Sydney rock oysters. It also revealed that proteins we identified by the iTRAQ approach as being differentially

expressed in response to metal stresses consisted predominantly of cytoskeletal and protein polymerization associated proteins. This reinforces our hypothesis that metal stress causes significant cytoskeletal damage.

From label-free analysis, 304 proteins were found to be expressed at one or more exposure conditions, and, of these, 185 proteins changed significantly in response to one or more metal stresses. Analysis of these proteins revealed that proteins involved in cell redox homeostasis, energy metabolism and protein metabolic processes showed greater response toward Cu and Zn toxicities, and over 95% of these proteins increased in abundance in response to metal stress. Proteins engaged in signal transduction were also found to be mostly up-regulated in response to Cu and Zn stress.

From iTRAQ analysis, 139 proteins were identified; it is worth noting that the software provides quantitative information only for those proteins present in all samples. However, iTRAQ analysis identified 12 proteins in total that changed significantly in response to Pb, Cu and Zn metal stress. These results showed that among the cytoskeletal proteins differentially expressed, filaminC, muscle lim protein Mlp84B, radixin and paramyosin were down-regulated in response to metal stress, but elongation factor and titin were up-regulated.

Furthermore, four out of 11 proteins showed statistical differential expression in response to both Pb and Cu metal stress, and each of those four proteins showed the same trend in abundance changes for both these metals. We found one unknown protein in our iTRAQ analysis, which did not match to any known protein in the literature and was termed as a novel ‘metal stress responsive protein’, similar to the other three novel metal stress responsive proteins identified from label-free quantitation. This novel metal stress responsive protein identified from iTRAQ analysis showed differential protein expression

in response to both Pb and Cu, in that it was increased in protein abundance relative to non-exposed controls. Therefore this protein may be more appropriately termed as a 'Pb/Cu stress responsive' protein.

Comparison of ratios between proteins in iTRAQ and label-free datasets shows very little correspondence between them. iTRAQ ratios are known to be artificially compressed and distorted by interference of contaminating reporter ions (near isobaric ions) that get co-isolated and co-fragmented at the MS/MS stage [337, 338]. In certain cases, spectral counting results in inflated expression ratio numbers due to zeroes being replaced by artificial fractions (0.5) of a spectrum. These fold-change ratios represented may be inflated, but they provide a mathematically valid way to represent missing data points, which iTRAQ does not have.

Spectral counting methodology is able to represent the presence and absence of proteins across samples, but iTRAQ is able to only pick differences among proteins reproducibly identified in all samples, and does not account for proteins that are present in one but absent in another. This means that any comparison between the two methods is unlikely to show a high degree of correspondence, as they are not looking at exactly the same sets of proteins. This has been highlighted in a recent publication from our laboratory using both iTRAQ and label-free shotgun proteomics techniques to study effects of cold stress in rice seedlings. The degree of consistency between the two different techniques was low, similar to what we observed here [235].

Comparisons of the technical aspects of labeled and label-free quantitation techniques have been further discussed in detail in one of our recent publications [21]. In spite of a few limitations in label-free approaches, in the context of this thesis we found that label-free shotgun proteomics is reliable, versatile, information-rich and cost-effective

compared to labeled quantitation techniques. These findings collectively show that iTRAQ analysis provided new information and complemented the results obtained using label-free shotgun proteomics (1DE and GPF approaches), although the number of reproducible protein identifications and differentially expressed proteins were both relatively low. Although the same amount of protein was analyzed for both iTRAQ and label-free experiments, the relatively low number of protein identifications in iTRAQ results may be due to, for example, fragmentation of only the top 3 ions. Fragmentation of just three ions in iTRAQ Q-TOF MS may not be adequate to successfully sample the abundance of the peptide pool from the eight samples, whereas the faster scanning ion-trap used in label-free experiments fragments the top 6 ions for each of the 16 fractions from each sample and each MS/MS spectrum is useful for peptide quantitation. Lastly, iTRAQ requires identification of at least three unique peptides to provide a statistical quantitation, whereas in label-free proteomics data protein identification matches with just one unique peptide with multiple shared peptides can be quantified.

#### **4.4 Concluding Remarks**

Analysing the response of Sydney rock oysters toward excess levels of heavy metals is essential as many Australian natural waters and ecosystems experience very high anthropogenic metal concentrations. Sydney rock oysters are endemic in Australia and possess high bioaccumulation capability. Performing proteomics studies on such species helps in understanding the biological implications and possibly in developing strategies to mitigate future contamination levels. The aim of this study was to utilise the recently released *C. gigas* oyster genome sequence data to identify and compare differentially expressed proteins in filter feeding Sydney rock oysters in response to Pb, Cu and Zn metal stress. We used both label-free shotgun proteomics and iTRAQ techniques for this

analysis, and our results indicate that they complement each other by identifying more in the combined dataset than is possible in each individually. The comparative analysis of proteomics data from the three metal stress conditions relative to non-exposed controls showed that Sydney rock oysters respond differently to different metals. The differentially expressed proteins identified in this study are highly reproducible and statistically significant in their abundance changes, making them potentially useful protein signatures or biomarkers suited for field trials. It is only recently that the first reports have been published investigating metal stress protein signatures in the field, such as the study recently conducted by Thompson *et al.*, in our laboratory [339].

In summary, results from this study suggest that metal stress causes oxidative damage to cells and tissues, especially cytoskeletal components. Since oysters need to maintain the structure, strength and integrity of their cytoskeletal tissues and structures, they may prefer to address those primary requirements to maintain survival by replacing or repairing damaged proteins in tissues using minimal expenditure of energy and cellular resources. Further demand for glucose, energy, and maintenance of cell redox homeostasis by counteracting metal stress induced ROS attack inside the cell were also found to be major stress responses. Results from using the Oyster genome sequence seemed more accurate in reflecting the cellular status of Sydney rock oysters under metal stress conditions, when compared to results obtained based on a cross-species *Bivalvia* protein sequence database in the absence of Oyster genome sequence in Chapter 3. We faced many characteristic challenges in oysters and other bivalves when compared to certain model organisms used in most other studies, such as relatively high biological variation due to high frequency SNPs, numerous peptide sequence repeats, higher than usual FDRs and relatively nascent genome curation. Nevertheless, our proteomics data has provided several useful molecular insights into Sydney rock oyster protein profiles in response to

metal stress and will potentially aid in addressing heavy metal pollution mitigation and early monitoring in our waterways and ecosystems.

### **Supplementary information**

The following Supplementary information for this study is available in the enclosed DVD

**Supplementary Information Table S4:** Proteins identified from GPM results for triplicates in each heavy metal stress treatment using either the 1DE approach or GPF.

**Supplementary Information Table S5:** NSAF values of reproducible proteins identified in each heavy metal stress exposure condition and controls, from either 1DE or GPF approaches.

**Supplementary Information Table S6:** iTRAQ peptide identification summary report generated by ProteinPilot from the 8plex iTRAQ experiment performed using Sydney rock oysters subjected to heavy metal stress.

**Supplementary Information Table S7:** iTRAQ protein identification summary report generated by ProteinPilot for the 8plex iTRAQ experiment performed using Sydney rock oysters subjected to heavy metal stress.

## Notes

The work presented in this chapter (Chapter 4) was performed after the release of the oyster genome. MS/MS data pertaining to Chapter 3 was re-analyzed using the *C. gigas* genome in order to obtain more closely relevant protein expression information in Sydney rock oysters in response to heavy metal stress. The work presented in this chapter has not been published yet.

Supplementary tables, including protein identification and quantitation information, referred to in-text can be found on the DVD attached to this thesis.

Other supplementary data are included in Appendix C as indicated.

In addition to re-analyzing all of previously generated MS/MS data from label-free experiments in this chapter, this project also describes additional experiments on heavy metal stress responses of Sydney rock oysters, quantified using label-dependant proteomics experiments. To do this, I used the same set of Sydney rock oyster hemolymph samples, mentioned in Chapter 3 which were provided by a fellow PhD student, Emma Thompson, but I conducted the iTRAQ experiments at the Australian Proteome Analysis Facility, Sydney. Using the recently available *C. gigas* genome, I also performed all of the data analysis for both the iTRAQ and label-free experiments, including the manual interpretation of data which led to identifying relevance of several differential proteins in the metal stress response in oysters and the majority of the manuscript preparation (approximately 95%).

---

## Chapter 5

### **Quantitative proteomics and biomarker discovery in response to Zn metal stress in the epibenthic amphipod *Melita plumulosa*.**

---

#### **5.1 Introduction**

In Australia, as in other parts of the world, estuaries are frequently areas where urban and industrial development is concentrated. As a consequence, estuaries receive large quantities of chemical pollutants, much of which accumulate in estuarine sediments at concentrations far in excess of those in the overlying waters. Disturbance of these sediments by various processes, such as dredging, storm events, and trophic transfer through benthic organisms, can remobilize these contaminants and, thereby, pose a threat to estuarine ecosystems and the wider ecosystems that they support. Several tools are available for monitoring the degradation of sediment quality as a consequence of contamination in sediments, including chemical analysis, sediment toxicity testing, and benthic community studies. Although chemical analyzes may provide information regarding the presence and nature of contaminants, biologically based tools provide indices of biological effect. Proteomics is a relatively new and effective tool which we believe can be useful for such assessments.

Sediments that occur around Sydney and other NSW regions provide a range of nutrients that is not easily simulated by commercial foods. However, such naturally occurring sediments come with inherent variability in their nutritional and non-nutritional compositions, and this has certain implications on toxicity tests that could affect the outcome when used in research studies. Naturally occurring sediments may be contaminated or contain extant flora or fauna that inhibit growth or survival of test organisms. Concentrations of metals, total polycyclic aromatic hydrocarbons and other organics (e.g. pesticides, PCBs) in the sediments should be below guideline trigger values for the sediment and associated pore water (ANZECC/ARMCANZ, 2000). This is an important consideration when planning and executing eco-toxicoproteomics studies. The physico-chemical properties of the sediment at the sites where amphipods were collected in this study are typical of silty sediments found at sites in the middle reaches of estuaries on the south-east coast of Australia, and should have properties that are within the geochemical requirements of the test species.

*Melita plumulosa* is an epibenthic amphipod, widely found in estuarine habitats in NSW, and is endemic to most of the Australian eastern coastline. It is used as a test species for whole sediment toxicity tests in Australia, to monitor the health of estuarine and marine sediments, as it has demonstrated high sensitivity to a variety of sediment-bound organic and metal toxicants [340-342]. It was also found to be one of the most sensitive benthic invertebrates under acute exposure to either dissolved or sediment-bound metals, namely copper and zinc [343, 340, 344, 164]. Exposure of *M. plumulosa* to metal-spiked sediments in a 13-day reproductive toxicity test resulted in a significant reduction in fecundity at concentrations that did not affect survival of the adults [341]. The amphipod reproduction test using the continuously breeding amphipod *M. plumulosa* spans two female molt cycles, and commences with all the females in a synchronous phase

of their ovarian cycle [345]. Within the ovary of these females, extant primary oocytes begin secondary vitellogenesis to form a new cohort of mature ova that ovulate on day 7 of the test, that subsequently contribute to the formation of the second-brood embryos that enter the marsupial pouch after a molt has occurred [345]. The test is terminated at some period within the second molt cycle, typically 10-13 days after commencing the test [345, 346].

In a previous study, an artificial substrate consisting of fine milled silica (Silica-300G, particle size <75  $\mu\text{m}$ ) that mimicked the particle-size composition of natural silty sediment was found to support the survival and fecundity of gravid *M. plumulosa* females over a 14-d period [347]. In addition, the toxicity of waterborne Zn to *M. plumulosa* increased if they are maintained on the nutrient-depleted fine silica substrate compared to a seawater-only exposure. It was suggested that the increased Zn toxicity to the amphipods was a consequence of their increased energy expended foraging in the silica substrate in concert with the likely increased exposure to Zn via the digestive tract in addition to exposure through the gills [347].

Although Silica-300G was found to be an unsuitable substrate for long term culture purposes, it did provide an inert substrate that supports good survival and reproduction of the epibenthic amphipod *M. plumulosa* over the duration of a 13-d reproduction toxicity test. Such a defined system provided an opportunity to examine the short-term proteomic response to low concentrations of Zn on the amphipod to be investigated, in the presence or absence of the silica substrate. Therefore, in this study we used fine silica without cellulose as our test sediment, as it has been previously tested and proven suitable for use in Zn toxicity studies on amphipods [347].

In a study on the amphipods *Gammarus pulex* and *Asellus aquaticus* investigating the effects of polycyclic aromatic hydrocarbon contaminants in sediments, survival and growth were reportedly not the most sensitive endpoints [173]. In the case of metal stressed amphipods, behavioral changes and cellular strategies to avoid Zn toxicity such as changes in protein expression in response to stress, increased demand for energy and carbohydrate would be significant steps in mitigating stress before physiological impact on survival and growth unfolds. Therefore, in this study we examined the hypothesis that the behavioral response of the amphipods to the presence of the silica substrate results in increased metabolic activity from foraging, and at the same time depletes metabolic resources for detoxification due to the additional exposure to zinc from the ingestion of contaminated particulates.

Amphipods may have a metal storage mechanism typical of other marine organisms that could handle metal sequestration across a whole range of exposure conditions regardless of metal concentration. There is reported evidence to support this where some studies on amphipods have shown the presence of equal distribution of metals in both cytosolic and insoluble fractions [348, 349]. When amphipods were exposed to a range of Cu and Zn conditions, accumulated metal concentrations increased quickly to LC-50 levels. Cu and Zn remained approximately equally distributed between cytosolic and insoluble fractions, and metal tolerance to Cu or Zn was not observed in these animals [349]. In addition, laboratory exposure experiments on native populations of amphipods to Cu and Zn caused greater metal induced effects from metal accumulation, oxidative stress responses, and lower LT-50 values [348]. Again, both native amphipods as well as those from a historically contaminated site showed similar sub-cellular distribution of Cu and Zn. This was attributed to their capacity to bind to metallothioneins and similar proteins, as well as metal binding granules and exoskeletal components.

Under Zn stress conditions, proteins with functions that are performed in the midgut region of the amphipods could help to identify useful biomarkers for Zn metal contamination scenarios in the environment. Midgut cells in amphipods could also develop changes in the cytoplasm similar to the findings seen in a study by Shu *et al.*, where cut worms were exposed to Zn stress [350]. Numerous electron-dense granules and vacuoles in the cytoplasm of the midgut cells, as shown by transmission electron microscopy, were indicative of changes caused by Zn stress as compared to non-exposed cells. The size, appearance and density of these structures closely correlated with the Zn accumulations in the midgut and such close correlation signifies the direct relationship existing between the midgut cells and metal stress.

Protein identification and measurement of differences in relative and absolute protein expressions between samples are essential steps toward understanding the function and roles of proteins in the cell. Mass spectrometry has become critically important in almost all areas of proteomics. Since the introduction of ESI in 1984 and MALDI in 1988, mass spectrometry has revolutionized proteomics [351, 23]. Although new proteomics methods have been developed to identify proteins in complex mixtures, most of these were developed to primarily address biological questions in, for example, bacteria, humans, mice, and other common species used in medical research. In the case of ecotoxicoproteomics, an area concerned with huge non-reversible environmental changes, most organisms are under-represented in proteomics research. Of the few studies that exist on this topic in literature, protein separation by 2DE and subsequent protein identification by MALDI-TOF mass spectrometry is still the most widely used proteomics technique [270]. Among the available mass spectrometric methods used for protein identification when adopting the 2DE protein differential display approach, ESI with tandem mass spectrometry (MS/MS) is an important technique used to gain additional data [181, 11,

352], and we have used this in facilitating protein identification from 2DE gels in this study.

Although protein profiles of many different organisms have been analyzed using 2DE with mass spectrometry [353], there have been relatively few studies using combined implementation of the two MS approaches (MALDI-TOF/TOF MS/MS and LC-MS/MS) for protein identification of 2DE separated proteins. This study demonstrates the feasibility of performing such analysis on organisms with unsequenced genomes, such as amphipods. Recently, Medzihradszky *et al.* compared the MALDI and ESI methods for peptide analysis and protein identification on rabbit intestine isolates separated by SDS-PAGE with Coomassie staining [354]. Upon analyzing a single band, two proteins were reportedly identified by MALDI-TOF/TOF MS but two additional proteins were identified by nanoLC-MS/MS. The two approaches for protein identification proved complementary in their analysis of a single band from SDS-PAGE, and similar scope exists when used with 2DE gel spots. However, these comparisons are not common and in many cases only MALDI data has been used for the identification of proteins from 2DE spots.

It is advantageous to have the genome available for organisms under study because protein identification is more effective. An illustration of this is the study conducted by Lim *et al.* [355] where proteins from two fully sequenced archaea, *Methanococcus jannaschii* and *Pyrococcus furiosus*, were separated by 2DE followed by maximizing success rates of protein identification by using both MALDI-TOF MS and LC-MS/MS [355]. This study reportedly identified 160 proteins from 2DE gels of the two organisms and compared several features of the two methods including the number of matched peptides, sequence coverage, effect of modifications for protein identification, and

sequence coverage. They found that while LC-MS/MS repeatedly performed better, the combination of these two methods enhanced proteomic results.

However, the lack of genomic sequence data for *M. plumulosa* and other closely related species, in addition to the relatively high cost of tandem mass spectrometry, has hampered proteomic investigations on amphipods in general. Detailed mechanisms of Zn stress response remain unknown, but interactions, gene mutations and changes in gene and protein expression are thought to be key aspects of such mechanisms. Comparative proteomic analysis of Zn metal exposed and non-exposed organisms including amphipods may reveal protein profiles reflecting metal stress-related phenotypes. The usefulness of employing a combination of several label-free proteomics approaches was verified in two of our previous research studies. We investigated the effects of Cu, Zn and Pb metal stress on oysters when exposed to toxic levels, and the various approaches used proved useful in terms of maximizing protein identifications and peptide quantitation (see Chapters 3 and 4). We hypothesized that a combination of experimental strategies would be equally effective when working with unsequenced organisms such as amphipods [11, 270].

In brief, the proteomics strategy adopted in this study included triplicate analysis of the extracted amphipod protein samples on 2DE, identification of a large number of protein features that showed statistical differential expression between metal exposed and non-exposed groups of amphipods, and consideration of their differential protein expressions and their role in a biological context. In particular, nanoflow reversed phase liquid chromatography coupled with tandem mass spectrometry (nLC-MS/MS) greatly increased the scope of our protein identifications.

The results of this study provide an extensive view of the effects that increased metal concentrations have on amphipods, by detailing the cascade of protein alterations

triggered by metal exposures. The strategy adopted in this study investigates statistical proteomic changes in the complete protein profile of amphipods, and contrasts with many previous studies which analyzed the effects of metals on individual molecules, such as heat shock protein 70, glyceraldehyde-3-phosphate dehydrogenase, glutathione transferase, superoxide dismutase, and ATP synthase. This challenge was also seen in our previous study concerning oysters and their stress responses when exposed to different heavy metals [11]. Although Zn is essential for the health of most organisms, excess Zn can be harmful. We present here important results from experiments aimed at recognizing the effects of zinc stress on the amphipod *M. plumulosa*, an abundant and important benthic organism.

## **5.2 Materials and Methods**

### **5.2.1 Materials and analytical chemistry**

All glassware, tubes and acrylic beaker-lids used for toxicity testing and chemical analyzes were cleaned by soaking in 10% (v/v) HNO<sub>3</sub> (BDH, Analytical Reagent grade) for a minimum of 24 h and then thoroughly rinsed with Milli-Q water. Subsequently, they were placed in a dishwasher (Lab999, Gallay Scientific Pty Ltd.) programmed for a phosphate-free detergent wash (Clean A, Gallay Scientific Pty Ltd.). All glassware was air dried for 6 h to prevent moisture interference. All chemicals used for the Zn exposure experiment were analytical reagent grade or equivalent analytical purity. Dissolved metal concentrations in seawater samples were acidified with ultra-pure nitric acid and analyzed with an Agilent 7700x inductively coupled plasma mass spectrometry (ICP-MS). The limit of reporting for the metals in seawater was 1 µg/L. As a check on analytical quality, blank seawater samples or test samples were fortified with a known concentration of dissolved zinc and recoveries for Zn of 82 to 87% were obtained.

### 5.2.2 Test organism

Cultures of *M. plumulosa* were established in the laboratory with animals collected from the northern shores of the Hawkesbury River near Brooklyn (33°32'3"S, 151°11'51"E), NSW, Australia (salinity, 27.0–33.8‰). The cultures were maintained under the conditions recommended by Hyne *et al.* [165] on silty sediments collected from Bonnet Bay, in the lower Woronora River, Sydney, Australia, (34°0'24"S, 151°3'27"E).

Adult amphipods were isolated from the cultures by slowly siphoning (tube diameter, 16mm) the surface layers of the sediment and retaining the amphipods on a sieve (mesh size, 710 µm). Juvenile amphipods were retained on a secondary sieve (mesh size, 212 µm) and maintained in separate culture trays to establish their growth and development. Amphipods (both males and females) were cultured for up to three adult generations prior to the experiment. Over 600 healthy sexually mature adult amphipods of uniform age were established and separated into two groups of males and females, and transferred to plastic trays containing a thin layer of natural sediment (2cm) with overlaying seawater. At 24 °C, the embryos are retained inside the marsupium of gravid females for seven days before hatching and subsequent release of 4-10 juveniles (see Figure 5.1). The number of gravid females required to generate subsequent generations was calculated on the expectation that each gravid female would produce at least three juveniles of similar size. Therefore, all ovigerous females were held for 7 days, to ensure the release of any pre-existing broods.

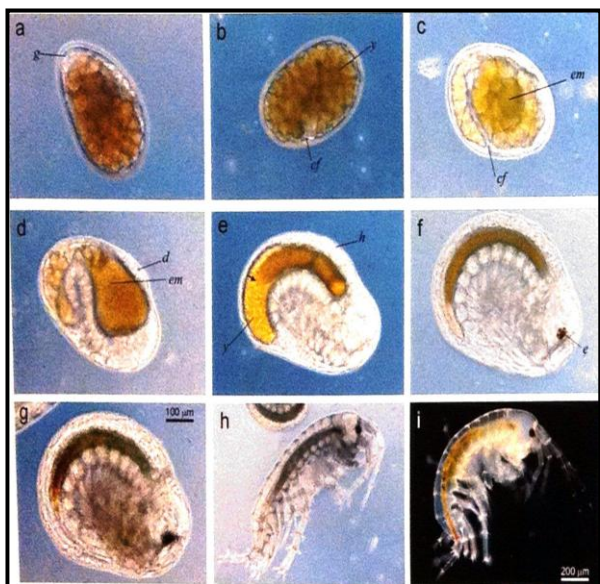


Figure 5.1. Stages of embryological development of *M. plumulosa*. All images in the sequence represent 1 day increments in development time starting with 1 day old embryos- stage 1 (a), 2 d – early stage 2 (b), 3 d – late stage 2 (c), 4 d – stage 3 (d), 5 d – stage 4 (e), 6 d – stage 5 (f), 7 d – pre hatch stage 6 (g), 7 d – post hatch stage 6 (h) and an eight day old free swimming juvenile (i). All photos are of whole embryos and are taken using a phase contrast illumination except i which is taken in dark field illumination. Plates a – g use scale bar in g. Plates h and i use scale bar in i. Structures indicated are: cf, caudal furrow; d, dorsal gland; e, eye; em, endodermal mass; g, germinal disc; h, heart; y, yolk.

**Figure 5.1** Different development stages in the amphipod life cycle beginning from an embryo through to a young amphipod (image adapted from [345]).

On day 8 after the separation of the sexes, the females were subsequently exposed to males which lead to approximately 80% of females becoming gravid over a 24 h period. This was done in order to synchronise the ovarian cycle of the female amphipods in preparation for the subsequent metal exposure experiments. Gravid females carrying embryos in stage 1 or 2 of their developmental cycle (Figure 5.1) were isolated for the Zn exposure experiment. Groups of stage 1 or 2 embryonic gravid females were used for exposure experiments. Gravid females were distinguished from males based on their smaller size and presence of much smaller second gnathopod, while non-gravid females were distinguished from gravid females by the presence of developing embryos in the

brood pouch marsupium by viewing under a Wild-Heerbrugg M3C dissecting microscope using low intensity dark field illumination.

### **5.2.3 Feeding**

Adult amphipods of a uniform size and age (8–10 mm; 2–3 months) were selected for the Zn exposure experiments. Amphipods were handled using a modified glass or plastic pipette and transferred to a watch glass with minimal water. Both male and female amphipods were fed with Sera<sup>®</sup> Micron (Heinsberg, Germany), a Spirulina-based dry powder food, at a rate of 0.5 mg per amphipod every 3 days during the holding and experimental period.

### **5.2.4 Test water**

Seawater was collected from Port Hacking (NSW, Australia) and stored in a fiberglass tank outside the laboratory until required. The seawater was filtered through a series of three filters (Stefani Australasia, Welshpool, Australia) consisting of a 5 mm particle cartridge, a 2 mm dual phase particle/organic adsorption cartridge and a 0.5 mm ion-exchange cartridge. The salinity was adjusted to 25‰ using Sydney tap-water that has been passed through a mixed bed filter and activated carbon filter and then allowed to stand for six weeks for dechlorination. This filtered seawater used for culturing and tests was stored in a plastic tank in the laboratory to allow temperature acclimation to  $21 \pm 1$  °C. Salinity of  $24 \pm 1$ ‰ and pH of 8.0–8.2 was maintained in waters used throughout this study.

### 5.2.5 Artificial sediment substrate

Sediment constituents were chosen to simulate the characteristics of natural sediment such as that of Bonnet Bay sediment, which has been shown to support amphipods survival and reproduction in previous studies with *M. plumulosa* [171, 80, 345, 341]. A commercially available milled silica (Silica-300G, Unimin Australia Limited, Sydney, Australia) was selected as a base substrate for the experiment. Silica-300G most closely replicated the particle size distribution of the natural sediment used in the amphipod cultures [356], with particles <75 µm in size, including 91.6% of the particles <38 µm in size. Silica-300G is devoid of organic carbon content unlike natural sediments, but previous studies have shown that this does not have significant effects on either the survival or fecundity of the amphipods [347]. Seawater was added to saturate the mixture, and the silica substrate was allowed to settle at 4°C for up to a week before using it for the experiments. The silica substrate was acclimated at room temperature ( $21 \pm 2^\circ\text{C}$ ) in 25‰ seawater for a minimum of 24 h prior to use.

### 5.2.6 Preparation of aqueous and silica-bound zinc

The exposures were set up in triplicates with 15 gravid female amphipods per replicate 1 L beaker maintained at a temperature of  $23 \pm 1^\circ\text{C}$  in a temperature controlled room set on a 12 h light/12 h dark cycle (light intensity of  $3.5 \mu\text{mol photons/s/m}^2$ ). The experiment was conducted over a period of 4 days. Water samples were taken from test beakers for metals analysis both at the start and termination of the test. A schematic representation of the experimental setup is shown in Figure 5.2. There were a total of four experimental groups, of which two contained silica substrate plus 25‰ seawater while the other two contained 25‰ seawater-only.

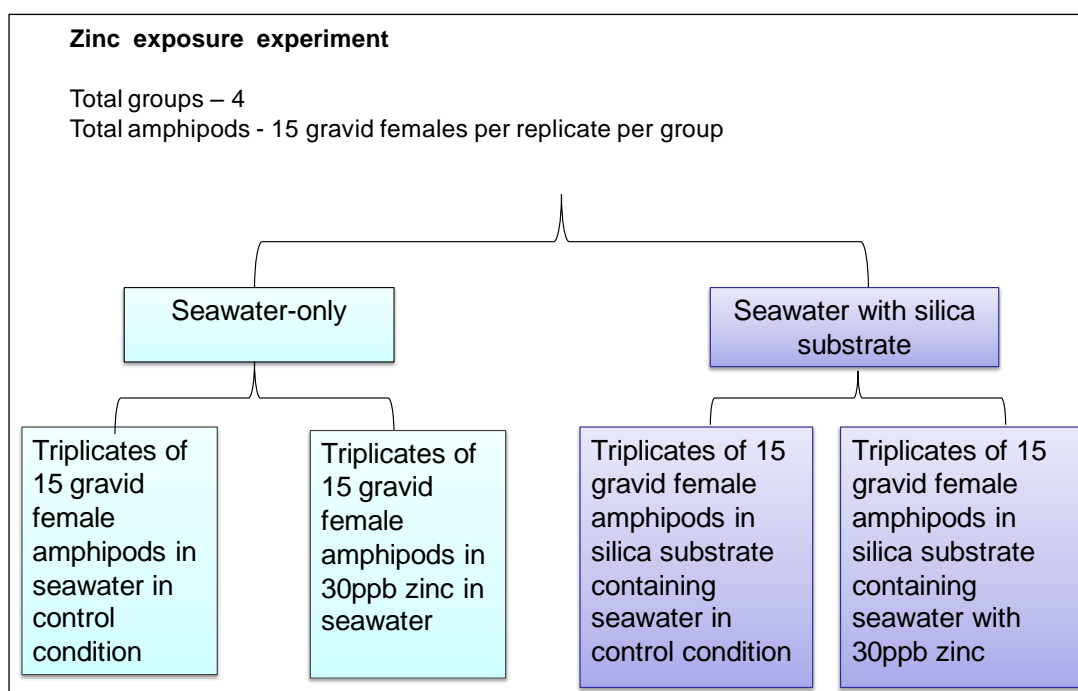


**Figure 5.2** Experimental groups setup used for the Zn exposure study on *M. Plumulosa* in 25‰ seawater.

The seawater-only Zn treatment was conducted in 1L beakers containing 900 mL of 25‰ seawater. Two nylon mesh strips (80 × 150 mm, 350 um mesh size,) were added to each beaker to provide a substrate for the amphipods. 30 µg Zn/L added as zinc sulfate was prepared by the addition of an aliquot from a 1.0 mg Zn/ml stock solution in milli-Q water to the 25‰ seawater. Prior to the commencement of the experiment each glass beaker used for the zinc exposure was pre-exposed to 30 µg Zn/L in 25‰ seawater for 24 h to saturate the inner glass walls with adsorbed zinc. This step was undertaken to minimise loss of zinc to the glass walls during zinc exposure experiments, thereby ensuring that the dissolved test concentrations of Zn remained stable [347]. Beakers used for controls were filled with the filtered 25‰ seawater without any addition of zinc. On the day of the experiment, solutions in the beakers were replaced with freshly prepared solution prior to the addition of the amphipods.

For the treatments with silica substrate, 50 g of Silica-300G substrate were placed into beakers and overlaid with 25% seawater. They were allowed to settle overnight for 1 day prior to the start of experiment. On the day of the test, this overlying water containing dust and other colloidal particulate was syphoned off and replaced with either 25% seawater containing 30 µg Zn/L or control 25% seawater. The solutions were poured without agitating the silica bed and allowed to settle again for 6 h before addition of amphipods.

After addition of the gravid female amphipods, all the test beakers were supplied with a gentle flow of air throughout the tests to maintain dissolved oxygen levels in overlying water at >85% saturation. Acrylic lids were placed over the beakers to minimise evaporation of seawater. Exposures were conducted for a period of 4 days with feeding once on day 3. For quality assurance purposes, physico-chemical parameters including dissolved oxygen at >85% saturation, pH (8.0–8.2), salinity ( $25 \pm 1\%$ ) and temperature ( $21 \pm 1$  °C) were monitored at the beginning and at test termination, in all replicate beakers per treatment to ensure that they remained within acceptable limits throughout the test. Test beakers were monitored daily to ensure that there was adequate aeration and minimal evaporation of the overlying water.

At the termination of the test, water samples collected from each beaker at the start and termination of the test were membrane-filtered (0.45 µm) immediately after collection, acidified with concentrated HNO<sub>3</sub> (2% (v/v), Trace Pur, Merck) to prevent metals from adhering to the plastic, and stored at 4°C until analysis. Dissolved metal concentrations in water samples collected at the start and end of the exposure tests were determined by inductively coupled plasma mass spectrometry (ICP-MS, Spectro Analytical Instruments) calibrated with matrix-matched standards (QCD Analysts). At the

termination of the test, the surviving amphipods in each beaker were gently removed counted, collected in pre-labeled cryo vials (Nalgene, Rochester, USA), and allowed to settle by gravity to remove the overlying water before immediately plunging the vials in liquid nitrogen to freeze-dry the amphipod pellet. Samples were stored at -80°C until protein extraction.

#### **5.2.7 Generation of survival data**

For the tests, amphipod survival data were expressed as a percentage  $\pm$  RSD.

#### **5.2.8 Protein extraction**

Proteins were extracted from 10-12 snap frozen amphipods into the 2DE rehydration buffer containing 6M urea, 2M thiourea, in 20mM Tris HCl with 4% CHAPS. The amphipods were homogenized into a fine powder with liquid nitrogen using a pre-chilled mortar and pestle, and further ground into a fine paste with the addition of 0.75mL LS tri-reagent (Sigma Aldrich, USA) and 0.25 mL of 2DE rehydration buffer (in the ratio 3:1 (v/v)), with 0.1% protease inhibitor cocktail (Roche Applied Science, Germany). Traces of RNA and DNA contained within each of the tissue homogenates were removed, and proteins were extracted and thoroughly washed according to methods described in Chapter 2, section 2.1.2. The protein pellets were air dried until the ethanol evaporated, and then solubilized in 100 $\mu$ L of IEF rehydration buffer consisting of 6M urea, 2M thiourea, 4% CHAPS in 100mM Tris-HCl (pH8.5) and 0.1% protease inhibitor cocktail (v/v). The concentration of protein in the solution was measured by Bradford assay.

### 5.2.9 Two dimensional poly-acrylamide gel electrophoresis (2DE)

To an aliquot of 250 µg of protein from each sample, 6 µL of 1M DTT, 0.5 µL of 4-7 IPG buffer (ampholytes), 0.5 µL of 3-10 IPG buffer, and 3 µL of bromophenol blue were added and the volume was adjusted to 215µL using IEF rehydration buffer consisting of 6M urea, 2M thiourea and 4% CHAPS in 100mM Tris-HCl (pH8.5). The sample solution was mixed thoroughly and centrifuged at 10,000 ×g for 5 min. This solution was used to rehydrate IPG strips of 11cm length and 4-7 pI range (Bio-Rad, Hercules, California). First, the IPG strip was passively rehydrated for 4 h to allow complete absorption of sample solution. Following this, the IPG strip was transferred to the focusing tray with the gel side facing down and aligned with the electrodes. Moist absorbent paper wicks were placed on top of each electrode underneath the strip, to aid in the removal of salts and other components of the sample which otherwise collect at the anode and cathode. Secondly, the IPG strip was subjected to active rehydration at 50v for 10 h. The strip was covered with mineral oil to prevent drying out during focusing. Isoelectric focusing was performed using a Biorad PROTEAN<sup>®</sup> IEF Cell unit where the voltage gradient was held at 50 µA per strip in 4 steps; starting at 200 v for 1 h, 1000 v for 1 h, 4000 v for 3 h, and 8000 v for 5 h. All steps were 'step-ups' to the next voltage, except for the transition from 1000-4000V, which was a linear gradient. Saturated wicks were replaced with fresh ones at the start of the 8000v ramp. This ensured that the voltage reached the maximum without going over the current limit. Volt hours measured at the end of the run were typically 40-50,000 VH.

Re-equilibration of focused protein spots under reducing and alkylating conditions were performed before fractionation by SDS-PAGE. The IPG strips were removed from the focusing tray and placed with gel side up on paper towels to remove oil from the back

of the strip. The IPG strips were first re-equilibrated at reducing conditions for 20 min with gentle rocking in buffer consisting of 6M urea, 20% glycerol, 2% SDS, 130 mM DTT in 50 mM Tris-HCl (pH 8.8) [170]. The strips were then subjected to alkylating conditions for 20 min with gentle rocking in buffer containing 6M urea, 20% glycerol, 2% SDS, 135 mM iodoacetamide in 50 mM Tris-HCl (pH 8.8) [170].

SDS-PAGE was carried out to separate proteins in the second dimension. IPG strips were equilibrated buffer for 25 min with gentle rocking in 1x Tris-glycine buffer containing 10% SDS. Precast 11 cm criterion SDS-PAGE gels of 10% acrylamide, IPG+1 well, were used (Bio-Rad). Bio-Rad unstained markers (7 $\mu$ L) were loaded in to the additional well on the gel. The IPG strip was sealed to the top of the SDS-PAGE gel with 0.5% agarose in running buffer, plus a trace of bromophenol blue. The SDS-PAGE running conditions were set to 70v for 12 min to allow high molecular weight proteins to slowly migrate to the stacking portion of the polyacrylamide gel, followed by 150v for 1 h 40 min to enable the low molecular weight proteins migrate to the bottom of the gel.

The gels were fixed with deep purple fixing solution consisting of 15% ethanol, 1% citric acid in water, with shaking overnight, and stained for 1 h using deep purple fluorescent protein stain (Gel Company) pre-mixed with 100 mM sodium borate solution in the ratio 1:200 (v/v). Gels were washed with 15% ethanol for 30 min to remove excess stain, and this was followed by acidification for 30 min in 15% ethanol in 1% citric acid solution. The gel was imaged by fluorescent scanning at 500 microns resolution, 510 PMT, 532 nm wavelength and normal sensitivity using a Typhoon scanner (GE Healthcare). Images were captured after adjusting scan settings to reduce saturation, and images from fluorescent stain were used for spot detection and spot analysis. The gels

were then re-stained with blue silver stain solution and imaged using a flat-bed scanner to aid spot picking for trypsin in-gel digestion.

## **5.2.10 Progenesis 2DE Image Analysis**

### **5.2.10.1 Image Quality check**

The images used for analysis were cropped, rotated and flipped prior to analysis if required. The images were then imported for image quality testing and a number of quality checks were performed on the images including bit depth, dynamic range and resolution. The images were grouped into the gels they originated from and a gold standard image for each exposure condition was created from high quality reference gels run for the same sample in preliminary experiments. The gold standard image was used as a baseline to compare with all corresponding gel images pertaining to the experiment. Gel images were tested against this gold standard by considering each spot individually and comparing values for the test gel against the range found in gold standards for each spot; this was done using standard deviations that measured the spread of values for each spot. For each exposure condition, gel images with 80% of spots within five standard deviations of the corresponding gold standard were representative of high image quality and were used for further image analysis. Further, selection of a reference image was vital for the alignment of other replicate gel images within the experiment. This was done by selecting a replicate gel image which was clear, represented the full spot pattern and had minimal distortion.

### **5.2.10.2 Experimental design and masking spots of disinterest**

The experimental design was set up such that the images of the triplicate gels were compared between groups. Therefore, triplicate gels from the two treatment groups (controls or Zn exposed) were compared between groups for each exposure condition

(seawater-only or silica substrate+seawater). Certain areas of the gel images such as the edges of the gels and saturated areas of the gel were masked to exclude them from image analyses and spot detection. Each of the 12 images was subsequently processed for alignment and spot detection.

#### **5.2.10.3 Alignment**

Alignment of the spots among gels is the most important stage in the Progenesis SameSpots workflow. Positional variations between protein spots on all gel images were corrected to ensure 100% matching between spots to enable statistical analysis. Each image was aligned both manually and automatically to obtain best matching. Reference image and gel images were first manually aligned by adding alignment vectors across the gel to ensure overall fitness, before proceeding to automatic alignment to fine-tune the alignment by adding automatic alignment vectors for all spots. The positional shifts caused by the alignment vectors were checked using visual tools to view the effect by switching to an aligned view. Using the focus grid size control box, each of the vectors was edited if required to improve the image alignment. Alignment criteria were set at 85% of the spots being within 3 standard deviations of the reference standard.

#### **5.2.10.4 Filtering and refining detected spots**

A spot was counted only if reproducibly present in triplicate gels for each treatment group. Average spot volumes were calculated for each reproducible spot and upon completion of filtering, the lists of spots detected were consolidated and normalisation of average spot volumes for all spots was reviewed. Spots were sorted based on p-value <0.05 and fold change based on normalised average spot volumes between control group and Zn exposed, to determine which spots were displaying significant

changes. For each spot from the list, spot expression profiles and 2D / 3D montage views were used to locate the spot on each of the gel images in each group, and spot editing was performed on spots where necessary. All spots that were selected were analyzed in Progenesis Stats.

#### **5.2.10.5 Progenesis stats**

As a multivariate and unsupervised statistical analysis tool, Progenesis Stats was used for data exploration, image quality control and visualisation of differentially expressed spots. Spots were checked for spot location, correlation analysis, false discovery test and Principal Components Analysis (PCA). For PCA, spot expression levels were used across the images and the principal axis of expression variation was determined. Plotting the expression data in PCA detected whether the images were clustered together as per their experimental groups. Any obvious outliers identified were manually examined.

#### **5.2.10.6 Viewing results**

To narrow down the relevant spots to be picked for mass spectrometric analysis, tags were used to group together spots with the same characteristics. Spots were filtered and tagged according to their  $p$ -value  $< 0.05$ , and fold change  $> 2$  based on differences between normalised average spot volumes corresponding to control group and Zn exposed. A color-coded list of differential spots within these characteristics was generated based on expression profiles using the correlation analysis.

#### **5.2.10.7 pI and M.Wt. calibration**

Spots were calibrated by adding an estimated pI or MW value to either known spots or a molecular weight ladder. Calibration values were updated on the fly as marker points were added. The pI and MW values were displayed alongside all the spot data.

#### **5.2.10.8 Spot picking and report generation**

A clean, non-distorted image, preferably a reference image used earlier in the alignment stage or a gold standard image for each group, was selected for spot picking. Spots selected for picking at this stage were annotated on the whole image view and the spot details were saved in the appropriate format. In the final stage, a report summarising spots and results was generated.

#### **5.2.11 Identification of proteins from 2DE spots using MALDI TOF/TOF and nanoLC-MS/MS**

Differential 2DE spots were excised and cut into 4-6 gel pieces and transferred into a microcentrifuge tube. The gel pieces were equilibrated in 100mM ammonium bicarbonate solution with slow vortexing for 5 min at room temperature prior to washing the gel pieces with 50mM ammonium bicarbonate / 50% acetonitrile (v/v) solution for stain removal. The steps for washing were repeated until gel pieces looked transparent and clear. After stain removal, subsequent in-gel trypsin digestion for each spot was carried out according to method described in Chapter 2, section 2.2.1.

For MALDI-TOF/TOF MS analysis, peptide extracts from the 2DE spots were concentrated and desalted using a C18 zip tip (Waters) (as described in chapter 2, section 2.2.1), reconstituted in 1  $\mu$ L matrix solution containing ( $\alpha$ )-cyano-4-hydroxycinnamic acid

dissolved in 70% methanol / 0.1% TFA (v/v) and loaded onto a MALDI sample target plate. BSA control digests (a zip tipped control and a non-desalted control) were also loaded as positive controls in adjacent wells. Peptide mix solution was used as calibration standards, and was prepared to contain bradykinin, neurotensin, angiotensin I (all 0.2 pmol/ $\mu$ L), and adrenocorticotrophic hormone residues 18-39 (0.8 pmol/ $\mu$ L), in 50% acetonitrile / 0.1 % TFA (v/v). The spots were air dried and the sample target plate was mounted onto the MALDI-TOF/TOF mass spectrometer (4800 Proteomics Analyzer, Applied Biosystems, Foster City, CA) and aligned before initiating analysis. Mass spectra were recorded in reflectron mode with an accelerating voltage of 25 kV, ions were extracted with 60 ns delay, each spectrum was averaged from 60-128 laser shots, and the top 8 ions in the MS spectrum were selected for MS/MS fragmentation.

MALDI spectral data for each spot was searched against all proteins from Refseq NCBI protein database (27,834,532 proteins as of Dec 2012) using GPM with search parameters similar to those described in chapter 2 section 2.6. The mass tolerance was limited to 50 ppm. MALDI MS/MS data for 2DE spots for which GPM resulted in no identifications were re-searched using the Mascot search engine with search parameters similar to that of GPM. Any resulting unmatched peptides with a significant Mascot score were subjected to BLAST search against all Swiss-Prot protein entries and those search results that showed at least 80% homology to a protein match were considered as true protein identifications for these spots.

For those spots for which MALDI TOF/TOF data was insufficient to identify a database match, a second set of 2DE spots were excised and tryptically digested to perform additional mass spectrometric analysis using nanoLC-MS/MS. They were resuspended in 10 $\mu$ L of 2% formic acid (v/v), centrifuged at 1000 rpm for 10min,

transferred to a 96 well plate and subjected to nanoESI LC-MS/MS analysis using a LTQ-XL linear ion trap mass spectrometer (Thermo, San Jose, CA). Samples were run as per methods described in sections 2.2 and 2.6 in chapter 2. Tandem MS spectra from the LTQ-XL were submitted for database search against the same Refseq NCBI protein database using both GPM and Mascot. Protein identifications from GPM for each 2DE spot were filtered to satisfy protein log(e) score  $< -3$  and minimum total peptide count  $\geq 2$  after correcting any unique and total peptide counts that resulted from multiple entries of the same protein corresponding to each spot.

## **5.3 Results and discussion**

### **5.3.1 Background**

Amphipods are an important component of benthic communities and are often highly sensitive when exposed to metal toxicants [186], particularly after the ingestion of metal-contaminated sediments [178, 340, 187]. These benthic invertebrates have become important bioindicators in sediment quality assessments [342]. Sediment ingestion has been shown to be an important pathway for toxicant entry in *M. plumulosa* when exposed to metal contaminated sites, and this stems from their epibenthic-sediment scavenging behaviour. Studies by King *et al.* [344, 164] with *M. plumulosa* maintained on copper and zinc contaminated sediments confirm the importance of sediment properties on metal uptake by *M. plumulosa*. Amphipods and other benthic organisms are a major part of the diet of small fishes, and thus metal contaminants from the sediments bioaccumulate into the aquatic food web over time.

### **5.3.2 Amphipod behavioural response to Zn exposure, when maintained either in seawater-only or in addition with silica substrate**

In this study, amphipods were exposed to Zn in two experiments maintained with or without the presence of Silica-300G substrate. Gravid female amphipods, synchronised at day 1 of their ovarian cycle, were exposed for 4 days with feeding on the 3<sup>rd</sup> day, to Zn added to the overlying seawater (25‰ salinity) in the presence or absence of Silica-300G substrate. Amphipod survival after 4 days was  $96 \pm 1\%$  following continuous exposure to a nominal concentration of  $30 \mu\text{g Zn/L}$  in the seawater-only treatment, compared to 100% survival for the water-only controls. In contrast, the presence of the silica substrate decreased amphipod survival after 4 days for both treatments, with  $62 \pm 2\%$  survival for the treatment containing an added nominal concentration of  $30 \mu\text{g Zn/L}$  compared to  $66 \pm 1\%$  survival for the silica substrate control. The initial measured zinc concentration through ICP-MS in the seawater-only treatment was  $28 \mu\text{g/L}$  indicating minimal adsorption of the Zn to the walls of the beaker, as found previously by Mann *et al* [347]. In comparison, the initial measured zinc concentration in the treatment containing the silica substrate was  $12 \mu\text{g Zn/L}$  indicating rapid adsorption of the Zn to the silica particles, as similarly reported previously [347]. The nominal concentration of  $30 \mu\text{g Zn/L}$  used in the seawater-only treatment was considerably lower than the previously reported 10-day LC50 value of  $490 \mu\text{g/L}$  for Zn in adult female amphipods grown in seawater-only [347], and so was not expected to affect the motility of the amphipods after the 4-day exposure period. In contrast, a measured initial concentration of  $12 \mu\text{g Zn/L}$  in the treatment containing silica substrate was similar to the previously reported zinc concentration of  $22 \mu\text{g/L}$  that caused a significant reduction in female fecundity [347]. Hence, the observed  $62 \pm 4\%$  survival after 4-d exposure found in this study was not unexpected. However, the observed survival of  $66 \pm 1\%$  for the silica substrate control was lower than the 100%

gravid female survival found previously, possibly because some samples of the Silica-300G contain sharp edges that would likely cause physical damage to the amphipods. Nevertheless, an assessment of the difference in the proteomic response between the two treatments containing silica substrate was still possible. In summary, continuous seawater-only exposure to low concentrations of waterborne Zn supported good survival of the adult amphipods, whereas, in contrast, the presence of the silica substrate resulted in increased sensitivity of the amphipod to added zinc.

During the experiment, although the fine silica-substrate was non-nutritional, the amphipods were observed to actively ingest the fine-grained silica particles as a result of their benthic foraging behaviour. As a consequence of this behaviour, almost all of the Zn that was partitioned into the sediment due to adsorption from the water column was bioavailable. Most likely, the adsorbed Zn on the silica was loosely bound when compared to the binding strength of Zn found in natural sediments. Natural sediments have the capacity to bind heavy metals facilitated by the presence of Fe- and Mn-(hydr)oxide phases and organic matter that acts as an additional substratum for further adsorption [357]. The presence of sediment greatly increases the benthic behaviour of amphipods, leading them to constantly scavenge for any available food.

The foraging behaviour by the amphipods would undoubtedly demand more energy and higher metabolic activity while increasing the exposure of Zn through the gut and the gills. We hypothesised that in response to the increased Zn uptake, the amphipods metabolic detoxification processes would be activated which, in turn, would also deplete metabolic resources and energy. This proposal was examined in the proteomic analysis of the Zn exposed amphipods to the corresponding non-exposed controls for amphipods maintained in either seawater-only or in addition on silica substrate.

Food availability has been a subject of investigation in toxicity tests and has been variously reported to either potentiate or mitigate the effects of metal toxicity. Cu metal toxicity was reportedly not ameliorated by the presence of algae containing food when supplied to *M. plumulosa* in a sediment toxicity test spanning 10 days; and the same study also concluded that starvation increased mortality by over 50% in amphipods over 10 days [358]. In another study, the addition of algal food was reported to increase toxicity effects [164], where the authors concluded that food supply led to increased non-selective foraging behaviour, and therefore ingestion of greater levels of metals from contaminated sediments. Although Silica-300G is an unsuitable substrate for long-term culture purposes as it provides no endogenous nutritional quality or microbial activity for nutrient recycling to prevent eutrophication, it does provide an inert substrate that supports good survival and reproduction of *M. plumulosa* over the duration of a toxicity test. Such a defined system enabled the short-term proteomic response to low concentrations of Zn on amphipod reproduction to be investigated, in the presence or absence of added food.

### **5.3.3 Proteomic analysis of Zn toxicity responsive proteins using 2DE and mass spectrometric identification of differential proteins**

For ease of understanding, we have used the term ‘protein spot’ to indicate a single spot on a 2DE gel. We are aware that a gel spot may contain more than one protein, and, conversely, a single protein may be found present in several spots. For the same reason, we have used the widely accepted terms ‘up-regulated’ and ‘down-regulated’ to indicate changes in protein expression, without formally investigating whether the observed differences were due to differential regulation or accumulation.

A numerical summary of protein detection data from amphipods maintained in 25‰ seawater-only or in addition with silica substrate and exposed to Zn or no Zn-

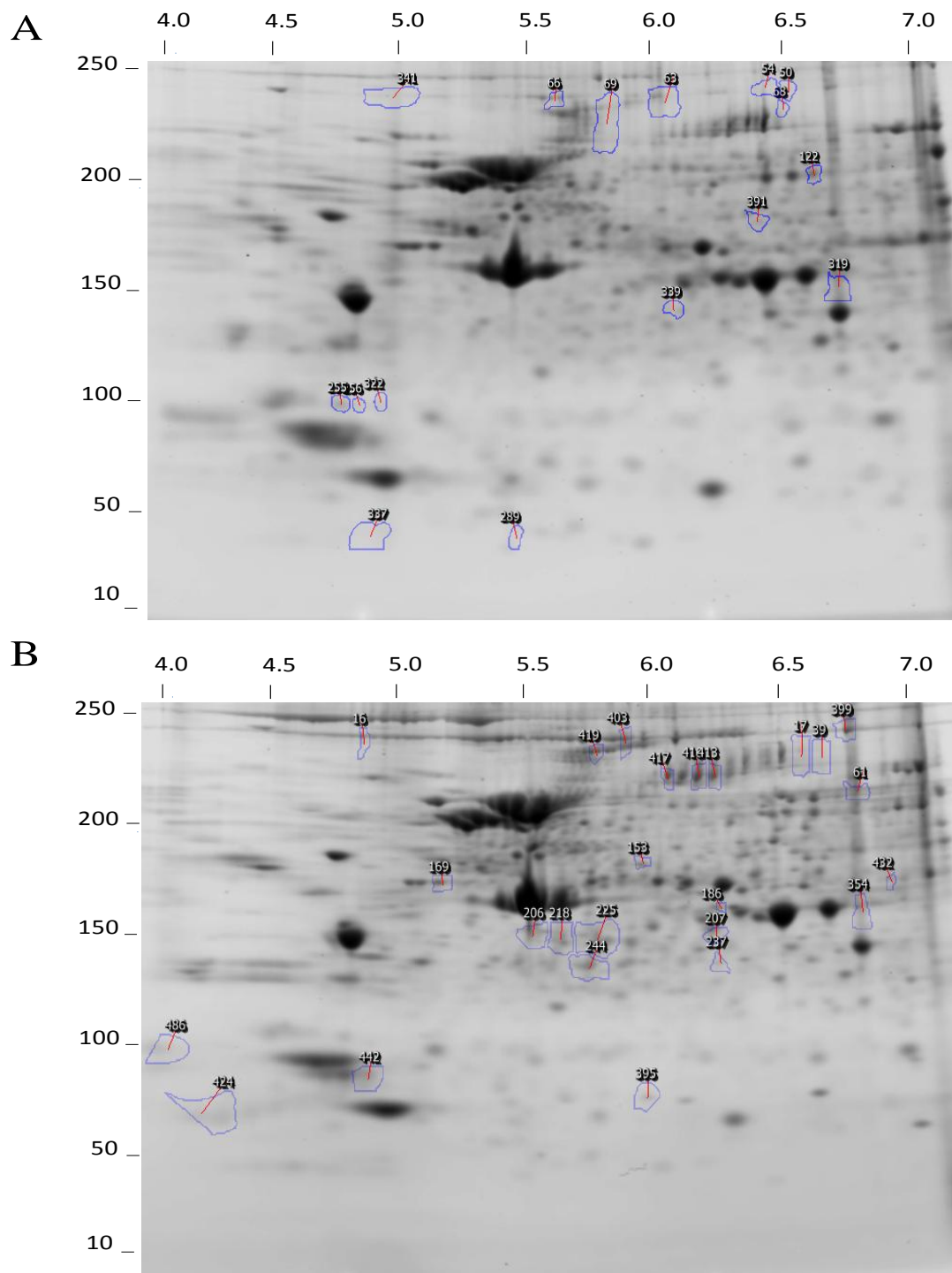
exposed (control) conditions are shown in Table 5.1. A total of 238 protein spots were detected and analyzed in each of the three biological replicate gels of controls and Zn-exposed amphipods maintained in the seawater-only treatments. In comparison, 264 protein spots were detected in the controls or Zn-exposed amphipods maintained on silica substrate in 25‰ seawater treatments. The gravid female amphipods (oocytes in primary vitellogenesis) cultured on sediment will undergo secondary vitellogenesis [359], but the oocytes of the female amphipods in the water-only treatments will not undergo secondary vitellogenesis [360]. This would explain the additional protein expression in the silica-substrate treatments.

The consistent number of protein spots identified in each gel among all exposures correlates well with the standardized amount of 250µg of protein analyzed for each experiment. All protein spots examined were within a pI range of 4-7 and protein molecular size from 10-250kDa. Statistical analysis of spot measurements showed good reproducibility between replicate gels of each group and also showed protein spots that changed in their protein expression in response to Zn exposure.

**Table 5.1      Summary of protein identifications**







<b>Data summary for amphipods exposed to Control / Zn conditions in 25‰ seawater-only</b>	
Total number of statistically reproducible protein spots detected	238
Total number of significant differentially expressed protein spots	11
Total up-regulated protein spots in comparison with controls	10
Total down-regulated protein spots in comparison with controls	1
Percentage of spots identified among the 11 differentially expressed proteins	100%
Total proteins identified	12
<b>Data summary for amphipods exposed to Control / Zn conditions maintained on silica substrate in 25‰ seawater</b>	
Total number of statistically reproducible protein spots detected	264
Total number of significant differentially expressed protein spots	25
Total up-regulated protein spots in comparison with controls	9
Total down-regulated protein spots in comparison with controls	16
Percentage of spots identified among the 25 differentially expressed proteins	96%
Total proteins identified	32
Non-redundant count of protein identifications (differentially expressed)	41

















In this study, we identified a total of 41 differentially expressed proteins from a total of 36 differential protein spots shown in Figure 5.3, arising from the two Zn exposure experiments for amphipods maintained in 25‰ seawater-only or maintained in addition with silica substrate. Protein spots were analyzed using both MALDI-TOF/TOF and nanoLC-MS/MS (LTQ) in order to maximize protein identification results.















**Figure 5.3** Fluorescent images of 2DE gels were acquired for amphipods exposed to Zn (A) when maintained in 25‰ seawater-only, and (B) when maintained on silica substrate in 25‰ seawater. Differentially expressed protein spots that were up- or down-regulated are marked with spot numbers and corresponding protein identifications are listed in Table 4.4.

Spot data from Progenesis analysis including spot volume values that directly reflect statistically distinct changes in protein expression levels from each exposure experiment are shown in Table 5.2.

**Table 5.2** Spot data for a total of 36 differentially expressed 2DE protein spots in response to Zn toxicity from amphipods (a) maintained in 25‰ seawater-only, (b) maintained on silica substrate in 25‰ seawater. 2DE gels of biological triplicates were analyzed between groups using Progenesis and those listed above were statistically significant, suited for further analysis. Coloured tags represent the following  edited;  Anova p-value  $\leq 0.05$ ;  down-regulated;  fold change  $\geq 2$ ;  up-regulated;  induced proteins compared to controls.

#	Spot Anova (p) value	Fold change	Tags	pI	MW	Average Normalised Spot Volumes <sup>†</sup>	
						Control seawater-only	Zinc seawater- only
319	7.66E-05	2.7		6.65	156	4324.104	1.15E+04
256	6.80E-04	2.4		4.85	97	520.785	1254.256
339	0.001	2.3		6.18	144	839.939	1967.57
341	0.002	3.4		5.0	232	3221.552	1.11E+04
54	0.006	3.4		6.4	246	1342.826	4520.643
69	0.009	2.7		5.8	237	7300.108	1.99E+04
122	0.014	2.0		6.7	252	1772.06	918.111
63	0.032	2.6		6.1	224	4368.764	1.15E+04
391	0.033	2.1		6.4	183	978.408	2063.468
50	0.035	3.7		6.5	241	506.437	1884.77
66	0.049	2.2		5.6	240	2221.951	4805.602
						Control silica	Zn Silica
61	0.02	3.1		6.73	213	9.69E+05	3.17E+05
237	0.018	3		6.18	135	1.30E+05	4.38E+04
218	0.023	3		5.55	145	9.94E+05	3.35E+05
413	0.007	2.8		6.17	218	1.57E+06	5.60E+05
244	3.05E-04	2.7		5.65	133	1.08E+06	3.91E+05

#	Spot Anova (p) value	Fold change	Tags	pI	MW	Average Normalised Spot Volumes <sup>†</sup>	
225	9.27E-04	2.7		5.69	143	2.41E+06	8.90E+05
416	0.004	2.7		6.1	216	2.39E+06	8.80E+05
16	0.005	2.7		4.74	236	2.50E+05	9.30E+04
186	0.011	2.7		6.18	161	1.53E+05	5.58E+04
399	0.008	2.6		6.7	237	1.52E+06	5.90E+05
403	0.015	2.6		5.8	233	1.30E+06	4.92E+05
39	0.031	2.6		6.57	225	4.37E+05	1.15E+06
207	0.032	2.6		6.17	150	4.92E+05	1.86E+05
354	0.006	2.4		6.75	159	8.36E+05	1.97E+06
417	0.015	2.4		5.98	217	1.04E+06	4.26E+05
486	0.019	2.4		4.0	96	5.56E+05	1.35E+06
432	0.01	2.3		6.88	171	1.25E+05	2.87E+05
153	0.011	2.2		5.87	179	2.11E+05	4.60E+05
419	0.031	2.2		5.67	228	1.03E+06	4.58E+05
206	0.004	2		5.42	150	1.06E+06	5.22E+05
169	0.021	2		5.04	171	5.49E+05	1.09E+06
424	0.039	2		4.18	65	6.85E+05	3.35E+05
442	0.044	2		4.71	85	1.04E+06	2.04E+06
17	0.046	2		6.49	236	7.53E+05	1.52E+06
395	0.001	2		5.9	74	2.08E+05	3.93E+05

<sup>†</sup>R.S.D values and spot volumes corresponding to differential 2DE spots in triplicates are given in Supplementary Information Table S8.

MALDI-TOF MS data were first searched against all proteins contained in NCBI nr database (as of December 2012) using GPM and for those with no significant match results, data were re-submitted for searches in Mascot followed by BLAST search of unmatched peptides against all entries in NCBI plus Swiss-Prot. For those protein spots for which MALDI data resulted in no identifications, nanoLC-MS/MS was used for subsequent identification, including database searching using GPM, Mascot and NCBI blast. Some spots were re-analyzed by both MALDI and LTQ to confirm identifications. Protein identifications were corrected for bias arising in peptide quantitation from peptide matches from multiple species contained with the nr database. These corrections were performed by using an in-house strategy similar to that previously developed in our laboratory and described in Muralidharan *et al* [11]. Table 5.3 lists all significant protein identifications that were obtained for each of the 36 spots that showed differential protein expression of the amphipods in response to Zn stress from both the silica and seawater-only experiments. Distinct protein identifications resulted from both MALDI-TOF MS and LC-MS/MS, as indicated in Table 5.3, demonstrating the complementarity of the two approaches. Each protein identified in a spot satisfied a minimum total peptide count of 2 and protein expectation value in GPM of less than or equal to  $\log(e) < -3$ . Spot numbers listed in Table 5.3 refer to those marked on the gel images in Figure 5.3A and B, and correspond to differential spots from amphipods maintained in 25‰ seawater-only and silica substrate in 25‰ seawater, respectively. Together they represent the statistically significant differentially expressed proteins identified in this study which are discussed further in this chapter. Supplementary Information Table S9 provides a detailed account of all differentially expressed proteins that were identified in response to Zn toxicity, along with peptide quantitation, peptide sequence and protein ontology information from the two Zn exposure experiments.

**Table 5.3** List of proteins identified for each of the 36 differentially expressed spots in response to Zn exposure when compared to controls (non-exposed amphipods) maintained in (a) 25‰ seawater-only (b) silica substrate in 25‰ seawater. These spots were statistically significant, with average normalized spot volumes showing p-value  $\leq 0.05$  and fold change  $\geq 2$ . Entries marked by ‘\*’ indicate results obtained for the spots for which unmatched peptides extracted from Mascot results were re-searched and identified by BLAST.

#	Spot Anova (p)	Fold change <sup>‡</sup>	Protein name	cU <sup>†</sup>	cT <sup>†</sup>	Protein log(e)	MS Meth
<b>A. Differential proteins from exposing amphipods to 30ppb Zinc in 25‰ seawater-only</b>							
50	0.035	3.7↑	actin	3	19	-55.1	Ltq
			tropomyosin	1	2	-4.7	Ltq
			ATP-dependent protease ATP-binding subunit	1	3	-4.2	Ltq
256	0.000068	2.4↑	GAPDH	7	10	-37.6	Ltq
			actin	14	18	-35	Ltq
			malate dehydrogenase	2	6	-9.1	Ltq
			tropomyosin	1	2	-5.5	Ltq
			serine threonine kinase associated protein	1	2	-4.1	Ltq
391	0.033	2.1↑	actin	11	13	-29.1	Ltq
			malic enzyme	2	5	-7.6	Ltq
			T-complex protein subunit $\alpha$	1	2	-3.8	Ltq
			GAPDH	2	3	-12.1	Ltq
122	0.014	2.0↓	actin	11	13	-47.2	Ltq
319	0.000076	2.7↑	GAPDH	14	22	-69	Ltq
			actin	11	15	-31.5	Ltq
			tropomyosin	1	2	-4	Ltq
54	0.006	3.4↑	actin	12	15	-41.1	Ltq
			myosin heavy chain	5	6	-18	Ltq/ Maldi
			catchin	1	2	-10.7	Ltq
			GAPDH	2	3	-8.4	Ltq / Maldi
			tropomyosin	1	2	-5.1	Ltq
341	0.002	3.4↑	myosin heavy chain	19	27	-96.5	Ltq/ Maldi
			catchin	1	2	-21.3	Ltq
			actin	8	10	-18.6	Ltq
			GAPDH	2	2	-9.2	Ltq

#	Spot Anova (p)	Fold change <sup>‡</sup>	Protein name	cU <sup>†</sup>	cT <sup>†</sup>	Protein log(e)	MS Meth
			tropomyosin	1	2	-7.2	Ltq
			leucyl-tRNA synthetase	1	2	-3.9	Ltq
69	0.009	2.7↑	Glycogen phosphorylase B	1	4	-3.3	Maldi
63	0.032	2.6↑	myosin heavy chain	1	2	-4.1	Maldi
339	0.001	2.3↑	guanine nucleotide-binding protein	2	2	-5.1	Maldi
66	0.049	2.2↑	myosin heavy chain	2	2	-3.4	Maldi
<b>B. Differential proteins from exposing amphipods to 30ppb Zinc on silica substrate in 25‰ seawater</b>							
61	0.02	3.1↓	GF23033 protein	2	2	-11.4	Ltq
			DHHC palmitoyltransferase	1	2	-3.2	Ltq
218	0.023	3↓	actin	27	71	-121.4	Ltq
237	0.018	3↓	cytokeratin	1	2	-5.2	Maldi
413	0.007	2.8↓	T cell receptor immunoglobulin domain beta chain	1	3	-5.1	Ltq
			hypothetical protein	1	2	-3.3	Ltq
			RNA-binding protein cabeza	2	2	-9.3	Ltq
244	3.05E-04	2.7↓	actin	2	2	-21.4	Maldi
			emrB/QacA family drug resistance transporter	2	2	-10	Ltq
			ARM like folded protein	2	2	-9.2	Ltq
225	9.27E-04	2.7↓	actin	3	3	-22.2	Maldi
			cell morphogenesis protein	1	2	-3.6	Ltq
416	0.004	2.7↓	ABC transporter permease	1	2	-3	Ltq
			xanthine dehydrogenase	1	2	-3.2	Ltq
16	0.005	2.7↓	conserved glycine rich protein	2	2	-4.1	Ltq
186	0.011	2.7↓	ATP-dependent DEAD/H RNA helicase	2	2	-9.2	Ltq
			arginine kinase	2	2	-10.7	Ltq
			heat shock protein 70	3	3	-9.2	Ltq
399	0.008	2.6↓	lon protease homolog	2	2	-9.2	Ltq
			DNA-damage-inducible protein	2	2	-10.5	Ltq
403	0.015	2.6↓	phosphatidylinositol:UDP- GlcNAc transferase	1	2	-3.5	Ltq
207	0.032	2.6↓	fructose-bisphosphate aldolase	1	4	-3.2	Maldi

#	Spot Anova (p)	Fold change <sup>‡</sup>	Protein name	cU <sup>†</sup>	cT <sup>‡</sup>	Protein log(e)	MS Meth
39	0.031	2.6↑	keratin 5	8	15	-92.6	Ltq
354	0.006	2.4↑	GAPDH	9	12	-15.3	Ltq/ Maldi
417	0.015	2.4↓	helicase-like protein	1	2	-4.4	Ltq
486	0.019	2.4↑	cytokeratin	2	2	-14.3	Maldi
432	0.01	2.3↑	hypothetical protein	2	2	-4.7	Ltq
153	0.011	2.2↑	DEAD (Asp-Glu-Ala-Asp) box polypeptide 39B	1	4	-4.1	Maldi
419	0.031	2.2↓	DNA polymerase epsilon	1	2	-3.8	Ltq
206	0.004	2↓	actin	1	1	-3.1	Maldi
169	0.021	2↑	ATP synthase beta subunit	1 9	19	-12	Maldi/ Ltq
424	0.039	2↓	DNA processing protein DprA	1	3	-4.2	Ltq
442	0.044	2↑	no protein identified				
17	0.046	2↑	hypothetical protein	1	2	-3.1	Ltq
395	0.001	2↑	glycerophosphodiester phosphodiesterase	1	1*	-6.4	Maldi/ blast
			GTP pyrophosphate synthetase	1	1*	-13.5	Maldi/ blast
			hypothetical protein	1	1*	0.033	Maldi/ blast
			hypothetical protein	1	1*	-13	Maldi/ blast
			tryptophan/ tyrosine permease	1	1*	-4.6	Maldi/ blast
			keratin 5	2	2	-11	Ltq
			sigma-54 dependent transcriptional regulator	2	2	-9.7	Ltq

<sup>‡</sup> Up and down regulation of proteins in response to metal stress relative to controls have been indicated by an upward arrow, '↑' and a downward arrow, '↓' respectively

<sup>†</sup> cU, represents corrected unique peptide count per protein from spot(s) identifying the same protein, where unique peptides resulting from multiple species were counted once only and added together after manual quantitation

<sup>‡</sup> cT, represents corrected highest total peptide count obtained for the protein from all matches that identified the same protein in the spot.

#### **5.3.4 Differentially expressed proteins from amphipods maintained in 25‰ seawater-only in response to zinc stress**

Among amphipods exposed to Zn in seawater-only, we obtained 12 statistically significant protein identifications from mass spectrometric analysis from eleven 2DE spots that showed differential protein expression compared to controls. A summary of these are listed in Table 5.3. Further detailed information on each of these protein identifications along with their peptide sequence and biological process information as found in KEGG and Uni-Prot is given in Appendix D1.

Of these 12 proteins, most were up-regulated including actin, ATP-dependent protease ATP-binding subunit, tropomyosin, myosin heavy chain protein and catchin, which had some of the highest protein expression changes extending up to 3.7-fold (Table 5.3). Actin was repeatedly identified in a few of these differential spots; however, all of them had unique peptides matches to distinct sequence entries as shown in Appendix D1. Although spot 122 was down-regulated, it was also identified as containing actin. This could possibly be due to acquired modifications in the isoelectric points of different isoforms of actin upon Zn metal exposure, or the possible presence of a novel actin isoform not identified previously in literature.

The 12 proteins were categorized based on their biological process information as found in KEGG and Uni-Prot, and the proteins were graphed first as a percentage in each biological process category as shown in Figure 5.4A-i. According to Figure 5.4A-i, it is evident that the largest groups of differential proteins in response to waterborne Zn toxicity on amphipods maintained in seawater-only belong to cytoskeleton and protein polymerization (34%) and carbohydrate metabolism (33%), followed by proteins involved

in protein metabolism (6%). Of the remaining, RNA metabolic processes and signal transduction processes comprised 8% each.

The 12 proteins were also re-graphed based on their abundance in each biological process category using the sum of all unique peptide counts per protein (Figure 5.4A-ii). According to Figure 5.4A-ii, the most abundant were the cytoskeleton and protein polymerization category of proteins (52%). Next in abundance were those belonging to carbohydrate metabolic processes (39%) followed by a small but significant portion of proteins involved in protein metabolic processes (5%).

Of the 12 proteins that were differentially expressed in response to exposure to waterborne Zn in 25‰ seawater, only actin and GAPDH were also similarly differentially expressed in amphipods exposed additionally to silica-bound Zn. Such varied biological responses likely stems from the differences in the two modes of Zn uptake by the amphipods [344]. In the seawater-only treatment, Zn uptake occurs by absorption of waterborne Zn, however, in the treatment containing silica substrate, additional Zn uptake by the amphipods can also occur after ingestion of silica-bound Zn particulates.

These alternate routes of Zn uptake resulted in considerable differences in the biological response of the amphipods to the Zn exposure in the two treatments after 4 days, with the amphipods exposed only to waterborne Zn having good survival in comparison to the amphipods also exposed to the silica-bound zinc. The 12 proteins that were differentially expressed by the amphipods in response to exposure to the waterborne Zn can be considered to be a metabolic response to Zn to maintain cellular homeostasis. In contrast, we have shown previously that the amphipods maintained on silica substrate in the presence of the added Zn would be undergoing toxicoses [347].

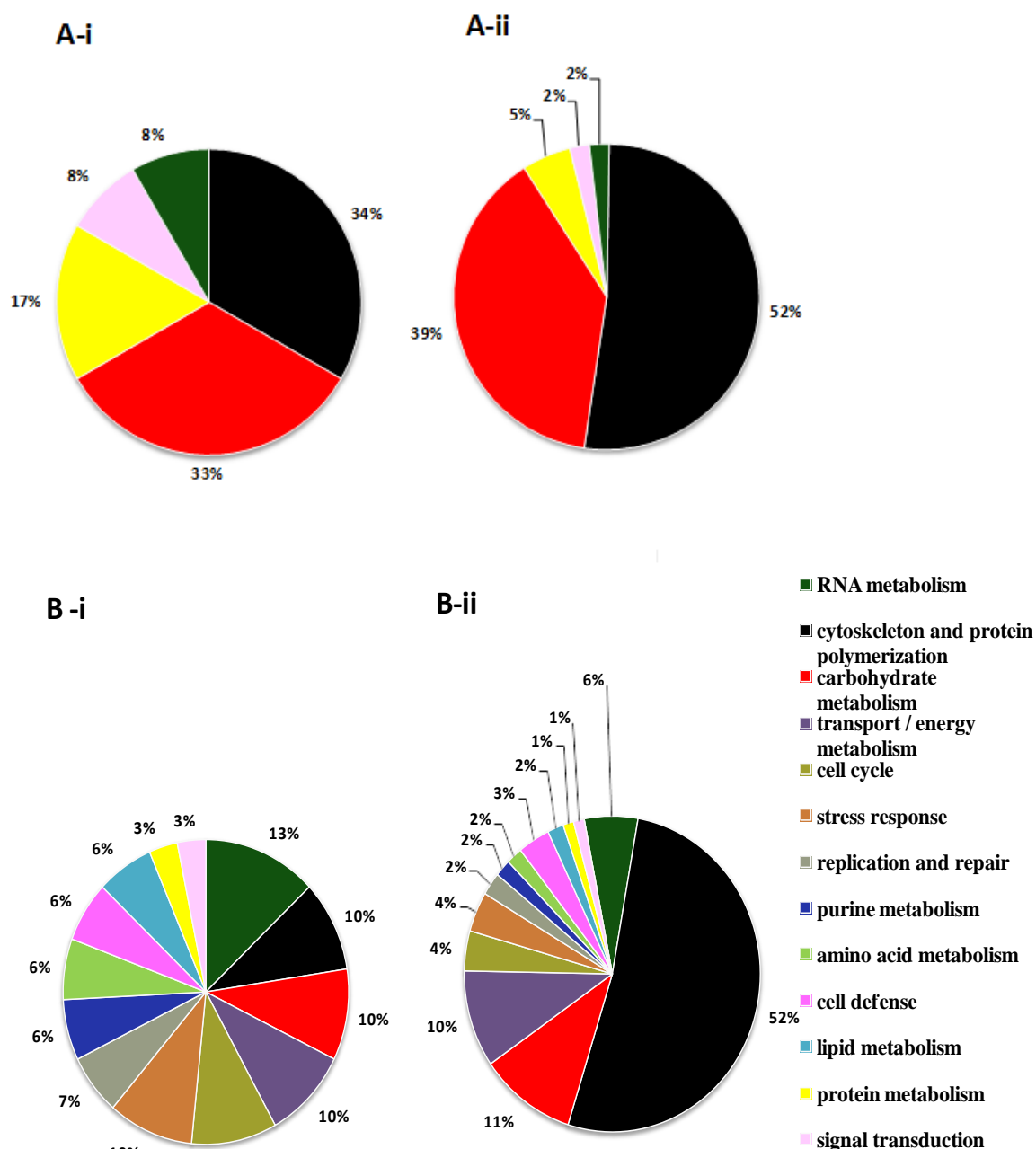


**Figure 5.4** Qualitative and quantitative distribution of proteins differentially expressed in amphipods in response to Zn exposure when (a) maintained in 25‰ seawater-only and (b) maintained on silica substrate in 25‰ seawater. Proteins with a known biological process were categorized based on (i) proteins as a percentage in each biological process category, and (ii) abundance of differentially expressed proteins in each biological process category, calculated from the sum of total counts of proteins in each biological process category. Total peptide count for each protein is the sum of total counts of each unique peptide detected for a protein.

### **5.3.5 Differentially expressed proteins from amphipods maintained on silica substrate in response to zinc stress**

Among amphipods exposed to Zn maintained on the silica substrate, we obtained 31 statistically significant protein identifications from mass spectrometric analysis of 25 2DE spots that showed differential protein expression compared to controls. A summary of this is listed in Table 5.3. Appendix D2 further provides detailed information on each of these protein identifications along with their peptide sequence and biological process information as found in KEGG and Uni-Prot.

Of these 31 proteins, 22 were down-regulated and 9 up-regulated. Among these proteins, the highest observed expression differences relative to controls ranged from 3.1-fold down regulation for GF23033 protein, DHHC palmitoyltransferase, and actin, to 2.4-fold up-regulation of glyceraldehyde-3-phosphate dehydrogenase. Many of the highest observed fold changes were down regulated-proteins including T-cell receptor immunoglobulin domain beta chain, ATP-dependent DEAD/H RNA helicase, ARM like folded protein, RNA-binding protein cabeza, emrB/QacA family drug resistance transporter protein, and ATP-dependent DEAD/H RNA helicase.

Of these 31 proteins, 30 had known biological process information; only GF23033 protein lacked gene ontology information even after BLAST protein homology searches. These 30 differentially expressed proteins were graphed as a percentage in each biological process category (Figure 5.4B-i) and discussed further in this chapter. From inspection of Figure 5.4B-i, it is evident that the largest groups of differential proteins in response to silica-bound Zn toxicity belong to RNA metabolism (13%), cytoskeleton and protein polymerization (10%), transport/energy metabolism (10%), carbohydrate metabolism

(10%), cell cycle (10%) and stress responsive proteins (10%). Proteins belonging to purine metabolism (6%) and DNA replication and repair (7%), were the next largest groups.

The 30 proteins were also re-graphed using the sum of all unique peptide counts per protein in each biological process category in order to represent their abundance (Figure 5.4B-ii). We realize that this approach is likely to be only semi-quantitative, as the lack of available genome sequence means not all peptides are identified. Despite this caveat, we felt that this approach gave us a quantitative estimate that revealed some interesting information. In contrast to Figure 5.4B-i, Figure 5.4B-ii shows that the most abundant were the cytoskeleton and protein polymerization category of proteins (52%). Next in abundance were those belonging to carbohydrate metabolic proteins (11%), followed by transport/energy metabolic processes (9%). A recent transcriptomics study that used microarrays to examine effects of Zn toxicity in *M. plumulosa* revealed differential expression of transcripts pertaining to the cytoskeleton after exposure to sediments spiked with 400 mg Zn Kg<sup>-1</sup>(ZnSO<sub>4</sub>.7H<sub>2</sub>O) [361]. Particularly, transcripts of actin isoforms were reported to be down-regulated, whereas myosin and tropomyosin were up-regulated in *M. plumulosa* following Zn toxicity; these findings are in good agreement to the results found in this study.

Expression of proteins in biological process categories of lipid metabolic process, amino acid metabolic processes and cell defence systems seem to be moderately affected by silica-bound Zn toxicity, as both their numbers as well as their abundance were low. However, changes in protein expression of some individual proteins may be crucial to the functionality of these metabolic processes.

### **5.3.6 Biological relevance of some of the 41 Zn toxicity responsive differential proteins expressed in amphipods found in this study**

The effect of Zn exposure on important metabolic pathways or processes of the amphipods were evaluated by examining the change in abundance of proteins/ enzymes involved in those processes.

#### **5.3.6.1 Proteins involved in RNA metabolism**

##### **5.3.6.1.1 Serine-Threonine kinase Receptor-Associated Protein**

Serine-Threonine kinase Receptor Associated Protein complex (STRAP) was up-regulated by 2.4 fold in amphipods exposed to Zn in 25‰ seawater-only (Figure 5.5). STRAP is known to play an essential role in negatively regulating transforming growth factor  $\beta$  signaling pathway, promoting tumor growth in Ewings sarcoma and several malignant tumors [362-364]. Increased protein expression of STRAP was seen in 70% of colorectal cancers and 68% of lung cancers in humans [363]. It is also involved in the cellular distribution of SMN complexes which co-regulate the cytoplasmic assembly of spliceosomal snRNPs, and is vital for pre-mRNA splicing in the nucleus [365]. It was also found to be up-regulated in HepG2 cell lines transfected with recombinant plasmid containing hepatitis B virus X protein gene [366]. STRAP could potentially be involved in progression of similar symptoms in amphipods under stress due to Zn toxicity.

##### **5.3.6.1.2 Arm-like folded protein**

Arm-like folded protein was down regulated by 2.7 fold in response to Zn toxicity in amphipods maintained on silica substrate in 25‰ seawater (Figure 5.5). This protein is known to perform several functions, mostly through interaction with various cell-binding receptors via an arginine rich motif. It serves as a structural protein facilitating

cytoskeletal polymerization and cell adhesion from associations with actins and microtubulins, as well as performing signaling functions such as binding RNA and regulating RNA metabolism [367]. Targeted ubiquitination and subsequent degradation of proteins is also a well-known cellular function mediated by ARM proteins, where they interact as a E3 ubiquitin ligase and directly transfer ubiquitin to target proteins [368]. In the Zn exposed amphipods, changes in expression of Arm-repeat proteins may suggest a possible protein degradation function, reduced splicing functions and/or other RNA metabolism associated with a reduction in amphipod fecundity. Collectively, these biological responses may create a ‘freight / flight / fight’ reaction in an effort to prevent expenditure of energy and other resources. Up-regulation of Arm-like repeat protein was observed in hepatocellular carcinoma cell lines [369].

#### **5.3.6.1.3 DEAD box RNA helicases**

ATP-dependent DEAD/H RNA helicase and helicase-like protein were down regulated by 2.7 and 2.4 fold respectively, in response to Zn toxicity in amphipods maintained on silica substrate in 25‰ seawater. Helicases catalyze the unwinding of double stranded nucleic acids. ATP binding and hydrolysis is a pre-requisite for the activity of ATP-dependent RNA helicases involved in pre-mRNA splicing required to remove introns and join exons. Previous studies report that translation initiation factor eIF4A, which is a RNA-dependent ATPase operating together with eIF4B as an RNA helicase, is a prototype of the DEAD-box RNA helicases [370]. The DEAD box helicases are involved in various aspects of RNA metabolism, including RNA repair, nuclear transcription, pre-mRNA splicing, ribosome biogenesis and transport, translation processes, and RNA degradation. Recent studies indicate differential gene regulation of DEAD box RNA helicase as a stress response to a variety of stressors including cold stress

in *A. thaliana* [371], salinity and dehydration in rice [372, 373], and chromium metal toxicity in midgut cells of *D. melanogaster* [374]. Further, it has been shown in cancer cells that Zn cytotoxicity disrupts post-transcriptional events of gene expression [375]. Although in the case of cancer cells the use of Zn toxicity seemed beneficial, it has given molecular insights on how Zn cytotoxicity causes stressful conditions by disrupting the expression levels of proteins involved in RNA metabolism, thereby affecting amphipod survival, as in the case of this study. Thus, in severe cytotoxic conditions in *M. plumulosa*, Zn stress has the potential to result in DNA damage and double strand breakage, and failure to repair these may result in cell death.

### **5.3.6.2 Zn toxicity responsive proteins that are involved in cytoskeleton and protein polymerization**

#### **5.3.6.2.1 Tropomyosin**

Tropomyosin was found to be up-regulated by 3.7 fold relative to controls in response to the exposure of the amphipods to low concentrations of Zn in 25‰ seawater-only (Figure 5.5). Tropomyosin is known to play a central role in the calcium dependent regulation of muscle contraction along with the troponin complex. The tropomyosin protein molecule resembles a coiled coil structure that is formed by 2 parallel polypeptide chains containing actin binding sites, and is present in both muscle and non-muscle cells. In striated muscle, tropomyosin regulates muscle contraction by mediating complex interactions between the troponin complex and actins [376]. Different cell types contain specific isoforms of this protein, created by differential mRNA splicing of the gene, but cell types vary quantitatively in the proportions of the isoforms present.

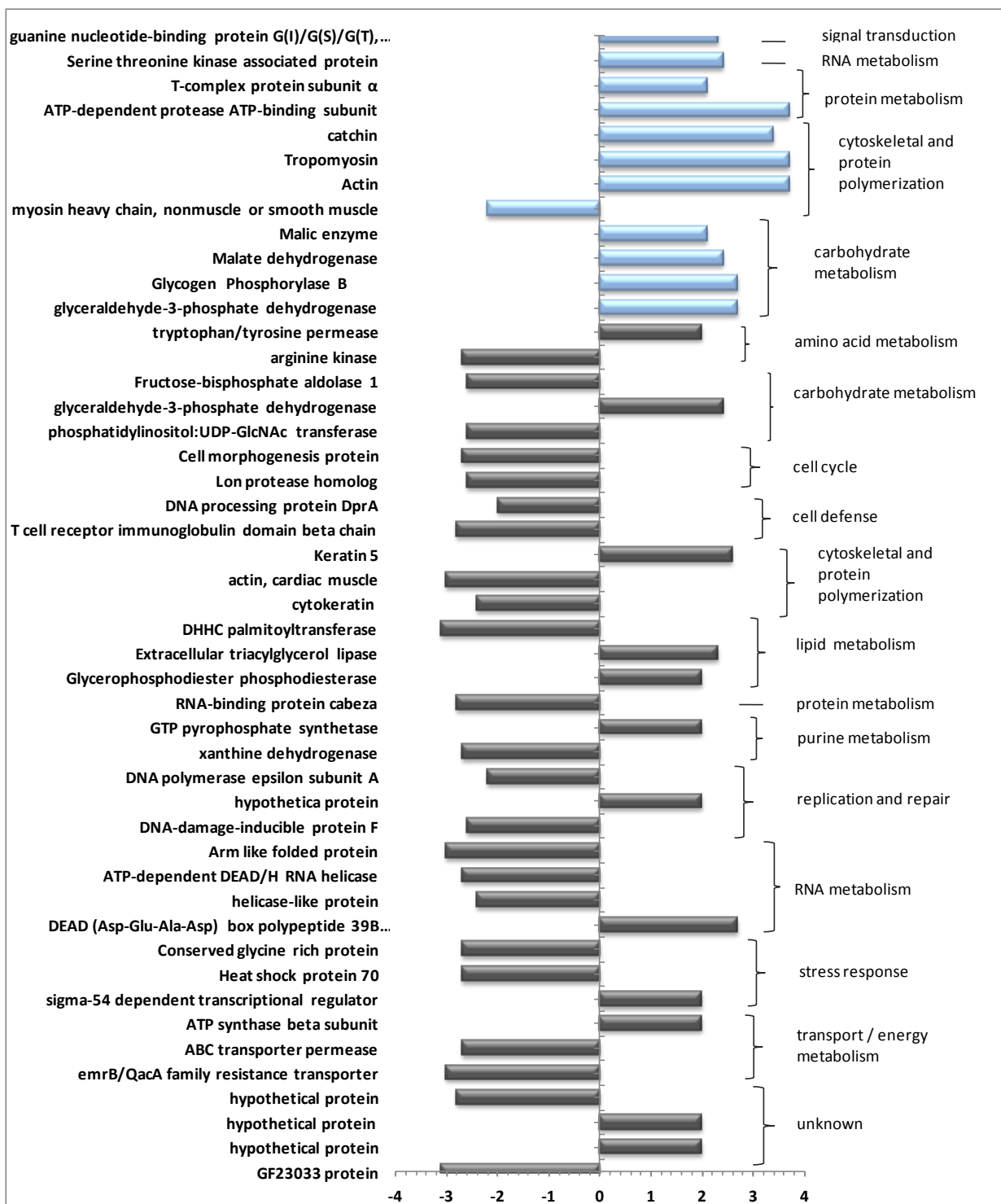


**Figure 5.5** Fold changes (up- or down-regulation) for all proteins differentially expressed in response to Zn exposure relative to controls. Protein ontology information was obtained from Uni-Prot and KEGG reference maps. Fold changes were calculated as spot volume ratio in metal-exposed amphipods relative to non-exposed controls. Proteins have been grouped based on their association with distinct functional pathways (see Table 5.3 for specific information on the responses of these proteins with respect to each metal exposure).

Muscle isoforms of tropomyosin are characterised by having 284 amino acid residues and a highly conserved N-terminal region, whereas non-muscle forms are generally smaller and are heterogeneous in their N-terminal region. Studies have suggested that different isoforms could have distinct functions and the ratio between them is important for correct development or morphogenesis [377]. However, the exact role of tropomyosin in non-muscle tissues is still not completely clear and hence there is a need for more research for further understanding.

#### **5.3.6.2.2 Actins**

Actins were found to be down-regulated by 2.7-fold in amphipods subjected to silica-bound Zn toxicity. Actins are highly conserved proteins that are involved in various types of cell motility, and in the formation of filaments that are major components of the cytoskeleton, and are ubiquitously expressed in all eukaryotic cells. These filaments interact with myosin to produce a sliding effect, which is the basis of muscular contraction and many aspects of cell motility, including cytokinesis. They are highly redox sensitive and their over-expression could be triggered indirectly as a response to oxidative stress. The possible relationship between metal stress and altered cellular plasticity and movement is highlighted in this study where major cytoskeletal proteins including actin, tropomyosin and myosin heavy chain were all altered in expression. Actin was also differentially expressed in recent studies on heavy metal stress including Zn stress [11, 378].

#### **5.3.6.2.3 Myosin heavy chain**

Myosin heavy chain proteins were up-regulated by 3.4-fold relative to non-exposed controls in amphipods exposed to Zn in seawater-only. Muscle contraction is

caused by sliding between the thick and thin filaments of the myofibril. Myosin heavy chain proteins are thick filaments and exist as a hexamer comprised of two heavy chains, two alkali light chains and two regulatory light chains. Myosin interacts with actin to convert chemical energy, in the form of ATP, to mechanical energy. Each actin protomer binds one molecule of ATP and has one high affinity site for either calcium or magnesium ions, as well as several low affinity sites. Under control conditions, the protein functions quickly where filaments form rapidly as salt concentration rises with ATP hydrolysis. Under metal stress, this protein showed reduced expression in spite of the need to replace those filaments that have been damaged due to oxidative metal stress due to reactive-oxygen species; this is most likely to avoid the increasing demand for energy and resources during such transitions. Therefore, the organism stops any further work on actin formation, possibly avoiding resource losses to help sustain survival under stressful conditions [11]. Multiple isoforms are also known to be involved in various cellular functions such as cytoskeleton structure, cell mobility, chromosome movement and muscle contraction.

#### **5.3.6.2.4 Catchin**

Catchin was up-regulated by 3.4-fold relative to non-exposed controls in amphipods exposed to low concentrations of Zn in seawater-only. This protein may be abundantly expressed only in the catch muscles and may become phosphorylated. A previous study has reported that it may play an important role in the catch contraction of molluscan smooth muscles [379].

### **5.3.6.3 Zn toxicity responsive proteins that are involved in DNA replication and repair**

#### **5.3.6.3.1 DNA polymerase**

DNA polymerase II was found to be down-regulated by 2.4-fold in amphipods subjected to silica-bound Zn toxicity. It is widely known this protein participates in chromosomal DNA replication, synthesizing new copies of DNA semi-conservatively by complementary base pairing, thus duplicating existing DNA molecules. Stress induced down-regulation of this protein compared to amphipods exposed to Zn in 25‰ seawater-only is most likely a result of the amphipods increased Zn uptake through ingesting silica-bound Zn, and probably lead to genotoxicity.

#### **5.3.6.3.2 DNA-damage-inducible protein**

DNA damage proteins were down regulated by up to 2.6-fold relative to controls in amphipods subjected to silica-bound Zn toxicity. The results of this study indicate that growth arrest, induction of DNA damage response proteins, oxidative damage to cytoskeletal proteins, and energy and carbohydrate depletion, are all associated with injury to amphipods subjected to silica-bound Zn toxicity. The DNA damage inducible proteins belong to a family of short proteins that are known to interact with a number of other proteins implicated in stress responses. They are reported to stimulate DNA excision repair *in vitro* and inhibit cell entry into the S phase of the cell cycle, thus preventing mitotic division of cells with damaged DNA. Therefore, in the case of amphipods under Zn stress, down-regulation of this protein with Lon protease is indicative of impairment of cell division due to Zn toxicity, resulting in a DNA damage-induced replication arrest.

#### **5.3.6.4 Zn toxicity responsive proteins that are involved in carbohydrate metabolisms**

##### **5.3.6.4.1 Glyceraldehyde-3-phosphate dehydrogenase (GAPDH)**

GAPDH was up regulated 2.4 fold in amphipods subjected to silica-bound Zn toxicity and 3.4 fold in those exposed to low concentrations of Zn in 25‰ seawater-only, relative to the respective controls. This enzyme is responsible for the interconversion of 1,3-diphosphoglycerate and glyceraldehyde-3-phosphate, a central step in glycolysis and gluconeogenesis. Besides having a well-defined glycolytic function, GAPDH has been lately regarded as one of the few multifunctional glycolytic proteins that can perform a variety of discrete molecular activities in numerous cellular processes, similar to some ancient proteins that have been found to be able to moonlight in performing other functions [380]. It has been characterized as having a number of non-glycolytic functions including DNA repair [381], apoptosis [382, 383], chromosomal binding and maintenance [384], and nuclear membrane fusion. To switch between and among its many functions, GAPDH functions as a monomer (DNA repair) [385], translocates to the nucleus (apoptosis, DNA repair, telomere binding) [386] and/or becomes post-translationally modified by carbonylation or S-nitrosation [386]. A study on acute Zn toxicity in mice suggested that Zn toxicity induces neuronal death followed by apoptosis, and this may partly be due to the inhibition of GAPDH following reduced NAD levels [387]. Another study also reported disruption of GAPDH when cells prepared from mouse cortices were subjected to chronic Zn toxicity [388]. This may also be the case with amphipods exposed to a critical cellular load of Zn, resulting in induced apoptosis caused by reduced glycolysis and energy failure. Thus, following reduced glycolysis, GAPDH may be triggered to cause Zn-induced apoptosis in amphipods. Although the mechanisms for the participation of GAPDH in apoptosis are not quite clear in such organisms, it is likely that

GAPDH may need some stress-induced post translational modification to occur in order to be translocated to the nucleus for mediating apoptosis.

Assigning multiple functions to the same protein could be energy efficient for cells, especially under energy deprived situations, as it entails synthesizing fewer proteins for various functions, and also implies that various cellular activities can be co-ordinately streamlined [380]. In the case of this ancient protein, it potentiates the coordination of carbohydrate metabolism with other processes, including apoptosis, which can be activated under metal-induced stress or other conditions. Since GAPDH catalyses fatty acid beta-oxidation in mitochondria, the up-regulation of this enzyme could be associated with the utilization of fatty acids as an alternate source of carbohydrate for energy replacement soon after the depletion of glycogen.

#### **5.3.6.4.2 Glycogen phosphorylase**

Glycogen phosphorylase was up regulated 2.7 fold in the amphipods exposed to low concentrations of Zn in seawater-only. Glycogen phosphorylase is an enzyme belonging to the family of glycosyltransferases with phosphorylase activities. The biosynthesis of disaccharides, oligosaccharides and polysaccharides involves the action of hundreds of different glycosyltransferases. Glycogen phosphorylase catalyses the transfer of carbohydrate moieties from active donors to specific acceptor molecules forming glycosidic bonds [389]. It uses the phosphate to break alpha (1,4) linkages between pairs of glucose residues on glycogen substrates at the end of long glucose polymers, and release alpha-D-glucose-1-phosphate. Thus it is apparent that its main activity is to provide phosphorylated glucose. In amphipods, over-expression of glycogen phosphorylase could also occur to meet greater demand for carbohydrate and energy, and this stress response may enable them to adapt more rapidly to changing conditions.

Glycogen phosphorylase was recently reported to be differentially expressed due to metal stress in a study conducted in oysters [11]. In normal conditions, glycogen storage is essential for reproduction [263, 390]. Forced utilization of glycogen reserves to disseminate the accumulated metal concentrations may cause depletion of glycogen thereby affecting vitellogenesis and development of embryos in the gravid *M. plumulosa*.

#### **5.3.6.4.3 Malate dehydrogenase**

Malic enzyme, also known as malate dehydrogenase due to its malate dehydrogenase activity, was found to be up-regulated by up to 2.4 fold in the amphipods exposed to low concentrations of Zn in seawater-only. Malic enzymes exist in three different enzymatic forms based on their NAD/ NADPH dependency and decarboxylating activities. This protein is involved in malate metabolic processes, has oxaloacetate-decarboxylating activity, and aids in NAD binding and divalent metal ion binding. It catalyzes the oxidative interconversion of malate to oxaloacetate with reduction of  $\text{NAD}^+$  to NADH. This is an important reaction in many important metabolic pathways, including the citric acid cycle, gluconeogenesis, and glyoxylate pathway which is a variant of the tricarboxylic acid cycle. There are three forms of the enzyme and this one is a NAD-dependent form that decarboxylates oxaloacetate. A previous study used detailed sequence analysis to study the activity of this enzyme and found a cysteine residue to be the point of alkylation, highlighting the important role of this residue in the activity of the enzyme [391].

#### **5.3.6.4.4      Phosphatidylinositol:UDP-GlcNAc transferase PIG-A (Glycosyl transferase 1)**

Phosphatidylinositol N-acetylglucosaminyltransferase was down-regulated by 2.6-fold in amphipods subjected to silica-bound Zn toxicity. This enzyme participates in the synthesis of N-acetyl-glucosaminyl phosphatidylinositol (GlcNAc-PI), which is the first transient biomolecule in glycan biosynthesis within carbohydrate metabolism. GlcNAc-PI forms the foundation of glycosphosphatidylinositol (GPI) glycolipid membrane anchors, which are used to anchor a wide variety of proteins in the cellular membrane. The role of this protein in Zn toxicity stress remains unclear, but it may have a disruptive effect on membrane structure and composition of the new cuticle being formed by the amphipods. This in turn would prevent the ability of males to copulate and subsequently for females to ovulate which is restricted to the early postmolt period of the females [392]. We have shown previously that the amphipods maintained on silica substrate had significantly reduced fecundity when exposed to 22µg Zn/L [347].

#### **5.3.6.4.5      Fructose biphosphate aldolase**

Fructose-bisphosphate aldolase was also found to be down-regulated by 2.6-fold in amphipods subjected to silica-bound Zn toxicity. Fructose-bisphosphate aldolase [393] is a glycolytic enzyme that catalyses the reversible aldol condensation reaction of fructose-1,6-bisphosphate into dihydroxyacetone-phosphate and glyceraldehyde 3-phosphate. This protein belongs to class I enzymes and is involved in glycolysis and gluconeogenesis. Fructose-1,6-bisphosphate was found to be affected by nickel toxicity in *E. coli*, where cells exposed to metal stress resulted in reduced levels of activity whereas overexpression of this enzyme resulted in restoration of cell growth [394]. It is highly likely that such a

direct connection of fructose-1,6-bisphosphate protein regulation may exist in Zn exposed amphipods, but further validation is required.

### **5.3.6.5 Zn toxicity responsive proteins that are involved in lipid metabolism**

#### **5.3.6.5.1 Glycerophosphodiester phosphodiesterase**

Glycerophosphodiester phosphodiesterase was found to be up-regulated 2-fold in amphipods exposed to Zn and maintained on silica substrate. Glycerophosphodiester phosphodiesterase is involved in the glycerol metabolic process and mediates the biochemical reactions with glycerophosphodiesters and related alcohols. It is also a significant intermediary in carbohydrate and lipid metabolism. Glycerol is primarily central to a major class of triglycerides, biological lipids and phosphatidyl phospholipids. Much information is available on the enzymes responsible for the formation of phospholipid metabolites, but little information is known regarding their catabolism by glycerophosphodiesterases.

A recent study in plants revealed that the release of phosphate from phospholipid, mediated via the lipid metabolic pathway during phosphate starvation, could be facilitated by glycerophosphodiester phosphodiesterase [395]. The role of this protein in Zn toxicity stress remains unclear, but it has been shown to be differentially expressed in *Borrelia lonestari* as part of an inflammatory response [396].

#### **5.3.6.5.2 Extracellular triacylglycerol lipase**

Triglyceride lipases are class 3 family lipases which are lipolytic enzymes that hydrolyse ester linkages of triglycerides. In amphipods, this enzyme could be a bifunctional enzyme with triacylglycerol lipase and lysophosphatidic acid acyltransferase or lysophosphatidylethanolamine acyltransferase activity, as seen in *S. cerevisiae*. They

are generally localized to lipid particles and involved in triacylglycerol mobilization. Down-regulation of this enzyme in this study is in agreement with results reported in a recent study on metal stress in *Drosophila* [397].

#### **5.3.6.5.3 DHHC palmitoyltransferase**

DHHC palmitoyltransferase protein was down-regulated in response to sediment silica-bound Zn toxicity by 3.1 fold relative to controls in amphipods subjected to silica-bound Zn toxicity, one of the highest fold changes in protein expression seen in this study. This enzyme anchors proteins to cell membranes through the process of palmitoylation, where it adds a palmitoyl chemical group to the proteins. Little is known about this protein in the context of Zn stress and Zn toxicity, even though it is essential for maintenance of vacuolar integrity under stress conditions [398]. Reduced effects of hepatic carnitine palmitoyltransferase I activity was observed in yellow catfish *P. fulvidraco* upon chronic exposure to low levels (<0.86mg/L) of water-borne Zn for a period of 8 weeks [399]. However, acute exposure to high levels (4.7mg/L Zn) of waterborne Zn caused increased activity of hepatic carnitine palmitoyltransferase I in the same study. The study concluded that the alterations in the mRNA levels of lipid metabolic genes were directly dependent on the amount of Zn exposure. Another recent study on hepatocytes of grass carp (*Ctenopharyngodon idellus*), observed that carnitine palmitoyltransferase I activity increased with increasing concentrations of Cu (0-100µM Cu) and exposure period (24-96 h) [400]. Lipogenesis and lipolysis mechanisms seem to be affected by Cu stress and a similar effect is seen to possibly occur in this study in amphipods in response to high Zn exposure over a period of 4 days. Excessive levels of ROS induced by metal stress may be causing lipid and protein damage in amphipods, resulting in changes in abundance of major proteins involved in fatty acid degradation or oxidation. Such changes in abundance

of these lipid proteins may indirectly interfere in vitellogenesis in amphipods exposed to Zn toxicity, but due to the lack of complete genome, this remains unclear and further research is needed.

#### **5.3.6.6 Zn toxicity responsive proteins that are involved in the cell cycle**

##### **5.3.6.6.1 Cell morphogenesis protein Las 1**

Las1 protein was down-regulated by 2.7-fold relative to controls in amphipods exposed to silica-bound Zn toxicity. This is an essential nuclear protein that is involved in cell morphogenesis and cell surface growth. Loss of function of this protein caused *S. cerevisiae* cells to arrest growth as 80% unbudded cells [401]. Down-regulation of this protein as a stress response in Zn exposed amphipods highlights the possibility that the amphipods may consider their need to grow or replicate less important after finding themselves in such stressful situations from ingesting toxic levels of metals. Rather, they may be diverting resources to meet basic needs for survival.

##### **5.3.6.6.2 Lon protease homolog**

Lon protease was down regulated by up to 2.6-fold relative to controls in amphipods subjected to silica-bound Zn toxicity. Lon protease has an ATP-dependent peptidase activity and recognizes the substrate directly, unlike most other enzymes for selective degradation of mutant and abnormal proteins, as well as certain short-lived regulatory proteins. It helps maintain cellular homeostasis by removing damaged or misfolded proteins, thus enabling survival of the organism during DNA damage and developmental changes induced by stress [402]. Lon protease was previously reported to be down-regulated under metal stress with intermittent hypoxia in *C. virginica* [403]. Reduced Lon protein expression in Zn exposed amphipods suggest that under controlled

conditions, the non-exposed amphipods were able to effectively defend their tissue energy status and ATP levels, whereas the Zn exposed amphipods may have experienced disturbance arising from energy depletion, thereby affecting survival and fecundity of the amphipods.

### **5.3.6.7 Zn toxicity responsive proteins that are involved in signal transduction**

#### **5.3.6.7.1 Guanine nucleotide binding proteins**

Guanine nucleotide binding proteins are alternatively known as G-proteins and are membrane-associated, heterotrimeric proteins composed of three subunits known for their involvement in varied signal transduction mechanisms such as the G-protein coupled receptor signaling pathway and the MAPK signaling pathway [404]. G-proteins and their receptors form one of the predominant signaling systems in animals and regulate a diverse range of sensory perceptions, cell growth and development [405]. G-proteins are central to the GTP/GDP exchange, binding of neurotransmitters and hormones, and transmitting signals from receptors to the cell surface to achieve cellular responses. G-protein was up regulated by 2.3-fold relative to controls in the amphipods exposed to low concentrations of Zn in seawater-only. This is suggestive of a possible role of G-proteins in the signaling process due to Zn stress in the amphipods that would lead to a disruption of the molting process and fecundity of *M. plumulosa*. This is because it is known that the ability of females to ovulate and mate is restricted to the early postmolt period [392]. Crustacean Y-organs produce and secrete ecdysone, the steroid molting hormone. In the case of amphipods, ecdysone is peripherally transformed into the active hormone, 20-hydroxyecdysone. The synthesis and secretion of ecdysone by the Y-organs are negatively regulated by the neuropeptide MIH [392]. Cell signaling pathways involving G-proteins may possibly link MIH receptor availability to changes in intracellular cAMP levels that

control Y-organ function. The  $\alpha$ ,  $\beta$  or  $\gamma$  subunits of the G-protein dimer may go on to activate distinct downstream effectors, such as phosphodiesterases, ion channels, phospholipases and adenylyl cyclase. These effectors in turn could regulate the secondary messengers ultimately leading to a physiological response, typically via increased gene transcription. This can target specific physiological processes in response to specific external stimuli [406, 407].

#### **5.3.6.8 Zn toxicity responsive proteins that are involved in transport/ energy metabolism**

##### **5.3.6.8.1 ATP synthase beta subunit and GRP-78**

ATP synthase beta subunit protein was up-regulated by 2-fold relative to controls in amphipods subjected to silica-bound Zn toxicity. ATP synthase beta subunit protein is known to play a role in ATP synthesis and hydrogen ion transport processes. Seventy-eight kilodalton glucose-regulated protein is also known to be involved in ATP binding. This suggests that the up-regulation of these two proteins indicates that when elevated levels of metal bioaccumulation occur, there is an increase in demand for ATP for energy production [11].

##### **5.3.6.8.2 emrB/ QaCA subfamily drug resistance transporter**

EmrB/ QaCA subfamily drug resistance transporter was down regulated by 2.7-fold relative to controls in amphipods exposed to silica-bound Zn toxicity. This protein belongs to the subfamily of efflux proteins which in turn is a part of the major facilitator family and known to be involved in cellular transport of drugs, metals and other biomolecules. In most cases, it functions as the efflux pump, a multidrug resistance

transporter in the major facilitator superfamily. It has been previously reported as a bile stress response protein in bacteria [408].

#### **5.3.6.8.3 ABC transporter permease**

ABC transporter permease was down regulated by 2.7-fold in amphipods subjected to silica-bound Zn toxicity. Differential expression of this protein was observed in several studies on environmental stress [409, 410], including one study that investigated genes responsive to iron stress in *Rhodobacter sphaeroides* [411]. ABC transporter permease proteins are involved in several transport mechanisms, for example, they carry out the uptake of choline required for glycine betaine biosynthesis. ABC transporters are conserved across all kingdoms, and are named for their soluble cytoplasmic ATPase subunits. ABC transporters import and export a variety of substrates including drug molecules and metals.

Proteomic analysis revealed Zn toxicity to *M. plumulosa* induced protein expression changes in many proteins. However, the effects of Zn stress on the biological response of *M. plumulosa* are apparent in a few metabolic pathways including carbohydrate metabolism, RNA metabolic processes, lipid metabolism, cytoskeletal organization and protein polymerization, and transport processes. Importantly, Zn stress was found to cause oxidative damage to the cytoskeletal proteins which in turn dampens microtubule contractions that are vital for swimming and foraging activities. Further, upon Zn stress, amphipods required more energy production to maintain normal metabolism. Therefore it is highly likely that amphipods may experience increased energy expenditure and production required to mitigate effects of Zn stress, including excessive oxidative damage caused by increased ROS levels, in addition to the energy required for normal

cellular homeostatic processes of the gravid female amphipods including oogenesis, embryo development and survival.

The finding in this study that the protein phosphatidylinositol N-acetylglucosaminyltransferase was down-regulated by 2.6-fold in amphipods subjected to silica-bound Zn toxicity, has potential as a biomarker for reproductive toxicity in *M. plumulosa*. This enzyme is necessary for the synthesis of N-acetylglucosaminyl-phosphatidylinositol, which has a key role for the foundation of GPI anchoring of membrane proteins such as the cuticle assembly protein Knickkopf [412]. Disruption by environmental contaminants of the molting process would cause reproductive toxicity since the ovarian and reproduction cycles of female gammaridean amphipods are closely correlated with molting. The ability of males to copulate and subsequently of females to ovulate is restricted to the early postmolt period of the females; hence, fecundity must be preceded by a molt [392].

The molting process in arthropods is hormonally initiated by 20-hydroxyecdysone and begins with the epidermis secreting what will become the outer layers of the new cuticle that separate the epidermal layer from the overlying old cuticle. An apolytic extracellular space then forms, separating new (inner) from old (outer) cuticles [412]. Molting fluid containing the enzyme chitinase is then secreted into the apolytic space to digest the inner layers of the old cuticle. A recent study suggested that the newly synthesized chitinous procuticle is protected from chitinase action by the cuticle assembly protein Knickkopf when it becomes incorporated into the cuticle after detachment from the plasma membrane by enzymatic cleavage of its GPI anchor [413]. Further down-regulation of the GPI anchored TcKnk protein resulted in molting defects in the red flour beetle [413].

A complete understanding of the biological metabolisms or mechanisms of amphipods has not yet been established in literature and needs more such research. This effort could be crucial to the understanding of the metabolic complexities and chaos caused by such threats to other organisms higher up in the food web. These differentially expressed proteins can potentially be used as biomarkers indicative of biological stress impacts and can be formulated as bioassays to help in biomonitoring Zn contamination in the environment.

## 5.4 Concluding Remarks

The substantial amount of biologically relevant data obtained from our study provided a greater insight into stress responses caused by metal toxicity in amphipods exposed to Zn and offers useful information for further studies. The proteomics methodology involving 2DE-coupled with MALDI-TOF/TOF and nanoLC-MS/MS mass spectrometry, and subsequent database search efforts using GPM, MASCOT and BLAST, was proved to be successful for use in studying the stress responses in *M. plumulosa*, an unsequenced organism. We obtained significant protein identification information for over 90% of differentially expressed 2DE spots selected for analysis. The differential metabolic responses seen in our study indicated that amphipods are more sensitive and have greater exposure to Zn toxicity from metal contaminated artificial sediments. As a result of Zn toxicity, several proteins changed in abundance. These differential metabolic responses were also reflective of the relationships that exist between metal stress effects, biological processes, and biological changes adopted by *M. plumulosa* as ways to mitigate stress. Since physical activity demands large amounts of oxygen supply and energy, under stressful situations amphipods may decrease most physical activities including fecundity and other cellular processes such as protein synthesis or cytoskeletal elongation or muscle

contraction. The amphipods would then be able to use the conserved energy to prolong survival, maintain important biological processes, and replace damaged proteins and cytoskeletal tissues, while adopting ways to efficiently metabolise available carbohydrates to generate more energy. In due course the free radicals generated as byproducts in the process of oxygen and energy metabolism may heighten stress levels by damaging cells and tissues resulting in several dysfunctions. Therefore, as a consequence of Zn stress, oxidative stress can be more pronounced and the collective damage is thought to be greater in cytoskeletal tissues and gills in *M. plumulosa*. When exposed to high levels of dissolved Zn, gills of *M. plumulosa* would experience increased sensitivity to oxidative damage, as a result of which gas exchange across gills may slow down or stop over the course of time with prolonged exposure causing tissue hypoxia; a similar effect was seen in gills of *C. virginica* exposed to high levels of dissolved silver [414]. At this point amphipods would experience severe stress from not being able to meet their oxygen requirements and the gut region, digestive tissues and reproductive cells would all be affected. The interaction between these responses appears to be complicated in nature and warrants more research on Zn stress responses in amphipods.

With a better understanding of the networking of genes and proteins involved in the heavy metal stress response, effective and useful early monitoring strategies could be developed to prevent disasters arising due to metal toxicities from affecting higher animals. Although there has been some progress in the development and availability of toxicity tests (both *in vivo* and *in vitro*), there remains a dearth of preventive signature biomarkers for early detection of toxicity impacts. Expressed protein profiles of oysters and amphipods are excellent indicators of their susceptibility to heavy metal stress and efforts to incorporate these as part of early monitoring systems could be the next step forward.

## **Supplementary Information**

The following Supplementary Information for this study is available in the enclosed DVD.

**Supplementary Information Table S8:** R.S.D values and spot volumes corresponding to differential 2DE spots in triplicate gels for amphipods when maintained on 25‰ seawater-only or in addition with silica substrate.

**Supplementary Information Table S9:** Protein and peptide identification and quantitation information, along with peptide sequence and protein ontology for differential proteins expressed in response to Zn toxicity, when maintained on 25‰ seawater-only or in addition with silica substrate.

## **Notes**

The work presented in this chapter has not been published yet. This work was partly conducted at the EPA laboratories, Department of Environment and Climate Change (NSW), Sydney.

Supplementary tables, including protein identification and quantitation information, referred to in-text can be found on the DVD attached to this thesis.

Other supplementary data are included in Appendix D as indicated.

I was involved in the experimental design and with the assistance of Dr. Ross Hyne, DECC, Sydney, I cultured the amphipods and performed the subsequent Zn exposure experiments at DECC. In addition to this, I also performed all of the proteomics experiments, data analysis including the manual interpretation of data which led to identifying relevance of several differential proteins in the metal stress response in amphipods and the majority of the manuscript preparation (approximately 99%).

---

## Chapter 6

# **Quantitative proteomics investigating ocean acidification effects on two breeds of Sydney rock oysters, wildtype and select QX disease resistant, and their metabolic responses toward increased levels of carbon dioxide**

---

### **6.1 Introduction**

Ocean acidification is increasing, caused by an increase in seawater  $p\text{CO}_2$  which leads to changes in the pH and the oceanic carbonate system. The hydrolysis of  $\text{CO}_2$  in seawater increases the  $\text{H}^+$  concentration and decreases the pH, while the proportions of the  $\text{HCO}_3^-$  and  $\text{CO}_3^{2-}$  ions are also affected. Currently, seawater pH ranges from 7.8 to 8.2, and has been estimated to drop by up to 0.4 units by 2100 due to the effects of ocean acidification. This process has already led to a decrease in pH by 0.1 pH units in surface seawater from  $\text{CO}_2$  absorptions since the beginning of the industrial revolution in the 1750s [209, 415].

Ocean acidification in response to hypercapnia arising from increased absorption of  $\text{CO}_2$  could lead to: (a) decreased calcification rates and increased dissolution rates of calcium carbonate, which is a basic mineral component needed for corals, shells and other body structures in a wide variety of organisms [204, 205]; (b) hypercapnia stress induced decreases in growth rates of many marine calcifying corals which provide habitat for at least a quarter of all marine species; (c) undersaturation of species with aragonite and

calcite structures in the ocean within next 50 years [416, 417, 202]; and (d) extinction of numerous marine species. All these stress responses will be backed by the down-regulation or up-regulation of relevant genes responsible for each physiological symptom. Corals and some other species are at the greatest risk of becoming extinct, similar to what has happened for several other species within the early 21st century [211]. Ocean acidification affects several types of calcifying oysters resulting in either reduced calcification or enhanced dissolution when exposed to reduced pH in ocean waters. Responses of an organism to hypercapnia stem from the need to protect the outer shell layer by an organic covering, slow down dissolution of their shells, or utilize excess nutrients in the form of inorganic carbon and  $\text{HCO}_3^-$  as part of a necessary increase in photosynthesis. Although specific mechanisms involved in these responses remain unconfirmed, it has been suggested that the impact of elevated atmospheric  $\text{pCO}_2$  on marine calcification would be more varied than previously thought [223]. Proteomics studies on understanding the effects of ocean acidification and hypercapnia are just beginning to gain momentum [418, 214, 267].

Sessile oysters must cope with harsh and dynamic shifts in marine environments. In addition to temperature and salinity fluctuations, metals and other anthropogenic pollutants or stressors affect oysters and pose serious challenges on a continuous basis. Oysters come in contact with a considerable flux of microbes, including pathogens, and if their cytoskeletal shell structure becomes fragile due to acidification effects, their shells become sensitive and they are unable to protect themselves and face a serious threat when exposed to pathogens. For instance, fertilization in oysters and mussels might not be affected by ocean acidification, but their larval development is affected [419]. The effects of lowered pH in the seawater column on brittle star species *Ophiura ophiura*, included the disruption of vitellogenesis processes [415]. The disruption of vitellogenesis highlights

the impact of such environmental stress on reproductive events resulting in declining rates of successful outcomes. Experimental evidence showed that larval morphology and growth are generally affected by ocean acidification [418]. However, it is not always easy to identify the specific mechanism or group of processes being affected.

The protozoan parasite *Marteilia sydneyi* causes QX disease in Sydney rock oysters, which has negatively impacted Australian oyster farming and the Sydney rock oyster industry in NSW and Queensland. This disease has been an important subject of research and development in Australia. Development of QX disease resistance in oysters was recently adopted as a priority for the benefit of the Sydney rock oyster industry by the NSW Department of Primary Industries, following several QX disease outbreaks [420]. Sydney rock oysters that survived QX disease outbreaks were presumed to have disease resistant abilities and were interbred to further generate selective QX disease resistant oyster populations (QXR). Several such mass selective breeding programs have generated disease resistant lines in other oyster populations, namely MSX disease resistance in American eastern oyster, *Crassostrea virginica* [421] and Bonamiasis resistance in European flat oyster, *Ostrea edulis* [422, 423]. Although selective breeding of QXR oysters proved successful in the oyster industry in reducing mortality, the molecular characteristics remains unclear.

This lack of understanding has recently begun to attract research interest. A recent study by Peters *et al.* [420] showed that suppression of the phenoloxidase enzyme cascade compromises the immune system of these oysters, decreasing their ability to control infection by *M. Sydneyi*, thus leading to the onset of QX disease. To further this understanding, a 2DE based proteomic approach was adopted in another study [420], where their results suggested that oysters that possessed a certain isoform of

phenoloxidase enzyme (PO<sup>b</sup>) were more susceptible to QX disease and those with PO<sup>b</sup> in less abundance were found to demonstrate QX disease resistance. Another study identified a few protein biomarkers possibly responsible for QX disease resistance [424]. Although these findings seem conclusive, much about factors influencing QX resistance still remains to be resolved. This is vital because oysters in general, and especially those bred to be QX disease resistant, can be impacted by other physical stressors such as global ocean acidification as a result of hypercapnia caused mainly by anthropogenic increase of CO<sub>2</sub> in marine waters. In order to investigate the effects of such a calamity, we exposed both wildtype oysters (WT) and QXR oysters to increased CO<sub>2</sub> conditions in marine water tanks and used proteomics to study the effects in comparison to non-CO<sub>2</sub>-exposed control oysters.

## **6.2 Materials and Methods**

Materials and methods that were specific to this study are described in sections 6.2.1 to 6.2.3. Section 6.2.4 gives a summary of proteomic analysis methods used, and a detailed description for these has been given in Chapter 2. All experiments were performed in biological triplicates.

### **6.2.1 Oyster breeds and CO<sub>2</sub> exposure conditions**

All oysters used for this study were Sydney rock oysters and were either wildtype randomly selected from the Port Stephens area, or from the QX resistant selectively bred lines produce by Port Stephens fisheries. They were acclimated for 2 weeks in filtered seawater in tanks maintained at 24°C and 34.6‰ salinity. Six groups of oysters, three groups for each breed, were then exposed to 856 µatm CO<sub>2</sub> for 4 weeks. They are referred to hereafter as stressed. Six other groups were cultured at controlled conditions under no

external exposure of CO<sub>2</sub> and are henceforth referred to as the controls. All oyster cultures were fed a combined algal diet of 50% *Chaetoceros muelleri*, 25% *Pavlova lutheri* and 25% Tahitian *Isochrysis* aff. *galbana* at a concentration of  $2.9 \times 10^{10}$  cells/mL per oyster per day. Complete water changes were made every 2 days using pre-equilibrated filtered seawater and oysters were rinsed daily with fresh water. Gill tissues of all oysters were excised after the stress period, transferred to cryovials, flash frozen in liquid nitrogen immediately and stored at -80°C. Hereafter non-exposed and CO<sub>2</sub> exposed Wildtype oysters are denoted as WT and WT<sub>CO<sub>2</sub></sub> respectively; whereas non-exposed and exposed select QX disease resistant oysters are denoted as QXR and QXR<sub>CO<sub>2</sub></sub> respectively.

### **6.2.2 Sample preparation for protein extraction**

Approximately 500mg of oyster gill tissues were ground to a fine powder using liquid nitrogen and homogenised in a mortar and pestle with 250µL 3M urea buffer and 1mL Tri reagent (Sigma Aldrich, USA), along with 1µL 7x protease inhibitor cocktail added to prevent proteolysis. Homogenates were transferred to pre-chilled RNase free eppendorf tubes, protein extractions were carried out similar to protocol described in Chapter 2, section 2.1.2, and proteins were quantified using the Bradford assay.

### **6.2.3 Filter Aided Sample Preparation method to digest proteins extracted from oyster gill tissues**

Aliquots of 100 µg protein extracted from homogenized oyster gill tissue were washed twice with 500 µL methanol and centrifuged at 1000 ×g. The proteins were reduced by adding 100 µL of reducing solution containing 50 mM DTT / 0.1 M ammonium bicarbonate in 50% Trifluoroethanol (TFE) (v/v), sonicated to mix completely, and incubated for 15 min at room temperature. The protein mixtures were

then transferred to 0.5 mL Amicon spin filters (filtration cutoff 10k) and filtered by centrifuging at 14,000  $\times$ g for 45 min or until retentate volume was less than 20  $\mu$ L. To the reduced proteins that were bound to the filtration bed of the spin filter, 50  $\mu$ L of alkylating solution containing 0.5 M iodoacetamide / 0.1 M ammonium bicarbonate in 50% TFE (v/v) was added, mixed in a thermomixer at 600  $\times$ g for 1 min, then incubated for 1 hr in the dark, then centrifuged at 14,000  $\times$ g for 45 min. The proteins bound on the spin filter were washed with 100  $\mu$ L of 0.1 M ammonium bicarbonate in 50% TFE, mixed for 1 min followed by centrifugation at 14,000  $\times$ g for 45 min or until retentate was less than 20  $\mu$ L. Flow through solutions collected in the receptacles were discarded. The above washing step was repeated four more times and each time flow throughs collected in the receptacles were discarded as necessary. After the washes, proteins were hydrated with 22.5  $\mu$ L of 0.1 M ammonium bicarbonate in 50% TFE. The first stage of protein digestion was carried out by adding 2.5  $\mu$ L of 1  $\mu$ g/ $\mu$ L Lys-C, mixing on a thermomixer for 5 min, and incubating overnight at 30°C in a tube box containing damp paper towel. This protein digestion was quenched with 175  $\mu$ L of 20% acetonitrile. The second stage of protein digestion was performed with 2.5  $\mu$ L of 1  $\mu$ g/ $\mu$ L trypsin in 50mM ammonium bicarbonate, mixed on a thermomixer at low speed for 1 min and incubated for 2 hr at 37°C. The protein digestion was stopped with 5  $\mu$ L of 50% formic acid. New receptacles were rinsed with 100 $\mu$ L of 50% acetonitrile / 2% formic acid (v/v) and fitted to the spin filters to replace the old ones. Peptide digests were extracted with 75  $\mu$ L of 50% acetonitrile / 2% formic acid (v/v) by mixing on a thermomixer for 10 min and centrifuging at 14,000  $\times$ g, 45 min. This step was repeated twice. Spin filters were removed and the receptacles containing the peptide digests in solution were dried down using a vacuum centrifuge to near dryness and reconstituted to 10  $\mu$ L with 50% formic acid / 50% TFE (v/v).

#### 6.2.4 Proteomic analysis

Each of the reconstituted peptide digests of triplicate sets of different treatments were diluted with 1% formic acid to a total volume of 80  $\mu$ L and centrifuged at 14,000  $\times g$  for 10 min. Peptides were analyzed by nanoLC-MS/MS coupled with gas phase fractionation in batches of 8 fractions per replicate, described in detail in Chapter 2. Raw files of data generated by mass spectrometry were converted to mzXML format and searched against the National Center for Biological Information (NCBI) *C. gigas* Reference Sequence (RefSeq) database (26,086 proteins, October 2012), using the X!Tandem algorithm incorporated into the GPM software (version cyclone 2011.12.01), same as Chapter 4. MS/MS spectra were also searched against the reverse database to generate possible false positives and estimate FDR rates. The 8 fractions of each replicate were processed sequentially and a merged, non-redundant output file was generated for protein and peptide identifications with protein and peptide log (e) values  $\leq -1$ . The 12 lists of proteins identified for three replicates in each of the four groups of oysters were filtered based on two criteria; a protein was retained if it was reproducibly identified in all replicates of at least one group of oysters and had a total spectral count of  $\geq 3$ . Peptide and protein FDRs were calculated for each replicate, and in an effort to minimise protein FDRs, data were further filtered for proteins with log (e)  $\leq 2$  at the protein level. After combining replicate data, protein and peptide FDRs were subsequently calculated and were found to be consistently  $< 0.1\%$  at the protein level and  $< 0.05\%$  at the peptide level; thus, further filtering of this data was not required. NSAF values for each protein were calculated using the method described in section 2.5 in Chapter 2. LogNSAF values were calculated for proteins in each replicate list in each treatment group and statistical analyses were performed using student's *t*-tests and ANOVA, implemented in the R stats package incorporated within the SCRAPPY program [232].

Data of all proteins expressed in the four treatment groups were partitioned based on their presence or absence at a given treatment, similar to a Venn diagram. Proteins were categorized based on different abundance patterns and six groups were selected for further analysis: proteins found only in select QX disease resistant oysters; proteins found only in wildtype oysters; proteins present only in non-exposed QXR controls; proteins found only in CO<sub>2</sub> exposed wildtype oysters; proteins found in all CO<sub>2</sub> exposed wildtypes and QXR oysters; and proteins found in all groups of oysters (i.e controls and CO<sub>2</sub> exposed of both wildtype and QXR oysters). In addition, we aimed to identify those proteins that were found to be statistically significantly differentially expressed in response to stress from hypercapnia. Proteins were annotated using various protein databases including InterPro, Uni-prot and KEGG and gene ontology information was inferred in terms of biological processes and metabolic pathways. Further, their distributions and involvement in specific biological processes were functionally categorized to determine the effect of stress from hypercapnia in certain metabolic pathways or processes.

## **6.3 Results and Discussion**

### **6.3.1 Protein identification and shotgun proteomic analysis**

The FASP – LC-MS/MS – GPF methodology proved to be reasonably successful in the proteomic analysis of gill tissues from Sydney rock oysters in studying the effects of hypercapnia. A total of 218 non-redundant proteins from gill tissues were identified in triplicates from the two different culture groups of oysters (WT and QXR) that were exposed to either 856  $\mu\text{atm}$   $\text{CO}_2$  or control conditions. The number of non-redundant proteins identified may seem relatively low when compared with those found in similar proteomics studies in other organisms, but this results from the high biological variability inherent in individual oysters [11, 267] (up to 51% of identified proteins) which lowers the number of reproducible proteins between triplicates in a group. This diversity could stem from the highly polymorphic genetic makeup of oysters, with greater frequency of single nucleotide polymorphisms, or the characteristic repeats in nucleotide and peptide sequences of several highly abundant proteins including collagen, pre-collagens, tubulins, and myosins [267]. These issues significantly increase the false positives in the protein lists, thus requiring stricter filtering protocols which further reduce the number of reproducible proteins. Such high degree of biological variability between oysters is unlike most mammals, insects or plant species, which are generally well documented in proteomics studies, but it is in agreement with the findings of previous studies in oysters [425-427, 11]. This may explain why the proteome of this species-rich mollusc family is relatively poorly explored.

Deciphering the oyster genome was a difficult task owing to its high levels of polymorphisms and sequence repeats. Researchers at the Beijing Genome Institute had to adopt a novel method to assemble the Pacific oyster genome, using a combination of short

reads and fosmid-pooling instead of adopting the usual *de novo* sequencing technique used to sequence the genomes of most other organisms [267]. The genomic and transcriptomic data of the pacific oyster genome revealed a wide-ranging set of genes (for instance, heat shock protein 70 family) that could be enabling these oysters to adapt and handle challenging environmental stresses, such as temperature variation and salinity changes and heavy metals. This was in fact evidenced in our previous proteomic study investigating the stress responses of Sydney rock oysters to heavy metals [11], where several peptide-to-spectrum matches indicated several HSP 70s from a wide range of bivalvia species, suggesting these different versions of HSP 70s may actually be responsible for making the oysters able to cope with the heavy metal stresses by bioaccumulation, in addition to protecting them from the continuously shifting marine waters. Supplementary Information Table S10 lists all proteins reproducibly identified in at least one triplicate set of the four treatment groups along with peptide quantitation and gene ontology information for each protein.

### **6.3.2 Presence and absence of proteins in different oyster groups**

The 218 proteins that were identified from four treatments were sorted based on the presence or absence of proteins at each treatment. This partitioning is shown in Figure 6.1, which reveals differences in the expression of proteins between WT oysters and the QXR breeding lines that had been held under the same environmental conditions in the laboratory, and thus are most likely the result of genetic changes associated with selective breeding. The group with the highest number of proteins (82) is those proteins present only in QXR<sub>controls</sub> that are unexposed to CO<sub>2</sub>. The selection process appears to have caused a significant change in the proteome of the QXR oysters indicated by unique expression of 82 proteins, as opposed to 25 or 13 proteins exclusively found in the

proteome of the other oyster groups. These unique proteins may be involved not only in conferring QX disease resistance, but also in better management of the health of oysters while regulating metabolism. Although there are a considerable number of proteins found in other groups and combinations, we focussed on those combinations with proteins unique to the two breeding lines and CO<sub>2</sub> exposure conditions. Proteins found in these combinations were annotated by extracting gene ontology information from UniProt and KEGG databases, and further analyzed for their distribution among different biological process categories.

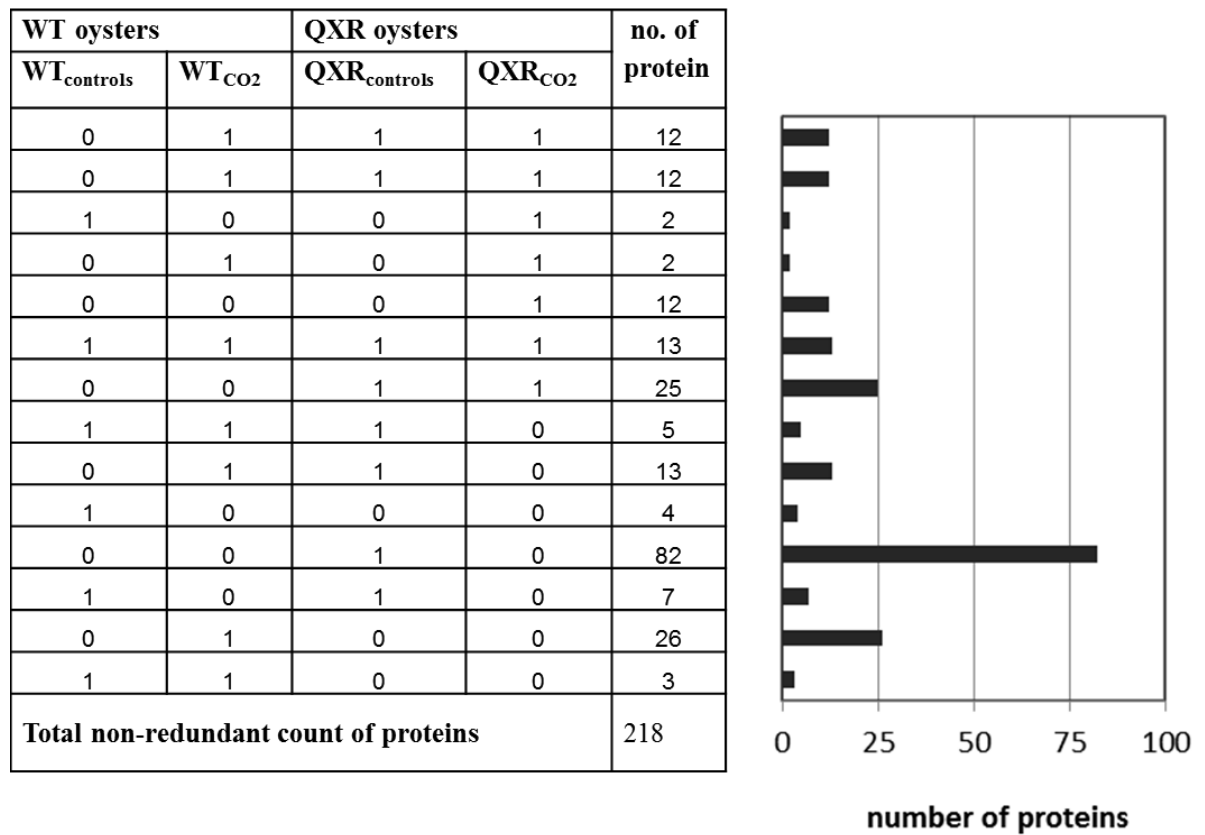


**Figure 6.1** Distribution of proteins across the two different oyster breeds that were either non-exposed controls or CO<sub>2</sub> exposed groups of oysters. Rows represent presence or absence of proteins in each culture group (presence, 1, absence, 0) in each cluster. The total number of proteins found in each combination is also given.

### 6.3.2.1 Proteins found only in QX disease resistant oysters

Proteins expressed only in QXR oysters are listed in Appendix D1, with their biological process categorised from the Uni-prot and KEGG databases. Proteins with a known biological process were graphed as a percentage in each biological process category (Figure 6.2A), and regraphed using combined NSAF values for each category to represent their abundance (Figure 6.2B). Figure 6.2A shows that most of the proteins unique to all oysters QXR disease resistant oysters (present in both CO<sub>2</sub> exposed as well as non-exposed) were involved in protein metabolic process (20%) and carbohydrate metabolism (20%), followed by proteins involved in cytoskeleton and protein polymerization (16%) and translation (16%). However, Figure 6.2B shows that most abundant among proteins unique to QXR<sub>controls</sub> were the cytoskeleton and protein polymerization proteins (49%), followed by those involved in energy metabolism (15%) and translation (12%).

Proteins belonging to the protein metabolic process category were mainly involved in proteolysis and protein folding. Proteasomes are protein degradative machines found in both the nucleus and cytoplasm of the cell. They are known to play a critical role in the removal of unwanted, damaged and misfolded proteins. These unwanted entities first get tagged with ubiquitins, which then act as a signal for subsequent degradation of the target entities from the cell. Since the proteasome complex destroys as well as recycles proteins, its functionality is quite useful when an organism needs to adapt itself to stressful conditions to aid survival. Such degradation of target proteins occurs within the central core of the proteasome complex and is essential for cellular responses to stress, and normal functioning of many other cellular processes including the immune system, cell cycle, growth, apoptosis, and gene expression and regulation [428]. It is possible that

successive breeding lines of QXR oysters may have adapted to continuous stress conditions, and greater protein turnover changes that occur under such stress, by altering how they synthesise new proteins. This could occur by recruiting the amino acids obtained from the degradation of other unwanted proteins, which is not seen in WT oysters. The identification of proteins involved in degradation including proteasome subunits alpha and beta, parkin co-regulated protein, and cytosolic non-specific dipeptidase, to be uniquely expressed in QXR oysters support this hypothesis. This is the first study to report identification of degradation proteins in QX disease resistant oysters, and we hypothesize they may be associated with imparting increased tolerance to environmental biotic and oxidative stresses. Ubiquitin and proteasome subunit beta type 7 were up regulated in QXR<sub>CO2</sub> oysters and such increased protein expression may be associated with increased levels of ubiquitin conjugates within the cell, or in imparting tolerance to hypercapnia stress conditions, or both. Increased expression of ubiquitin conjugates and proteasome subunit beta was also seen in a recent study on *Mytilus trossulus* in response to heat stress [292]. This suggests that hypercapnia shares similarities with responses to other stresses and it is possible that these response mechanisms may be related. Another protein in this category, T complex protein-1-beta subunit was previously shown to be involved in protein folding, especially actins and tubulins [429].

The other most abundant group of proteins uniquely expressed only in QXR oysters (in both CO<sub>2</sub> exposed and non exposed oyster groups) were the carbohydrate metabolic proteins which include phosphoglycerate kinase, 6-phosphogluconate dehydrogenase, glyceraldehyde-3-phosphate dehydrogenase (GAPDH), citrate synthase and isocitrate dehydrogenase. These were associated with roles in pentose shunt, glycolysis and TCA cycle. The TCA cycle, or the Krebs cycle, revolves around the utilization and regeneration of citric acid through oxidation of acetates obtained from the

breakdown of complex carbon molecules from carbohydrates and lipid nutrient reserves to produce usable energy. In the TCA cycle, citrate synthase catalyses the conversion of oxaloacetate to citrate, and isocitrate dehydrogenase catalyses the conversion of isocitrate to ketoglutarate generating 28 equivalents of ATP after one complete cycle [430]. This is used to meet energy and sugar demands to maintain metabolic homeostasis of the oyster. A resourceful avenue of carbon source is via protein catabolism where unwanted proteins get broken down by protein degrading proteasome units into component amino acids, as mentioned earlier in this section. The carbon backbone of these amino acids can become a source of energy by being converted to acetyl-CoA and entering into the citric acid cycle. Another avenue of carbon source can be from fat catabolism where triglycerides may be broken down into fatty acids and glycerol by hydrolysis. The glycerol can be converted into glucose via dihydroxyacetone phosphate and glyceraldehyde-3-phosphate by way of gluconeogenesis.

Phosphoglycerate kinase plays a critical role in glycolysis, in the first ATP-generating step of glycolysis, where it catalyzes the conversion of 1,3-bisphosphoglycerate to 3-phosphoglycerate and transfers the phosphate group from 1,3-bisphosphoglycerate to ADP to yield ATP. Phosphoglycerate kinase catalyses the reverse of the above reaction in gluconeogenesis, generating ADP and 1,3-bisphosphoglycerate as part of reactions that generate ribulose-1,5-phosphate, which is useful in nucleic acid metabolism. This enzyme has been previously shown to impart thiol reductase activity on plasmin, inhibiting angiogenesis and tumour growth. It was also shown to take part in DNA replication and repair in mammalian cell nuclei [431]. Overexpression of this enzyme was associated with gastric cancer cells as seen in *in vitro* studies [432]. 6-phosphogluconate dehydrogenase participates in the pentose shunt where generation of energy and ribulose-5-phosphate (useful for nucleic acid synthesis), and erythrose-4-phosphate (useful for amino acid

synthesis) are primary outcomes of the pathway [433]. Pentose sugars derived from the digestion of nucleic acids may also be used to meet sugar and energy requirements and can be metabolized through the pentose shunt pathway. It is possible that the abundance of CO<sub>2</sub> in hypercapnia conditions may trigger oysters to utilize excess fixed carbon from CO<sub>2</sub> and water, with the help of photosynthetic bacteria to make carbon compounds via the reverse Krebs's cycle [434]. It is also possible that oysters may possess the ability to convert lipids to glucose via glyoxylate cycle, as previously seen in nematodes at early stages of development [435], chicken liver [435], rat cartilage [436], and in black bear brown adipose tissues [437]. These possibilities warrant further research and investigation.

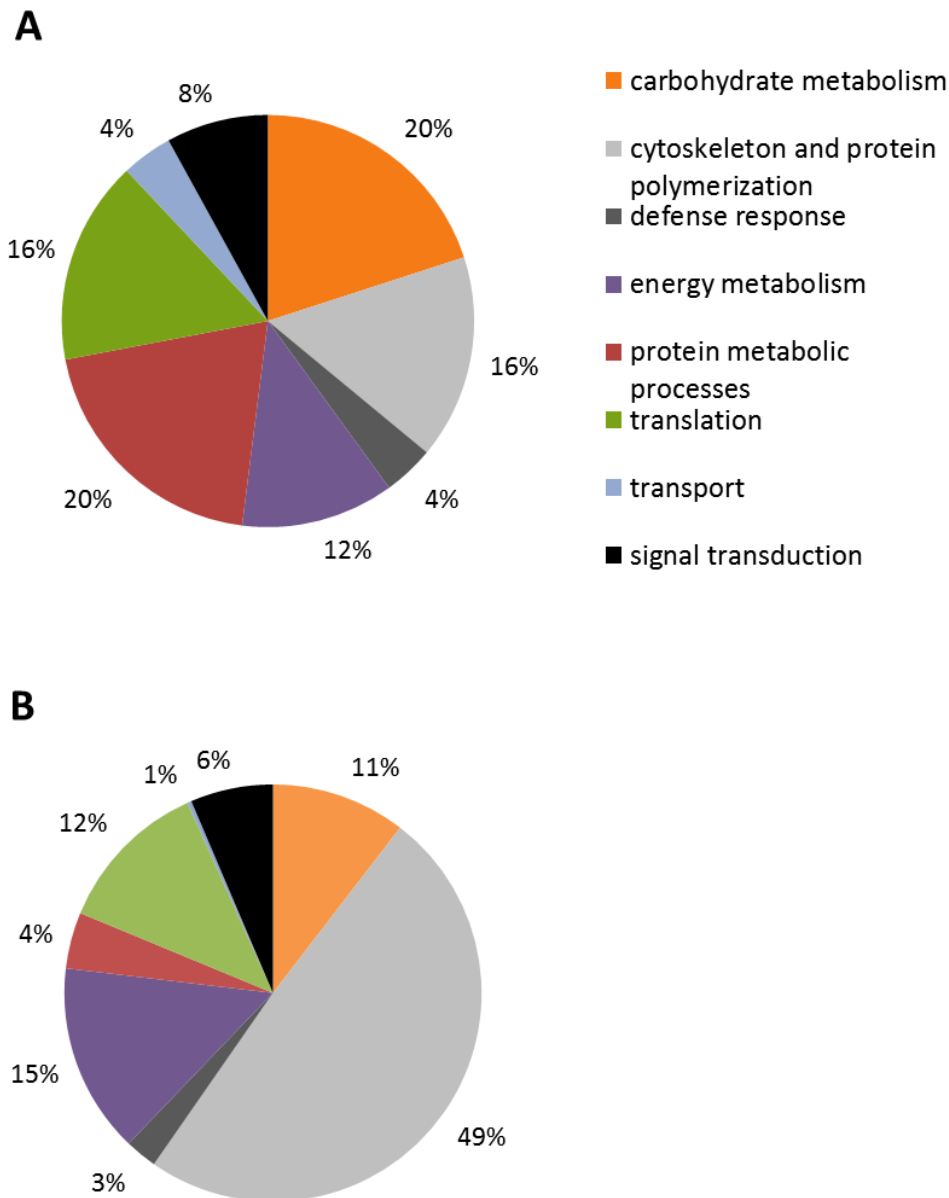


**Figure 6.2** Qualitative and quantitative distribution of proteins found only in QXR oysters. Proteins with a known biological process were categorized as a (A) percentage of protein number in each biological process category and (B) as a percentage of protein abundance in each biological process category represented by the sum of NSAF of proteins in each biological process category. NSAF of each protein represents the average NSAF of the biological triplicate.

GAPDH catalyses the cytosolic breakdown of glucose to carbon and energy in the glycolysis and gluconeogenesis pathways. In this catalysis, D-glyceraldehyde-3-phosphate is converted to D-glycerate-1,3-bisphosphate by oxidation and phosphorylation, releasing energy in the form of reducing equivalents of  $\text{NADH}^+$ , and these are further utilised to replenish oxidised glutathione responsible for counteracting reactive oxygen species prevalent in stress conditions. The  $\text{NAD}^-/\text{NADH}^+$  ratio is an important component of the redox state of the cell, and the equilibrium between these oxidised and reduced forms of NAD are specific to each of the several metabolic activities and is an indirect clue of the health of cells [438]. This is an important pathway surrounding energy and carbon generation vital for the organism's survival. GAPDH and NADH dehydrogenase I were previously shown to be differentially expressed in oysters exposed to heavy metals [11].

GAPDH was previously known mainly for its central role in metabolism but recent evidence has proved GAPDH has multi-faceted roles in other cellular processes, thus demonstrating how nature chooses to efficiently and resourcefully recruit a single protein to perform a variety of functions in the cell. In 2003, Zheng *et al.* discovered that GAPDH alone can sufficiently activate gene transcription [439]. In 2005, Hara *et al.* observed the ability of GAPDH to translocate to the nucleus and initiate apoptosis in response to cytotoxicity [386]. The same study also reported that as a result of acute cytotoxicity, macrophages are apoptotically activated by endotoxins, and this signals the generation of nitric oxide which causes GAPDH to become s-nitrosylated. S-nitrosylation of GAPDH triggers its binding to a ubiquitin ligase, translocating it to the nucleus which lead to degradation of nuclear proteins, and the initiation of the apoptosis cycle. Although oysters are robust organisms naturally adapted to withstand a variety of stresses in the intertidal sea, long term ocean acidification conditions typically lead to acute changes in pH, temperature (seawater warming), and carbonate chemistry (high  $\text{CO}_2$  and  $\text{HCO}_3^-$ , lower

$\text{CO}_3^{2-}$ ). These changes could stimulate GAPDH in activating apoptosis and it is quite possible for such a signalling cascade to occur in oysters in response to cytotoxicity. Hence, understanding this sort of signalling pathway associated with cytotoxicity is vital, and useful in studies inclined toward investigating environmental stress responses such as ocean acidification. Hence, these proteins, especially GAPDH, have become vital to understanding the cellular mechanisms related to cell growth and development in oxidative or reductive stresses arising from environmental stress conditions.

Proteins engaged in cytoskeleton and protein polymerization include cysteine and glycine-rich protein 3, known for its role in myogenesis, cytoplasmic actin, tubulin alpha-1C chain, and tubulin beta chain. These proteins, in addition to myosins, comprise the major cytoskeletal proteins in Sydney rock oysters, and their identification by mass spectrometry is in good agreement with other published studies. In our previous study where Sydney rock oysters were exposed to heavy metals, actins and tubulins were identified as among the most abundant proteins, and some of them showed differential protein expression in response to heavy metal stress [11]. Expression of some of these proteins was also found to be modulated in response to  $\text{CO}_2$  exposure relative to  $\text{QXR}_{\text{controls}}$  as discussed later in this chapter.

Stress-induced metabolic changes are generally used to restore the metabolic balance, and ensure the survival of the organism, specifically by ensuring the fitness of the calcified structures such as shells. Previous studies on calcifying marine invertebrates such as molluscs indicated that biomineralization is a critical and energetically expensive process, because shell structures require production of inorganic calcite and/or aragonite crystals or a proteinaceous organic matrix to enable growth. Therefore, stressful

environmental imbalances that affect the integrity of the organisms external structures will have direct consequences for the organisms fitness to survive.

Many proteins involved in translation were uniquely expressed in all oysters of the QXR breeding line (Figure 6.2A and B). These include 40S ribosomal protein S4 (X linked), 40S ribosomal protein S27, 40S ribosomal protein S12 and 60S ribosomal protein L23. Ribosomal proteins are an important group of proteins and have been associated with environmental stress response in bivalves, as previously seen in *Argopecten purpuratus* [246] and Sydney rock oysters [11]. These proteins mainly drive protein synthesis.

#### **6.3.2.2 Proteins unique only to WT oysters**

Proteins expressed uniquely in all WT oysters were severin, which is involved in cytoskeleton and protein polymerization, calcium-regulated heat stable protein 1, which is involved in transcription and cathepsin B, which is involved in protein metabolic process. These are also listed in Appendix D2. They shared equal distribution both as a percentage as well as in abundance in each biological process category. Cathepsin B has also been recently observed to be involved in conferring innate immune response in pearl oysters [440] and flat oysters [441]. The lack of expression of proteins involved in protein metabolic processes or translation may be have been due to reduced protein biosynthesis which could be the cause for the low number of proteins identified among wildtype oysters.

### 6.3.2.3 Proteins found in all groups of oysters

Proteins expressed in this group include those expressed in controls as well as CO<sub>2</sub> exposed oysters of both WT and QXR lines, as shown in Appendix D3 with their biological process categories. Of these, proteins with a known biological process were graphed as a percentage in each biological process category (Figure 6.3A). The largest group of proteins were those involved in energy metabolism (23%) followed by carbohydrate metabolic proteins (16%), proteins involved in nucleosome assembly (15%), cytoskeleton and protein polymerization (15%), and those involved in signal transduction (15%). Upon regraphing based on relative abundance using combined NSAF values for each category (Figure 6.3B), the most abundant category of proteins were found to be those belonging to nucleosome assembly (61%), followed by proteins involved in cytoskeleton and protein polymerization processes (21%). Although the abundance seems to be low in carbohydrate metabolic proteins, translation, signal transduction and those involved in transport, the fairly sizable number of proteins belonging to each of these categories suggests they may be essential for driving these metabolic processes. Proteins found in all groups of oysters and involved in energy metabolism include peroxiredoxin-5, mitochondrial nucleoside diphosphate kinase and ATP synthase beta subunit. Proteins involved in nucleosome assembly included histone H2B and histone H4. It is clear that the two histone proteins are expressed in high abundance and contribute 61% in quantitative distribution compared to other proteins in this list. Selectively bred QXR oysters had more than twice the levels of growth than non-selectively bred (wild type) oysters when exposed to elevated CO<sub>2</sub>. Proteins expressed in all treatments irrespective of whether exposed to CO<sub>2</sub> stress or not may be those vital for the survival, sustenance, maintenance and development of oysters.

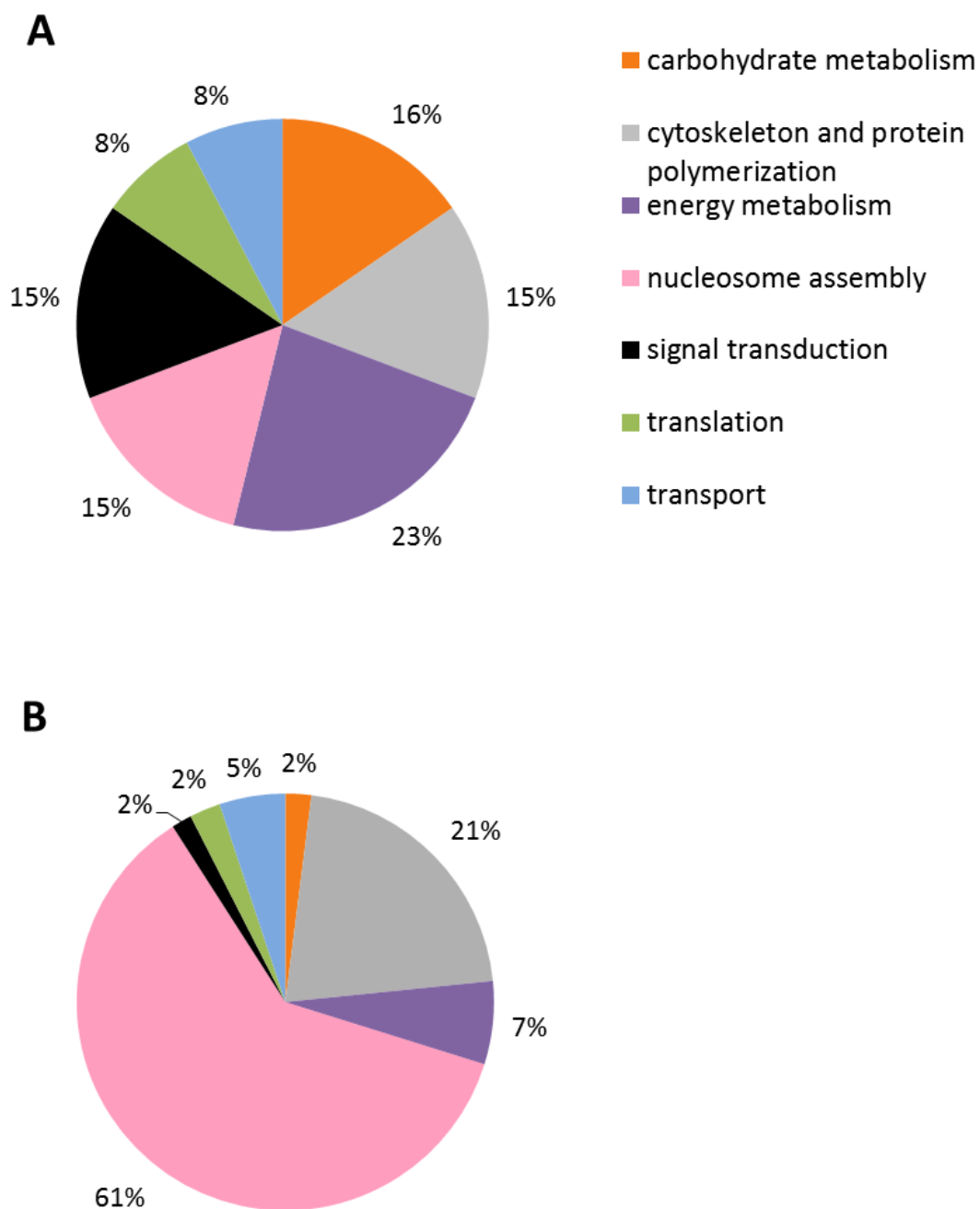


**Figure 6.3** Qualitative and quantitative distribution of proteins in all groups of oysters. Proteins with a known biological process were categorized as a (A) percentage of protein number in each biological process category and (B) as a percentage of protein abundance in each biological process category represented by the sum of NSAF of proteins. NSAF of each protein represents the average NSAF of the biological triplicate.

#### **6.3.2.4 Proteins unique to all CO<sub>2</sub> exposed oysters from both WT and QXR breeds**

The proteins belonging to this group include actin 2/3 and guanine nucleotide-binding protein subunit beta-2, of which actin 2/3 was more abundant. Of all proteins identified in this study, these two proteins could be centrally affected by hypercapnia and may highlight possible reasons for the exclusive expression of these two proteins under stressful CO<sub>2</sub> conditions. Firstly, these proteins may be adaptive responses. Secondly, actin expression is affected by ROS species and reactive nitrogen species. Therefore, increased expression may be necessary to replace ROS/RNS damaged actin forms in these oysters. Alternatively, post-translational modifications might be a way to avoid damage by ROS, hence the identifications of various isoforms of actins in this study.

Under low pH conditions caused by hypercapnia, muscles are more prone to experience extracellular acidosis which causes decreased rate and force of muscle contraction of the heart and nervous systems. Hypercapnic acidosis was reported to directly affect vasodilation and muscle contraction in rat cerebral artery vessels [442], and increased P<sub>CO2</sub> in the hemolymph of snails resulted in a decrease in intracellular pH of myocytes, reducing contractile force [443]. Therefore, actin proteins could be victims of extracellular acidosis caused by the negative effects of lowering of pH arising from hypercapnia, rather than changes in intracellular pH. This is because oysters in general have fewer mechanisms to regulate changing CO<sub>2</sub> or pH conditions and are reported to also face intracellular and extracellular acidosis due to seawater acidification [444].

#### **6.3.2.5 Proteins found uniquely in WT oysters exposed to hypercapnia**

This group represents proteins expressed uniquely in CO<sub>2</sub> exposed WT oysters but absent in QXR<sub>CO<sub>2</sub></sub>, WT<sub>controls</sub> or QXR<sub>controls</sub> oysters. Proteins belonging to this group are listed in Appendix D4 along with biological process information. Proteins with a known biological process were graphed as a percentage in each biological process category (Figure 6.4A) and regraphed based on relative abundance using combined NSAF values for each category (Figure 6.4B). Figure 6.4A revealed that the largest group of proteins were those involved in cytoskeleton and protein polymerization (35%) followed by protein metabolic processes (18%) and transcription (17%). These proteins also showed similar patterns of distribution in each biological process categories in terms of abundance of proteins, where the most abundant proteins belonged to cytoskeleton and protein polymerization (30%) followed by protein metabolic processes (25%) and transcription (21%). Interestingly, although the percentage of proteins involved in nucleosome assembly was only about 9%, their abundance was almost twice as great and encompassed 16% of proteins unique to CO<sub>2</sub> exposed wildtype oysters (Figure 6.4B). It is clear that CO<sub>2</sub> stress highly affected these biological process categories in wildtype Sydney rock oysters. Expression of proteins in the biological process categories of organelle organization, spermatogenesis, and signal transduction may be low in number and abundance, but many of these individual proteins may be significantly affected in response to CO<sub>2</sub> stress.

Proteins involved in cytoskeleton and protein polymerization in this group include non-neuronal cytoplasmic intermediate filament protein, radixin, myosin regulatory light chain sqh, actin-3, paramyosin, tropomyosin, calponin-2 and tektin-3. Most of these proteins are crucial to the formation and maintenance of the integrity of the shell, adductor muscle, mantle and non-muscle tissues, and extracellular matrices. In a recent study on the

effects of elevated pCO<sub>2</sub> on the mantle tissues of eastern oysters, *Crassostrea virginica*, proteomic analysis revealed differential expression of 54 protein spots, of which 17 proteins were identified and belonged to two major classes: cytoskeletal proteins and oxidative stress responsive proteins. Of the cytoskeletal proteins that were differentially expressed in that study, actin, calponin-2, actin polymerization factor and collagens were reported as the proteins that changed in expression in response to stress caused by elevated pCO<sub>2</sub> [214], which is in agreement with our results found in this study. In other recent ocean acidification studies, some benthic marine invertebrates have been reported to show reduced calcification rates [445] and decreased metabolism (hypometabolism) [446] as common effects of elevated CO<sub>2</sub>. However, in some species increased rates of physiological processes that require energy could also be paralleled by an increase in metabolic activity; this relationship was seen by Wood *et al.* in their study on starfish, *Amphiura filiformis*, where calcification rate, growth and metabolism was preliminarily increased to maintain cytoskeletal integrity under hypercapnia conditions, but survival, arm movement and reproductive success were affected by ocean acidification [415]. Although this study reported loss of muscle mass and damage to internal structures of arm muscle leading to arm muscle wastage and declined motility in lowering pH conditions, no significant decrease in egg size of *A. Filiformis*, was observed [415]. Since arm movement is vital for feeding, burrow creation and locomotion, a loss of arm function could result in the release of gametes within the starfish burrows resulting in fewer gametes being released into the water column, as is necessary during spawning. Therefore, reduction in the numbers of successful reproductions is possible not only for *A. filiformis* but also in other marine relatives such as oysters when subjected to stress in the form of ocean acidification.

Among the proteins involved in protein metabolic processes, the majority were responsible for protein folding and ubiquitin dependent protein catabolism. These included peptidyl-prolyl cis-trans isomerase, an uncharacterized protein (GI 405959327), protein disulfide-isomerase, and S-phase kinase-associated protein. This uncharacterized protein was reported in the Uni-prot database to be involved in protein folding. However, BLAST searches against all protein entries in NCBI and Swissprot did not result any significant similarities or identity to matches to a known protein, where a match greater than 80% was considered significant identity, while the BLAST result for this protein showed matches to less than 50% identity. (see also Appendix D6).

Transcription related proteins unique to WT<sub>CO2</sub> and QXR<sub>CO2</sub> oysters included heterogeneous nuclear ribonucleoprotein A/B, Transcription factor BTF3-like protein 4, heterogeneous nuclear ribonucleoprotein Q and heterogeneous nuclear ribonucleoprotein A2-like protein 1, all of which were mainly involved in pre-mRNA processing, mRNA metabolism and splicing activities.

Histone H3 and protein SET were the two nucleosome assembly related proteins that showed greater abundance than the remaining proteins. These were involved in organelle organisation, signal transduction, stress response or spermatogenesis, so these may play important roles in stress adaptation in oysters and need deeper understanding which requires further research.

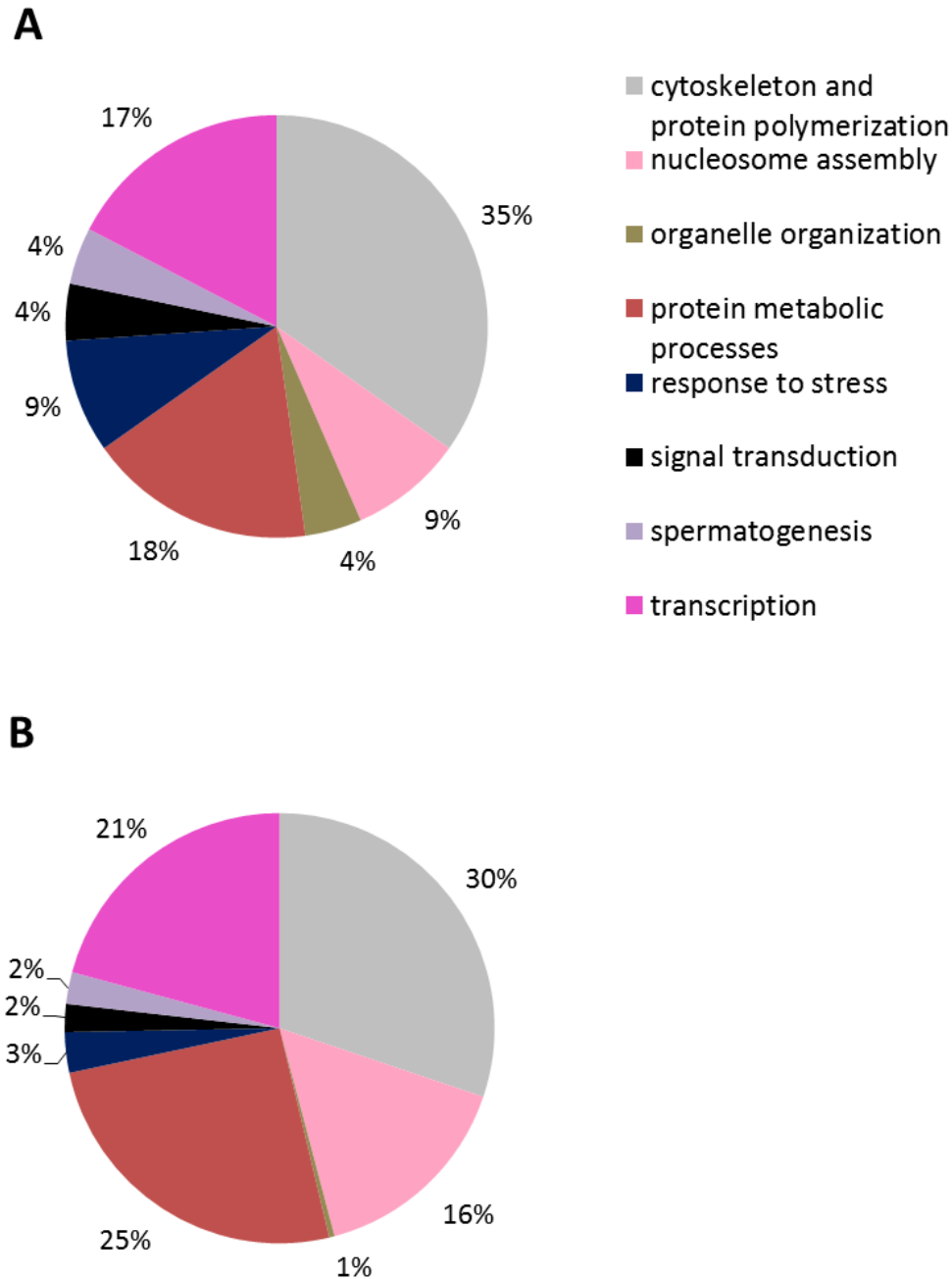


**Figure 6.4** Qualitative and quantitative distribution of proteins unique to CO<sub>2</sub> exposed WT oysters. Proteins with a known biological process were categorized as a (A) percentage of protein number in each biological process category and (B) as a percentage of protein abundance in each biological process category represented by the sum of NSAF of proteins in each biological process category. NSAF of each protein represents the average NSAF of the biological triplicate.

### 6.3.2.6 Proteins found only in QXR oysters exposed to hypercapnia

This group represent proteins expressed uniquely in CO<sub>2</sub> exposed QXR oysters but absent in WT<sub>CO<sub>2</sub></sub>, QXR<sub>controls</sub> or WT<sub>controls</sub> oysters. Proteins expressed only in CO<sub>2</sub> exposed QXR select oysters are listed in Appendix D5, with their biological process categorised from Uni-prot and KEGG.

Proteins unique to CO<sub>2</sub> exposed QXR oysters with a known biological process were graphed as a percentage in each biological process category (Figure 6.5A) and regraphed based on relative abundance using combined NSAF values for each category (Figure 6.5B). Figure 6.5A indicate that many of these proteins belonged to carbohydrate metabolism (34%) and transport (25%) biological process categories. Figure 6.5B reveals that proteins involved in protein metabolic process and transport share the highest abundance (23%) followed by carbohydrate metabolic proteins. Of the proteins involved in protein metabolic processes, ubiquitin was the greatest in abundance at 23% of the total and is known to be associated with protein destruction or catabolism. Transport related proteins that were next in terms of abundance included ankyrin, ras-related protein Rab-1A, and Rab GDP dissociation inhibitor beta.

Carbohydrate metabolic proteins included glycogen phosphorylase, isocitrate dehydrogenase subunit alpha, succinyl-CoA ligase subunit alpha and aldehyde dehydrogenase. Isocitrate dehydrogenase was previously reported as differential protein in response to CO<sub>2</sub> stress [418]. All of the above carbohydrate metabolic proteins were up-regulated in response to hypercapnia (>800 uatm CO<sub>2</sub>). Aldehyde dehydrogenase oxidises several aliphatic and aromatic aldehydes, and under inhibition of CO<sub>2</sub> aldehyde dehydrogenase has been reported to catalyse the metabolism of formaldehyde, but its role in relation to CO<sub>2</sub> stress remains unclear. Succinyl coA ligase (also known as succinyl

COA synthetase) and isocitrate dehydrogenase are both involved in the TCA cycle through which oysters can generate energy by oxidation of carbohydrates, proteins and fats to CO<sub>2</sub> and water. Upregulation of these enzymes could be associated with the utilization of fatty acids or glycogen reserves as an alternate source of sugar for energy replacement soon after the depletion of glucose. In normal conditions, glycogen storage is essential for reproduction. Forced utilization of glycogen reserves to meet high energy demands for cytoskeletal maintenance, sustenance and survival under CO<sub>2</sub> stress may cause depletion of glycogen thereby affecting reproduction and development of oysters.

All these proteins may therefore play roles in helping the already resilient QXR oysters cope with newer stressful conditions coming from the environmental changes in terms of greater levels of seawater CO<sub>2</sub> and the resulting lowering of pH. Hence, the biological processes involving these proteins eventually become affected in response to CO<sub>2</sub> stress.

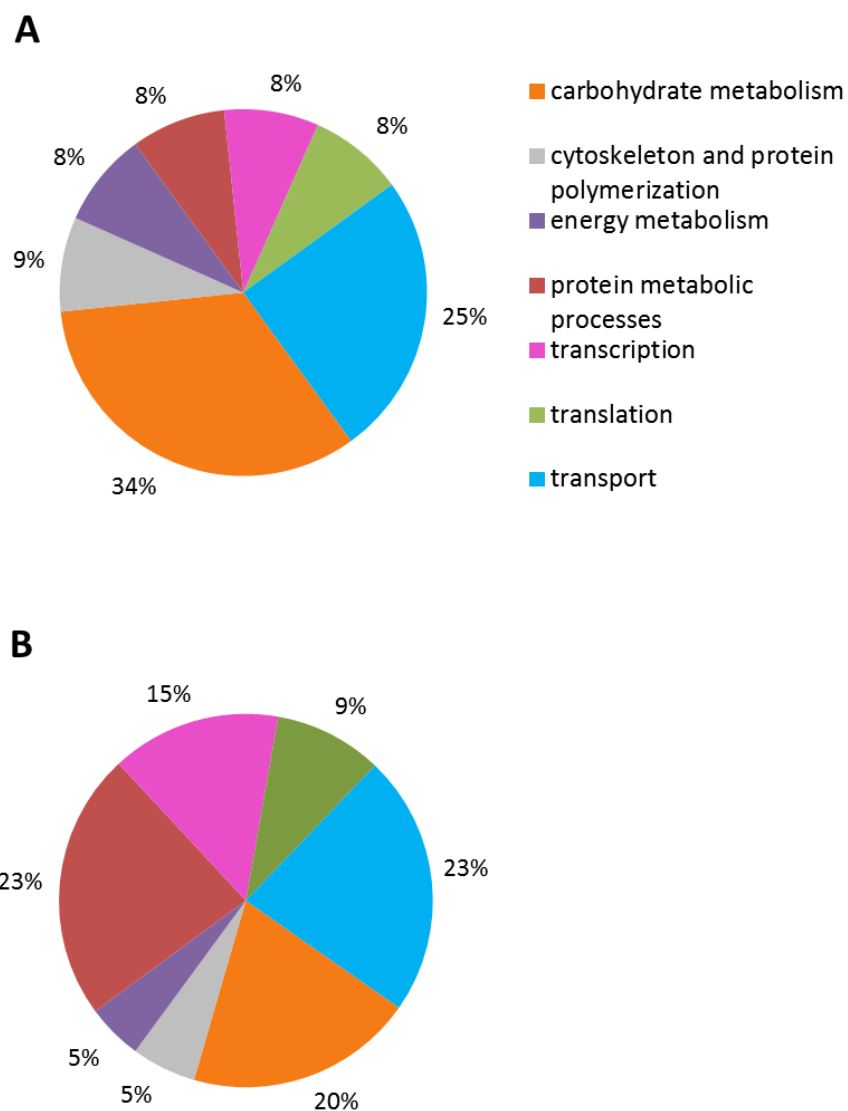


**Figure 6.5** Qualitative and quantitative distribution of proteins unique to CO<sub>2</sub> exposed QXR oysters. Proteins with a known biological were categorized as a (A) percentage of protein number in each biological process category and (B) as a percentage of protein abundance in each biological process category represented by the sum of NSAF of proteins. NSAF of each protein represents the average NSAF of the biological triplicate.

### 6.3.3 Statistically significant differentially expressed proteins among CO<sub>2</sub> exposed oysters

Student's t-test analysis was performed to identify the statistically differentially expressed proteins in response to elevated CO<sub>2</sub> stress in both breeding lines of Sydney rock oysters. The LogNSAF values, characteristic of protein abundance, were plotted for each reproducible protein in each treatment against respective controls for all oysters breeds of the CO<sub>2</sub> exposure experiments, and these were indicative of the distribution of differentially expressed proteins amongst unchanged proteins. Figure 6.6a represents the LogNSAF plot corresponding to QXR breed of oysters (QXR<sub>controls</sub> plotted against QXR<sub>CO2</sub>) and Figure 6.6b represents LogNSAF plot corresponding to WT oyster (WT<sub>controls</sub> plotted against WT<sub>CO2</sub>). In each CO<sub>2</sub> stress experiment, statistically differentially expressed proteins in terms of protein abundance relative to controls were clearly distinguishable from unchanged proteins, as evidenced from these LogNSAF plots (Fig. 6.6A and B). Supplementary Information Table S11 provides NSAF values of all proteins in each replicate list in each treatment group for the two oyster breeds.

These plots provide an informative visual display of both the total number of significantly differentially expressed proteins and the overall trend of their differential expression.

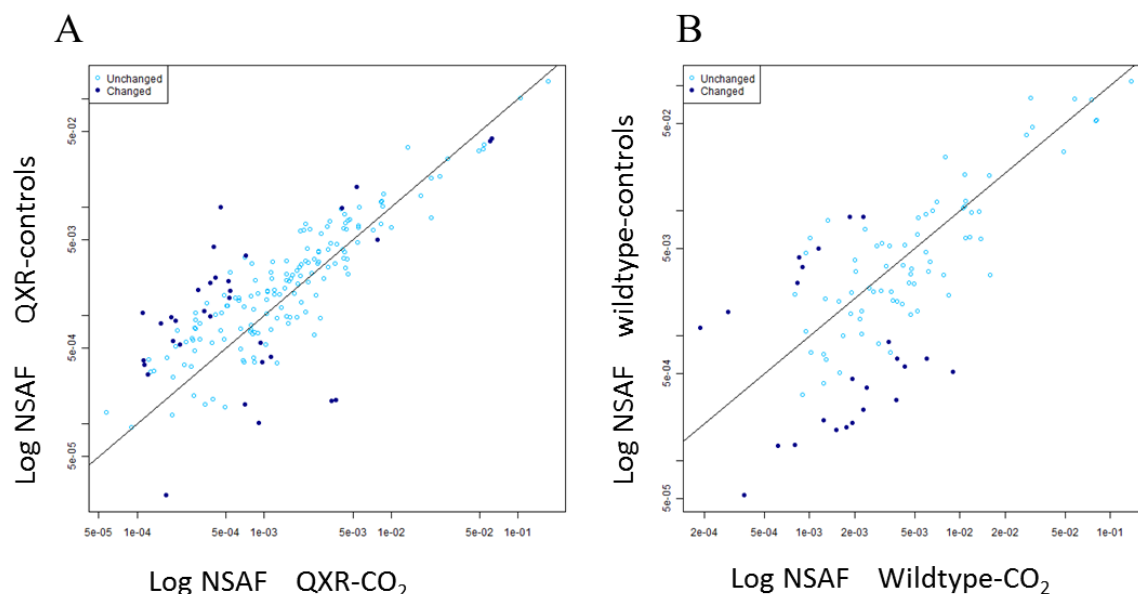


**Figure 6.6** Log NSAF plots of differential and unchanged proteins in each CO<sub>2</sub> treatment relative to controls (A) QXR oysters, (B) WT oysters. Proteins with significant differential expression are shown as darker spots. Proteins with expression levels that did not differ significantly between metal exposures and controls are shown as lighter hollow spots. Up- and down-regulated proteins are shown as darker spots below and above the diagonal respectively.

A total of 56 proteins changed significantly (p-value <0.05) in their expression profiles in response to elevated CO<sub>2</sub> stress from both oyster breeds, of which 32 proteins were differentially expressed in response to CO<sub>2</sub> stress in QXR oysters relative to controls, whereas 24 proteins were differential in WT<sub>CO<sub>2</sub></sub> oysters relative to WT<sub>controls</sub>. A complete list of these 56 significantly differentially expressed proteins in response to CO<sub>2</sub> stress, with annotation and quantitation information, is shown in Table 6.1 for QXR oysters and Table 6.2 for WT oysters. Of the 56 differential proteins in response to CO<sub>2</sub> stress, one

differentially expressed protein was common to both QXR as well as WT oysters, which was small nuclear ribonucleoprotein Sm D1.

#### **6.3.4 Differentially expressed proteins among QXR<sub>CO2</sub> oysters relative to QXR<sub>controls</sub>**

Differentially expressed proteins corresponding to QXR oyster breed exposed to elevated CO<sub>2</sub> were comprised of 10 up-regulated proteins and 22 down-regulated proteins. The top up-regulated proteins in QXR oysters in response to CO<sub>2</sub> stress include ubiquitin-b, isocitrate dehydrogenase [NAD] subunit alpha, inorganic pyrophosphatase, and ankyrin-1. Ubiquitin-b showed the highest differences by being up regulated by 20 fold, followed isocitrate dehydrogenase by 9 fold and ankyrin by 7.7 fold (Table 6.1). Among the 22 down-regulated proteins, peptidyl-prolyl cis-trans isomerase, plastin-1, saccin, ubiquitin, and 40S ribosomal proteins S19 and S7 were the most significant, with expression levels reduced from 4.6 to 20 folds relative to QXR<sub>controls</sub>.

**Table 6.1** Statistically differentially expressed proteins among QXR oysters exposed to CO<sub>2</sub> relative to their respective controls.

GI number	UniProt AC	Protein name	Average peptide count	Biological process category*	Fold change relative to controls
<b>Proteins down regulated in QXR<sub>CO2</sub> oysters in response to hypercapnia</b>					
gi 405965410	K1Q2Y1	40S ribosomal protein S15	4	translation	3.1
gi 405951077	K1QC22	40S ribosomal protein S19	8	translation	10.7
gi 405972954	K1RSZ6	40S ribosomal protein S7	4	translation	5.6
gi 405965232	K1Q2L2	60S ribosomal protein L12	23	translation	2.3
gi 405976099	K1RAI3	annexin	4	transport	5.2
gi 405972655	K1QUT9	calcineurin subunit B type 1	2	PMP	3.0
gi 405964165	K1PZN1	calcium/calmodulin-dependent protein kinase type II delta chain	2	signal transduction	2.3
gi 405965382	K1QHW8	ferritin	2	energy metabolism	3.3
gi 405974984	K1QRQ2	glutamate dehydrogenase	2	energy metabolism	3.4
gi 405952674	K1PFT9	myophilin	41	CY/P	2.9
gi 405978738	K1R1I0	peptidyl-prolyl cis-trans isomerise (FKBP-type domain)	4	PMP	5.4
gi 405968843	K1QAU8	peptidyl-prolyl cis-trans isomeraseE (cyclophilin-domain)	3	PMP	4.4
gi 405960658	K1Q5Q2	plastin-1	4	CY/P	5.3
gi 405959092	K1Q8G0	Radial spoke head protein 9-like	2	CY/P	2.5
gi 405977015	K1QX44	Ras-related protein Rab-11B	5	signal transduction	3.9
gi 405962281	K1Q227	Sacsin	7	PMP	9.5
gi 405973087	K1R2P2	SH3 domain-binding glutamic acid-rich protein	2	PMP	3.03
gi 405969415	K1QKN1	Small nuclear ribonucleoprotein F	4	transcription	4.9

GI number	UniProt AC	Protein name	Average peptide count	Biological process category*	Fold change relative to controls
gi 405953653	K1PR03	nexin-12	3	PMP	2.7
gi 405951523	K1PD36	Ubiquitin	19	PMP	21.9
gi 405975080	K1RXH3	Uncharacterized protein	2	stress response	2.6
gi 405964389	K1Q087	Uncharacterized protein	4	unknown	5.4
<b>Proteins up regulated in QXR<sub>CO2</sub> oysters in response to hypercapnia</b>					
gi 405966634	Q8TA69	Actin 1	193	CY/P	1.5
gi 405973339	K1QWP8	Actin-2/3	200	CY/P	1.5
gi 405973865	K1RBG6	Actin-3	35	CY/P	1.6
gi 405969724	K1QCS6	Ankyrin-1	2	transport	7.7
gi 405962800	K1Q3F4	Inorganic pyrophosphatase	2	energy metabolism	4.7
gi 405968311	K1Q9G3	Isocitrate dehydrogenase [NAD] subunit alpha, mitochondrial	2	carbohydrate metabolism	9.0
gi 405962686	K1PVF6	Proteasome subunit beta type	2	PMP	1.7
gi 405973300	K1QMH5	Small nuclear ribonucleoprotein Sm D1	5	transcription	2.6
gi 405972882	K1R294	T-complex protein 1 subunit beta	5	PMP	2.8
gi 405978203	K1RA77	Ubiquitin-b	6	PMP	20.9

\* Cy/P and PMP refer to the biological process categories, cytoskeleton and protein polymerization and protein metabolic processes respectively.

All of the differentially expressed proteins with respect to QXR oysters were first categorized based on their function as a percentage of the total number of proteins (Figure 6.7A), and then recategorized as a percentage of protein abundance within each functional category based on NSAF values (Figure 6.7B). Comparison of the two plots showed that the total number of differential proteins within a functional category often followed a

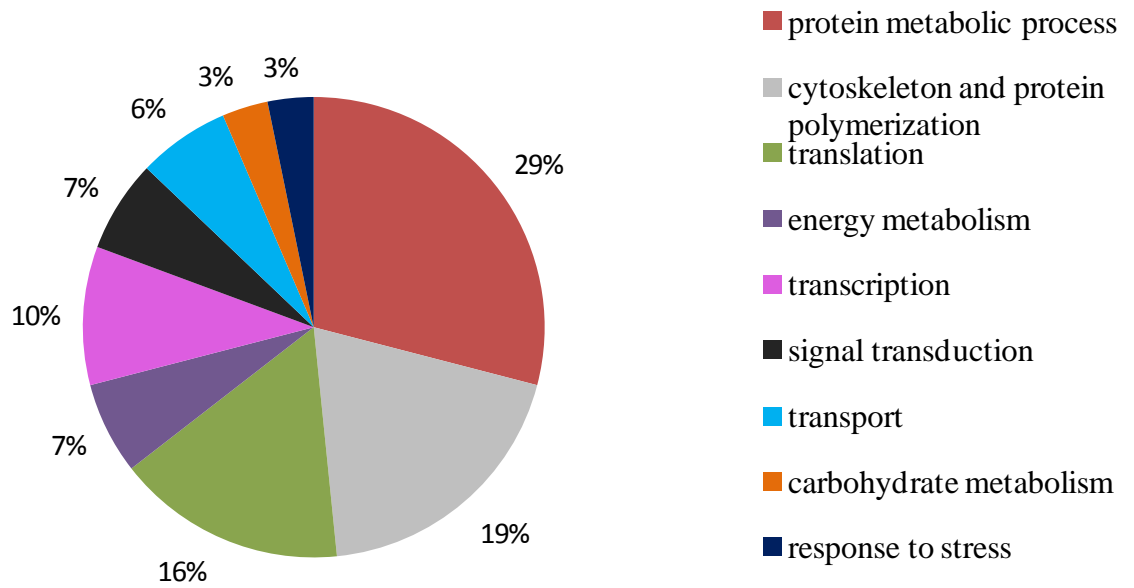
different trend than when functional categories were quantified based on their overall protein abundance. Figure 6.7A shows that protein metabolic process (29%) comprised the highest percentage of proteins, followed by cytoskeleton and protein polymerization category (19%) and translation (16%), while Figure 6.7B shows that proteins involved in cytoskeleton and protein polymerization processes were the greatest in abundance (76%), followed by translation (11%) compared to all other biological process categories.

Of the 32 differentially expressed proteins seen in response to hypercapnia in QXR oysters, protein metabolic process category comprised one third of the proteins, and included nexin-12, saccin, glutamate dehydrogenase, calcineurin subunit B type 1, peptidyl-prolyl cis-trans isomerase, SH3 domain-binding glutamic acid-rich protein, proteasome subunit beta type, T-complex protein 1 subunit beta and ubiquitin, as listed in Table 6.1. Although the number of proteins related to cytoskeleton and protein polymerization biological process category was less than half when compared to protein metabolic process, they formed the most abundant functional category, also shown in Figure 6.13. The six differentially expressed cytoskeletal proteins were myophilin, radial spoke head protein 9-like protein, plastin-1, actin-2/3, actin 1 (adductor muscle) and actin-3 (Table 6.1), and their expression changes ranged from 1.5 to 5.5 fold. Actin isoforms have been found to be sensitive to elevated CO<sub>2</sub> stress and oxidative stress from ROS, and this explains their increased abundance to counteract stress and possibly aid in maintenance of cellular and muscular integrity. However, in terms of fold changes these actin forms were some of the lowest compared to other differentially expressed proteins in QXR oysters. Such low fold changes for differentially expressed actins were also observed by Tomanek *et al.* where protein expression changes in actins in response to elevated pCO<sub>2</sub> in oysters ranged between 1.3 and 2.3 fold, quantitated using 2DE [214]. The increased expression, or perhaps post-translational modifications of these forms of actin,

may be triggered by Rab 11b, a small G-protein of the Ras family, recently found to be involved in actin-cytoskeleton organization [447]. Further Rab-11b protein is also associated with protein localization to the cell surface, ion channels, and endocytic recycling, affecting a number of transmembrane proteins during membrane trafficking. In conjunction with its role in actin-associated cytoskeleton organization, Rab-11b was also up regulated in response to extracellular acidosis at the protein level in HSG salivary ducts [448], and may be a crucial regulator of translocation of acid-base ( $H^+$  and  $HCO_3^-$ ) transporters in Sydney rock oysters facing extracellular acidosis as a consequence of ocean acidification caused by elevated levels of  $CO_2$ .

A recent study reported the effects of elevated temperatures and elevated levels of  $pCO_2$  on eastern oysters by measuring the whole-organism standard metabolic rate, total antioxidant capacity, and levels of several known oxidative stress biomarkers, and observed that the combination of stresses from increased temperature and  $CO_2$  levels could impact greatly on biomineralization, structural hardness and dissolution of cytoskeletal carbonate structures of shells when compared to stress arising from increased  $pCO_2$  alone [226]. Therefore, these differential proteins are indicative of stress in  $CO_2$  exposed QXR oysters relative to controls and could act as potential biomarkers for hypercapnia in response to  $CO_2$  stress.

**A**



**B**

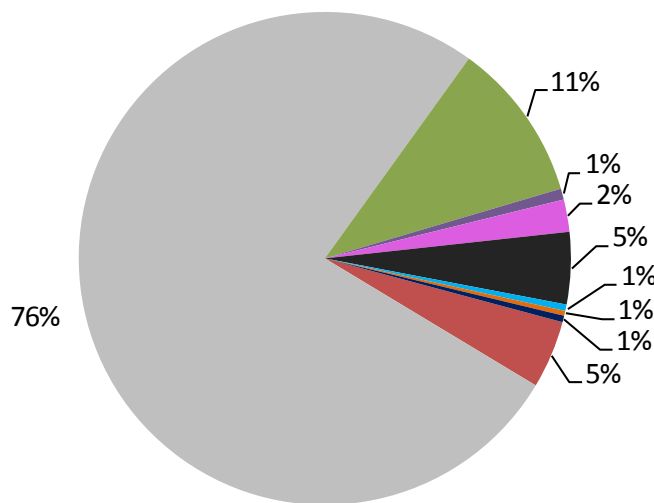


**Figure 6.7** Quantitative and qualitative distribution of differentially expressed proteins QXR oysters in response to CO<sub>2</sub> exposures represented as (a) percentage of proteins in each biological process category and, (b) abundance of proteins in each biological process category represented by summed NSAFs.

### **6.3.5 Differentially expressed proteins among WT<sub>CO2</sub> oysters relative to WT<sub>controls</sub>**

Differentially expressed proteins corresponding to WT oysters exposed to elevated CO<sub>2</sub> were comprised of 16 up-regulated proteins and 8 down-regulated proteins, which are shown in Table 6.2 with biological process and peptide quantitation information. The proteins that increased most in abundance among the up-regulated proteins include tropomyosin, actin-2, myosin regulatory light chain sqh, uncharacterized protein (GI 405957528), 78 kDa glucose-regulated protein, heterogeneous nuclear ribonucleoprotein Q and rootletin. These are listed in decreasing order of fold changes ranging from 17.3 fold down to 7 fold. Many of these up-regulated proteins were found to be involved in cytoskeleton and protein polymerization processes in addition to transcription and translation.

Several proteins decreased in abundance in WT oysters in response to CO<sub>2</sub> stress, including small nuclear ribonucleoprotein Sm D1, elongation factor 1-alpha, 40S ribosomal protein S16, small nuclear ribonucleoprotein Sm D3, ras-related protein Rab-7a, dynein light chain roadblock-type 2, natterin-1 and 40S ribosomal protein S13, listed in decreasing order of fold changes, ranging from 6.1 to 3.1 fold. Of these proteins, tropomyosin, actin 3, heterogeneous nuclear ribonucleoprotein Q, myosin regulatory light chain sqh, uncharacterized proteins (GI405958653 and GI405957528), 78 kDa glucose-regulated protein and small nuclear ribonucleoprotein Sm D1 showed some of the highest fold changes ranging from 17- 6.1 fold (Table 6.2). Many of these proteins were involved in transcription and translation processes and may play an important role in CO<sub>2</sub> stress response.

**Table 6.2** Statistically significant differentially expressed proteins among WT oysters exposed to CO<sub>2</sub> relative to WT<sub>controls</sub>.

GI number	UniProt AC	Protein name	Average peptide count	Biological process category	Fold change relative to controls
<b>Proteins down regulated in WT<sub>CO2</sub> oysters in response to hypercapnia</b>					
gi 405966326	K1QRZ3	40S ribosomal protein S13	2	translation	3.2
gi 405958969	K1PM50	40S ribosomal protein S16	2	translation	5.0
gi 405957468	K1QQC1	Dynein light chain roadblock-type 2	4	transport	4.0
gi 405967949	K1QGS8	Elongation factor 1-alpha	3	translation	5.4
gi 405945673	K1Q7Q8	Natterin-1	2	cytolysis	3.9
gi 405961849	K1PZ08	Ras-related protein Rab-7a	4	signal transduction	4.4
gi 405973300	K1QMH5	Small nuclear ribonucleoprotein Sm D1	3	transcription	6.2
gi 405976315	K1QVD0	Small nuclear ribonucleoprotein Sm D3	5	transcription	4.9
<b>Proteins up regulated in WT<sub>CO2</sub> in response to hypercapnia</b>					
gi 405950429	K1PHM8	14-3-3 protein zeta	2	signal transduction	4.3
gi 405976088	K1R4D4	40S ribosomal protein S2	2	translation	6.3
gi 405968607	K1QIR8	78 kDa glucose-regulated protein	3	response to stress	8.5
gi 405965392	K1QHY0	Actin-3	5	CY/P	12.3
gi 405973812	K1R4R1	Coiled-coil domain-containing protein 19, Heterogeneous nuclear	2	unknown	5.9
gi 405977263	K1QXS6	ribonucleoprotein A2-like protein 1	5	transcription	7.6
gi 405972362	K1R7I9	Heterogeneous nuclear ribonucleoprotein Q	4	transcription	9.5
gi 405974681	K1QQR1	Major vault protein	2	transport	6.0
gi 405964694	K1Q122	Myosin regulatory light chain sqh	4	CY/P	9.2

GI number	UniProt AC	Protein name	Average peptide count	Biological process category	Fold change relative to controls
gi 405950795	K1PBC0	Non-neuronal cytoplasmic intermediate filament protein	9	CY/P	5.8
gi 405966986	K1QTC1	Paramyosin	2	CY/P	4.7
gi 405971092	K1QGF9	Rootletin	3	organnelle organization	6.9
gi 405967947	K1RG91	Transgelin-2	2	CY/P	3.7
gi 405967637	K1QNV6	Tropomyosin	12	CY/P	17.3
gi 405958653	K1QT31	Uncharacterized protein	3	cellular metabolic process	8.8
gi 405957528	K1PIB2	Uncharacterized protein	3	unknown	9.6

\* Cy/P refers to the biological process category cytoskeleton and protein polymerization.

Transport related proteins may particularly be indicators that oysters may be responsive to the change in the ion gradient caused by the rapid diffusion of CO<sub>2</sub> in seawater by which H<sup>+</sup> and HCO<sub>3</sub><sup>-</sup> ions dissociate in greater number. This is because elevated CO<sub>2</sub> has greater impact on calcification when animals generally pass bicarbonate HCO<sub>3</sub><sup>-</sup> ions transported for carbon source through their epithilium, instead of carbonate CO<sub>3</sub><sup>2-</sup> ions, thus requiring more transport proteins.

All of the differentially expressed proteins corresponding to WT oysters exposed to elevated CO<sub>2</sub> were analyzed for their distribution pattern among different biological process categories. The differential proteins were first categorized based on their function as a percentage of the total number of proteins (Figure 6.8A), and then recategorized as a percentage of protein abundance within each functional category based on summed NSAF values (Figure 6.8B). Comparison of these two plots showed that the total number of

differential proteins within a functional category in WT oysters followed a fairly similar trend when functional categories were quantified based on their overall protein abundance. Figure 6.8A shows that cytoskeleton and protein polymerization category (28%) comprised the highest percentage of proteins, followed by transcription (19%), translation (19%) and transport (9%). In the context of distribution of protein abundance, Figure 6.8B shows that proteins involved in cytoskeleton and polymerization processes were also the greatest in abundance (35%) followed by transcription (22%), translation (15%) and transport proteins (14%), all of which were of moderate abundance, while the remaining functional categories were relatively less abundant.

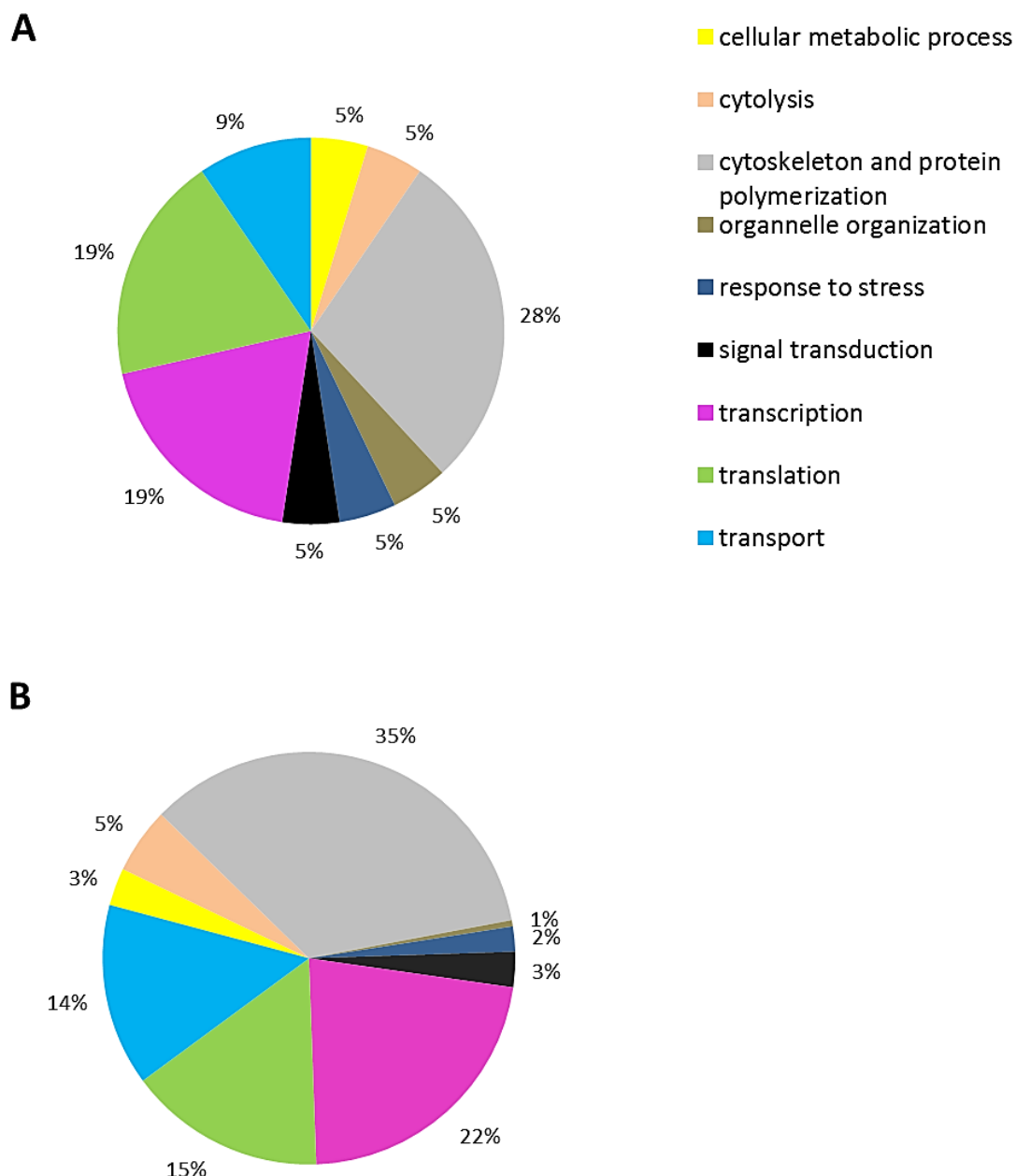


**Figure 6.8 Quantitative and qualitative distribution of differentially expressed proteins in WT oysters in response to CO<sub>2</sub> exposures relative to WT<sub>controls</sub> represented as (a) percentage of proteins in each biological process category and, (b) abundance of proteins in each biological process category represented by summed NSAFs.**

### **6.3.6 Metabolic pathway analysis**

The effects of stress from seawater acidification caused by excess CO<sub>2</sub> levels on important metabolic pathways featured in oysters were determined by examining abundance changes in proteins and enzymes involved in those metabolic pathways.

#### **6.3.6.1 Cytoskeleton and protein polymerization**

Acidification of seawater by elevated CO<sub>2</sub> levels negatively impacts the calcification rate, biomineralization and cytoskeleton formation of calcifying marine species such as oysters. Many studies have established this effect on cytoskeletal maintenance and processes [224, 204, 415, 246]. In a study on sea urchins, mRNA transcripts for genes that are core to the skeletal formation and calcification processes were found to decrease under moderate CO<sub>2</sub> exposures as well as high CO<sub>2</sub> conditions [418]. This may mean that sea urchin larvae were incapable of fueling certain biomineralization pathways to restore the damage effects caused by elevated CO<sub>2</sub>. The same could apply to oyster larvae if subjected to moderate and elevated CO<sub>2</sub>, and they may not be able to handle the increasing effort required to steer biomineralization processes for restoration works, leading to poor survival in these conditions.

Differentially expressed CO<sub>2</sub> stress responsive proteins pertaining to WT oysters involved in cytoskeleton and protein polymerization processes were graphed based on the average NSAF values from triplicates for each protein. Changes in NSAF protein abundance factors revealed that most proteins of the cytoskeleton and protein polymerization category were up-regulated in protein expression in WT oysters exposed to elevated CO<sub>2</sub> compared to controls, as shown in Figure 6.9.

Myosins are responsible for most muscle contractions, which occur by sliding motions between thick and thin myosin filaments of the myofibril. The mechanical energy required for this muscle contraction is usually obtained by the interaction of myosins with actins to convert ATP chemical energy to mechanical energy [449]. On the other hand, tropomyosin is known to be present in both muscle and non-muscle cells and it also interacts with actin to aid in muscle contraction. Paramyosin forms the core structure of the thick filaments of many catch muscles [450]. Changes in proteins related to muscle contraction in oysters has the potential to become a useful bioindicator of prevailing CO<sub>2</sub> stress conditions in the marine environment.

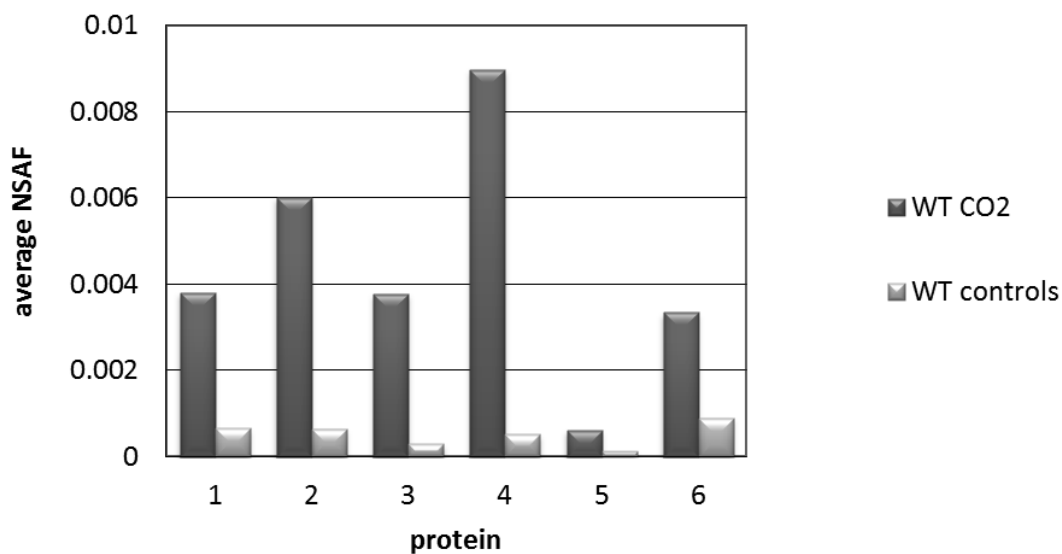


**Figure 6.9** Abundance of statistically significant differentially expressed proteins involved in cytoskeleton and protein polymerization in WT oysters. Numbers 1 -6 on the horizontal axis refer to names of proteins; (1) non-neuronal cytoplasmic intermediate filament protein, (2) myosin regulatory light chain sqh, (3) actin-3, (4) tropomyosin, (5) Paramyosin, (6) Transgelin-2. Y-axis represents average NSAF value from biological triplicates.

Differentially expressed proteins involved in cytoskeleton and protein polymerization that were either up- or down-regulated in QXR oysters exposed to CO<sub>2</sub> when compared to QXR<sub>controls</sub> were also graphed based on the average NSAF values from triplicates for each protein (Figure 6.10). Changes in NSAF protein abundance factors revealed interesting metabolic changes in response to CO<sub>2</sub>. Proteins belonging to this metabolic process that were differentially expressed in QXR oysters include up-regulated proteins which were all different forms of actin proteins, namely actin-2/3, actin-3 and actin 1.

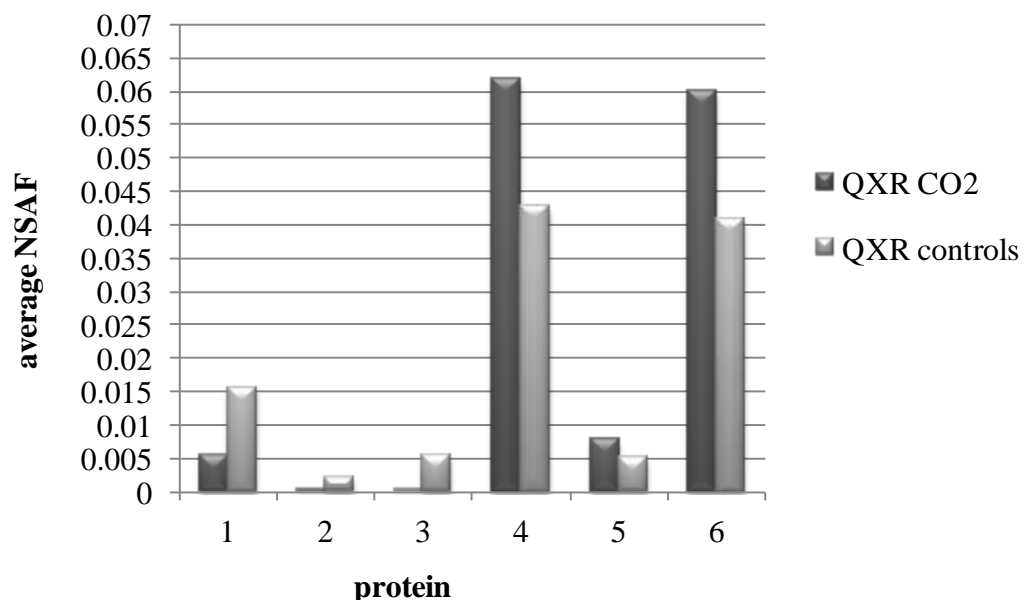


**Figure 6.10** Abundance of statistically significant differentially expressed proteins involved in cytoskeleton and protein polymerization in QXR oysters. Numbers 1 -6 on the horizontal axis refer to names of proteins; (1) Myophilin, (2) Plastin-1 (3) Radial spoke head protein 9-like protein, (4) Actin-2/3, (5) Actin-3, (6) Actin 1 (adductor muscle). Y-axis represents average NSAF value from biological triplicates.

These showed less than 50% similarity with several unique peptides to each, hence these were retained as separate proteins to best represent the cellular status instead of grouping them as a single protein. The other proteins of this category include myophilin, plastin-1 and radial spoke head protein 9-like protein which were all down-regulated in response to CO<sub>2</sub> stress in QXR oysters.

#### **6.3.6.2 Translation**

Differentially expressed proteins in wildtype oysters involved in translation were graphed based on their average NSAF values from triplicates of each protein, as shown in Figure 6.11. Changes in NSAF protein abundance factors revealed that 40S ribosomal protein S16, 40S ribosomal protein S13 and elongation factor 1-alpha were down regulated in WT<sub>CO<sub>2</sub></sub> oysters (Figure 6.11), suggesting that this will impact negatively on protein production at elevated CO<sub>2</sub> conditions. However, 40S ribosomal protein S2 was increased in abundance in CO<sub>2</sub> exposed WT oysters compared to WT<sub>controls</sub>. RPS2 protein was also up-regulated in response to Pb stress in our previous study using Sydney rock oysters [11], and in *C. gigas* in response to environmentally relevant pesticide exposure [451].

Ribosomal proteins are important for translation and protein synthesis and play an active role in streamlining the protein biosynthesis, decoding and processing peptide transfers as well as working outside the ribosomes in some circumstances. The role of these ribosomal proteins as stress adaptive proteins needs further research. Their down-regulation could possibly be to reduce energy expenditure, utilize alternate resources for energy and foods, and prevent newer protein syntheses which are typically energy demanding. Up-regulation of RPS2 may be vital for maintaining the stability and assembly of 40S subunit, and play an essential role in the final maturation of the 40S

ribosome subunits. Under hypercapnia conditions, the Sydney rock oysters could be using the available energy for survival, and using proteins as nitrogen and amino acid sources for sustenance and renewal of damaged proteins.

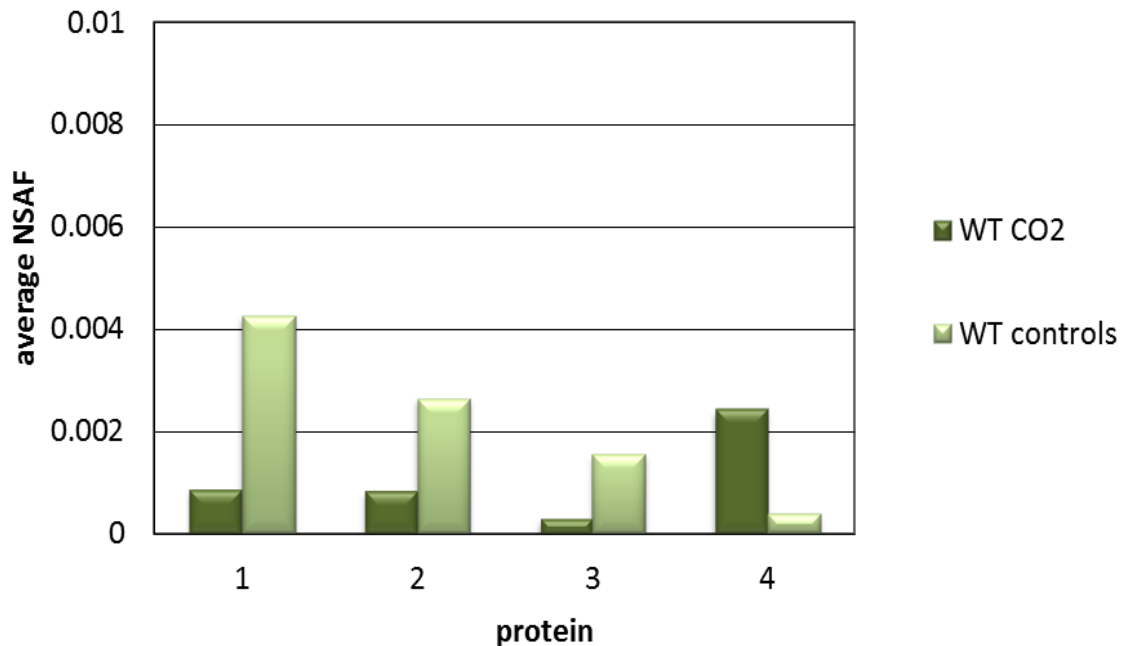


**Figure 6.11** Abundance of statistically significant differentially expressed proteins involved in translation in WT oysters. Numbers 1-4 on the horizontal axis refer to names of proteins; (1) 40S ribosomal protein S16, (2) 40S ribosomal protein S13, (3) Elongation factor 1-alpha (4) 40S ribosomal protein S2. Y-axis represents average NSAF value from biological triplicates.

Differentially expressed proteins involved in translation in QXR oysters exposed to CO<sub>2</sub> were also graphed with their average NSAF protein abundance factors, and changes in NSAF abundance values relative to controls revealed that translation related proteins were down regulated in their protein expressions in response to CO<sub>2</sub> acidification (Figure 6.12). The 40S ribosomal protein S15 gene is known to be associated with tumor

development, colon cancers, and esophageal cancers [452]. All of these ribosomal proteins including ubiquitin were identified in our previous study and were found to be over-expressed in Sydney rock oysters in response to heavy metal stress.

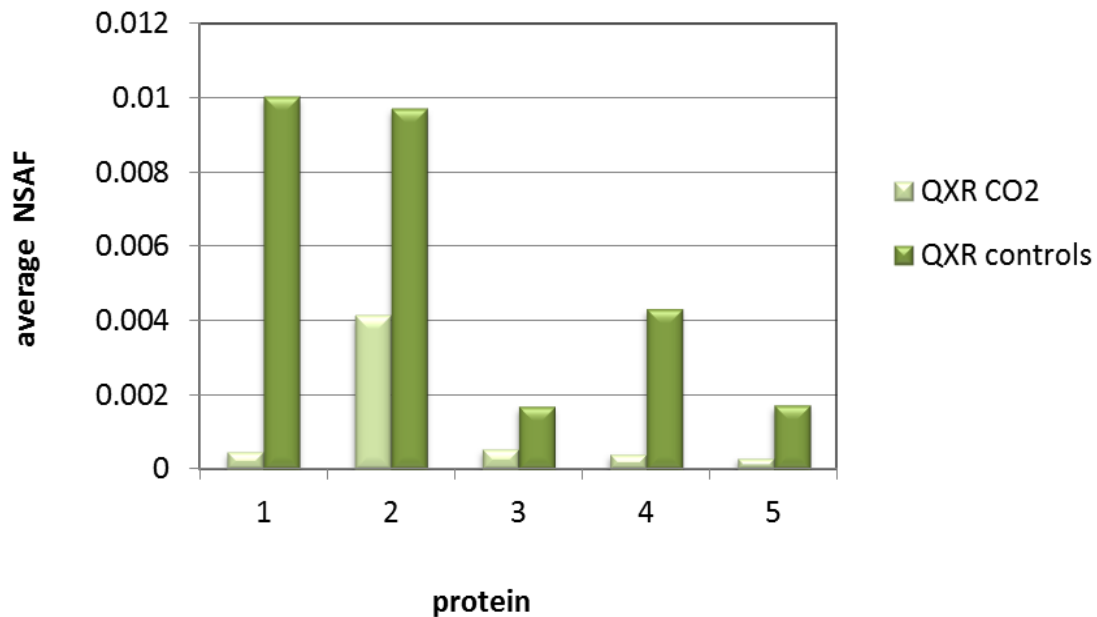


**Figure 6.12** Abundance of statistically significant differentially expressed proteins involved in translation in QXR oysters. Numbers 1 -5 on the horizontal axis refer to names of proteins; (1) Ubiquitin, (2) 60S ribosomal protein L12, (3) 40S ribosomal protein S15, (4) 40S ribosomal protein S19, (5) 40S ribosomal protein S7. Y-axis represents average NSAF value from biological triplicates.

However, the significant down-regulation of these proteins in this experiment suggests a possible future research direction in deciphering their relationship with CO<sub>2</sub> stress.

### 6.3.6.3 Transcription

Differentially expressed proteins in WT oysters involved in transcription were graphed based on their average NSAF values from triplicates of each protein and this revealed that ribonucleoprotein Sm D1 and D3 were down-regulated in WT oysters exposed to CO<sub>2</sub> when compared to WT<sub>controls</sub> (Figure 6.13). Decrease in protein abundance in these two proteins as a consequence of stress response may reflect reduced metabolic activities in pathways involving intronic non-coding RNA in Sydney rock oysters under stress. However, heterogeneous nuclear ribonucleoprotein A2-like protein 1 and heterogeneous nuclear ribonucleoprotein Q were up-regulated by 7.6 fold and 9.4 fold, respectively, in WT<sub>CO2</sub> compared to controls. Cloning studies in pearl oyster, *P. fucata*, revealed that the heterogenous small ribonucleoproteins were present only in the nuclei [453], and hence these were confirmed to be nuclear ribonucleoproteins. These ribonucleoproteins are common core proteins that are present in the spliceosome and are responsible for the splicing of pre-mRNAs. The differential expression of these proteins has not been previously reported in literature in the context of CO<sub>2</sub> stress in marine organisms, hence this is the first such report to the best of our knowledge.

Due to the increased prevalence of such ribonucleoproteins in gill tissues, their differential expression could be useful biomarkers for stress response to hypercapnia in Sydney rock oysters. Further studies on these RNA binding protein biomarkers in gonads and viscera tissues, where they are highly abundant, may provide additional information on their regulation patterns and metabolic responses under stress conditions.

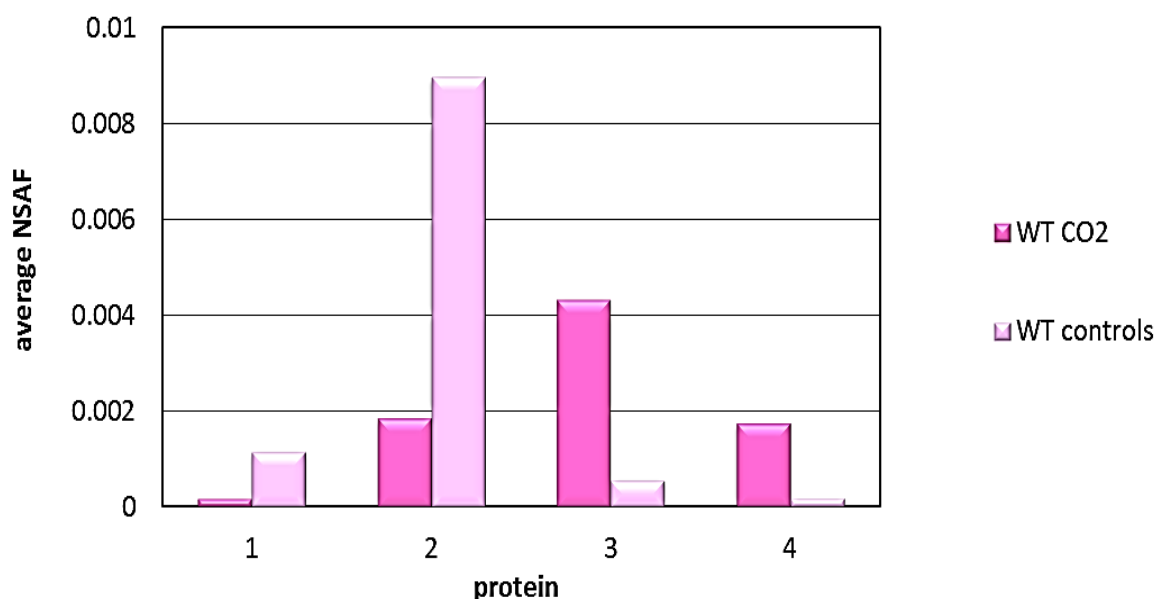


**Figure 6.13** Abundance of statistically significant differentially expressed proteins involved in transcription in WT oysters. Numbers 1-4 on the horizontal axis refer to names of proteins; (1) small nuclear ribonucleoprotein Sm D1, (2) small nuclear ribonucleoprotein Sm D3, (3) heterogeneous nuclear ribonucleoprotein A2-like protein 1, (4) heterogeneous nuclear ribonucleoprotein Q. Legend represents WT<sub>controls</sub>/ WT<sub>CO2</sub> exposed Y-axis represents average NSAF value from biological triplicates.

Differentially expressed proteins in QXR oysters involved in transcription were graphed based on their average NSAF values from triplicates of each protein and this revealed that peptidyl-prolyl cis-trans isomerase E and small nuclear ribonucleoprotein F1 were down regulated in QXR oysters exposed to CO<sub>2</sub> compared to QXR<sub>controls</sub> (Figure 6.14). Although essentially involved in protein folding, peptidyl-prolyl cis-trans isomerase has been recently reported to modulate stress-induced dephosphorylation of Tau, a key regulator of microtubule dynamics [454], and has been suggested to gradually become inactive leading to cardiovascular morbidity under stressful conditions [455]. Therefore, reduced abundance of this protein could be a significant response to hypercapnia in QXR

Sydney rock oysters, and could be a useful bioindicator for preventing oyster mortalities for future tests.

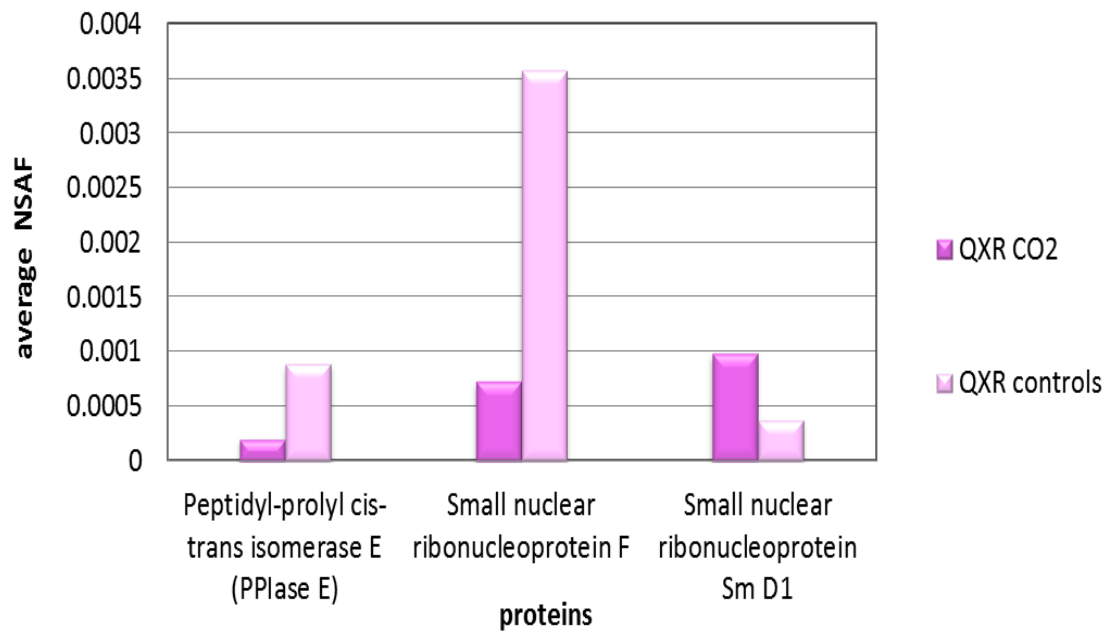


**Figure 6.14** Abundance of statistically significant differentially expressed proteins involved in transcription in QXR oysters. Numbers 1-4 on the horizontal axis refer to names of proteins; (1) Peptidyl-prolyl cis-trans isomerase E, (2) small nuclear ribonucleoprotein F, (3) small nuclear ribonucleoprotein Sm D1. Y-axis represents average NSAF value from biological triplicates.

#### 6.3.6.4 Protein metabolic processes

Nine differentially expressed proteins involved in protein metabolic processes in QXR oysters exposed to CO<sub>2</sub> relative to QXR<sub>controls</sub> were graphed based on the average NSAF values for each protein, as shown in Figure 6.15. Changes in NSAF revealed significant differences in their protein expression, where six of those proteins were down-regulated when QXR oysters were exposed to CO<sub>2</sub>. Up-regulation of proteasome subunit beta type, T-complex protein 1 subunit beta, and ubiquitin indicate the possible need within the cell to recycle unwanted damaged proteins affected by ROS mediated oxidative stress and CO<sub>2</sub> induced stresses, or possibly repair these damaged proteins while adapting to stress conditions.

Many proteins involved in protein folding and sorting were differentially expressed in response to stress (Figure 6.15), namely nexin-12, saccin, peptidyl-prolyl cis-trans isomerase E, peptidyl-prolyl cis-trans isomerase, T-complex protein 1 subunit beta and calcineurin subunit B type. In addition to being involved in protein folding, peptidyl-propyl cis trans isomerase was recently reported as being involved in biomineralisation in a study on sea urchin larvae affected by CO<sub>2</sub> driven ocean acidification [418]. Since correct folding and sorting of proteins is vital not only to maintain their activity but also to enable them to perform the correct function, the differential expression of several proteins involved in protein folding may indicate the possibility of a critical role played in relation to stress. Further research on these proteins may expand our understanding and help in early biomonitoring. Glutamate dehydrogenase is involved in amino acid metabolism and nitrogen metabolism and this could be working in conjunction with the ubiquitin protein degradation system in breaking down unwanted proteins and utilizing amino acids as a

temporary nutrient and energy source. Some of these proteins have also been shown to be differentially expressed in sea urchins in response to CO<sub>2</sub> stress [418].

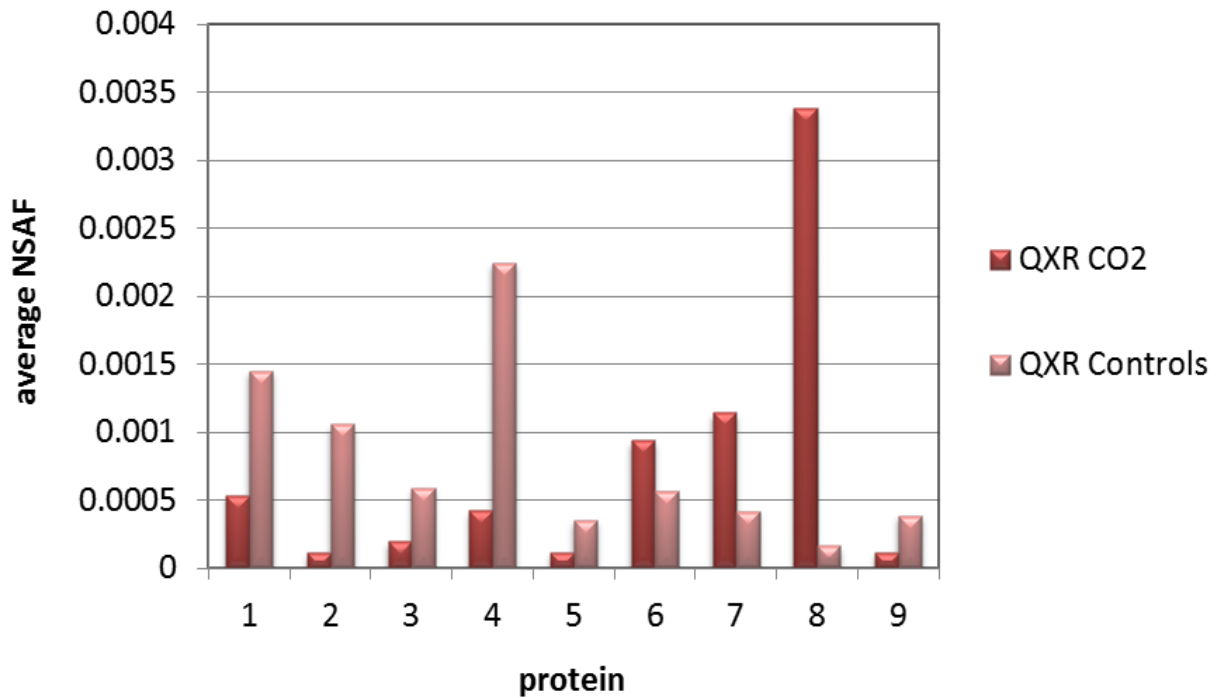


**Figure 6.15** Abundance of statistically significant differentially expressed proteins involved in protein metabolic processes in QXR oysters. Numbers 1 -9 on the horizontal axis refer to names of proteins; (1) sorting nexin-12, (2) saccin (3) calcineurin subunit B type 1, (4) peptidyl-prolyl cis-trans isomerase, (5) SH3 domain-binding glutamic acid-rich protein, (6) proteasome subunit beta type , (7) T-complex protein 1 subunit beta, (8) ubiquitin (9) glutamate dehydrogenase. Y-axis represents average NSAF value from biological triplicates.

## 6.4 Concluding Remarks

Maintenance and sustenance of cytoskeletal integrity, physiological and metabolic activities, in addition to survival, are all huge demands for oysters when individuals are exposed to stress caused by CO<sub>2</sub> acidification. These demands are often energy-expensive and have an elevated metabolic cost. Lowering of pH, imbalance in ionic gradient (H<sup>+</sup>, HCO<sub>3</sub><sup>-</sup>, CO<sub>3</sub><sup>2-</sup>), calcification, and greater dissolution rates of cytoskeletal structures of calcifying organisms are the more high-risk effects of CO<sub>2</sub> acidification. However, more proteomic studies could verify if reproduction events such as gonad production are affected in addition to growth and survival. The down-regulation we observed of proteins in numerous metabolic pathways could be a way for the cells to avoid energy and resource expenditure, restore and defend cell homeostasis and survive by trying to adapt to stressful hypercapnia conditions.

The 56 differentially expressed proteins seen in response to hypercapnia from both breeds, namely wildtypes and QXR Sydney rock oysters, highlight the dynamic metabolic changes deployed to utilise available resources efficiently and reduce wastage. The differential proteins with the highest fold changes that were either up- or down-regulated in response to stresses caused by hypercapnia have the potential to be used as biomarkers indicative of stressful conditions of CO<sub>2</sub> exposure; such biomarkers are often more useful when employed in combination rather than as single proteins. It is also clear that proteins from “housekeeping” genes (previously widely used as internal standards), such as actins and tubulins, undergo considerable modulation in response to CO<sub>2</sub> stress, as seen in this study. Therefore, it may not be advisable to use them as internal protein standards, especially since their differential expression has been previously reported in response to other toxicological agents [181, 11].

The results from this study provide insights into the metabolic behaviour of WT and QXR Sydney rock oysters, among proteins and within biological process categories, under high CO<sub>2</sub> acidification conditions. Further research using proteomic analysis of ocean acidification effects on early stage juveniles and adult oysters, and validation of results using orthogonal proteomic techniques, would be an obvious future direction. Juveniles contain aragonite rich, more sensitive, shell structures, posing a risk of faster dissolution, while adults contain more stable calcite structures which have slower dissolution. Using such an approach, we could obtain a deeper understanding on the effects of CO<sub>2</sub> on oyster populations as a whole, and generate more detailed information regarding the proteomic mechanisms of how and when calcification structures of marine organisms are affected by seawater acidification caused by hypercapnia. It would then be possible to use these significant molecular insights for early monitoring of marine environments for signs of CO<sub>2</sub> acidification, and in the development of mitigating strategies.

### **Supplementary Information**

The following Supplementary Information for this study is available in the enclosed DVD.

**Supplementary Information Table S10** Proteins identified reproducibly in at least one triplicate set of the four treatment groups along with peptide quantitation and gene ontology information for each protein.

**Supplementary Information Table S11** NSAF values of all proteins identified in all four treatment groups.

.

## Notes

The work in this chapter was performed after the release of the oyster genome and has not been published yet.

Supplementary tables, including protein identification and quantitation information, referred to in-text can be found on the DVD attached to this thesis.

Other supplementary data are included in Appendix E as indicated.

This project was also performed in collaboration with a fellow PhD student, Emma Thompson and her supervisor Prof. David Raftos, of the Department of Biological Sciences, Macquarie University, Sydney. Emma was involved in the Oyster exposure experimental design, culturing of oysters and CO<sub>2</sub> exposures. I performed the extraction and purification of proteins and peptides from the haemolymph of these oysters, and all other proteomics experiments including MS/MS analysis using two different label-free experiments. I also performed all of the data interpretation and analysis of the quantitation of peptide data, which led to identifying the relevance of differential expression of several proteins toward metal stress response in Sydney rock oysters, and prepared the manuscript (approximately 95%).

---

## Chapter 7      Conclusions and future directions

---

The work described in this thesis investigated differential metabolic responses of Sydney rock oysters and amphipods upon exposure to high levels of toxicity from heavy metals and hypercapnia, specifically aimed at determining proteomic changes that occurred when animals were subjected to these stressors in seawater conditions which mimic high levels of toxicity in the marine environment.

In order to gain a fundamental understanding, proteomic responses of Sydney rock oysters were initially analyzed after being exposed to a range of metal stresses (Pb, Cu and Zn), using two different quantitative label-free shotgun proteomic techniques. These analyses enhanced our understanding of the nature of metabolic responses that occurred due to different metal stresses in these oysters. We identified over two hundred non-redundant reproducibly identified proteins expressed at one or more metal stress conditions, from both proteomics approaches, and found 56 proteins to be statistically significantly differentially expressed in response to metal stress. In both analyses, many proteins expressed uniquely at different metal stress conditions were identified. The lack of oyster genome sequence at the time of the initial study made this work challenging, and thus our results were of general significance to researchers working with oysters. We successfully solved several problems encountered during the analysis of our spectral counting (SpC) quantitative datasets by (i) construction of an in-house *Bivalvia* database to compensate for the unavailability of a complete oyster genome sequence; (ii) using peptide (rather than protein)  $\log(e)$  filtering to help minimize protein and peptide FDR;

(iii) development of a manual curation strategy for quantitation of SpC data in order to account for shared and unique peptides between proteins from similar species. This was the first study to use shotgun proteomics in oysters (or bivalves), and the first to identify and quantify hundreds of proteins in oysters in a biologically relevant experimental system.

Analysis of metabolic pathways and processes in Sydney rock oysters revealed that translation, cytoskeleton and protein polymerization processes, nucleosome assembly and carbohydrate metabolism were greatly responsive to metal toxicity. Furthermore, our data suggested that in Sydney rock oysters, metal stress has maximum impact on cytoskeletal proteins in the form of oxidative damage. Significant up-regulation of ribosomal proteins was observed, which may be linked to the need to repair and replace damaged muscle proteins in order to maintain cytoskeletal integrity and shell structure at all times.

We believe that heavy metal stress is catastrophic for oysters because they are able to bio-accumulate metals at very high levels, and are very poor at de-contamination. Hence, heavy metal stress affects large numbers of proteins as many of the cellular systems are negatively impacted. It is clear from our results that lead poisoning affects far more proteins than the other metals studied, which is consistent with previously published data from other species. We have no way of verifying whether proteins present in hemolymph are produced by circulating hemocytes, or secreted by other tissues; this is an interesting question, but beyond the scope of this work.

Subsequent validation of the heavy metal stress data was achieved by reanalysing the data using the *Crassostrea gigas* genome sequence, which became publicly available early in 2013, and differential metabolic changes were re-examined. Although many differentially expressed proteins were reconfirmed, some proteins were newly identified to

be metal stress responsive from this analysis. Further, upon reanalysing our Sydney rock oyster shotgun metal stress data using the new oyster genome sequence, we identified four novel metal stress responsive proteins, and provided them with putative initial functional annotations. In addition to using the quantitative label-free shotgun proteomic techniques, iTRAQ analysis was performed to provide validation by an orthogonal technique. While these two approaches complemented each other, the label-free technique (SDS-PAGE coupled with nanoLC-MS/MS) was better at identifying uniquely expressed proteins from a given metal stress condition. Both techniques revealed the importance of metal-induced oxidative damage to oyster muscle tissues and proteins with regard to metal stress tolerance.

The potential biomarkers identified here may be able to act as an early warning system to prevent heavy metal stress from affecting the health and growth of marine biota. Although we have identified these indicative protein signatures, it is acknowledged that complex mixtures of contaminants and conditions in the environment might limit their utility for field biomonitoring. Therefore, further validation and development of these biomarkers as assays is vital before they can be considered for field use.

The study on Zn toxicity in amphipods investigated the metabolic effects of Zn toxicity on female gravid amphipods for four days, as well as changes in metabolic effects between amphipods exposed to Zn with and without silica-300G substrate sediment. Although the fine silica-substrate sediment was non-nutritional, the benthic foraging behaviour of amphipods enabled active ingestion of the sediment particles. Due to this behaviour, almost all of the Zn that was partitioned into the sediment due to adsorption from the seawater column was bioavailable. This increases bioavailability through the gut and gills, especially as Zn is more likely to be fairly loosely bound to sediment ligands

compared to those found in natural sediments. Due to the lack of available genome sequence data for either amphipods or any close relatives, this study was performed using the 2DE-MS/MS approach, where differential protein spots were analyzed using both MALDI-TOF/TOF and LC-MS/MS analyses as a means of maximising protein and peptide identification. A total of 43 differentially expressed proteins were identified in total, of which 31 and 12 proteins corresponded to amphipods exposed to Zn toxicity in the presence and absence of silica-substrate sediment respectively. Moreover, cellular responses included an indirect increase in enzymatic activities related to carbohydrate and lipid metabolic pathways. These responses indicated an increased regulation of various sugar and lipid substrates which may be useful resources for energy production. Under stressful situations amphipods were observed to decrease most physical activities, including fecundity, and modulate cellular processes such as protein synthesis, cytoskeletal elongation, and muscle contraction. Our data are consistent with our hypothesis that during metal stress conditions several key process are primary for amphipod survival, including conservation of energy expenditure, which is directly linked to utilisation of this conserved energy and other resourceful cellular machinery for repair and maintenance of damage caused by oxidative stress from free radicals.

Our analyses also showed that moderate to high toxicity from a mixture of metal stresses may result in a greater change in the proteome, when compared to changes seen with high toxicity from single metals. This observation highlighted the importance of designing metal stress studies appropriately if the results are to have any relevance in field conditions. In the context of metal stress in marine waters, this is especially important with the increase of global ocean acidification from elevated CO<sub>2</sub> (hypercapnia). The occurrence of a multifaceted stressful marine environment, where animals and plants

experience significant metal toxicity in conjunction with hypercapnia, will most likely result in a more threatening situation than either considered separately.

In our study investigating ocean acidification effects from hypercapnia, 56 proteins were differentially expressed in response to stress among wild type and QX disease resistant Sydney rock oysters. The observed differences in protein expression shed light on the metabolic changes directed towards efficient utilisation of available resources, reduction of cellular wastage, defending cell homeostasis, and survival while trying to adapt to stressful hypercapnia conditions. The differential proteins with the highest fold changes, that were either up- or down-regulated in response to hypercapnia in this study, have the potential to be used as biomarkers indicative of stressful conditions of CO<sub>2</sub> exposure. As seen in previous studies these biomarkers would likely be most useful when employed in combination rather than as single proteins.

The studies contained in this thesis add valuable molecular insights into metal stress response in Sydney rock oysters and amphipods, and stress responses toward hypercapnia caused by ocean acidification in Sydney rock oysters. They provide a basis for future work that would broaden our understanding about metal stress and effects of elevated CO<sub>2</sub> and subsequent ocean acidification in marine organisms.

Among multiple studies that can be carried out to further the progress of this research in the future, the following would be some of the most useful future directions:

- A combinational metal toxicity study, including both a time course analysis as well as different toxicity levels, which would enable identification of protein expression patterns in multiple dimensions, as our study was only a snapshot of changes after four days of high levels of metal toxicity stress.

- Investigation of proteomic changes in other organs (in addition to gills and hemolymph) as well as reproductive tissues of oysters, which would help to gain a broader understanding of stress responses amidst complex environmental stresses, with the possibility of correlating differential tissue responses.
- Comparative studies to investigate the proteomic responses of different marine animals of ecological importance, including other types of oysters (such as pearl oysters) and important commercially farmed aquaculture species (such as salmon).
- Changes in low abundance proteins could be investigated in all of the abovementioned studies by analysing proteomes after more complex sample preparation or depletion of known highly abundant proteins.
- Apart from proteomic studies, transcriptomic and metabolomics studies could be undertaken to provide a broader picture of cellular level responses.

In this thesis, we have shown that expressed protein profiles of oysters and amphipods act as excellent indicators of stress responses. Stress-responsive proteins identified in this study are therefore ideal candidates for detailed biochemical characterization and development for use in bioassays useful for marine and agricultural monitoring of the environment. There is obviously a very long way to go before the results here can be used in environmental monitoring with the aim of improving the health of our oceans and ecosystems. However, we believe we have taken the essential first steps along this path.

**Appendix A of this thesis has been removed due to copyright reasons**

## **Appendix B**

**Appendix B1: Quantitation and peptide sequence information of 56 differentially expressed proteins in response to Pb, Cu or Zn metal stress.**

S.no	Identifier, Protein name and Fold change	Spectrum	m+h	Peptide log(e)	Peptide sequences
<b>Elements in response to Cu stress only</b>					
1.	gi 220979902  cell division cycle 42; Cu↑ 5.7	2724.1.r1	1198.5773	-3.1	YVECSALTQK
		2975.1.r2	2317.062	-5.0	IGGEPYTLGLFDTAGQEDYDR
		2740.1.r3	1060.546	-5.7	CVVVGDGAVGK
		2741.1.r3	1313.677	-5.5	TCLLISYTTNK
		2867.1.r3	2332.239	-3.6	TPFLLVGTQVDLRDDATTIEK
2.	gi 40642728  Phosphoglucomutase; Cu↑ 10	1110.1.r1	1106.580	-7.2	LSGTGSSGATIR
		136.1.r2	1883.939	-4.3	KADNFSYTDPVDTALVK
		1033.1.r2	1618.633	-4.4	YDYENCESEPAK
		1059.1.r3	1688.864	-3.9	NAFFVTPSDSLAVLAH
3.	gi 40642990  Ribosomal protein L5; Cu↑5.7	331.1.r1	1338.665	-4.4	GAADGGDLIPHSTK
		482.1.r1	1094.566	-3.3	CYLDVGLVR
		122.1.r2	1586.764	-5.0	NHIFGQHVANYMR
4.	gi 152003987  sarco/endoplasmic reticulum calcium ATPase; Cu↑ 32.4	2835.1.r1	1615.713	-5.6	CFNMIFDVIDTNK
		2834.1.r1	1886.841	-7.3	CFNMIFDVIDTNKDR
5.	gi 34484251  Sodium/potassium ATPase α; Cu↑ 11.2	2830.1.r2	2304.101	-3.2	MAIGIYVGCATVGAAAWFMI
		109.1.r2	1157.580	-4.3	TGDGVNDAPALK
		103.1.r2	1045.552	-6.2	NAESAIEALK
		104.1.r2	1966.946	-13.0	SLPSVETLGCTSIICSDK
		107.1.r2	1468.688	-6.6	TGTLTTNQMSVCR
6.	gi 21388656  Twitchin; Cu↑ 4.5	459.1.r1	1145.5909	-5.8	NALGESNATIR
		264.1.r2	1101.521	-3.7	NPFDTDPAPK
		199.1.r3	2539.292	-3.0	NNAGVGDWAQTSQAIKARAAPVAPK
7.	gi 44885729  Arginine kinase; Cu↓ 2.8	2248.1.r1	1671.849	-6.9	TFLVWLNEEDHLR
		2054.1.r1	1075.556	-8.7	LGGTLADCIR
		2198.1.r1	1853.812	-3.2	NDDKMLGDAGGYNGWPK
		2861.1.r1	1381.621	-3.2	MLGDAGGYNGWPK
		2202.1.r1	1079.548	-19.8	GGDVGEVYKR
		2201.1.r1	923.447	-6.3	GGDVGEVYK
		2203.1.r1	1850.922	-10.0	HGYLTFCPTNLGTTLR
		2207.1.r1	1988.946	-14.1	LGLTEYQAMQEMYNGIK
		2150.1.r2	2896.270	-5.0	YYSLETMTPEENQQLIDHFMFK
		2142.1.r3	1028.501	-4.8	PPVSTDEQR
		182.1.r2	1446.742	-7.1	YFPTQALNFA FK
		4924.1.r3	1045.546	-2.4	CIRSGALNL

**Appendix B1 (continued)**

S.no	Identifier, Protein name and Fold change	Spectrum	m+h	Peptide log(e)	Peptide sequences
8.	gi 40642982  ribosomal protein S25; Cu↑ 18.6	234.1.r1	1100.631	-2.5	LITPSVVSER
		234.1.r1	1100.631	-2.5	DKLNNLILFDK
		416.1.r2	1332.752	-3.2	AAWEPKKPDPKAGAKGGKAPAKKKEG
9.	gi 51315721  Histone H4; Cu↓ 8.7	2848.1.r1	989.578	-3.1	VFLENVIR
		2847.1.r1	1325.754	-3.2	DNIQGITKPAIR
		135.1.r2	1180.621	-3.6	ISGLIYEETR
		2797.1.r3	1310.702	-9.6	TVTAMDVVYALK
10.	gi 146326704  DNA-directed RNA polymerase β; +Control- Cu 6.6 ;+Control-Zn 12.8	341.1.ur1	920.484	-3.6	VADLFEAR
<b>Elements in response to Pb stress only</b>					
11.	gi 229891605  ribosomal protein S2; Pb↑ 1.7	1228.1.r1	1219.643	-2.4	FASATGATPIAGR
		2150.1.r2	3126.5185	-3.0	NRHEATRADAAPAGGRGGFRGGFGSGERGR G
		1200.1.r3	2156.061	-2.6	DPEEAEKEEQTVVEKPAVK
		383.1.r3	1444.828	-2.8	RKPDGVYIINLR
		563.1.r2	1698.860	-4.0	FTPGTFTNQIAAFR
12.	gi 40642988  ribosomal protein S3a; Pb↑ 24	611.1.r1	1517.753	-2.1	NVLTNFHGMDLTR
		68.1.r1	906.487	-3.2	APSMFVVR
		1518.1.r2	1688.858	-7.7	ACQGIYPLHDVFIR
		977.1.r2	1032.514	-2.5	LMAEEVQGR
13.	gi 78172537  NADH dehydrogenase subunit I; Pb↑ 44	489.1.r1	1497.900	-4.2	GLVQAVADGVKLLSK
14.	gi 27363140  ribosomal protein L12; Pb↑ 10.1	2426.1.r1	881.545	-4.3	IGPLGLSPK
		3456.1.r1	1383.748	-13.6	AVGGEVPATSSLAPK
15.	gi 40642996  ribosomal protein L24; Pb↑ 36	3534.1.r1	1219.5664	-4.5	IELCSYSGYK
16.	gi 40642980  ribosomal protein S10; Pb↑ 33.3	3674.1.r1	1679.937	-10.9	DYLHLPAEIVPATLK
		3673.1.r1	2018.976	-10.7	HYYWYLTNEGIIQYLR
		3671.1.r1	1510.838	-3.9	HPEIDVPNLHVIK
17.	gi 40642986  ribosomal protein S11; Pb↑ 81.6	3731.1.r1	1150.567	-6.1	CPFTGNVSIR
		3465.1.r1	1250.645	-5.8	EAMLGTYIDKK
18.	gi 146336951  ribosomal protein S13; Pb↑ 27.9	3720.1.r1	1437.679	-5.8	LTSEDVQEQIMK
		3696.1.r1	968.491	-4.1	DSHGVAQVR
		3505.1.r1	1253.758	-7.7	GLTPSQIGVILR
		3695.1.r1	1381.853	-3.5	KGLTPSQIGVILR
		2638.1.r2	1091.584	-3.8	GISQSALPYR
19.	gi 27363138  ribosomal protein S14; Pb↑ 22.5	3734.1.r1	3019.458	-12.8	EGENVFGVAHIFASFNDTFVHVTDLSGK
20.	gi 82408382  ribosomal protein S15;	3700.1	2049.077	-9.2	NMIIVPEMIGSIIGVYNGK
		3528.1	1277.710	-10.2	EAGPLEKPEVVK

**Appendix B1** (continued)

S.no	Identifier, Protein name and Fold change	Spectrum	m+h	Peptide log(e)	Peptide sequences
	Pb↑ 25.2				
21.	gi 40643042  ribosomal protein S17; Pb↑ 62.8	3627.1.r1 3624.1.r1 3622.1.r1 3621.1.r1 3613.1.r1	2489.315 2718.278 1102.608 1386.766 1244.675	-17.1 -3.4 -3.2 -7.7 -5.8	ALDFGNLQGLQVTQPITAVQGYR DNYVPEISYIDQHDIEVDPDTK VAGFVTHLMK VCEEIAILPSKK LTLDHFHTNKR
22.	gi 40643006  ribosomal protein S19; Pb↑ 36	3726.1.r1 3725.1.r1 3751.1.r1	1236.677 1364.772 1004.544	-3.6 -6.7 -4.5	QMIVDVLHPGK KQMIVDVLHPGK VLQSLEGMK
23.	gi 61619986  ribosomal protein S23; Pb↑ 17.2	3688.1.r1 3687.1.r1	1174.719 1205.675	-7.8 -3.3	VANVSLLALFK KGHAVGDIPGVR
24.	gi 22203724  ribosomal protein S27E; Pb↑ 27.9	3735.1.r1 3510.1.r1	1527.751 1465.765	-10.4 -8.2	LVQSPNSYFMDVK DLLHPSLEEEKR
25.	gi 18565104  Actin ; Pb↓ 2.4	2436.1.r1 2438.1.r1 2437.1.r1 1980.1.r1 1592.1.r1 1593.1.r1 2883.1.r1 1387.1.r1 2460.1.r1 1637.1.r1 1640.1.r1 3087.1.r1 1754.1.r1 2015.1.r1 1748.1.r1 1648.1.r1 1669.1.r1 1691.1.r1 548.1.r1 3832.1.r1 1716.1.r1 1755.1.r1 2233.1.r1 1730.1.r1 2714.1.r1 3601.1.r1 1760.1.r1 3327.1.r1 1644.1.r1 2720.1.r1 1764.1.r1 1719.1.r1	976.448 1794.961 1198.7055 1028.600 881.532 2393.086 1171.571 1198.522 1515.749 1954.064 1854.996 1783.959 3165.658 2712.352 1371.675 998.486 1132.527 2550.174 2682.265 1790.892 2329.149 2216.055 1161.618 2602.337 2273.066 1516.703 1878.857 3169.599 1357.659 3178.399 2212.096 2201.054	-6.3 -4.6 -6.1 -3.5 -3.8 -4.3 -14.5 -10.4 -10.1 -10.1 -8.1 -8.4 -15.5 -5.4 -8.1 -3.4 -7.0 -18.4 -3.5 -13.2 -19.0 -6.2 -5.9 -6.2 -5.8 -28.8 -9.6 -12.1 -8.1 -5.3 -6.8 -10.2	AGFAGDDAPR DDAPRAVFPSIVGRPR AVFPSIVGRPR FPSIVGRPR PSIVGRPR HQGVMVGMGQKDSYVGDEAQS K HQGVMVGMGQK DSYVGDEAQS K IWHHTFYNELR VAPEEHPVLLTEAPLNPK APEEHPVLLTEAPLNPK PEEHPVLLTEAPLNPK TTGIVLDSGDGVTHTVPIYEGYALPHAILR TTGIVLDSGDGVTHTVPIYEGYALPH TTGIVLDSGDGVTH DLTDYLMK GYSFTTTAER LCYVALDFEQEMATAASSSSLEK SYELPDGQVITIGNERFRCPEAM KDLYANTVLSGGSTMYPGIADR SYELPDGQVITIGNER DLYANTVLSGGTTMFPGIADR EITALAPSTMK YSVWIGGSILASLSTFQQMWISK QMWISKQEYDESGPSIVHR QEYDESGPSIVHR GDEDIVALVVDNGSGMCK TTGIVLDSGDGVSHTVPIYEGYALPHAIMR TTGIVLDSGDGVSH CPEAMFQPSFLGMESGSIHETSYSIMK DLYANIVLSGGTTMFPGIADR DLYANTVLSGGSTMYPGIADR

Appendix B1 (continued)					
S.no	Identifier, Protein name and Fold change	Spectrum	m+h	Peptide log(e)	Peptide sequences
		1112.1.r2	1612.885	-6.1	PIYEGYALPHAILR
		1154.1.r2	909.552	-6.0	VIAPPERK
		2657.1.r1	3174.458	-5.1	CPESLFQPSFLGMESAGIHETTYNSIMK
		1154.1.r1	3297.649	-3.3	DLYANTVLSSGGTTMFPGIADRMQKEITALAP
26.	gi 14422379  Calponin-like protein; +Control-Pb 15.8	2619.1.r1	895.445	-3.9	GMTGFGAVR
		1729.1.r2	1410.697	-5.1	QSHGTIGLQSGTNK
27.	gi 73665577  myosin essential light chain; +Control-Pb 55.3	97.1.r1	1011.558	-4.3	HLLSSLGER
		50.1.r2	1251.552	-2.4	MSGTDPEETLR
		272.1.r3	1224.568	-2.1	EAFTMIDQNR
28.	gi 118596568  Cytochrome c oxidase subunit I; Pb↓ 2.4	2433.1.r1	1899.033	-3.9	RVNLAQPAGLYVEVSQL
		2692.1.r2	1261.609	-3.8	KMADIPAGDAEK
		935.1.r3	941.614	-4.1	GVALSLLIR
		1109.1.r1	1891.954	-3.3	SYFSTMTMVIAIPTGIK
		913.1.r1	927.442	-3.3	PGALLGDDQ
		2622.1.r1	1773.909	-3.1	TYFTSATMVIAVPTGAK
		332.1.r2	2577.135	-5.9	IRYETPMLWMMGFIMMFTTG G
		2806.1.r2	2496.259	-3.9	MSYWLLLGPLAMLLMSGLVE GGA
		1433.1.r3	2155.245	-4.0	WLLLLSLPVLAGGLTMLITD
		3112.1.r3	1601.788	-4.0	SMLLFLGSAYVDGGVG
Elements in response to Zinc stress only					
29.	gi 194068375  beta-tubulin; Zn↑ 2.7	516.1.r1	2111.049	-4.4	MREIVHIQAGQCGNQIGAK
		125.1.r1	1822.923	-5.1	EIVHIQAGQCGNQIGAK
		320.1.r1	1328.648	-4.2	INVYYNEATGGK
		517.1.r1	1615.836	-5.0	AILVDLEPGTMDSVR
		1334.1.r1	2798.343	-10.1	SGPFGQIFRPDNFVFGQSGAGNNWAK
		934.1.r1	1964.936	-4.4	RPDNFVFGQSGAGNNWAK
		935.1.r1	1958.982	-8.6	GHYTEGAELVDSVLDVVR
		324.1.r1	1979.990	-3.7	EYPDRIMNTFSVVPSPK
		327.1.r1	1335.698	-5.7	IMNTFSVVPSPK
		1339.1.r1	2708.338	-10.1	LTTPTYGDLNHLVSATMSGVTTCLR
		60.1.r1	1258.690	-7.1	FPGQLNADLRK
		128.1.r1	1130.595	-3.3	FPGQLNADLR
		133.1.r1	1143.634	-6.3	LAVNMVPFPR
		749.1.r1	1636.830	-5.5	LHFFMPGFAPLTSR
		751.1.r1	1691.867	-3.9	ALTVPELTQQMFDAK
		136.1.r1	1065.427	-7.5	NMMAACDPR
		137.1.r1	1071.566	-2.7	YLTVAAMFR
		520.1.r1	1446.689	-2.7	EVDEQMLNVQNK
		752.1.r1	1696.833	-4.8	NSSYFVEWIPNNVK
		141.1.r1	1028.519	-6.5	TAVCDIPPR
		939.1.r1	1843.926	-8.8	MSATFVGNSTAIQELFK
		329.1.r1	1229.598	-3.8	ISEQFTAMFR
		354.1.r2	1808.835	-2.6	PDNFVFGQSGAGNNWAK
		839.1.r2	3312.519	-9.2	EAESDCIQGFQLTHSLGGGTGAGMGTLLIS K
		82.1.r2	1143.634	-3.7	IAVNMVPFPR

**Appendix B1** (continued)

S.no	Identifier, Protein name and Fold change	Spectrum	m+h	Peptide log(e)	Peptide sequences
		363.1.r2	2506.279	-2.6	TAVCDIPPRGLKMSATFVGNSTAI
		189.1.r3	1271.729	-4.8	KIAVNMVPFPR
		1346.1.r1	3116.423	-2.4	FWEVISDEHGIDPTGTYHGSDLQLER
		1347.1.r1	3439.629	-4.1	KEAESCDCQLQGFQLTHSLGGGTGSGMGTLII SK
		550.1.r2	1782.905	-2.7	QLTHSLGGGTGAGMGTLII
		217.1.r3	2031.995	-3.1	GDLNHLVSATMSGVTTCLR
		213.1.r3	1977.974	-3.4	EYPDRIMNTFSVVPSPK
30.	gi 51701479  Histone H2A; Zn↑ 4	250.1.r1	1760.007	-2.3	MSGRGKGGKAKAKAKSR
		1389.1.r1	2871.561	-4.3	VGAGAPVYLAADVLEYLAAEVLELAGNAAR
		1258.1.r1	2301.39	-12.0	LLSGVTIAQGGVLPNIQAVLLPK
		660.1.r2	944.531	-2.7	AGLQFPVGR
		34.1.r2	850.526	-3.7	HLQLAIR
		120.1.r2	1092.678	-3.6	PNIQAVLLPK
31.	gi 207008800  Histone H2B; Zn↑ 15.1	799.1.r1	1773.830	-9.1	AMSIMNSFVNDIFER
		228.1.r2	1305.684	-2.8	RESYAIYIK
32.	gi 116008297  mitochondrial H+ ATPase α; Zn↑ 5.4	369.1.r1	1330.740	-2.3	ISVKEPMQTGIK
		370.1.r1	2002.939	-2.1	MNDDNGGSLTALPVIETQA
		563.1.r1	1424.833	-2.3	GVRPAINVGLSVSR
		793.1.r3	1982.019	-2.1	HTAGASAEVSSILEERILG
		794.1.r3	1000.579	-2.1	VLSIGDGIAR
		124.1.r3	1197.647	-7.9	VVDALGNPIDGK
		984.1.r3	2408.184	-11.1	EVAFAAQFGSDLDQATQNLNR
		570.1.r1	1553.738	-2.2	EAYPGDVLYLHRS
33.	gi 58219310  Tubulin; Zn↑ 2.6	1215.1	2007.893	-14.9	TIGGGDDSFNTFFSETGAGK
		754.r1	1687.890	-8.4	AVFVDLEPTVVDEVR
		756.r1	2418.160	-3.5	QLFHPEQLITGKEDAANNYAR
		331.r1	1393.747	-8.0	QLFHPEQLITGK
		207.r1	1071.604	-2.4	EIVDLVLDR
		459.r1	1457.869	-11.8	LIGQIVSSITASLR
		757.r1	1784.995	-3.8	IHFPLVTYAPVISAER
		1362.r1	2750.291	-6.6	AYHEQLSVAEITNACFEPANQMVK
		333.r1	1267.509	-4.5	YMACCMLYR
		208.r1	1015.578	-5.1	DVNAAIATIK
		467.r1	1598.767	-8.3	TIQFVDWCPTGFK
		949.r1	1864.904	-5.7	AVCMLSNTTAIAEAWAR
		337.r1	1380.698	-2.2	LDHKFDLMYAK
		1217.r	3533.720	-6.7	KLADQCTGLQGFLIFHSFGGGTSGFTSLLM R
		1220.2.r1	2409.209	-9.7	FDGALNVDLTFEQTNLVPYPR
		467.1.r1	1598.76	-8.3	TIQFVDWCPTGFK
		947.1.r1	1824.98	-2.7	VGINYQPPTVVPGGDLAK
		772.1.r1	2638.439	-4.3	NLVPYPRIHFPLATYAPVISAER
		774.1.r2	3405.625	-12.0	LADQCTGLQGFLIFHSFGGGTSGFTSLLME R
		5.1.r3	887.433	-2.5	FDLMYAK
		1058.1.r3	2786.244	-3.9	ECMACCMLYRGDVVPKDVNAAIAT
		128.1.r3	1015.578	-4.5	DVNAAIATIK

**Appendix B1** (continued)

S.no	Identifier, Protein name and Fold change	Spectrum	m+h	Peptide log(e)	Peptide sequences
		584.1.r3	2397.275	-2.3	ATIKTKRTIQ FVDWCPTGFK
34.	gi 148717307  Calreticulin; Zn↑ 26	1448.1.r1	1490.669	-7.9	HEQNIDCGGGYIK
		1449.1.r1	1147.662	-3.7	KVHVIFNYK
		1450.1.r1	1725.848	-11.5	YDDIGAVGFDLWQVK
		2756.1.r3	1019.567	-3.6	VHVIFNYK
		1433.1.r3	1666.817	-11.0	SGTIFDNILVTDDEK
35.	gi 46909221  fructose-bisphosphate aldolase; Zn↑ 3.2	2167.1.r1	1298.69	-4.5	VTEQVLAFTYK
		2002.1.r1	3464.829	-5.9	FAKWRCVLKIQKETPSYQAMLENANVLAR
		2159.1.r1	3438.627	-8.0	YASICQQNGLVPIVEPEVLPDGEHDLDTAEK
		2289.1.r2	952.499	-4.0	ELLFTSDK
36.	gi 46391574  G protein β; Zn↑ 2.6	2143.1.r1	1336.610	-7.8	IYAMHWASDSR
		2146.1.r1	1213.552	-8.6	TFVSGACDASAK
		2433.1.r2	1802.913	-9.0	SSELEALRQETEQLK
		2302.1.r3	1309.679	-3.5	LIVWDGYTTNK
37.	gi 115501910  Receptor of Activated Kinase C 1; Zn↑ 8.9	2300.1.r1	860.451	-3.3	IWDLEGK
		2302.1.r1	1047.540	-4.7	VWQVSMAAR
		2457.1.r2	1090.571	-5.0	LWNTLGVCK
		2475.1.r3	1366.682	-6.8	YWLCAATGPSIK
38.	gi 33337635  Rho-GDI related protein ; Zn↑ 9.2	2791.1.r1	1105.662	-3.4	LKEQVFTIK
		2881.1.r2	872.520	-4.3	LSLVVEGR
		2882.1.r2	1090.563	-4.7	ELDLTGDLK
39.	gi 22758856  ribosomal protein L19; Zn↑ 37.2	2688.1.r1	2912.468	-9.5	VLKCGKNKVWLDPNETNEIANANSR
		2688.1.r1	1942.925	-16.1	VWLDPNETNEIANANSR
		2403.1.r1	1233.608	-6.1	HLYHELYMK
40.	gi 22758866  ribosomal protein L23a; Zn↑ 28.2	2558.1.r1	1064.599	-5.4	LESGNFAWGSEAITR
		2562.1.r1	1227.669	-7.3	SCIVQIDATPFR
		2901.1.r2	1404.701	-3.4	LAEKEEAVLK CDGYILEGK
41.	gi 40643000  ribosomal protein S8; Zn↑ 37.2	2675.1.r1	1653.787	-8.9	LESGNFAWGSEAITR
		2676.1.r1	1406.710	-9.0	SCIVQIDATPFR
		2406.1.r1	1129.646	-7.2	LAEKEEAVLK
		2590.1.r1	1054.487	-3.9	CDGYILEGK
42.	gi 46909451  triosephosphate isomerase; Zn↑ 6.9	2410.1.r1	1581.794	-3.5	EKGFTGDISANMIK
		2411.1.r1	1435.706	-17.3	NVFGESDQLIGEK
		2578.1.r2	1591.807	-8.8	RNVFGESDQLIGEK
		2448.1.r3	1670.796	-4.9	DIGCEWVILGHSE
		2599.1.r3	1321.663	-3.2	VFGESDQLIGEK
		1571.1.r1	1957.570	-3.6	DDDDDDDDDDASADEADE
43.	gi 5817598  Myosin heavy chain; Zn↓ 4.5	1405.1.r1	2728.397	-2.4	STQENVEDLERVKRELEENVRR
		1015.1.r1	2732.422	-2.8	QQLEDLQAQLSKREEEVQHALLK
		215.1.r2	1370.696	-4.0	NLYSTHPHFVR
		217.1.r2	1911.931	-2.5	DLEEASLQHEAQISALR

Appendix B1 (continued)					
S.no	Identifier, Protein name and Fold change	Spectrum	m+h	Peptide log(e)	Peptide sequences
		309.1.r2	2334.122	-3.7	LEDMANMTYLNEASVLHNL
		244.1.r2	1223.638	-2.9	AGVLAHLEEEER
		1111.1.r3	2809.411	-2.3	SSVSVQRSSVSASNPGMLSTANLVGR
		412.1.r3	1467.773	-3.9	SVSFIGLLDIAGFE
		1314.1.r1	3503.676	-5.0	QSMNPPKFEKLEDMANMTYLNEASVLHNL
		988.1.r1	2755.307	-2.5	FEKLEDMANM TYLNEASVLHNL
		536.1.r1	1435.768	-10.9	IAGADIETYLLEK
		396.1.r1	1303.675	-11.0	SSAFQTISAVHR
		1479.1.r1	1572.812	-3.4	ELEEQNVTLLEQK
		258.1.r1	1000.579	-3.3	AQLEIATVR
		1318.1.r1	2058.036	-5.5	KLEQDINELEVALDASNR
		1335.1.r1	2230.135	-14.3	GSLEDQIIQANPVLEAYGNAK
		396.1.r1	1303.675	-11.0	SSAFQTISAVHR
		536.1.r1	1435.768	-10.9	IAGADIETYLLEK
		982.1.r1	942.468	-5.3	GYSaelFR
		985.1.r1	1899.084	-3.1	MRKTLEITIKELHVR
		562.1.r2	2496.202	-6.3	LQQFFNHFFVLEQEEYKK
		964.1.r2	2185.146	-12.3	KKLEQDINEL EVALDASNR
		354.1.r2	1463.705	-2.3	ALDSMQASLE AEAk
		125.1.r3	1084.659	-4.2	RLQQLSAIR
		921.1.r3	3231.656	-2.2	ESLNKLMKNLYSTHPSFVRCIIPNELK
		325.1.r3	1500.842	-6.9	VLLALQLDPAEYR
		327.1.r3	1616.813	-5.2	LDEAGGATSAQIELNK
Elements in response to both Copper and Zinc stress					
44.	gi 22758854  ribosomal protein L11; Cu↑ 41.4 ; Zn↑ 10.2	502.1.cr1	1573.858	-5.0	VLEQLTGQQPVFSK
		371.1.cr3	1492.68	-2.5	LCLNICVGESGDR
		2808.1.zr1	975.551	-6.6	YDGILPGK
		3095.1.zr2	937.489	-4.5	PGFNIA YR
45.	gi 32169292  ribosomal protein L7; Cu↑ 30 ; Zn↑ 102.9	220.1.cr1	1216.632	-4.1	NFGIGQDIQPK
		727.1.cr2	2570.406	-2.4	KRPRNFGIGQDIQPKRDLSR F
		581.1.cr3	1648.873	-5.6	IAEPFITWGYPNLK
		375.1.zr1	1256.646	-8.0	YAANFLWPFK
46.	gi 28475277  glyceraldehyde 3- phosphate dehydrogenase; Cu↑ 3.1; Zn↑ 2.3	823.1.cr1	1819.904	-7.5	IVSNASCTTNCLAPLAK
		359.1.r1	1385.738	-6.1	GAAQNIIPSTGAAK
		470.1.cr1	2332.215	-5.0	LTGMAFRVPVPDVSVDLTCR
		472.1.cr1	1555.815	-10.2	VPVPDVSVDLTCR
		830.1.cr1	1813.860	-9.8	GILGYTEDDVVSQDFR
		203.1.cr1	1161.626	-6.6	AGIALNDNFVK
		553.1.cr1	1455.780	-2.1	QNIIPSTGAAKAVG
		368.1.cr2	2067.058	-3.0	FGIVEGLMTTVHAYTATQK
		1023.1.cr2	4306.229	-2.5	TVHATTATQKTVDGPSNKDWRGGRGAAQ- NIIPSTGAAK
		239.1.ur1	1027.521	-2.9	DPANIPWSK
		1328.1.ur1	2194.198	-2.3	KRSSIFDAKAGIALNDNFVK
		2222.1.zr3	1537.772	-10.5	FGIVEGLMTTVHAY

**Appendix B1** (continued)

S.no	Identifier, Protein name and Fold change	Spectrum	m+h	Peptide log(e)	Peptide sequences
47.	gi 18073531  heat shock protein 70; Cu↑ 2.9 ; Zn↑ 2.8	515.1.cr1	1509.838	-4.9	DKIHDIVLVGSTR
		479.1.cr1	1487.701	-7.2	TTPSYVAFTDTER
		694.1.cr1	1663.8108	-6.3	NQVAMNPTNTIFDAK
		352.1.cr1	1292.646	-3.1	MVNHFIQEFK
		353.1.cr1	1372.714	-4.4	ELEGVCNPIITK
		354.1.cr1	2015.870	-2.2	GAPGGGMPGGMPNFGGGDKGGGAP
		479.1.cr1	1487.701	-7.2	TTPSYVAFTDTER
		873.1.cr1	2949.318	-2.4	CNPIVTKLYQGAGGAPGGMPGGMPGGMPG GM
		482.1.cr1	2222.857	-2.7	MPGGMPGGMPGGMPGGADGASTGGGGG
		487.1.cr2	1465.812	-4.0	AQIHDIIVLVGGSTR
		884.1.cr2	2842.495	-2.1	ETAAYLGKTVTNAVVTVPAILNDSQR
		491.1.cr2	2208.893	-2.9	YQGAGGAGGMPGGMPGGMPGGMPGGA
		490.1.cr2	2342.010	-2.3	GGAPGGMPNFGGAAPGGGSEGGSSGGPT
		700.1.cr2	1645.880	-6.2	IVNEPTAAALAYGLDK
		303.1.cr3	1303.599	-6.0	NSLESYAFNMK
		149.1.cr3	1215.669	-3.1	DAGTISGLNVLR
		289.1.cr3	2125.856	-3.0	QGAGGAPGGMPGGMPGGMPGGMPGGA
		150.1.cr3	1720.690	-2.6	MPGGMPGGADSQSTGGSGGP
		568.1.cr3	1667.854	-3.7	HWPFDVVNVEGKPK
		237.1.ur1	1215.669	-5.0	DAGTISGLNVLR
		1461.1.ur1	4192.326	-2.8	VQDLLLLDVTPLSLGIETAGGVMTNLIKRN TIPTKQTQ
		1065.1.ur2	3178.425	-3.4	VCNPIVTKLYQGAGGAGGMPGGMPGGMPG GMPGG
		1007.1.ur2	2009.009	-3.0	TINNAVVTVPAYFNDSQR
		1056.1.ur2	4352.368	-2.3	MVNHVFVQEFK RKHKKDISDNKRAVRRRLRTACERAK
		786.1.zr1	1707.720	-4.4	STSGDTHLGGEDFDNR
		304.1.zr2	2381.057	-3.3	GGAGAPGGMPNFGGAAPGGAPDAGTGGPT
		889.1.zr1	1228.628	-8.1	VEIANDQGNR
		1061.1.zr1	1480.754	-6.5	ARFEELNADLFR
		1065.1.zr1	2260.146	-18.2	SINPDEAVAYGAAYQAAILSGDK
		902.1.zr1	2169.046	-17.6	TTYSDNQPGVLIQVYEGER
		1383.1.zr2	2774.327	-5.2	QTQTFTTYSDNQPGVLIQVYEGER
		1106.1.ur1	1691.726	-5.3	STAGDTHLGGEDFDNR
		753.1.ur2	1628.868	-6.5	QKELEGVCNPIITK
		793.1.ur3	1240.624	-10.1	MKETAEAYLGK
		932.1.ur3	1313.674	-9.4	NQLESYVFSVK
		805.1.ur3	975.511	-5.0	LSKDEIDR
48.	gi 73427346  mantle gene 2; Cu↑ 3.7; Zn↑ 2	498.1.cr1	1444.758	-11.7	AGQNIIGLQMGTNK
		993.1.cr1	2171.966	-3.0	TGEPVNTCGDPENFHEQLK
49.	gi 50512854  Glycogen phosphorylase; Zn↑ 3.5 ; +Control-Cu 24.5	1331.1.cr1	2350.157	-7.2	LAACFLDSMATLGLAAYGYGIR
		1333.1.cr1	2021.143	-7.7	LKQEYFLVAATLQDILR
		963.1.cr1	1861.944	-2.3	TFAYTNHTVLPEALER
		964.1.cr1	1998.084	-3.7	RWLLCNPGLSDIIAEK
		965.1.cr1	1841.983	-2.4	WLLCNPGLSDIIAEK
		572.1.cr2	893.415	-2.5	YGNPWEK

Appendix B1 (continued)					
S.no	Identifier, Protein name and Fold change	Spectrum	m+h	Peptide log(e)	Peptide sequences
		1000.1.zr1	1301.710	-6.2	GIAPVENVVEFK
		1001.1.zr1	1900.871	-5.8	IEDGWQVEEPDEWLR
		1004.1.zr1	1352.637	-6.4	IGEEWVTDLYQ
		782.1.zr1	1126.516	-5.2	FADDENFLR
		646.1.zr1	1263.535	-4.4	EFYEMYPER
		437.1.ur1	2462.208	-7.2	IIPAADLSEQISTAGTEASGTGNMK
50.	gi 113207854  phosphoenolpyruvate carboxykinase; Cu↓ 2.6 ; Zn↓ 1.7	1102.1.cr1	1043.555	-6.3	SMGPIGGPLSK
		1107.1.cr1	1188.549	-6.2	SESTAAAEHTGK
		1223.1.cr1	1393.606	-3.6	IMHDPMAMRPF
		850.1.cr1	1910.975	-12.5	TMYVIPFSMGPIGGPLSK
		851.1.cr2	1086.428	-3.5	CVHSMGCPR
		853.1.cr2	2118.983	-3.5	DEGWLAEHMLIMGLTNEK
		855.1.cr2	1973.928	-4.3	FVCAAFPSACGKTNLAMI
		855.1.cr2	1314.597	-14.2	FVCAAFPSACGK
		857.1.cr2	1321.643	-4.6	IGMPGNAAHPNSR
		859.1.cr2	1078.510	-5.1	IGMPGNAAHPN
		1011.1.cr3	1041.566	-3.4	IMIGHFPAR
		1014.1.cr3	1109.559	-5.1	GSGYGGNSLLGK
		43.1.ur1	801.462	-2.6	GILGQWK
Elements in response to all Copper, Lead and Zinc					
51.	gi 86156234  ATP synthase beta subunit Cu↑ 16.3 ; Pb↑ 19 ; Zn↑ 23.2	374.1.cr1	1262.641	-6.7	TIAMDGTEGLVR
		477.1.cr1	1617.805	-5.9	VSLVYGQMNEPPGAR
		478.1.cr1	1435.754	-7.5	FTQAGSEVSALLGR
		436.1.cr2	1367.753	-2.3	IINVIGEPIDER
		70.1.cr2	975.562	-2.7	IGLFGGAGVGK
		528.1.pr1	1457.840	-7.4	TVLIMELINNVAK
		529.1.pr1	1406.681	-9.4	AHGGYSVFAGVGER
		1296.1.pr1	1439.789	-3.2	VALTGLTVAEYFR
		2034.1.pr2		-3.4	GSITSVQAIYVPADDLTDP PATTF AHL DATTVLSR
		1728.1.pr2	1987.013	-3.9	GIAELGIYPAVDPLDSNSR
		354.1.zr1	1352.615	-2.4	ESCLDTGYPIR
		510.1.zr2	1626.994	-2.7	SKWLITGVGGIKGLVV
		333.1.zr3	2386.250	-2.4	DATTVLSRGIAELGIYPAVDPLD
52.	gi 46359618  78kDa glucose regulated protein; Cu↑ 32.8 ; Pb↑ 40.6; Zn↑ 2.1	512.1.cr1	1583.770	-4.1	ITPSYVAFTADNER
		410.1.cr2	1217.631	-4.2	DAGTIAGLNVMR
		572.1.cr3	1719.855	-12.4	NQLTSNPENTIFDVK
		976.1.pr1	963.515	-3.9	EIAEGFLGK
		273.1.pr1	1183.647	-3.2	FDLTGIPPAPR
		2021.1.pr2	2034.077	-5.4	KINNAVITVPAYFNDAQR
		2166.1.pr2	2683.457	-2.3	DNHLLGKFDLTGIPPAPRGVPQIEV
		571.1.pr3	1234.665	-2.1	AMVLGKMREIA
		688.1.pr3	1787.990	-7.8	IINEPTAAAIA YGLDKK

Appendix B1 (continued)					
S.no	Identifier, Protein name and Fold change	Spectrum	m+h	Peptide log(e)	Peptide sequences
		687.1.pr3	1659.895	-5.1	IINEPTAAAIAYGLDK
		1204.1.pr3	3826.859	-2.7	KELEEIVQPIMTKLYQGAGGAPPPSGEEGAD EKDEL
		889.1.zr1	1228.628	-8.1	VEIANDQGNR
		968.1.zr1	2287.036	-12.1	LYQGAGGAPPPSGEEGADEKDEL
		752.1.zr3	2100.997	-11.0	IEIESLFDGEDFSETLTR
53.	gi 229485193	370.1.cr1	1261.682	-10.7	VIDSLQLTMNK
	Peroxiredoxin 6	509.1.cr1	1539.853	-4.4	VFPQGVTVQPVPSGK
	Cu↑ 19.3 ; Pb↑ 7.4;Zn↑ 15.1	1210.1.pr1	1209.630	-2.9	LSMLYPATTGR
		1721.1.pr2	1931.863	-8.0	MIALSCDDVPSHEGWSK
		1966.1.pr2	3085.577	-4.3	DKSRDLAVKLGMDPAEKDNAGLPLTCR
		1968.1.pr2	2057.015	-11.9	LGMVDPAEKDNAGLPLTCR
		379.1.zr3	1450.809	-3.2	LKLSMLYPATTGR
		145.1.zr3	1087.651	-3.2	AVFIIGPDKK
		973.1.zr3	3399.545	-3.3	FHDFVGDSWCILFHPADYTPVTTELGK
54.	gi 219806594	2034.1.cr1	1447.764	-6.2	LQTATEKLEE ASK
	Tropomyosin	952.1.cr1	1387.681	-11.2	VLENLNNASE ER
	Cu↓ 4.1; Pb↓100.9 ; Zn↓ 6.7	1737.1.cr1	1721.870	-5.4	LIAEEADKKY DEAARSLEISEQEASQR
		1738.1.cr1	1376.665	-9.6	SLEISEQEASQR
		2038.1.cr1	1742.812	-4.0	AISDELDQTFAGELAGY
		2237.1.cr1	1114.585	-4.3	AEQLEQQLR
		1955.1.cr2	1843.940	-7.6	EVDRLEDELLAEKER
		1775.1.pr2	1189.631	-3.4	IEEDLTTLQK
		2293.1.zr2	1286.731	-4.8	KLAITEVDLER
		1994.1.zr3	1431.726	-5.1	RIQLLEEDMER
		1997.1.zr3	1291.620	-3.8	IQLLEEDMER
		1528.1.ur2	2510.175	-10.3	TLQVQNDQASQREDSYEETIR
		2781.1.ur2	1388.763	-9.5	AKIEEDLTTLQK
		39.1.ur3	2499.148	-14.2	SLEISEQEASQREDSYEETIR
Elements in response to both Lead and Zinc					
55.	gi 40643024	3629.1.pr1	1160.704	-6.6	NLFVIAVSGIK
	ribosomal protein L17A; Pb↑ 44 ; Zn↑ 26	3849.1.pr1	1465.718	-19.5	MPAAGAGDMFVATVK
		3850.1.pr1	2013.992	-4.1	NGVFIYFEDNAGVIVNNK
		3633.1.pr1	900.515	-10.4	GSAITGPVAK
		3678.1.pr1	1984.053	-20.1	ISLALPVGAVINCADNTGAK
		2873.1.zr2	833.436	-3.2	IASNASSIA
56.	gi 164510092	3690.1.pr1	1787.927	-12.5	TITLEVEPSDTIENVK
	Ubiquitin; Pb↑ 12.3 ; Zn↑ 33.7	106.1.pr1	1081.552	-3.4	TLSDYNIQK
		3693.1.pr1	1067.621	-3.5	ESTLHLVLR
		2548.1.zr1	1523.781	-7.1	IQDKEGIPPDQQR

**Appendix B2: List of all 451 distinct proteins that were identified in the heavy metal stress study on Sydney rock oysters, prior to the release of the Oyster genome.**

These proteins were identified in atleast one replicate list among the four treatments using SDS-PAGE and/or GPF proteomic approaches. These protein identifications were results from matching mass spectra to the protein sequences of species within the ‘Bivalvia’ class. *Candidatus Vesicomysocius okutanii* is a gammaproteobacteria and is an endosymbiont harbored in many bivalves including oysters. Protein identifications that matched *Candidatus Vesicomysocius* sp. have also been included in this list.

Identifier	Protein name	Species	UniProt ID
gi 110559485	galectin	<i>Crassostrea virginica</i>	ABG75998
gi 112144576	elongation factor-1 alpha	<i>Crassostrea</i> sp. THS-2006	ABI13286
gi 113207852	glucose-6-phosphate 1-dehydrogenase	<i>Crassostrea gigas</i>	CAJ28912
gi 113207854	phosphoenolpyruvate carboxykinase	<i>Crassostrea gigas</i>	CAJ28913
gi 113207856	pyruvate kinase	<i>Crassostrea gigas</i>	CAJ28914
gi 113431892	APS reductase	<i>Lucinoma</i> aff. kazani	CAJ85653
gi 113927399	alanopine dehydrogenase 1	<i>Crassostrea gigas</i>	CAH18004
gi 115501910	Receptor of Activated Kinase C 1	<i>Mya arenaria</i>	CAL48986
gi 116008297	mitochondrial H <sup>+</sup> ATPase a subunit	<i>Pinctada fucata</i>	ABJ51956
gi 116171	G2/mitotic-specific cyclin-A	<i>Spisula solidissima</i>	P04962
gi 116180	G2/mitotic-specific cyclin-B	<i>Spisula solidissima</i>	P13952
gi 118151639	major vault protein	<i>Mytilus galloprovincialis</i>	ABK63640
gi 118596568	cytochrome c oxidase subunit I	<i>Pinctada maxima</i>	BAF37943
gi 119852227	tyrosinase-like protein	<i>Pinctada fucata</i>	BAF42771
gi 119874551	vacuolar ATP synthase subunit B	<i>Mytilus edulis</i>	ABM05752
gi 121200	Globin I	<i>Calyptogeno soyoe</i>	P14805
gi 121308649	hypothetical protein	<i>Pinctada fucata</i>	BAF43717
gi 121582241	non muscle myosin	<i>Mizuhopecten yessoensis</i>	BAF44480
gi 122056400	putative neurotrypsin precursor	<i>Mytilus galloprovincialis</i>	ABM66067
gi 122056406	membrane selenoprotein P	<i>Mytilus galloprovincialis</i>	ABM66070
gi 122063213	Calmodulin	<i>Patinopecten</i> sp	P02595
gi 124055243	polyprotein	<i>Mizuhopecten yessoensis</i>	ABM90393
gi 124265190	nucleoside diphosphate kinase	<i>Chlamys farreri</i>	ABM98102

**Appendix B2** (continued)

Identifier	Protein name	Species	UniProt ID
gi 124298385	cytochrome oxidase subunit II	<i>Lemiox rimosus</i>	ABN04293
gi 13309811	mucoperlin mucin-like nacre protein	<i>Pinna nobilis</i>	AAK18045
gi 13383378	perlin precursor	<i>Perna canaliculus</i>	AAK20952
gi 134317	Sarcoplasmic calcium-binding protein	<i>Mizuhopecten yessoensis</i>	P02637
gi 142886017	shematin-8	<i>Pinctada margaritifera</i>	ABO92760
gi 14422379	calponin-like protein	<i>Mytilus galloprovincialis</i>	BAB60813
gi 144227414	interleukin 17	<i>Crassostrea gigas</i>	ABO93467
gi 144952800	RNA-binding protein	<i>Pinctada fucata</i>	ABP04054
gi 144952812	thioester-containing protein	<i>Chlamys farreri</i>	ABP04060
gi 145308426	KRMP-10	<i>Pinctada margaritifera</i>	ABP57448
gi 146325997	chromosomal replication initiator protein DnaA	<i>C. Vesicomysocius</i>	BAF61140
gi 146326000	phosphoribulokinase	<i>C. Vesicomysocius</i>	BAF61143
gi 146326001	leucyl-tRNA synthetase	<i>C. Vesicomysocius</i>	BAF61144
gi 146326003	dethiobiotin synthase	<i>C. Vesicomysocius</i>	BAF61146
gi 146326010	preprotein translocase SecA subunit	<i>C. Vesicomysocius</i>	BAF61153
gi 146326012	bifunctional riboflavin biosynthesis protein RibF	<i>C. Vesicomysocius</i>	BAF61155
gi 146326013	homoserine O-succinyltransferase	<i>C. Vesicomysocius</i>	BAF61156
gi 146326015	aminotransferase	<i>C. Vesicomysocius</i>	BAF61158
gi 146326021	1-deoxy-D-xylulose 5-phosphate reductoisomerase	<i>C. Vesicomysocius</i>	BAF61164
gi 146326042	cell division protein FtsK	<i>C. Vesicomysocius</i>	BAF61185
gi 146326053	translation initiation factor IF-2	<i>C. Vesicomysocius</i>	BAF61196
gi 146326058	methyltransferase	<i>C. Vesicomysocius</i>	BAF61201
gi 146326065	3-phosphoglycerate kinase	<i>C. Vesicomysocius</i>	BAF61208
gi 146326066	pyruvate kinase	<i>C. Vesicomysocius</i>	BAF61209
gi 146326067	fructose-bisphosphate aldolase, class II	<i>C. Vesicomysocius</i>	BAF61210
gi 146326068	glucose inhibited division protein A GidA	<i>C. Vesicomysocius</i>	BAF61211
gi 146326071	ribosomal large subunit pseudouridine synthase C	<i>C. Vesicomysocius</i>	BAF61214
gi 146326077	DNA polymerase I	<i>C. Vesicomysocius</i>	BAF61220
gi 146326079	ATP-dependent DNA helicase	<i>C. Vesicomysocius</i>	BAF61222
gi 146326083	adenylsulfate reductase	<i>C. Vesicomysocius</i>	BAF61226
gi 146326089	H <sup>+</sup> translocating pyrophosphate synthase	<i>C. Vesicomysocius</i>	BAF61232
gi 146326091	6-phosphofructokinase	<i>C. Vesicomysocius</i>	BAF61234
gi 146326092	conserved hypothetical protein	<i>C. Vesicomysocius</i>	BAF61235
gi 146326096	3-isopropylmalate dehydrogenase	<i>C. Vesicomysocius</i>	BAF61239
gi 146326104	DNA-directed RNA polymerase sigma-70 factor	<i>C. Vesicomysocius</i>	BAF61247
gi 146326111	hypothetical protein	<i>C. Vesicomysocius</i>	BAF61254
gi 146326118	acetyl-CoA carboxylase carboxyl transferase subunit alpha	<i>C. Vesicomysocius</i>	BAF61261
gi 146326121	Na(+):phosphate symporter	<i>C. Vesicomysocius</i>	BAF61264
gi 146326123	ATP-dependent RNA helicase RhIE	<i>C. Vesicomysocius</i>	BAF61266
gi 146326129	cell division protein FtsH	<i>C. Vesicomysocius</i>	BAF61272

<b>Appendix B2 (continued)</b>			
gi 146326131	phosphoglucosamine mutase	<i>C. Vesicomysocius</i>	BAF61274
gi 146326139	hypothetical protein	<i>C. Vesicomysocius</i>	BAF61282
gi 146326140	succinyl-CoA synthetase alpha subunit	<i>C. Vesicomysocius</i>	BAF61283
gi 146326145	argininosuccinate synthase	<i>C. Vesicomysocius</i>	BAF61288
gi 146326147	UDP-N-acetylmuramoylalanyl-D-glutamyl-2,6-diaminopimelate--D-alanyl-D-alanine ligase	<i>C. Vesicomysocius</i>	BAF61290
gi 146326149	sulfur oxidation protein SoxB	<i>C. Vesicomysocius</i>	BAF61292
gi 146326150	polysialic acid capsule expression protein	<i>C. Vesicomysocius</i>	BAF61293
gi 146326153	translation elongation factor EF-G	<i>C. Vesicomysocius</i>	BAF61296
gi 146326155	30S ribosomal protein S10	<i>C. Vesicomysocius</i>	BAF61298
gi 146326156	50S ribosomal protein L3	<i>C. Vesicomysocius</i>	BAF61299
gi 146326157	50S ribosomal protein L4	<i>C. Vesicomysocius</i>	BAF61300
gi 146326168	50S ribosomal protein L5	<i>C. Vesicomysocius</i>	BAF61311
gi 146326181	DNA-directed RNA polymerase alpha subunit	<i>C. Vesicomysocius</i>	BAF61324
gi 146326182	50S ribosomal protein L17	<i>C. Vesicomysocius</i>	BAF61325
gi 146326203	glutamate-1-semialdehyde 2,1-aminomutase	<i>C. Vesicomysocius</i>	BAF61346
gi 146326204	HAD-superfamily hydrolase	<i>C. Vesicomysocius</i>	BAF61347
gi 146326212	conserved hypothetical protein	<i>C. Vesicomysocius</i>	BAF61355
gi 146326218	NADH dehydrogenase I chain C	<i>C. Vesicomysocius</i>	BAF61361
gi 146326236	phosphoribosylglycinamide formyltransferase	<i>C. Vesicomysocius</i>	BAF61379
gi 146326239	DnaA family protein	<i>C. Vesicomysocius</i>	BAF61382
gi 146326246	succinyl-diaminopimelate desuccinylase	<i>C. Vesicomysocius</i>	BAF61389
gi 146326264	peptide chain release factor RF-2	<i>C. Vesicomysocius</i>	BAF61407
gi 146326266	lauroyl acyltransferase	<i>C. Vesicomysocius</i>	BAF61409
gi 146326270	DNA topoisomerase IV subunit A	<i>C. Vesicomysocius</i>	BAF61413
gi 146326271	6-pyruvoyltetrahydropterinsynthase	<i>C. Vesicomysocius</i>	BAF61414
gi 146326273	3-deoxy-7-phosphoheptulonate synthase	<i>C. Vesicomysocius</i>	BAF61416
gi 146326274	DNA gyrase subunit A GyrA	<i>C. Vesicomysocius</i>	BAF61417
gi 146326283	RNA methyltransferase	<i>C. Vesicomysocius</i>	BAF61426
gi 146326289	arsenate reductase	<i>C. Vesicomysocius</i>	BAF61432
gi 146326296	formamidopyrimidine-DNA glycosylase	<i>C. Vesicomysocius</i>	BAF61439
gi 146326297	conserved hypothetical protein	<i>C. Vesicomysocius</i>	BAF61440
gi 146326298	hypothetical protein	<i>C. Vesicomysocius</i>	BAF61441
gi 146326300	Na <sup>+</sup> :H <sup>+</sup> antiporter NhaD	<i>C. Vesicomysocius</i>	BAF61443
gi 146326305	3-dehydroquinate synthase	<i>C. Vesicomysocius</i>	BAF61448
gi 146326308	glutamyl-tRNA (Gln) amidotransferase subunit A	<i>C. Vesicomysocius</i>	BAF61451
gi 146326316	cation/multidrug efflux pump	<i>C. Vesicomysocius</i>	BAF61459
gi 146326321	Trk system, membrane component	<i>C. Vesicomysocius</i>	BAF61464
gi 146326324	two-component sensor histidine kinase	<i>C. Vesicomysocius</i>	BAF61467
gi 146326332	3-isopropylmalate dehydratase large subunit	<i>C. Vesicomysocius</i>	BAF61475
gi 146326336	SsrA-binding protein	<i>C. Vesicomysocius</i>	BAF61479
gi 146326338	Fe-S-cluster redox enzyme	<i>C. Vesicomysocius</i>	BAF61481
gi 146326342	1-deoxy-D-xylulose-5-phosphate synthase	<i>C. Vesicomysocius</i>	BAF61485

**Appendix B2** (continued)

gi 146326346	phosphoribosylformylglycinamide synthase	<i>C. Vesicomysocius</i>	BAF61489
gi 146326354	DNA polymerase III	<i>C. Vesicomysocius</i>	BAF61497
gi 146326357	porphobilinogen synthase	<i>C. Vesicomysocius</i>	BAF61500
gi 146326360	GTP-binding protein	<i>C. Vesicomysocius</i>	BAF61503
gi 146326384	conserved hypothetical protein	<i>C. Vesicomysocius</i>	BAF61527
gi 146326401	pyruvate dehydrogenase complex E1 component	<i>C. Vesicomysocius</i>	BAF61544
gi 146326403	IMP dehydrogenase	<i>C. Vesicomysocius</i>	BAF61546
gi 146326405	valyl-tRNA synthetase	<i>C. Vesicomysocius</i>	BAF61548
gi 146326407	DNA polymerase III tau and gamma subunit	<i>C. Vesicomysocius</i>	BAF61550
gi 146326413	glutamyl-tRNA synthetase	<i>C. Vesicomysocius</i>	BAF61556
gi 146326414	uridylyltransferase	<i>C. Vesicomysocius</i>	BAF61557
gi 146326420	exodeoxyribonuclease VII small subunit	<i>C. Vesicomysocius</i>	BAF61563
gi 146326421	geranyltranstransferase	<i>C. Vesicomysocius</i>	BAF61564
gi 146326423	fatty acid/phospholipid synthesis protein PlsX	<i>C. Vesicomysocius</i>	BAF61566
gi 146326430	heat shock protein HtpG	<i>C. Vesicomysocius</i>	BAF61573
gi 146326434	glutamine synthetase	<i>C. Vesicomysocius</i>	BAF61577
gi 146326447	guanosine-3',5'-bis(diphosphate) 3'-pyrophosphohydrolase	<i>C. Vesicomysocius</i>	BAF61590
gi 146326449	biopolymer transport protein TolB	<i>C. Vesicomysocius</i>	BAF61592
gi 146326453	NAD <sup>+</sup> synthase	<i>C. Vesicomysocius</i>	BAF61596
gi 146326456	ribonucleoside-diphosphate reductase beta subunit		BAF61599
gi 146326462	ribonuclease R	<i>C. Vesicomysocius</i>	BAF61605
gi 146326464	ATP phosphoribosyltransferase regulatory subunit	<i>C. Vesicomysocius</i>	BAF61607
gi 146326474	lipoic acid synthetase	<i>C. Vesicomysocius</i>	BAF61617
gi 146326475	multidrug efflux system	<i>C. Vesicomysocius</i>	BAF61618
gi 146326483	bacterial surface antigen family protein	<i>C. Vesicomysocius</i>	BAF61626
gi 146326485	3R-hydroxymyristoyl ACP dehydrase	<i>C. Vesicomysocius</i>	BAF61628
gi 146326486	UDP-N-acetylglucosamine acyltransferase	<i>C. Vesicomysocius</i>	BAF61629
gi 146326492	chaperonin GroEL	<i>C. Vesicomysocius</i>	BAF61635
gi 146326495	trans-regulatory protein ExsB	<i>C. Vesicomysocius</i>	BAF61638
gi 146326497	3-oxoacyl-[acyl-carrier-protein] synthase I/II	<i>C. Vesicomysocius</i>	BAF61640
gi 146326499	oligopeptidase A	<i>C. Vesicomysocius</i>	BAF61642
gi 146326506	iron-sulfur cofactor synthesis protein	<i>C. Vesicomysocius</i>	BAF61649
gi 146326507	cysteine desulfurase	<i>C. Vesicomysocius</i>	BAF61650
gi 146326508	Fe-S cluster-containing transcription factor	<i>C. Vesicomysocius</i>	BAF61651
gi 146326509	serine O-acetyltransferase	<i>C. Vesicomysocius</i>	BAF61652
gi 146326510	lipid A biosynthesis lauroyl acyltransferase	<i>C. Vesicomysocius</i>	BAF61653
gi 146326512	hypothetical protein	<i>C. Vesicomysocius</i>	BAF61655
gi 146326519	conserved hypothetical protein	<i>C. Vesicomysocius</i>	BAF61662
gi 146326526	hypothetical protein	<i>C. Vesicomysocius</i>	BAF61669
gi 146326531	signal recognition particle, subunit SRP54	<i>C. Vesicomysocius</i>	BAF61674
gi 146326540	ribonuclease III	<i>C. Vesicomysocius</i>	BAF61683

<b>Appendix B2 (continued)</b>			
gi 146326541	conserved hypothetical protein	<i>C. Vesicomysocius</i>	BAF61684
gi 146326544	transcriptional regulator ArsR family	<i>C. Vesicomysocius</i>	BAF61687
gi 146326546	carboxyl-terminal protease	<i>C. Vesicomysocius</i>	BAF61689
gi 146326553	D-3-phosphoglycerate dehydrogenase	<i>C. Vesicomysocius</i>	BAF61696
gi 146326554	phosphoserine aminotransferase	<i>C. Vesicomysocius</i>	BAF61697
gi 146326557	glycine hydroxymethyltransferase	<i>C. Vesicomysocius</i>	BAF61700
gi 146326562	phenylalanyl-tRNA synthetase beta subunit	<i>C. Vesicomysocius</i>	BAF61705
gi 146326566	translation initiation factor IF-3	<i>C. Vesicomysocius</i>	BAF61709
gi 146326568	single-stranded-DNA-specific exonuclease RecJ	<i>C. Vesicomysocius</i>	BAF61711
gi 146326570	FAD dependent oxidoreductase	<i>C. Vesicomysocius</i>	BAF61713
gi 146326573	peptidyl-prolyl cis-trans isomerase D	<i>C. Vesicomysocius</i>	BAF61716
gi 146326575	thiol:disulfide interchange protein DsbE	<i>C. Vesicomysocius</i>	BAF61718
gi 146326576	cytochrome c-type biogenesis protein CcmE	<i>C. Vesicomysocius</i>	BAF61719
gi 146326595	conserved hypothetical protein	<i>C. Vesicomysocius</i>	BAF61738
gi 146326607	nitrate transporter	<i>C. Vesicomysocius</i>	BAF61750
gi 146326608	nitrite reductase (NAD(P)H) large subunit	<i>C. Vesicomysocius</i>	BAF61751
gi 146326611	molybdopterin biosynthesis protein MoeA	<i>C. Vesicomysocius</i>	BAF61754
gi 146326619	respiratory nitrate reductase alpha subunit	<i>C. Vesicomysocius</i>	BAF61762
gi 146326620	molybdenum cofactor biosynthesis protein B	<i>C. Vesicomysocius</i>	BAF61763
gi 146326625	iron ABC transporter permease	<i>C. Vesicomysocius</i>	BAF61768
gi 146326647	negative regulator of ferric iron uptake	<i>C. Vesicomysocius</i>	BAF61790
gi 146326649	peptidase S49	<i>C. Vesicomysocius</i>	BAF61792
gi 146326653	S-adenosyl-L-homocysteine hydrolase	<i>C. Vesicomysocius</i>	BAF61796
gi 146326668	UDP-N-acetylmuramate--alanine ligase	<i>C. Vesicomysocius</i>	BAF61811
gi 146326676	threonine synthase	<i>C. Vesicomysocius</i>	BAF61819
gi 146326684	methionyl-tRNA formyltransferase	<i>C. Vesicomysocius</i>	BAF61827
gi 146326685	ATP-dependent Clp protease ATP-binding subunit ClpB	<i>C. Vesicomysocius</i>	BAF61828
gi 146326689	rod shape-determining protein MreB	<i>C. Vesicomysocius</i>	BAF61832
gi 146326695	bifunctional riboflavin biosynthesis protein RibD	<i>C. Vesicomysocius</i>	BAF61838
gi 146326704	DNA-directed RNA polymerase beta subunit	<i>C. Vesicomysocius</i>	BAF61847
gi 146326707	50S ribosomal protein L10	<i>C. Vesicomysocius</i>	BAF61850
gi 146326710	transcription antitermination protein NusG	<i>C. Vesicomysocius</i>	BAF61853
gi 146326712	translation elongation factor EF-Tu	<i>C. Vesicomysocius</i>	BAF61855
gi 146326713	malate dehydrogenase	<i>C. Vesicomysocius</i>	BAF61856
gi 146326719	dihydrodipicolinate reductase	<i>C. Vesicomysocius</i>	BAF61862
gi 146326729	bifunctional protein FolD	<i>C. Vesicomysocius</i>	BAF61872
gi 146326730	3-deoxy-manno-octulosonate cytidyltransferase	<i>C. Vesicomysocius</i>	BAF61873
gi 146326736	oxaloacetate decarboxylase, beta subunit	<i>C. Vesicomysocius</i>	BAF61879
gi 146326748	intracellular sulfur oxidation protein DsrO	<i>C. Vesicomysocius</i>	BAF61891
gi 146326758	intracellular sulfur oxidation protein DsrA	<i>C. Vesicomysocius</i>	BAF61901
gi 146326760	50S ribosomal protein L19	<i>C. Vesicomysocius</i>	BAF61903
gi 146326761	transcription elongation factor GreA	<i>C. Vesicomysocius</i>	BAF61904

**Appendix B2** (continued)

gi 146326762	carbamoyl-phosphate synthase large subunit	<i>C. Vesicomysocius</i>	BAF61905
gi 146326763	surface lipoprotein VacJ	<i>C. Vesicomysocius</i>	BAF61906
gi 146326774	UTP--glucose-1-phosphate uridylyltransferase	<i>C. Vesicomysocius</i>	BAF61917
gi 146326782	permease	<i>C. Vesicomysocius</i>	BAF61925
gi 146326791	ribonuclease II family protein	<i>C. Vesicomysocius</i>	BAF61934
gi 146326793	glycine cleavage system aminomethyltransferase	<i>C. Vesicomysocius</i>	BAF61936
gi 146326802	glycerol-3-phosphate dehydrogenase (NAD(P)+)	<i>C. Vesicomysocius</i>	BAF61945
gi 146326815	histidinol-phosphate aminotransferase	<i>C. Vesicomysocius</i>	BAF61958
gi 146326820	conserved hypothetical protein	<i>C. Vesicomysocius</i>	BAF61963
gi 146326826	pyruvate dehydrogenase complex E3 component	<i>C. Vesicomysocius</i>	BAF61969
gi 146326828	conserved hypothetical protein	<i>C. Vesicomysocius</i>	BAF61971
gi 146326830	polypeptide deformylase	<i>C. Vesicomysocius</i>	BAF61973
gi 146326834	UbiH/COQ6 monooxygenase family protein	<i>C. Vesicomysocius</i>	BAF61977
gi 146326844	sulfur deprivation response regulator	<i>C. Vesicomysocius</i>	BAF61987
gi 146326848	adenylosuccinate lyase	<i>C. Vesicomysocius</i>	BAF61991
gi 146326857	conserved hypothetical protein	<i>C. Vesicomysocius</i>	BAF62000
gi 146326860	3-hydroxydecanoyl-[acyl-carrier-protein] dehydratase	<i>C. Vesicomysocius</i>	BAF62003
gi 146326863	preprotein translocase SecD subunit	<i>C. Vesicomysocius</i>	BAF62006
gi 146326865	seryl-tRNA synthetase	<i>C. Vesicomysocius</i>	BAF62008
gi 146326868	thioredoxin	<i>C. Vesicomysocius</i>	BAF62011
gi 146326869	rhodanese family protein	<i>C. Vesicomysocius</i>	BAF62012
gi 146326870	nitrate/nitrite response regulator	<i>C. Vesicomysocius</i>	BAF62013
gi 146326875	glutamate synthase (NADPH) large chain	<i>C. Vesicomysocius</i>	BAF62018
gi 146326878	transcription-repair coupling factor	<i>C. Vesicomysocius</i>	BAF62021
gi 146326882	acetyl-CoA carboxylase carboxyl transferase subunit beta	<i>C. Vesicomysocius</i>	BAF62025
gi 146326889	tryptophan synthase beta subunit	<i>C. Vesicomysocius</i>	BAF62032
gi 146326891	hypothetical protein	<i>C. Vesicomysocius</i>	BAF62034
gi 146326901	F0F1-type ATP synthase beta subunit	<i>C. Vesicomysocius</i>	BAF62044
gi 146326906	F0F1-type ATP synthase C subunit	<i>C. Vesicomysocius</i>	BAF62049
gi 146326918	citrate synthase	<i>C. Vesicomysocius</i>	BAF62061
gi 146326920	hypothetical protein	<i>C. Vesicomysocius</i>	BAF62063
gi 146326925	phosphoglycerate mutase	<i>C. Vesicomysocius</i>	BAF62068
gi 146326926	ribulose-phosphate 3-epimerase	<i>C. Vesicomysocius</i>	BAF62069
gi 146326928	translation elongation factor EF-Ts	<i>C. Vesicomysocius</i>	BAF62071
gi 146326929	hypothetical protein	<i>C. Vesicomysocius</i>	BAF62072
gi 146336951	ribosomal protein S13	<i>Pinctada martensi</i>	ABQ23589
gi 147907866	mitochondrial mortalin splice variant	<i>Mya arenaria</i>	ABQ52471
gi 148717303	glucose-regulated protein 94	<i>Crassostrea gigas</i>	BAF63637
gi 148717303	glucose-regulated protein 94	<i>Crassostrea gigas</i>	BAF63637
gi 148717305	calnexin	<i>Crassostrea gigas</i>	BAF63638
gi 148717307	calreticulin	<i>Crassostrea gigas</i>	BAF63639

<b>Appendix B2 (continued)</b>			
gi 148717309	hypothetical protein	<i>Crassostrea gigas</i>	BAF63640
gi 148717311	voltage-dependent anion channel	<i>Crassostrea gigas</i>	BAF63641
gi 15004986	integrin beta cgh	<i>Crassostrea gigas</i>	BAB62173
gi 150378658	tolloid-like protein	<i>Crassostrea ariakensis</i>	ABR68098
gi 15128115	multidrug resistance-associated protein	<i>Mytilus edulis</i>	AAK84397
gi 15150336	RNA helicase p47	<i>Spisula solidissima</i>	AAK85400
gi 15150338	translation initiation factor eIF4A	<i>Spisula solidissima</i>	AAK85401
gi 151573941	catalase	<i>Crassostrea gigas</i>	ABS18267
gi 152003987	sarco/endoplasmic reticulum calcium ATPase isoform C	<i>Pinctada fucata</i>	ABS19817
gi 152205944	chitin synthase	<i>Pinctada fucata</i>	BAF73720
gi 1524127	MLH3	<i>Mytilus edulis</i>	CAA92785
gi 153123674	NADH dehydrogenase subunit 2	<i>Argopecten irradians</i>	YP_001382285
gi 153793258	heat shock protein 90	<i>Argopecten irradians</i>	ABS50431
gi 154551047	ABCC/MRP-like protein	<i>Mytilus californianus</i>	ABS83557
gi 154623288	myticin C precursor	<i>Mytilus galloprovincialis</i>	CAM56808
gi 156254294	mannose-6-phosphate isomerase	<i>Mytilus trossulus</i>	ABU62655
gi 156571895	mitochondrial aconitase-like protein	<i>Crassostrea virginica</i>	ABU84875
gi 156630609	nuclear receptor subfamily 1 DEF	<i>Mytilus galloprovincialis</i>	ABU89803
gi 156630629	nuclear receptor subfamily 1 group D variant3	<i>Mytilus galloprovincialis</i>	ABU89809
gi 157154407	macrophage expressed protein 1-like protein	<i>Crassostrea gigas</i>	ABV24918
gi 157804881	AprA	<i>Bathymodiolus azoricus</i>	ABV80101
gi 157815791	NADH dehydrogenase subunit 5	<i>Mytilus californianus</i>	ABV81046
gi 157830922	Hemoglobin I	<i>Lucina pectinata</i>	1EBT_A
gi 158515777	vitellogenin	<i>Saccostrea glomerata</i>	ABW69671
gi 158563793	ribosomal protein L8	<i>Modiolus modiolus</i>	ABW74352
gi 158563818	ribosomal protein S9	<i>Modiolus modiolus</i>	ABW74360
gi 158936908	Msx protein	<i>Corbicula fluminea</i>	BAF91569
gi 158957547	putative tumor suppressor QM protein	<i>Hyriopsis schlegelii</i>	ABW86313
gi 159145792	precollagen-NG	<i>Mytilus californianus</i>	ABW90433
gi 162417703	taurine transporter	<i>Bathymodiolus septemdierum</i>	BAF95543
gi 164418955	shematrin 2	<i>Pinctada fucata</i>	ABY54785
gi 164510092	ubiquitin	<i>Mytilus edulis</i>	CAJ32650
gi 164551492	lysosomal hexosaminidase	<i>Mytilus galloprovincialis</i>	ABY60965
gi 168824098	hexokinase	<i>Crassostrea gigas</i>	ACA30403
gi 169264926	p38 MAPK 5A	<i>Crassostrea gigas</i>	BAG12303
gi 18073531	heat shock protein 70	<i>Crassostrea gigas</i>	CAC83683
gi 18157445	cytochrome b	<i>Venerupis philippinarum</i>	BAB83775
gi 18565104	Actin	<i>Crassostrea gigas</i>	BAB84579
gi 187370560	peptidoglycan recognition protein S1S	<i>Crassostrea gigas</i>	BAG31896
gi 187762800	NADH dehydrogenase subunit 6	<i>Crassostrea gigas</i>	ACD35420
gi 187948617	histone H3	<i>Euvola ziczac</i>	ACD42742
gi 19070255	6-phosphogluconate dehydrogenase	<i>Sphaerium striatinum</i>	AAL83782

**Appendix B2** (continued)

gi 193248438	hypothetical protein	<i>Crassostrea nippona</i>	BAG50305
gi 193506923	15-hydroxyprostaglandin dehydrogenase	<i>Crassostrea gigas</i>	ACF19426
gi 194068375	beta-tubulin	<i>Saccostrea kegaki</i>	BAG55008
gi 194068377	tektin	<i>Saccostrea kegaki</i>	BAG55009
gi 194068379	actin-related protein 2/3	<i>Saccostrea kegaki</i>	BAG55010
gi 194068385	high mobility group 1 protein	<i>Saccostrea kegaki</i>	BAG55013
gi 194293520	alpha2-macroglobulin	<i>Cristaria plicata</i>	ACF39935
gi 197091707	phosphoinositide 4-kinase beta	<i>Crassostrea gigas</i>	ACH42086
gi 197091709	tyrosine phosphatase	<i>Crassostrea gigas</i>	ACH42087
gi 197091711	semaphorin	<i>Crassostrea gigas</i>	ACH42088
gi 197091717	nicastrin	<i>Crassostrea gigas</i>	ACH42091
gi 197690576	putative strombine dehydrogenase	<i>Crassostrea gigas</i>	CAL35825
gi 20269883	pholasin	<i>Pholas dactylus</i>	AAM18085
gi 207008800	Histone H2B	<i>Mytilus galloprovincialis</i>	CAR80313
gi 20804395	octopine dehydrogenase	<i>Mizuhopecten yessoensis</i>	BAB92087
gi 209869983	beta-glucosidase	<i>Corbicula japonica</i>	BAG75455
gi 209921945	calcineurin A subunit	<i>Pinctada fucata</i>	ACI96106
gi 209921947	calcineurin B subunit	<i>Pinctada fucata</i>	ACI96107
gi 209962626	3-ketoacyl-coenzyme A thiolase	<i>Mytilus galloprovincialis</i>	ACJ02108
gi 209981331	leucine aminopeptidase-like protein	<i>Crassostrea gigas</i>	ACJ05346
gi 211939928	PMMG1	<i>Pinctada maxima</i>	ACJ13444
gi 212374118	ribosomal protein	<i>Mytilus galloprovincialis</i>	CAQ63456
gi 21262971	protein phosphatase IIA	<i>Dreissena polymorpha</i>	AAM44817
gi 21388656	twitchin	<i>Mytilus galloprovincialis</i>	BAC00784
gi 215415905	hypoxia-inducible factor 1 alpha	<i>Crassostrea gigas</i>	BAG85183
gi 217273135	p63/p73	<i>Mya arenaria</i>	ACK28180
gi 218944225	cathepsin D	<i>Chlamys farreri</i>	ACL13150
gi 219566992	molluscan prismatic and nacreous layer 88 kDa protein lack7	<i>Pinctada fucata</i>	BAH05014
gi 2196556	troponin T	<i>Mizuhopecten yessoensis</i>	BAA20456
gi 219806594	tropomyosin	<i>Crassostrea gigas</i>	BAH10152
gi 2204081	insoluble protein	<i>Pinctada fucata</i>	BAA20466
gi 220979902	cell division cycle 42	<i>Mytilus sp. ZED-2008</i>	CAQ64775
gi 22203712	ribosomal protein L3	<i>Chlamys farreri</i>	AAM94270
gi 22203722	ribosomal protein L4	<i>Chlamys farreri</i>	AAM94273
gi 22203724	ribosomal protein S27E	<i>Chlamys farreri</i>	AAM94274
gi 22203726	ribosomal protein S20	<i>Chlamys farreri</i>	AAM94275
gi 22203734	small nuclear ribonucleoprotein D2-like protein	<i>Chlamys farreri</i>	AAM94277
gi 224925976	TNF-alpha factor	<i>Pinctada fucata</i>	ACN70008
gi 225111255	forkhead box L2	<i>Crassostrea gigas</i>	ACN80999
gi 226192454	cyclophilin A	<i>Vesicomys pacifica</i>	ACO37504
gi 226192476	ADP/ATP translocase	<i>Calymptogena kilmeri</i>	ACO37511
gi 226295502	Rab7-like protein	<i>Pinctada martensi</i>	ACO40522

<b>Appendix B2 (continued)</b>			
gi 227002095	cytochrome c oxidase subunit III	<i>Mytilus galloprovincialis</i>	ACP04326
gi 227476596	glutathione S-transferase pi-class	<i>Corbicula fluminea</i>	CAY36349
gi 22758848	ribosomal protein L30	<i>Argopecten irradians</i>	AAN05584
gi 22758850	ribosomal protein L22	<i>Argopecten irradians</i>	AAN05585
gi 22758854	ribosomal protein L11	<i>Argopecten irradians</i>	AAN05587
gi 22758856	ribosomal protein L19	<i>Argopecten irradians</i>	AAN05588
gi 22758866	ribosomal protein L23a	<i>Argopecten irradians</i>	AAN05592
gi 22758868	ribosomal protein S4	<i>Argopecten irradians</i>	AAN05593
gi 22758886	ribosomal protein S7	<i>Argopecten irradians</i>	AAN05602
gi 22758898	ribosomal protein L26	<i>Argopecten irradians</i>	AAN05608
gi 227908937	aryl hydrocarbon receptor	<i>Chlamys farreri</i>	ACL80140
gi 229472826	bactericidal permeability increasing protein	<i>Crassostrea gigas</i>	ACQ72917
gi 229485193	peroxiredoxin 6	<i>Saccostrea glomerata</i>	ACQ73550
gi 229485195	extracellular superoxide dismutase	<i>Saccostrea glomerata</i>	ACQ73551
gi 229503981	defensin	<i>Crassostrea gigas</i>	ACQ76286
gi 229891605	ribosomal protein S2	<i>Pinctada fucata</i>	A3RLT6
gi 229893916	cytochrome P450	<i>Hyriopsis cumingii</i>	ACQ90303
gi 238768474	peptidoglycan recognition protein L	<i>Crassostrea gigas</i>	BAH66800
gi 2388676	precollagen P	<i>Mytilus edulis</i>	AAB80719
gi 241913774	ribosomal protein S6	<i>Pinctada maxima</i>	ACS72283
gi 241913776	ribosomal protein S12	<i>Pinctada maxima</i>	ACS72284
gi 253683357	endo-1,4-beta-xylanase	<i>Corbicula japonica</i>	BAH84830
gi 254028663	scavenger receptor cysteine-rich protein	<i>Chlamys farreri</i>	ACT53266
gi 2570788	putative c-myc homolog	<i>Crassostrea virginica</i>	AAB82270
gi 27363138	ribosomal protein S14	<i>Chlamys farreri</i>	AAO11522
gi 27363140	ribosomal protein L12	<i>Chlamys farreri</i>	AAO11523
gi 2739487	abductin	<i>Argopecten irradians</i>	AAB94679
gi 2772914	precollagen D	<i>Mytilus edulis</i>	AAB96638
gi 28475271	GDF2 precursor	<i>Crassostrea gigas</i>	CAD67714
gi 28475277	glyceraldehyde 3-phosphate dehydrogenase	<i>Crassostrea gigas</i>	CAD67717
gi 29119647	DNA ligase	<i>Crassostrea gigas</i>	CAD79339
gi 29122671	matrix metalloproteinase	<i>Crassostrea gigas</i>	BAC66058
gi 29468327	aldolase	<i>Pecten maximus</i>	AAO85503
gi 3023823	Guanine nucleotide-binding protein G(o) subunit alpha	<i>Mizuhopecten yessoensis</i>	O15976
gi 3046767	dystrophin-like protein	<i>Pectinidae</i>	CAA68071
gi 30842644	Binding protein 2 like protein	<i>Crassostrea gigas</i>	CAD91435
gi 31335670	insulin-related peptide receptor	<i>Crassostrea gigas</i>	CAD59674
gi 32169288	SRC Kinase Associated Phosphoprotein 2	<i>Crassostrea gigas</i>	CAD88601
gi 32169292	ribosomal protein L7	<i>Crassostrea gigas</i>	CAD89885
gi 32250973	beta-1,3-glucanase	<i>Pseudocardium sachalinensis</i>	AAP74223
gi 32479251	ferritin GF2	<i>Crassostrea gigas</i>	AAP83794
gi 33114058	histone H1	<i>Mytilus galloprovincialis</i>	AAP94647

**Appendix B2** (continued)

gi 33337631	EGF-like related protein	<i>Crassostrea gigas</i>	AAQ13466
gi 33337635	Rho-GDI related protein	<i>Crassostrea gigas</i>	AAQ13468
gi 33337637	ribophorin related protein	<i>Crassostrea gigas</i>	AAQ13469
gi 33337639	plastin related protein	<i>Crassostrea gigas</i>	AAQ13470
gi 33337643	BAT1 homolog	<i>Crassostrea gigas</i>	AAQ13472
gi 33352160	BMP type 1b receptor	<i>Crassostrea gigas</i>	CAE11917
gi 34328768	NADH dehydrogenase subunit 4	<i>Mytilus galloprovincialis</i>	AAQ63685
gi 34484251	sodium/potassium ATPase alpha subunit	<i>Lampsilis cardium</i>	AAQ72760
gi 3513512	nongradient byssal precursor	<i>Mytilus edulis</i>	AAC33847
gi 37524027	G-protein a-subunit s class	<i>Pinctada fucata</i>	AAQ92314
gi 38146755	small 22kd heat shock protein	<i>Chlamys farreri</i>	AAR11780
gi 40642728	phosphoglucosyltransferase	<i>Crassostrea gigas</i>	CAD54445
gi 40642980	ribosomal protein S10	<i>Crassostrea gigas</i>	CAD91124
gi 40642982	ribosomal protein S25	<i>Crassostrea gigas</i>	CAD91125
gi 40642986	ribosomal protein S11	<i>Crassostrea gigas</i>	CAD91419
gi 40642988	ribosomal protein S3a	<i>Crassostrea gigas</i>	CAD91420
gi 40642990	ribosomal protein L5	<i>Crassostrea gigas</i>	CAD91421
gi 40642992	ribosomal protein L18	<i>Crassostrea gigas</i>	CAD91422
gi 40642996	ribosomal protein L24	<i>Crassostrea gigas</i>	CAD91424
gi 40643000	ribosomal protein S8	<i>Crassostrea gigas</i>	CAD91426
gi 40643002	ribosomal protein L9	<i>Crassostrea gigas</i>	CAD91427
gi 40643006	ribosomal protein S19	<i>Crassostrea gigas</i>	CAD91429
gi 40643010	ribosomal protein L31	<i>Crassostrea gigas</i>	CAD91431
gi 40643012	Adseverin-like protein	<i>Crassostrea gigas</i>	CAD91432
gi 40643020	ribosomal protein S3	<i>Crassostrea gigas</i>	CAD91437
gi 40643024	ribosomal protein L17A	<i>Crassostrea gigas</i>	CAD91439
gi 40643042	ribosomal protein S17	<i>Crassostrea gigas</i>	CAD91448
gi 40891625	vasa-like protein	<i>Crassostrea gigas</i>	AAR37337
gi 42559342	Paramyosin	<i>Mytilus galloprovincialis</i>	O96064
gi 44885729	arginine kinase	<i>Crassostrea gigas</i>	BAD11950
gi 46359618	78kDa glucose regulated protein	<i>Crassostrea gigas</i>	BAD15288
gi 46391574	G protein beta subunit	<i>Pinctada fucata</i>	AAS90835
gi 46909221	fructose-bisphosphate aldolase	<i>Mytilus edulis</i>	AAT06128
gi 46909371	methionine adenosyltransferase	<i>Nucula proxima</i>	AAT06203
gi 46909451	triosephosphate isomerase	<i>Nucula proxima</i>	AAT06243
gi 48476113	cavortin	<i>Crassostrea gigas</i>	AAT44352
gi 48476117	isocitrate dehydrogenase	<i>Crassostrea gigas</i>	AAT44354
gi 50512854	glycogen phosphorylase	<i>Crassostrea gigas</i>	AAS93901
gi 50726950	ras	<i>Mytilus edulis</i>	AAT81171
gi 51315721	Histone H4	<i>Mytilus edulis</i>	Q7K8C0
gi 51701479	Histone H2A	<i>Mytilus edulis</i>	Q8I0T3
gi 520509	RNA polymerase II, largest subunit	<i>Crassostrea gigas</i>	AAA50225
gi 56718386	glycogen synthase	<i>Crassostrea gigas</i>	AAS93900

<b>Appendix B2 (continued)</b>			
gi 57165227	endo-1,3-beta-D-glucanase	<i>Mizuhopecten yessoensis</i>	AAW34372
gi 57335436	hemocyanin isoform 1	<i>Nucula nucleus</i>	CAH10286
gi 57335438	hemocyanin isoform 2	<i>Nucula nucleus</i>	CAH10287
gi 5817598	myosin heavy chain	<i>Pecten maximus</i>	AAD52842
gi 58219310	tubulin	<i>Crassostrea gigas</i>	BAD88768
gi 5902774	Alpha-amylase	<i>Pecten maximus</i>	P91778
gi 60548046	foot protein 2	<i>Mytilus edulis</i>	AAX23970
gi 61105830	serine protease inhibitor	<i>Argopecten irradians</i>	AAX38588
gi 61619986	ribosomal protein S23	<i>Crassostrea gigas</i>	AAX47435
gi 61815768	ikk-like protein	<i>Pinctada fucata</i>	AAX56336
gi 61815774	astacin-like protein	<i>Pinctada fucata</i>	AAX56337
gi 61967932	defender against apoptotic cell death 1	<i>Argopecten irradians</i>	AAX56947
gi 62086387	Xlox-like homeodomain protein	<i>Mizuhopecten yessoensis</i>	BAD91661
gi 62086389	cdx-like homeodomain protein	<i>Mizuhopecten yessoensis</i>	BAD91662
gi 63055693	foot protein 3 variant 6	<i>Mytilus californianus</i>	AAZ29129
gi 6682323	catchin protein	<i>Mytilus galloprovincialis</i>	CAB64664
gi 66865864	ETS-family transcription factor	<i>Chlamys farreri</i>	AAU11487
gi 66947665	putative multidrug resistance protein 1	<i>Brachidontes pharaonis</i>	CAI99869
gi 68655616	aspartate aminotransferase	<i>Crassostrea gigas</i>	CAD42721
gi 68989138	ATP synthase F0 subunit 6	<i>Crassostrea virginica</i>	YP_254653
gi 71040619	ribosomal protein S5	<i>Crassostrea gigas</i>	BAE16013
gi 71040621	ribosomal protein S18	<i>Crassostrea gigas</i>	BAE16014
gi 71063300	mantle protein 9	<i>Pinctada fucata</i>	AAZ22318
gi 72132971	tyrosinase	<i>Pinctada fucata</i>	AAZ66340
gi 73427346	mantle gene 2	<i>Pinctada fucata</i>	AAZ76256
gi 73656362	cytosolic malate dehydrogenase	<i>Mytilus californianus</i>	AAZ79368
gi 73665577	myosin essential light chain	<i>Pinctada fucata</i>	AAZ79490
gi 7524150	E3 ubiquitin-protein ligase	<i>Mya arenaria</i>	AAD34642
gi 76058057	nerve hemoglobin	<i>Spisula solidissima</i>	CAJ31108
gi 76573377	60S ribosomal protein L13A	<i>Mytilus edulis</i>	ABA46793
gi 7689377	poly(A)-binding protein	<i>Spisula solidissima</i>	AAF67755
gi 78172537	NADH dehydrogenase subunit I	<i>Lampsilis fasciola</i>	ABB29392
gi 80971720	inhibitor protein kappa B	<i>Crassostrea gigas</i>	ABB52821
gi 81367459	C-type lectin B	<i>Chlamys farreri</i>	ABB71673
gi 82408382	ribosomal protein S15	<i>Mytilus edulis</i>	ABB73035
gi 83288255	Serine/threonine-protein kinase	<i>Pinctada fucata</i>	Q4KTY1
gi 83699763	cytochrome P450-like protein	<i>Mytella strigata</i>	ABC40757
gi 84782834	LMPX protein	<i>Crassostrea gigas</i>	ABC61696
gi 85792106	foot protein-4 variant-2	<i>Mytilus californianus</i>	ABC84185
gi 86156234	ATP synthase beta subunit	<i>Pinctada fucata</i>	ABC86835
gi 86156234	ATP synthase betasubunit	<i>Pinctada fucata</i>	ABC86835
gi 86439930	aspartate racemase	<i>Scapharca broughtonii</i>	BAE78960
gi 91179150	vasa	<i>Chlamys farreri</i>	ABE27759

**Appendix B2** (*continued*)

gi 91179152	pl10-like protein	<i>Chlamys farreri</i>	ABE27760
gi 92110430	Chit2 protein	<i>Crassostrea gigas</i>	CAI96025
gi 92110434	Chit3 protein	<i>Crassostrea gigas</i>	CAI96027
gi 92110438	Clp1 protein	<i>Crassostrea gigas</i>	CAI96029
gi 93102305	shematin-4	<i>Pinctada fucata</i>	BAE93436
gi 93102311	shematin-7	<i>Pinctada fucata</i>	BAE93439
gi 94961054	EF-hand calcium-binding protein	<i>Pinctada fucata</i>	ABF48089
gi 957315	Myc homolog	<i>Crassostrea virginica</i>	AAB34577
gi 974720	two-domain chain of the polymeric hemoglobin (intracellular)	<i>Barbatia lima</i>	BAA09964
gi 9957079	omega-crystallin	<i>Placopecten magellanicus</i>	AAG09204
gi 998666	vitelline coat lysin M3=acrosomal protein	<i>Mytilus edulis</i>	AAB33369

## **Appendix C**

# Appendix C1 Proteins found in all metal-exposed as well as non-exposed Sydney rock oysters

Gene Identifier	Uni-prot AC	Protein name	Average NSAF	Biological Process Category
gi 405958790	K1PLF9	Arginine kinase	0.006750	amino acid metabolism
gi 405957058	K1Q350	Glyceraldehyde-3-phosphate dehydrogenase	0.015654	carbohydrate metabolism
gi 405959090	K1PU26	Malate dehydrogenase (EC 1.1.1.37)	0.001128	carbohydrate metabolism
gi 405961263	K1QEA6	Phosphoenolpyruvate carboxykinase [GTP]	0.002019	carbohydrate metabolism
gi 405963427	K1R4Z3	Malate dehydrogenase, mitochondrial	0.001916	carbohydrate metabolism
gi 405964948	K1R8R6	Fructose-bisphosphate aldolase	0.005590	carbohydrate metabolism
gi 405965040	K1Q948	glycogen phosphorylase (EC 2.4.1.1)	0.001277	carbohydrate metabolism
gi 405969875	K1R115	Succinate dehydrogenase [ubiquinone] flavoprotein subunit B, mitochondrial	0.000785	carbohydrate metabolism
gi 405970867	K1QX37	Enolase (EC 4.2.1.11)	0.000639	carbohydrate metabolism
gi 405976318	K1RH70	6-phosphogluconate dehydrogenase, decarboxylating (EC 1.1.1.44)	0.002085	carbohydrate metabolism
gi 405953867	K1PCA0	Septin-7	0.008597	cell cycle
gi 405957670	A7M7T7	Non-selenium glutathione peroxidase	0.001586	cell redox homeostasis
gi 405964323	K1QLW5	Extracellular superoxide dismutase [Cu-Zn]	0.171700	cell redox homeostasis
gi 405950190	K1P339	Vinculin	0.000589	Cy/P
gi 405950538	K1PI02	Talin-1	0.000658	Cy/P
gi 405950795	K1PBC0	Non-neuronal cytoplasmic intermediate filament protein	0.003659	Cy/P
gi 405952674	K1PFT9	Myophilin	0.002994	Cy/P
gi 405954086	K1PCV0	Severin-1	0.002262	Cy/P
gi 405954824	K1PE57	Severin-2	0.006141	Cy/P
gi 405959361	K1PN21	Tubulin beta chain	0.010370	Cy/P
gi 405961655	K1QEZ3	Fascin	0.001948	Cy/P
gi 405962295	K1PUJ1	Radixin	0.001278	Cy/P
gi 405962873	K1PW06	Filamin-C	0.003241	Cy/P
gi 405964579	K1Q0U8	Actin-3	0.007506	Cy/P
gi 405965637	K1QII6	Tubulin alpha-1C chain	0.007570	Cy/P
gi 405966634	Q8TA69	Actin 2 (adductor muscle)	0.084379	Cy/P
gi 405966986	K1QTC1	Paramyosin	0.010708	Cy/P
gi 405971145	K1QXX7	Myosin heavy chain, non-muscle (Fragment)	0.001954	Cy/P
gi 405972818	K1RSS3	Myosin heavy chain, striated muscle	0.005859	Cy/P
gi 405972952	K1R2D6	Plastin-3	0.001356	Cy/P
gi 405973142	K1QLZ1	Actin-related protein 3	0.000893	Cy/P
gi 405973339	K1QWP8	Actin-2/3	0.006150	Cy/P

**Appendix C1** *(continued)*

<b>Gene Identifier</b>	<b>Uni-prot AC</b>	<b>Protein name</b>	<b>Average NSAF</b>	<b>Biological Process Category</b>
gi 405973340	C4NY62	Actin-1	0.073191	Cy/P
gi 405973341	K1RA57	Actin related protein	0.040191	Cy/P
gi 405973516	K1R401	Spectrin alpha chain	0.000474	Cy/P
gi 405973865	K1RBG6	Actin-1/3	0.001396	Cy/P
gi 405974681	K1QQR1	Major vault protein	0.000747	Cy/P
gi 405974805	K1R781	Muscle LIM protein Mlp84B	0.004458	Cy/P
gi 405975056	K1QRU8	Myosin heavy chain alpha	0.004732	Cy/P
gi 405975057	K1R1B3	Myosin heavy chain 2	0.004285	Cy/P
gi 405975242	K1R1X5	Calponin-2	0.005536	Cy/P
gi 405975785	K1RZ99	Filamin-A	0.001546	Cy/P
gi 405978716	K1RH58	Alpha-actinin, sarcomeric	0.003354	Cy/P
gi 405965075	K1QNT7	Aldehyde dehydrogenase, mitochondrial	0.000932	energy metabolism
gi 405974703	K1R6Z7	ATP synthase subunit alpha	0.001164	energy metabolism
gi 405974790	K1RWW5	ATP synthase subunit beta	0.003077	energy metabolism
gi 405959333	K1PUI8	Fibrinogen C domain-containing protein 1	0.006658	immune response
gi 405972837	K1R266	Retinal dehydrogenase 1	0.002070	metabolic process
gi 405958653	K1QT31	Uncharacterized protein	0.000909	metabolic process
gi 405973417	K1R3V1	Neurotrypsin	0.000321	metabolic process
gi 405962347	K1PUQ5	Histone H2B	0.005411	nucleosome assembly
gi 405975240	K1RXS6	Histone H2A	0.003758	nucleosome assembly
gi 405955982	K1PV35	Kyphoscoliosis peptidase	0.000938	protein metabolic process
gi 405959675	K1PNQ5	Heat shock protein HSP 90-1	0.001528	protein metabolic process
gi 405978782	K1RHA5	Nucleoside diphosphate kinase B	0.002135	purine metabolism
gi 405955698	K1Q1L4	Uncharacterized protein	0.000906	response to stress
gi 405968607	K1QIR8	78 kDa glucose-regulated protein	0.000999	response to stress
gi 405969523	K1QTD6	Catalase	0.002713	response to stress
gi 405963584	K1R5F2	14-3-3 protein epsilon	0.006004	signal transduction
gi 405965548	K1QI97	Adenylyl cyclase-associated protein	0.000251	signal transduction
gi 405957597	K1PII9	Reelin	0.000617	signal transduction
gi 405967652	K1QFW9	Uncharacterized protein	0.000548	signal transduction
gi 405950098	K1P9N7	14-3-3 protein zeta	0.001196	signal transduction
gi 405963584	K1R5F2	14-3-3 protein epsilon like protein	0.004501	signal transduction

**Appendix C1** *(continued)*

<b>Gene Identifier</b>	<b>Uni-prot AC</b>	<b>Protein name</b>	<b>Average NSAF</b>	<b>Biological Process Category</b>
gi 405974926	K1R0Y3	Ras-related protein Rap-1b	0.001711	signal transduction
gi 405976470	K1S151	Rab GDP dissociation inhibitor beta	0.001668	signal transduction
gi 405977015	K1QX44	Ras-related protein Rab-11B	0.001713	signal transduction
gi 405963560	K1Q5G7	Sarcoplasmic calcium-binding protein	0.003055	signal transduction
gi 405965232	K1Q2L2	60S ribosomal protein L12	0.003111	translation
gi 405967949	K1QGS8	Elongation factor 1-alpha	0.005448	translation
gi 405973234	K1QWC3	40S ribosomal protein S3	0.002015	translation
gi 405975071	K1QRW4	Coronin	0.000713	transport

## Appendix C2 Proteins found only in oysters exposed to Zn toxicity

Gene Identifier	Uni-prot AC	Protein name	Average NSAF	Biological Process Category
gi 405953427	K1PXH5	Putative saccharopine dehydrogenase	0.000164	amino acid metabolism
gi 405958953	K1PM29	Glucose-6-phosphate 1-dehydrogenase	0.000657	carbohydrate metabolism
gi 405947958	K1PN47	Succinate dehydrogenase iron-sulfur subunit, mitochondrial	0.000638	carbohydrate metabolism
gi 405963909	K1R647	Lactoylglutathione lyase	0.001265	carbohydrate metabolism
gi 405952700	K1PW08	glycogen debranching enzyme	6.31E-05	carbohydrate metabolism
gi 405971692	K1R5P2	Tumor protein D54	0.000508	carcinogenesis
gi 405973087	K1R2P2	SH3 domain-binding glutamic acid-rich protein	0.000293	cell redox homeostasis
gi 405957134	K1PHC4	Fibroleukin	0.001208	Cy/P
gi 405964694	K1Q122	Myosin regulatory light chain sqh	0.00078	Cy/P
gi 405964580	K1Q821	cytoplasmic actin 3	0.00607	Cy/P
gi 405955250	K1QL59	Talin-1	0.002635	Cy/P
gi 405973201	K1QM61	Uncharacterized protein	0.000484	Cy/P
gi 405968537	K1RHJ4	beta actin	0.004434	Cy/P
gi 405978684	K1RH30	Collagen alpha-1(IV) chain	0.001053	Cy/P
gi 405957279	K1PPF4	NADH dehydrogenase Fe-S protein4	0.000688	energy metabolism
gi 405963253	K1QCF5	Fumarate hydratase class I, aerobic	0.000387	energy metabolism
gi 405960099	K1QWZ6	Dolichyl-diphosphooligosaccharide--protein glycosyltransferase subunit 1	0.000223	glycan biosynthesis and metabolism
gi 405963180	K1PWR0	Protein SET	0.000539	nucleosome assembly
gi 405949985	K1PGH0	Vacuolar protein sorting-associated protein 29	0.001338	protein metabolic process
gi 405968717	K1QIZ7	Programmed cell death protein 6	0.000782	protein metabolic process
gi 405965865	K1QJ51	Proteasome subunit beta type-8	0.000201	protein metabolic process
gi 405964525	K1QMD8	Proteasome subunit alpha type	0.001137	protein metabolic process
gi 405971643	K1QS07	Proteasome subunit beta type-3	0.001329	protein metabolic process
gi 405961865	K1R1M7	Ubiquitin-like modifier-activating enzyme 1	0.000564	protein metabolic process
gi 405977961	K1S4Q2	T-complex protein 1 subunit delta	0.000418	protein metabolic process
gi 405977525	K1R866	Puromycin-sensitive aminopeptidase	0.000257	protein metabolic process
gi 405966599	K1Q5G6	60 kDa heat shock protein	0.000434	response to stress
gi 405970591	K1QWC6	Universal stress protein A-like protein	0.002008	response to stress
gi 405973525	K1QX26	Endoplasmic	0.002419	response to stress
gi 405961849	K1PZ08	Ras-related protein Rab-7a	0.002592	signal transduction
gi 405958669	K1Q086	Ankyrin-2	3.28E-05	signal transduction
gi 405971056	K1QGA2	Flotillin-2	0.000308	signal transduction
gi 405954479	K1QJN6	Angiopoietin-4	0.000765	signal transduction

### Appendix C2 (continued)

Gene Identifier	Uni-prot AC	Protein name	Average NSAF	Biological Process Category
gi 405972778	K1QL55	Protein phosphatase 1B	0.000149	signal transduction
gi 405972710	K1QUZ5	Integrin beta	0.000414	signal transduction
gi 405970601	K1QWE5	Ras-related protein Rab-18-B	0.000902	signal transduction
gi 405976041	K1RGQ0	Ras-related C3 botulinum toxin substrate 1	0.002596	signal transduction
gi 405973892	K1RV41	Guanine nucleotide-binding protein subunit beta-2-like 1	0.002864	signal transduction
gi 405951708	K1PDL3	Ribosomal protein L19	0.00145	translation
gi 405952182	K1PEP0	40S ribosomal protein S8	0.001412	translation
gi 405947752	K1PG60	60S ribosomal protein L17	0.001146	translation
gi 405965438	K1QI14	40S ribosomal protein S3a	0.000584	translation
gi 405957444	K1PPW8	Coatomer subunit beta	0.00028	transport
gi 405962570	K1QAB1	AP-2 complex subunit alpha-2	0.000196	transport
gi 405950556	K1QAM7	Copine-7	0.000534	transport
gi 405971077	K1QQ16	AP-2 complex subunit beta	0.000441	transport
gi 405965094	K1R973	Chloride intracellular channel exc-4	0.000472	transport
gi 405962347	K1PUQ5	Histone H2B	0.01646	nucleosome assembly
gi 405965171	K1Q2H5	Uncharacterized protein	0.000818	unknown
gi 405969976	K1QUG6	Uncharacterized protein	0.001082	unknown

### Appendix C3 Proteins found only in control oysters

Gene Identifier	Uni-prot AC	Protein name	Average NSAF	Biological Process Category
gi 405967637	K1QNV6	Tropomyosin	0.005584	cytoskeleton and protein polymerization
gi 405968541	K1QXE8	Actin, cytoplasmic	0.011926	cytoskeleton and protein polymerization
gi 405959643	K1QAU8	Peptidyl-prolyl cis-trans isomerase E (PPIase E) (EC 5.2.1.8)	0.000124	protein metabolic process
gi 405961891	K1Q8F7	Alpha-crystallin B chain	0.000689	protein metabolic process
gi 405968843	K1QVS3	Thimet oligopeptidase	0.001137	protein metabolic process
gi 405962950	K1QIB2	Mitogen-activated protein kinase 1	0.000193	signal transduction
gi 405976099	K1RAI3	Annexin-2	0.001668	transport
gi 405960811	K1QYT5	Phosphate carrier protein, mitochondrial	0.000196	transport

#### Appendix C4 Proteins found only in oysters exposed to Pb toxicity

Gene Identifier	Uni-prot AC	Protein name	Average NSAF	Biological Process Category
gi 405962372	K1R2R2	Uncharacterized protein	0.001178	carbohydrate metabolism
gi 405952131	K1P8D9	SH3 domain-binding glutamic acid-rich-like protein 3	0.00149	cell redox homeostasis
gi 405965638	K1QQ68	Tubulin alpha-1C chain	0.007538	Cy/P
gi 405969939	Q70MM3	Ferritin	0.001288	energy metabolism
gi 405952151	K1PUL2	Long-chain-fatty-acid--CoA ligase 1	0.000201	lipid metabolism
gi 405953127	K1QGU5	Allene oxide synthase-lipoxygenase protein (Fragment)	0.00022	lipid metabolism
gi 405951793	K1PLJ5	Histone H3.3	0.000846	nucleosome assembly
gi 405951393	K1PK85	Cullin-associated NEDD8-dissociated protein 1	0.000219	protein metabolic process
gi 405969319	K1QZJ6	Ras like family protein	0.000783	signal transduction
gi 405957027	K1Q324	Heterogeneous nuclear ribonucleoprotein K	0.000589	transcription
gi 405977575	K1R8C6	40S ribosomal protein S12	0.00418	translation
gi 405958969	K1PM50	40S ribosomal protein S16	0.0013	translation
gi 405955817	K1PUV4	40S ribosomal protein S24	0.002153	translation
gi 405962281	K1Q227	Sacsin	0.000556	translation
gi 405965410	K1Q2Y1	40S ribosomal protein S15	0.000956	translation
gi 405967288	K1QF01	40S ribosomal protein S4, X isoform	0.001834	translation
gi 405952804	K1QGB4	40S ribosomal protein S17	0.002902	translation
gi 405953356	K1QHF0	40S ribosomal protein S27	0.002609	translation
gi 405964878	K1QN79	40S ribosomal protein S11	0.003053	translation
gi 405966326	K1QRZ3	40S ribosomal protein S13	0.001819	translation
gi 405965901	K1RB07	60S ribosomal protein L27a	0.000577	translation
gi 405977517	K1RK12	40S ribosomal protein S23	0.000168	translation
gi 405957760	Q70MT4	40S ribosomal protein S10 (Ribosomal protein S10)	0.00128	translation
gi 405976100	K1RGT2	Annexin-1	0.003176	transport
gi 405950430	K1PPQ1	14-3-3 protein gamma	0.003158	signal transduction
gi 405974926	K1R0Y3	Ras-related protein Rap-1b	0.002637	signal transduction

## Appendix C5 Proteins found only in oysters exposed to Cu toxicity

Gene Identifier	Uni-prot AC	Protein name	Average NSAF	Biological Process Category
gi 405977978	K1R9E9	Aldehyde dehydrogenase family 16 member A1	0.000154	amino acid metabolism
gi 405951823	K1P7P6	Glutamate decarboxylase-like protein1	0.000882	amino acid metabolism
gi 405952567	K1PFG1	$\beta$ -1,3-glucan-binding protein	0.000183	carbohydrate metabolism
gi 405971478	K1QRD4	S-formylglutathione hydrolase	0.001280	carbohydrate metabolism
gi 405966541	K1QSB0	Fructose-1,6-bisphosphatase 1	0.000592	carbohydrate metabolism
gi 405970598	K1RM80	Citrate synthase	0.000967	carbohydrate metabolism
gi 405964146	K1Q6X5	Protein disulfide-isomerase	0.001386	cell redox homeostasis
gi 405959834	K1QW72	Catalase	0.000665	cell redox homeostasis
gi 405963072	K1R473	Tubulin alpha-3 chain	0.005951	Cy/P
gi 405977054	K1S2I2	Kinesin heavy chain	0.000243	Cy/P
gi 405950693	K1PIH2	V-type proton ATPase subunit E	0.000549	energy metabolism
gi 405950221	K1Q9V3	V-type proton ATPase catalytic subunit A	0.000333	energy metabolism
gi 405978156	K1QZU8	Plasma membrane calcium-transporting ATPase 3	0.000224	energy metabolism
gi 405969654	K1R0L4	Sodium/potassium-transporting ATPase subunit alpha	0.000656	energy metabolism
gi 405964521	K1Q0N6	Dolichyl-diphosphooligosaccharide--protein glycosyltransferase subunit STT3A	0.000211	glycan biosynthesis and metabolism
gi 405965244	K1QHM2	Dolichyl-diphosphooligosaccharide--protein glycosyltransferase subunit 2	0.000919	glycan biosynthesis and metabolism
gi 405962319	K1Q9K6	Histone H3	0.002044	nucleosome assembly
gi 405953294	K1PQ64	Kyphoscoliosis peptidase	0.001754	protein metabolic process
gi 405953774	K1PRB5	Tyrosyl-tRNA synthetase, cytoplasmic	0.000576	protein metabolic process
gi 405965139	K1Q9D7	Sorting nexin-2	0.001315	protein metabolic process
gi 405970092	K1QDM2	26S proteasome non-ATPase regulatory subunit 2	0.000294	protein metabolic process
gi 405959342	K1QUZ1	Putative leucine aminopeptidase	0.000959	protein metabolic process
gi 405963058	K1R466	T-complex protein 1 subunit gamma	0.000340	protein metabolic process
gi 405976915	K1R6F1	Proteasome subunit beta type 2	0.003885	protein metabolic process
gi 405972436	K1R7N7	Cystatin-A2	0.007227	protein metabolic process
gi 405978203	K1RA77	Ubiquitin	0.005051	protein metabolic process

**Appendix C5** (*continued*)

<b>Gene Identifier</b>	<b>Uni-prot AC</b>	<b>Protein name</b>	<b>Average NSAF</b>	<b>Biological Process Category</b>
gi 405964548	K1QG22	Heat shock protein 70 B2	0.002974	response to stress
gi 405962799	K1PVR8	Tyrosine-protein kinase transforming protein Src	0.001561	signal transduction
gi 405950485	K1QAF2	Tyrosine-protein kinase HTK16	0.000183	signal transduction
gi 405950642	K1QAV0	Guanine nucleotide-binding protein G(Q) subunit alpha	0.000395	signal transduction
gi 405962909	K1QBJ5	G protein-coupled receptor kinase 1	0.000199	signal transduction
gi 405977709	K1RKL1	Tyrosine-protein phosphatase non-receptor type 11	0.000216	signal transduction
gi 405974949	K1RXA0	cAMP-dependent protein kinase regulatory subunit	0.000378	signal transduction
gi 405952464	K1PF96	Spliceosome RNA helicase BAT1	0.000393	transcription
gi 405965439	K1QPM8	40S ribosomal protein S3a	0.000521	translation
gi 405971144	K1QQB3	Glycyl-tRNA synthetase	0.000323	translation
gi 405973144	K1R2V1	Importin subunit beta-1	0.000164	translation
gi 405977322	K1RJH5	Polyadenylate-binding protein 4	0.000236	translation
gi 405971461	K1RPF7	60S ribosomal protein L5	0.000486	translation
gi 405952344	K1P8W6	60S ribosomal protein L4	0.004043	translation
gi 405951708	K1PDL3	Ribosomal protein L19	0.006484	translation
gi 405972789	K1QL67	60S ribosomal protein L7a	0.004284	translation
gi 405973234	K1QWC3	40S ribosomal protein S3	0.004030	translation
gi 405960081	K1QWX2	60S acidic ribosomal protein P0	0.005363	translation
gi 405961297	K1PZP6	Coatomer subunit gamma	0.000236	transport
gi 405964042	K1QET2	Coatomer subunit alpha	0.000259	transport
gi 405961646	K1R0Y9	ADP,ATP carrier protein	0.002435	transport
gi 405966815	K1Q620	Uncharacterized protein	0.001041	unknown
gi 405954873	K1QKD6	Uncharacterized protein	0.000513	unknown

**Appendix C6 Protein and peptide identification data for 185 statistically significant differentially expressed proteins in response to metal stress in Sydney rock oysters, with biological process and quantitation information.**

Ratio of differential expression <sup>a,b</sup>	Identifier	Uniprot AC	Protein name	BP category	Average NSAF Metal	Average NSAF Control	p value
<b>Proteins in response to Cu stress only</b>							
<b>-Control+Cu↑60.7</b>	gi 405966815	K1Q620	Uncharacterized protein	unknown	1.18E-03	1.95E-05	0.003
<b>-Control+Cu↑34.4</b>	gi 405969654	K1R0L4	Sodium/potassium-transporting ATPase subunit alpha	energy metabolism	7.41E-04	2.16E-05	0.002
<b>-Control+Cu↑31.8</b>	gi 405965244	K1QHM2	Dolichyl-diphosphooligosaccharide-protein glycosyltransferase subunit 2	glycan biosynthesis and metabolism	1.03E-03	3.25E-05	0.001
<b>-Control+Cu↑31.3</b>	gi 405954873	K1QKD6	Uncharacterized protein	unknown	5.80E-04	1.85E-05	0.008
<b>-Control+Cu↑30.66</b>	gi 405959695	K1PNR3	Clathrin heavy chain 1	transport	1.23E-03	4.02E-05	0.004
<b>-Control+Cu↑23.39</b>	gi 405952567	K1PFG1	β-1,3-glucan-binding protein	carbohydrate metabolism	2.06E-04	8.80E-06	0.002
<b>-Control+Cu↑20.8</b>	gi 405946057	K1PFH4	Talin-2	Cy/P	4.08E-03	1.96E-04	0.022
<b>-Control+Cu↑20.01</b>	gi 405953294	K1PQ64	Kyphoscoliosis peptidase	protein metabolic process	1.96E-03	9.79E-05	0.001
<b>-Control+Cu↑18.6</b>	gi 405962799	K1PVR8	Tyrosine-protein kinase transforming protein Src	signal transduction	1.76E-03	9.47E-05	0.007
<b>-Control+Cu↑18.1</b>	gi 405971478	K1QRD4	S-formylglutathione hydrolase	carbohydrate metabolism	1.45E-03	8.03E-05	0.012
<b>-Control+Cu↑17.39</b>	gi 405953394	K1QHK9	Dynein heavy chain, cytoplasmic	Cy/P	2.39E-04	1.37E-05	0.009
<b>-Control+Cu↑16.6</b>	gi 405973144	K1R2V1	Importin subunit beta-1	translation	1.86E-04	1.12E-05	0.007
<b>Cu↑16.1</b>	gi 405964118	K1Q6W3	Talin-3	Cy/P	1.96E-03	1.22E-04	0.001
<b>-Control+Cu↑15.1</b>	gi 405978156	K1QZU8	Plasma membrane calcium-transporting ATPase 3	energy metabolism	2.50E-04	1.66E-05	0.002
<b>-Control+Cu↑14.7</b>	gi 405970598	K1RM80	Citrate synthase	carbohydrate metabolism	1.10E-03	7.44E-05	0.010
<b>-Control+Cu↑13.6</b>	gi 405964548	K1QG22	Heat shock protein 70 B2	response to stress	3.21E-03	2.36E-04	0.002
<b>+Control-Cu↓13.46</b>	gi 405961702	K1Q801	Myosin regulatory light chain A, smooth adductor muscle	Cy/P	2.28E-04	3.06E-03	0.002
<b>-Control+Cu↑13.2</b>	gi 405957027	K1Q324	Heterogeneous nuclear ribonucleoprotein K	transcription	3.59E-03	2.72E-04	0.008
<b>-Control+Cu↑12.6</b>	gi 405970092	K1QDM2	26S proteasome non-ATPase regulatory subunit 2	protein metabolic process	3.27E-04	2.59E-05	0.001
<b>-Control+Cu↑11.9</b>	gi 405971144	K1QQB3	Glycyl-tRNA synthetase	translation	3.54E-04	2.97E-05	0.000
<b>+Control-Cu↓11.9</b>	gi 405971258	K1QY95	Alanopine dehydrogenase 2	lipid metabolism	1.64E-04	1.95E-03	0.009
<b>-Control+Cu↑11.4</b>	gi 405977054	K1S2I2	Kinesin heavy chain	Cy/P	2.73E-04	2.39E-05	0.006

Ratio of differential expression <sup>a,b</sup>	Identifier	Uniprot AC	Protein name	BP category	Average NSAF Metal	Average NSAF Control	p value
-Control+Cu↑11.42	gi 405959834	K1QW72	Catalase	cell redox homeostasis	7.47E-04	6.54E-05	0.006
-Control+Cu↑11.32	gi 405951823	K1P7P6	Glutamate decarboxylase-like protein 1	carbohydrate metabolism	9.96E-04	8.79E-05	0.009
-Control+Cu↑11.1	gi 405965139	K1Q9D7	Sorting nexin-2	protein metabolic process	1.46E-03	1.32E-04	0.004
+Control-Cu↓11	gi 405963559	K1PY28	Sarcoplasmic calcium-binding protein 2	signal transduction	7.91E-04	8.69E-03	0.019
-Control+Cu↑10.62	gi 405950221	K1Q9V3	V-type proton ATPase subunit A	energy metabolism	3.76E-04	3.54E-05	0.008
-Control+Cu↑10.61	gi 405953774	K1PRB5	Tyrosyl-tRNA synthetase, cytoplasmic	translation	6.48E-04	6.11E-05	0.006
-Control+Cu↑10.12	gi 405961297	K1PZP6	Coatomer subunit gamma	transport	2.60E-04	2.57E-05	0.000
-Control+Cu↑9.8	gi 405952464	K1PF96	Spliceosome RNA helicase BAT1	transcription	4.43E-04	4.52E-05	0.011
-Control+Cu↑9.8	gi 405963058	K1R466	T-complex protein 1 subunit gamma	protein metabolic process	3.84E-04	3.92E-05	0.011
-Control+Cu↑9.8	gi 405966541	K1QSB0	Fructose-1,6-bisphosphatase 1	carbohydrate metabolism	6.67E-04	6.81E-05	0.006
-Control+Cu↑9.5	gi 405964042	K1QET2	Coatomer subunit alpha	transport	2.89E-04	3.04E-05	0.008
Cu↑9.36	gi 405959342	K1QUZ1	Putative aminopeptidase W07G4.4	protein metabolic process	1.08E-03	1.15E-04	0.005
-Control+Cu↑9.3	gi 405967652	K1QFW9	Uncharacterized protein	signal transduction	2.66E-03	2.85E-04	0.032
-Control+Cu↑9.2	gi 405972789	K1QL67	60S ribosomal protein L7a	translation	4.67E-03	5.07E-04	0.000
Cu↑8.9	gi 405978082	K1QZI3	Myosin-Ie	Cy/P	6.83E-04	7.71E-05	0.047
Cu↑8.8	gi 405967698	K1Q7T5	Protein disulfide-isomerase A3	cell redox homeostasis	2.37E-03	2.69E-04	0.006
-Control+Cu↑8.71	gi 405962038	K1PTY5	Protocadherin Fat 4	Cy/P	1.29E-04	1.48E-05	0.001
+Control-Cu↓8.6	gi 405969780	K1RKC1	Far upstream element-binding protein 3	RNA binding	2.79E-04	2.41E-03	0.018
-Control+Cu↑8.3	gi 405964146	K1Q6X5	Protein disulfide-isomerase	protein metabolic process	1.54E-03	1.86E-04	0.017
-Control+Cu↑8.13	gi 405962909	K1QBJ5	G protein-coupled receptor kinase 1	signal transduction	2.24E-04	2.75E-05	0.006
-Control+Cu↑7.66	gi 405961646	K1R0Y9	ADP,ATP carrier protein	transport	2.73E-03	3.57E-04	0.047
-Control+Cu↑7.62	gi 405957670	A7M7T7	Non-selenium glutathione peroxidase (Peroxiredoxin-6)	cell redox homeostasis	2.07E-02	2.72E-03	0.019
-Control+Cu↑7.48	gi 405950485	K1QAF2	Tyrosine-protein kinase HTK16	signal transduction	2.03E-04	2.71E-05	0.006
-Control+Cu↑7.5	gi 405974949	K1RXA0	cAMP-dependent protein kinase regulatory subunit	signal transduction	4.17E-04	5.58E-05	0.001

Ratio of differential expression <sup>a,b</sup>	Identifier	Uniprot AC	Protein name	BP category	Average NSAF Metal	Average NSAF Control	p value
-Control+Cu↑7.31	gi 405950642	K1QAV0	Guanine nucleotide-binding protein G(Q) subunit alpha	signal transduction	4.44E-04	6.07E-05	0.015
-Control+Cu↑7.31	gi 405950693	K1PIH2	V-type proton ATPase subunit E	energy metabolism	6.17E-04	8.44E-05	0.015
-Control+Cu↑7.3	gi 405964521	K1Q0N6	Dolichyl-diphosphooligosaccharide-protein glycosyltransferase subunit STT3A	glycan biosynthesis and metabolism	2.36E-04	3.23E-05	0.004
-Control+Cu↑7.1	gi 405976915	K1R6F1	Proteasome subunit alpha type (EC 3.4.25.1)	protein metabolic process	4.18E-03	5.87E-04	0.009
-Control+Cu↑6.9	gi 405978841	A5LGH1	Voltage-dependent anion channel (Voltage-dependent anion-selective channel protein 2)	signal transduction	3.76E-03	5.42E-04	0.006
-Control+Cu↑6.5	gi 405972436	K1R7N7	Cystatin-A2	protein metabolic process	7.89E-03	1.21E-03	0.002
Cu↑5.5	gi 405976470	K1S151	Rab GDP dissociation inhibitor beta	signal transduction	3.87E-03	7.09E-04	0.016
Cu↓5.2	gi 405963560	K1Q5G7	Sarcoplasmic calcium-binding protein 1	signal transduction	7.32E-04	3.84E-03	0.001
-Control+Cu↑5.1	gi 405977322	K1RJH5	Polyadenylate-binding protein 4	translation	2.62E-04	5.13E-05	0.016
Cu↑4.85	gi 405950190	K1P339	Vinculin	Cy/P	1.26E-03	2.60E-04	0.048
+Control-Cu↓4.84	gi 405961968	K1QFS4	Actin-related protein 2	Cy/P	4.96E-04	2.40E-03	0.007
-Control+Cu↑4.42	gi 405952700	K1PW08	Glycogen debranching enzyme	carbohydrate metabolism	1.26E-04	2.84E-05	0.026
-Control+Cu↑4.11	gi 405962772	K1Q3C4	Ras suppressor protein 1	signal transduction	6.21E-04	1.51E-04	0.038
Cu↑3.97	gi 405959090	K1PU26	Malate dehydrogenase	carbohydrate metabolism	2.51E-03	6.32E-04	0.028
Cu↑3.91	gi 405955275	K1PEZ6	Kyphoscoliosis peptidase	protein metabolic process	5.85E-03	1.50E-03	0.009
Cu↑3.66	gi 405953867	K1PCA0	Septin-7	cell cycle	1.62E-03	4.43E-04	0.002
+Control-Cu↓3.6	gi 405971646	K1RQ26	Potassium voltage-gated channel subfamily H member 7	signal transduction	1.53E-04	5.51E-04	0.006
Cu↑3.35	gi 405954086	K1PCV0	Severin	Cy/P	5.90E-03	1.76E-03	0.046
+Control-Cu↓3.16	gi 405961891	K1Q8F7	Alpha-crystallin B chain	protein metabolic process	2.34E-04	7.40E-04	0.033
Cu↑2.6	gi 405976318	K1RH70	6-phosphogluconate dehydrogenase, decarboxylating (EC 1.1.1.44)	carbohydrate metabolism	3.95E-03	1.52E-03	0.030
Cu↑2.6	gi 405963584	K1R5F2	14-3-3 protein epsilon	signal transduction	1.14E-02	4.45E-03	0.013
Cu↓2.44	gi 405958790	K1PLF9	Arginine kinase	amino acid metabolism	3.06E-03	7.47E-03	0.026

Ratio of differential expression <sup>a,b</sup>	Identifier	Uniprot AC	Protein name	BP category	Average NSAF Metal	Average NSAF Control	p value
Cu↓1.7	gi 405964323	K1QLW5	Extracellular superoxide dismutase [Cu-Zn]	cell redox homeostasis	2.33E-01	3.93E-01	0.026
<b>Proteins in response to Pb stress only</b>							
-Control+Pb↑208.4	gi 405973339	K1QWP8	Actin-2	Cy/P	8.07E-02	3.87E-04	0.000
+Control-Pb↓75.6	gi 405967637	K1QNV6	Tropomyosin	Cy/P	8.33E-05	6.30E-03	0.000
-Control+Pb↑29.2	gi 405964878	K1QN79	40S ribosomal protein S11	translation	3.46E-03	1.18E-04	0.003
-Control+Pb↑20.25	gi 405952804	K1QGB4	40S ribosomal protein S17	translation	3.27E-03	1.62E-04	0.002
-Control+Pb↑19.29	gi 405955817	K1PUV4	40S ribosomal protein S24	translation	2.39E-03	1.24E-04	0.000
-Control+Pb↑12.55	gi 405953356	K1QHF0	40S ribosomal protein S27	translation	2.88E-03	2.30E-04	0.001
-Control+Pb↑10.15	gi 405957760	Q70MT4	40S ribosomal protein S10 (Ribosomal protein S10)	translation	1.47E-03	1.45E-04	0.005
-Control+Pb↑10.1	gi 405965901	K1RB07	60S ribosomal protein L27a	translation	6.37E-04	6.32E-05	0.001
-Control+Pb↑7.9	gi 405965410	K1Q2Y1	40S ribosomal protein S15	translation	1.09E-03	1.38E-04	0.014
-Control+Pb↑7.1	gi 405968450	K1QA13	Calcium-transporting ATPase sarcoplasmic/endoplasmic reticulum type	signal transduction	1.68E-04	2.36E-05	0.027
Pb↑7.1	gi 405971745	K1R5V4	GTP-binding nuclear protein Ran	signal transduction	3.37E-03	4.75E-04	0.044
-Control+Pb↑6.7	gi 405969319	K1QZJ6	Uncharacterized protein (Fragment)	signal transduction	8.69E-04	1.30E-04	0.015
-Control+Pb↑5.8	gi 405977517	K1RK12	40S ribosomal protein S23	translation	1.89E-04	3.29E-05	0.001
-Control+Pb↑5.48	gi 405962281	K1Q227	Sacsin	translation	6.31E-04	1.15E-04	0.035
-Control+Pb↑5.5	gi 405975834	K1RZE2	Isocitrate dehydrogenase [NADP] (EC 1.1.1.42)	carbohydrate metabolism	1.77E-03	3.22E-04	0.011
-Control+Pb↑5.24	gi 405958969	K1PM50	40S ribosomal protein S16	translation	1.49E-03	2.84E-04	0.039
Pb↑5.2	gi 405968827	K1RI08	60S ribosomal protein L6	translation	4.39E-03	8.51E-04	0.005
-Control+Pb↑5.1	gi 405966326	K1QRZ3	40S ribosomal protein S13	translation	2.04E-03	3.99E-04	0.035
+Control-Pb↓4.7	gi 405976463	K1RBC9	Transketolase-like protein 2	carbohydrate metabolism	4.38E-04	2.05E-03	0.036
-Control+Pb↑4.47	gi 405952131	K1P8D9	SH3 domain-binding glutamic acid-rich-like protein 3	protein metabolic process	1.63E-03	3.64E-04	0.041
-Control+Pb↑4.1	gi 405977575	K1R8C6	40S ribosomal protein S12	translation	4.40E-03	1.09E-03	0.009
<b>Proteins in response to Zn stress only</b>							
-Control+Zn↑92.1	gi 405965393	K1QPJ1	Actin, cytoplasmic	Cy/P	3.68E-02	3.99E-04	0.000
-Control+Zn↑24.7	gi 405961865	K1R1M7	Ubiquitin-like modifier-activating enzyme 1	protein metabolic process	5.90E-04	2.39E-05	0.000
-Control+Zn↑23.8	gi 405965171	K1Q2H5	Uncharacterized protein	unknown	8.52E-04	3.59E-05	0.000

Ratio of differential expression <sup>a,b</sup>	Identifier	Uniprot AC	Protein name	BP category	Average NSAF Metal	Average NSAF Control	p value
+Control-Zn↓23.3	gi 405966532	K1Q5A6	Tripartite motif-containing protein 2	protein metabolic process	5.06E-05	1.18E-03	0.001
-Control+Zn↑21.72	gi 405959640	K1PVA1	Transitional endoplasmic reticulum ATPase	protein metabolic process	1.05E-03	4.83E-05	0.004
-Control+Zn↑21.1	gi 405976041	K1RGQ0	Ras-related C3 botulinum toxin substrate 1	signal transduction	2.76E-03	1.31E-04	0.012
-Control+Zn↑14.8	gi 405970591	K1QWC6	Universal stress protein A-like protein	response to stress	2.13E-03	1.44E-04	0.022
+Control-Zn↓14.6	gi 405975785	K1RZ99	Filamin-A	Cy/P	2.30E-04	3.37E-03	0.001
-Control+Zn↑14.55	gi 405950556	K1QAM7	Copine-7	transport	5.64E-04	3.88E-05	0.003
-Control+Zn↑12.72	gi 405949985	K1PGH0	Vacuolar protein sorting-associated protein 29	protein metabolic process	1.40E-03	1.10E-04	0.003
-Control+Zn↑12	gi 405978684	K1RH30	Collagen alpha-1(IV) chain	Cy/P	1.24E-03	1.03E-04	0.006
-Control+Zn↑11.6	gi 405963909	K1R647	Lactoylglutathione lyase	carbohydrate metabolism	1.32E-03	1.14E-04	0.000
-Control+Zn↑11.5	gi 405966599	K1Q5G6	60 kDa heat shock protein, mitochondrial	response to stress	4.50E-04	3.92E-05	0.002
-Control+Zn↑10.9	gi 405971077	K1QQ16	AP-2 complex subunit beta	transport	4.70E-04	4.31E-05	0.024
-Control+Zn↑10.8	gi 405963253	K1QCF5	Fumarate hydratase class I, aerobic	energy metabolism	4.03E-04	3.72E-05	0.001
-Control+Zn↑10.7	gi 405949998	K1P2H1	Fatty acid-binding protein, adipocyte	transport	1.76E-03	1.64E-04	0.007
-Control+Zn↑10.68	gi 405957444	K1PPW8	Coatamer subunit beta	transport	2.99E-04	2.80E-05	0.047
-Control+Zn↑10.3	gi 405974897	K1R7F8	Peroxisomal protein 5, mitochondrial	cell redox homeostasis	1.45E-03	1.41E-04	0.001
+Control-Zn↓10	gi 405966986	K1QTC1	Paramyosin	Cy/P	2.14E-04	2.13E-03	0.001
-Control+Zn↑9.8	gi 405962570	K1QAB1	AP-2 complex subunit alpha-2	transport	2.09E-04	2.13E-05	0.042
-Control+Zn↑9.6	gi 405976181	K1QV25	Transcription elongation factor B polypeptide 2	protein metabolic process	1.76E-03	1.84E-04	0.013
-Control+Zn↑9.49	gi 405958953	K1PM29	Glucose-6-phosphate 1-dehydrogenase (EC 1.1.1.49)	carbohydrate metabolism	6.74E-04	7.10E-05	0.034
-Control+Zn↑9.4	gi 405964801	K1Q1A5	Glycogen phosphorylase	carbohydrate metabolism	6.15E-04	6.54E-05	0.012
Zn↑9.2	gi 405974681	K1QQR1	Major vault protein	Cy/P	1.59E-03	1.73E-04	0.002
-Control+Zn↑9.09	gi 405961849	K1PZ08	Ras-related protein Rab-7a	signal transduction	2.68E-03	2.94E-04	0.023
-Control+Zn↑9	gi 405970601	K1QWE5	Ras-related protein Rab-18-B	signal transduction	9.35E-04	1.03E-04	0.031
-Control+Zn↑8.76	gi 405962347	K1PUQ5	Histone H2B	nucleosome assembly	1.88E-02	2.14E-03	0.015
-Control+Zn↑8.00	gi 405962731	K1QHR5	Uncharacterized protein	protein metabolic process	5.20E-04	6.50E-05	0.033
-Control+Zn↑7.8	gi 405965438	K1QI14	40S ribosomal protein S3a	translation	6.16E-04	7.88E-05	0.008

Ratio of differential expression <sup>a,b</sup>	Identifier	Uniprot AC	Protein name	BP category	Average NSAF Metal	Average NSAF Control	p value
-Control+Zn↑7.7	gi 405968717	K1QIZ7	Programmed cell death protein 6	protein metabolic process	8.19E-04	1.06E-04	0.001
-Control+Zn↑7.65	gi 405953427	K1PXH5	Putative saccharopine dehydrogenase	amino acid metabolism	1.70E-04	2.22E-05	0.010
-Control+Zn↑7.6	gi 405973087	K1R2P2	SH3 domain-binding glutamic acid-rich protein	cell redox homeostasis	3.05E-04	4.00E-05	0.000
-Control+Zn↑7.6	gi 405969976	K1QUG6	Uncharacterized protein	unknown	1.13E-03	1.48E-04	0.001
-Control+Zn↑7.4	gi 405972362	K1R7I9	Heterogeneous nuclear ribonucleoprotein Q	transcription	6.67E-04	8.98E-05	0.047
-Control+Zn↑7	gi 405965094	K1R973	Chloride intracellular channel exc-4	transport	4.95E-04	7.11E-05	0.006
-Control+Zn↑6.75	gi 405947752	K1PG60	60S ribosomal protein L17	translation	1.19E-03	1.76E-04	0.003
-Control+Zn↑6.7	gi 405963180	K1PWR0	Protein SET	nucleosome assembly	5.60E-04	8.32E-05	0.017
Zn↑6	gi 405968237	K1QHH8	Putative 10-formyltetrahydrofolate dehydrogenase ALDH1L2	one carbon metabolic process	5.96E-04	9.87E-05	0.000
-Control+Zn↑5.98	gi 405957279	K1PPF4	NADH dehydrogenase [ubiquinone] iron-sulfur protein 4, mitochondrial	energy metabolism	7.13E-04	1.19E-04	0.003
-Control+Zn↑5.95	gi 405947958	K1PN47	Succinate dehydrogenase [ubiquinone] iron-sulfur subunit, mitochondrial	carbohydrate metabolism	6.63E-04	1.11E-04	0.012
-Control+Zn↑5.8	gi 405970027	K1R1E2	Actin-related protein 2/3 complex subunit 2	Cy/P	2.15E-03	3.73E-04	0.037
-Control+Zn↑5.49	gi 405957134	K1PHC4	Fibroleukin	Cy/P	1.26E-03	2.29E-04	0.040
Zn↑5.4	gi 405974790	K1RWW5	ATP synthase subunit beta (EC 3.6.3.14)	energy metabolism	4.92E-03	9.18E-04	0.014
Zn↑4.74	gi 405954100	K1PJ59	Triosephosphate isomerase (EC 5.3.1.1)	carbohydrate metabolism	2.80E-03	5.92E-04	0.034
-Control+Zn↑4.7	gi 405966436	K1QCM0	Rho GDP-dissociation inhibitor 1	signal transduction	1.55E-03	3.31E-04	0.020
-Control+Zn↑4.7	gi 405964694	K1Q122	Myosin regulatory light chain sqh	Cy/P	8.06E-04	1.73E-04	0.012
-Control+Zn↑4.6	gi 405971056	K1QGA2	Flotillin-2	signal transduction	3.19E-04	6.86E-05	0.008
Zn↑4.3	gi 405977015	K1QX44	Ras-related protein Rab-11B	signal transduction	4.36E-03	1.03E-03	0.020
Zn↑4	gi 405973516	K1R401	Spectrin alpha chain	Cy/P	8.45E-04	2.10E-04	0.021
Zn↑3.2	gi 405974703	K1R6Z7	ATP synthase subunit alpha	energy metabolism	1.92E-03	5.99E-04	0.005
-Control+Zn↑3.12	gi 405952673	K1P9L2	Myophillin-1	Cy/P	1.03E-03	3.31E-04	0.047
Zn↑2.4	gi 405975071	K1QRW4	Coronin	transport	1.20E-03	4.96E-04	0.009
Zn↑1.99	gi 405959361	K1PN21	Tubulin beta chain	Cy/P	4.61E-02	2.31E-02	0.038
Proteins in response to lead and copper							

Ratio of differential expression <sup>a,b</sup>	Identifier	Uniprot AC	Protein name	BP category	Average NSAF Metal	Average NSAF Control	p value
- Control+Pb↑166.1; - Control+Cu↑143.26	gi 405965638	K1QQ68	Tubulin alpha-1C chain	Cy/P	8.68E-03	5.22E-05	0.001
-Control+Cu↑55.4; -Control+Pb↑7.1	gi 405968450	K1QA13	Calcium-transporting sarcoplasmic ATPase	signal transduction	1.25E-03	2.26E-05	0.000
- Control+Cu↑51.28; -Control+Pb↑15.96	gi 405950430	K1PPQ1	14-3-3 protein gamma	signal transduction	4.51E-03	8.79E-05	0.000
Pb↑5.6; Cu↑4.9	gi 405978203	K1RA77	Ubiquitin		1.76E-03	3.15E-04	0.007
<b>Proteins in response to copper and zinc</b>							
- Control+Cu↑39.44; -Control+Zn↑20.96	gi 405961963	K1QFR9	Spectrin beta chain	Cy/P	5.92E-04	1.50E-05	0.005
- Control+Cu↑30.19; -Control+Zn↑24.26	gi 405959469	K1Q2B5	Talin-1	Cy/P	1.24E-03	4.11E-05	0.001
- Control+Cu↑17.63; -Control+Zn↑6.5	gi 405957030	K1PNK5	Ras GTPase-activating-like protein IQGAP1	signal transduction	6.79E-04	3.85E-05	0.022
- Control+Cu↑16.54; Control+Zn↑6.17	gi 405960427	K1PQ23	PDZ and LIM domain protein 5	unknown	7.51E-04	4.54E-05	0.002
- Control+Cu↑16.11; -Control+Zn↑10.18	gi 405959086	K1Q1D1	UTP--glucose-1-phosphate uridylyltransferase	carbohydrate metabolism	7.06E-04	4.38E-05	0.001
-Control+Cu↑13.1; -Control+Zn↑10.9	gi 405964355	K1Q056	Calpain-A	protein metabolic process	2.86E-04	2.18E-05	0.008
-Control+Cu↑9.59; -Control+Zn↑4.19	gi 405951856	K1PTI6	Glucose-6-phosphate isomerase (EC 5.3.1.9)	carbohydrate metabolism	5.66E-04	5.90E-05	0.003
-Control+Cu↑9.15; -Control+Zn↑7.05	gi 405960244	K1QBI9	Cytosolic purine 5'-nucleotidase	purine metabolism	3.56E-04	3.90E-05	0.011
-Control+Cu↑8.6; - Control+Zn↑6	gi 405971461	K1RPF7	60S ribosomal protein L5	translation	5.39E-04	6.27E-05	0.001
Cu↓7.22; Zn↓5.97	gi 405959333	K1PUI8	Fibrinogen C domain-containing protein 1 (Fragment)	immune response	1.46E-03	1.06E-02	0.003
Cu↑5.7; Zn↑4.3	gi 405973142	K1QLZ1	Actin-related protein 3	Cy/P	1.86E-03	3.26E-04	0.024
Cu↑4.4; Zn↑1.8	gi 405969875	K1R115	Succinate dehydrogenase [ubiquinone] flavoprotein subunit B, mitochondrial	carbohydrate metabolism	1.67E-03	3.82E-04	0.009
Cu↑3.82; Zn↑3.26	gi 405958653	K1QT31	Uncharacterized protein	unknown	1.71E-03	4.49E-04	0.003
Cu↑3.41; Zn↑1.96	gi 405962873	K1PW06	Filamin-C	Cy/P	6.73E-03	1.97E-03	0.005
+Control-Cu↓3.3; Zn↑2.7	gi 405963261	K1PWZ3	Guanine nucleotide-binding protein subunit beta	signal transduction	8.99E-04	2.97E-03	0.009
Cu↑2.82; Zn↑1.99	gi 405957058	K1Q350	Glyceraldehyde-3-phosphate dehydrogenase	carbohydrate metabolism	3.51E-02	1.24E-02	0.001
-Control+Zn↑37.2; -Control+Cu↑24.8	gi 405972993	K1QVS0	Ras-like GTP-binding protein Rho1	signal transduction	2.41E-03	6.48E-05	0.001

Ratio of differential expression <sup>a,b</sup>	Identifier	Uniprot AC	Protein name	BP category	Average NSAF Metal	Average NSAF Control	p value
- Control+Zn↑20.83; -Control+Cu↑16.51	gi 405962453	K1PJ53	Cdc42-like protein	signal transduction	2.29E-03	1.10E-04	0.014
- Control+Zn↑18.84; -Control+Pb↑14.30	gi 405961802	K1PTH4	ADP-ribosylation factor	signal transduction	3.55E-04	1.88E-05	0.002
- Control+Zn↑15.43; -Control+Cu↑10.0	gi 405951708	K1PDL3	Ribosomal protein L19	translation	1.54E-03	9.95E-05	0.003
- Control+Zn↑14.65; -Control+Cu↑9.79	gi 405950592	K1PQD4	Phosphoglucosyltransferase-1	carbohydrate metabolism	5.29E-04	3.61E-05	0.008
-Control+Zn↑14.2; -Control+Cu↑10.6	gi 405977633	K1QYM7	1,4-alpha-glucan-branching enzyme	carbohydrate metabolism	4.21E-04	2.95E-05	0.000
-Control+Zn↑12.9; -Control+Cu↑7.8	gi 405970574	K1QNG9	60S ribosomal protein L23a	translation	2.73E-03	2.12E-04	0.017
-Control+Zn↑11.7; -Control+Cu↑11.4	gi 405965075	K1QNT7	Aldehyde dehydrogenase, mitochondrial	carbohydrate metabolism	1.75E-03	1.49E-04	0.009
+Control-Zn↓5; +Control-Cu↓4.7	gi 405973417	K1R3V1	Neurotrypsin	protein metabolic process	2.47E-04	1.24E-03	0.001
Zn↑3.72; Cu↑3.32	gi 405952674	K1PFT9	Myophilin-2	Cy/P	5.77E-03	1.55E-03	0.000
Zn↑3.5; Cu↑2.7	gi 405965040	K1Q948	Phosphorylase (EC 2.4.1.1)	carbohydrate metabolic process	2.33E-03	6.71E-04	0.011
<b>Proteins in response to lead and zinc</b>							
+Control-Pb↓9.9; +Control-Zn↓8.3	gi 405975056	K1QRU8	Myosin heavy chain, striated muscle	Cy/P	1.89E-05	1.87E-04	0.007
-Control+Pb↑35.1; -Control+Zn↑14.1	gi 405974492	K1QQB6	40S ribosomal protein S14	translation	5.64E-03	1.61E-04	0.000
- Control+Pb↑16.19; -Control+Zn↑9.31	gi 405961012	K1QDI4	Superoxide dismutase [Fe-Mn]	response to stress	2.66E-03	1.65E-04	0.002
Pb↑15; Zn↑9	gi 405965232	K1Q2L2	60S ribosomal protein L12	translation	8.34E-03	5.57E-04	0.001
-Control+Pb↑13.1; -Control+Zn↑9.5	gi 405967540	K1QFN1	60S ribosomal protein L23	translation	2.23E-03	1.70E-04	0.011
Pb↑5; Zn↑3.8	gi 405978782	K1RHA5	Nucleoside diphosphate kinase (EC 2.7.4.6)	energy metabolism	4.67E-03	9.42E-04	0.020
<b>Proteins in response to lead, copper and zinc</b>							
-Control+Cu↑37.8; -Control+Zn↑29.3; -Control+Pb↑7	gi 405963233	K1QCC1	Phosphoglycerate kinase	carbohydrate metabolism	4.27E-03	1.13E-04	0.001
Cu↑3.4; Pb↑3.4; Zn↑3.9	gi 405974805	K1R781	Muscle LIM protein Mlp84B	Cy/P	5.65E-03	1.65E-03	0.009
Cu↑2.5; Zn↑2.2; - Control+Pb↑7.9	gi 405968607	K1QIR8	78 kDa glucose-regulated protein	response to stress	1.59E-03	6.43E-04	0.007
Cu↓2.2; Zn↓2; Pb↑1.4	gi 405967949	K1QGS8	Elongation factor 1-alpha	translation	3.21E-03	7.14E-03	0.042

## Appendix D

**Appendix D1 Protein and peptide identification and quantitation data for the 12 differentially expressed proteins in amphipods exposed to Zn conditions in 25‰ seawater-only in comparison to non-exposed controls.**

Trend <sup>‡</sup>	Gel spot/s	Prot loge	Fold change	Unique peptides	Total peptides	Gene Identifier	Protein name	Peptide sequence from spectra
↑; except 122 ↓	50, 256, 391, 122, 319, 54, 341	-55.1	3.7	24	31	gi 3907620 ; cytoskeleton and protein polymerization	Actin	VAPEESPVLLTEAPLNPK TTGIVLDTGDGVTHTVPIYEGYALPHAILR SYELPDGQVITIGNER EITALAPSTIK TTGIVLDSGDGVSHTVPIYEGYALPHAILR DLYANIVMSGGTTMYPGIADR DLYANNVLSGGTTMYPGIADR KDLFANIVMSGGTTMYPGIADR DLFANIVMSGGTTMYPGIADR TTGIVLDSGDGVTHTVPIYEGYALPHAILR VAPEDDPVLLTEAPLNPK MKCDVDIRKDLYGNIIVMSGGTTMYPGIADR CYTALNFEREMATAAASSSLEK DLYANNVMSGGTTMYPGIADR SYELPDGKVITIGNER AAHSSAIEKSYELPDGQVITIGNER KDLYANIVMSGGTTMYPGIADR LSGXTTMYPGIADR SFYNELRVAPPEESPVLLTEAPLNPK GYSFTTTAER TFYNELRVAPPEELPVLLTEAPLNPK CHTVPIYEGYALPHAILR TTGIVLDSXDGVSHTVPIYEGYALPHAILR SYKLDPGQVITIGNER
↑	50	-4.2	3.7	1	3	gi 84686589 ; protein metabolism	ATP-dependent protease ATP-binding subunit	EGASAG
↑	50, 256, 319	-4.7	3.7	1	2	gi 14285796 ; cytoskeleton and protein polymerization	Tropomyosin	SITDELDTFSELSGY
↑	54, 341	-21.3	3.4	1	2	gi 6682323 ; cytoskeleton and protein polymerization	catchin	LDEAGGATSAQIELNK ALDSMQASLEAEAK
↑	54, 63, 66, 341	-18	2.2-3.4	23	35	gi 195386602 ; cytoskeleton and protein polymerization	myosin heavy chain	TLHSTSPHFIR DIEDLELSVQK LTQEA VSDLER ALDSMQASLEAEAK LDEAGGATSAQIELNK IQEKEEEFDNTR QEVDRRIQEKEEEFDNTR IQEKEEEFDNTR NLNDEIAHQDELINK LEEAGGATSAQIELNK VDDLAAELDASQKECR MQDLVDKLQKQ QIEEAEIEAALNLAK AQQELEEAEER DIEDLELSVQKSEQDKATK LEDEQSLVSK EQVEEEAEAKADIQR MKVDDLAAELDASQKECR MKVDDLAAELDASQK AIDSMQASLEAEAK RANALHGELEESR RANALHGELEESR LASEYREQYGIAER
↑	319, 256, 391, 54, 341	-69	2.7	15	24	gi 190014502 ; carbohydrate metabolism	glyceraldehyde-3-phosphate dehydrogenase	VIISAPSADAPMFVM DMTIVSNASCTTNCLAPIAK LTGMAFRVPTPD VPTPDVSVVDLTVR VVSWDNEYGYSNR LVSWYDNEYGYSNR YDSTHGVEFKGEVK GAEVAVNDPF VIISAPSADAPMFVMGVN GAGQNIIPSSGAAK SLKVVSNASCTTNCLAPLAK VIISAPSADAPMFVMGVNNKDYTK VIISAPSADAPMYVMGVN VIISAPSADAPMYVM TSDTVVSNASCTTNCLALAK

## Appendix D1 (continued)

Trend ‡	Gel spot/s	Prot loge	Fold change	Unique peptides	Total peptides	Gene Identifier	Protein name	Peptide sequence from spectra
↑	69	-3.3	2.7	1	4	gi 442605 ; carbohydrate metabolism	Glycogen phosphorylase B	GMAFSLEER
↑	256	-9.1	2.4	2	6	gi 195146792  ; carbohydrate metabolism	Malate dehydrogenase	IFKAQGQAIENFAK AQGQAIENFAK
↑	256	-4.1	2.4	1	2	gi 125809382  ; RNA metabolism	Serine threonine kinase associated protein	FSPDGELYASGSEDGTLR
↑	339	-5.1	2.3	2	2	gi 212514462  ; signal transduction	guanine nucleotide- binding protein G(I)/G(S)/G(T), subunit beta,	ELPGHTGYLSCCR QTTPGHESDINAVTFFPNGQAFATGSDDATC
↑	391	-3.8	2.1	1	2	gi 125774917  ; protein metabolism	T-complex protein subunit α	YFVEAGAMAVR
↑	391	-7.6	2.1	2	5	gi 187608085  ; carbohydrate metabolism	Malic enzyme	LNKGMAFSLEER GMAFSLEER
‡ Up and down regulation of proteins in response to metal stress relative to controls have been indicated by an upward arrow, '↑' and a downward arrow, '↓' respectively								

**Appendix D2 Protein and peptide identification and quantitation data for the 35 differentially expressed proteins in amphipods exposed to 30ppb Zinc on silica substrate in 25‰ seawater-only in comparison to non-exposed controls.**

Trend <sup>‡</sup>	Gel spot/s	Protein log(e)	Fold change	Unique peptide count	Total peptide count	Gene Identifier	Protein name	Peptide sequence from spectra
↓	244, 225, 206, 218	-121.4	2.0-3.0	27	71	gi 17137090 ; cytoskeleton and protein polymerization	actin, cardiac muscle	EIVRDIKEKLCYVALDFEQEMATAAASTA- -LEKSYELPDGQVITIGNER ELTALAPSTMKIK AGFAGDDAPR AVFPSIVGRPR HQQVMVGMGQKDAYVGDEAQ SKR HQQVMVGMGQK DAYVGDEAQSKR DAYVGDEAQSKR DAYVGDEAQSKR IWHHTFYNEL R TTGIVLDSGDGVSHTVPIYEGYALPHAILR GYSFTTTAER SYELPDGQVITIGNER MQKEITSLAPSTIK EITSLAPSTI K VSPLVVDNGSGMVK VAPEESPVLLEAPLNPK DLTAYLMK DLFANIVMSG GTTMYPGIADR VAPEDDPVLLTEAPLNPK VGMGHKDAYVGDEAQSKR APEDDSILLT EAPLNPK VAPEEQPVLL TEAPLNPK TYELPDGQVI TIGNER EITALAPSTI K TTGIVLDSGDGVTHTVPIYE GYALPHAILR EEYEESGPGI VHR VAPEESPILLTEAPLNPK
↓	244	-10	2.7	2	2	gi 134298203 ; Transport / energy metabolism	EmrB/QacA family drug resistance transporter	TSATTFRSIGGTGLGMTVLG LVMNHQSVE IPGLQSGPFSGMLTK
↓	244	-9.2	2.7	2	2	gi 71003470 ; RNA metabolism	Arm like folded protein	EFRRTKVTVMMSGASPYRRTQEKLSLC VTVMMSGASPYRR
↓	225	-3.6	2.7	1	2	gi 67541304 ; cell cycle	Cell morphogenesis protein	ALGVVG
↑	395	-9.7	2.0	2	2	gi 28872507 ; stress response	sigma-54 dependent transcriptional regulator	PPPGGG KHGLTFGDGSG GASDDND
↑	395	-14.7	2.0	1	1*	ZP_08710717 ; lipid metabolism	Glycerophosphodiesterase	GVDCVITNYPDLVRR (BLAST 4e-07, 100%, maxscore52.8)
↑	395	-13.5	2.0	1	1*	ZP_08651839 ; purine metabolism	GTP pyrophosphate synthetase	GSIPIDMAYSIHTDVGNSTTGAR (BLAST 3e-14, 100%, maxscore75.3)
↑	395	-3.5	2.0	1	1*	EKE41550 ; unknown	Hypothetical protein	SNKATIEIHK (BLAST0.00033, 100%, maxscore37.5)
↑	395	-13.0	2.0	1	1*	An08g08790 ; unknown	hypothetical protein	YSPSCNPNGSPRPEMLDFPTTR (BLAST 8e-15, 100%, Score76.6)
↑	395	-4.6	2.0	1	1*	gi 400533027 ; amino acid metabolism	Tryptophan/ tyrosine permease	GANGLCLMLDPATR (BLAST 2e-05, 100%, 47.5 score)
↓	416	-3.2	2.7	1	2	gi 148260158 ; purine metabolism	xanthine dehydrogenase	AGGDAP
↓	416	-3	2.7	1	2	gi 148257208 ; Transport / energy metabolism	ABC transporter permease	GPGGEA
↓	16	-4.1	2.7	2	2	gi 121709089 ; stress response	Conserved glycine rich protein	GGGGGGRGGG SSGGSSGGR LPPAGG
↑	354	-15.3	2.4	9	12	gi 190014502 ; carbohydrate metabolism	glyceraldehyde-3-phosphate dehydrogenase	VVSWYDNEYG YSNR GGRGAGQNII PSSTGA ECSYDDIKAAMK KVIISAPSAD APMFVMGVNH TSYTK GAGPTG YTTVGGVEGF DGSK GGDGSS GEDAPGLLVQ SIGGGGGR DGGGGGG VINDTFGIAD GLMTTVHSIT ATQK TAAGGP
↓	413	-5.1	2.8	1	3	gi 10304601 ; cell defense	T cell receptor immunoglobulin β	TAAGGP
↓	413	-3.3	2.8	1	2	gi 46122919 ; unknown	hypothetical protein	GGPSST

## Appendix D2 (continued)

Trend <sup>‡</sup>	Gel spot/s	Protein log(e)	Fold change	Unique peptide count	Total peptide count	Gene Identifier	Protein name	Peptide sequence from spectra
↓	413	-9.3	2.8	2	2	gi 212508796 ; protein metabolism	RNA-binding protein cabeza	GGFGRRGGPGDGGGGPGNPK GDGGGGP
↓	399	-9.2	2.6	3	2	gi 116196404 ; cell cycle	Lon protease homolog	ILCFVGPPGVGKTSIGK TTEKPRLPLKVPESVHVTIGKDNLD GAGSGSG
↓	399	-10.5	2.6	2	2	gi 67641091 ; replication and repair	DNA-damage-inducible protein F	GAATAT APSAAG
↑	432	-4.7	2.3	2	2	gi 67539214 ; lipid metabolism	Extracellular triacylglycerol lipase	GDLSGG GDGANG
↑	153	-4.1	2.2-2.7	1	4	gi 4758112 ; RNA metabolism	DEAD (Asp-Glu-Ala-Asp) box polypeptide 39B spliceosome RNA helicase	ILVATNLFGR
↓	186	-9.2	2.7	2	2	gi 71413014 ; RNA metabolism	ATP-dependent DEAD/H RNA helicase	ESGSSFAGNE AAAAVATMEK PAGDAS
↓	186	-10.7	2.7	2	2	gi 161597835 ; amino acid metabolism	arginine kinase	EMEDKVSSTL SGLEGELK LIDDFHFLFKE GDRFLQAANA CR
↓	186	-9.2	2.7	3	3	gi 7960186 ; stress response	heat shock protein 70	QATKDAGTIS GLNVLR GPGGSS MPGFPGGAPG AGGAAPGGGP GLASGS
↓	417	-4.4	2.4	1	2	gi 33313525 ; RNA metabolism	helicase-like protein	
↓	403	-3.5	2.6	1	2	gi 189208973 ; carbohydrate metabolism	phosphatidylinositol: UDP-GlcNAc transferase	GTDLLVAAIP HIVAANPNVR
↓, ↑	237, 486	-14.3	2.4-3.0	2	3	gi 52789 ; cytoskeleton and protein polymerization	cytokeratin	SLNNKFASFIDKVR GGGFGGGSSSF GGGSGFSGGG FGGGGFGGGR THNLEPYFESFINLRR
↓	61	-11.4	3.1	2	2	gi 194764709 ; unknown	GF23033	SGCGSGGGPG SGGPGPAAP GSGR GPGSGG
↓	61	-3.2	3.1	1	2	gi 156551463 ; lipid metabolism	DHHC palmitoyltransferase	SSSSSSSSSSSSGSSGSSR
↑	169	-42.3	2	19	19	gi 126002169 ; Transport/ energy metabolism	ATP synthase beta subunit	LVLEVAQHLGENTVR FTQAGSEVSALLGR LTIAEYFRDVEGQDVLLFIDNIFRFTQAG- -SEVSALLGR GIAELGIYPAVDPLDSTSR LVLEVAQHLGESTVRTIAMDATEGL- -VRGARVTDGSPISVPVGDAGR QIASLGIYPAVDPLDSTSR FTQAGSEVSALLGR DIAAQAIFFAVDPLDSTSR DVLLFVDNIFRFTQACSEVSALLGR TIAMDGTEGLVR GGKIGLFGGAGVGK ENVVRCIAMDGTEGLVR GGKIGLFGGAGVGKTVNMM GAAVSD ENVVRTIAMDGTEGLVR EGSITSIQAI YVPADDLTDPAPATTFAHLDAITVLSR GPGGSV LILEVAQHLGDSRVR LVVEVAQHLGENTVR
↑	39, 395	-92.6	2.6	10	15	gi 87045985 ; cytoskeleton and protein polymerization	Keratin	LQSSSASYGG FGFGGSCQLGGGR VRALEEANADLEV ALEEANADLEV ALEEANADLEV LKYENELALRQSV EADINGL VLAEMREQYEAMAER EVSTNTAMIQTSK TLQGLEIELQSLSMK ALEESNYELEGK SQYEQLAEQNRK
↓	419	-3.8	2.2	1	2	gi 58260822 ; replication and repair	DNA polymerase epsilon	AFEEGGAVAT VDEAK
↓	207	-3.2	2.6	1	4	gi 1703238 ; carbohydrate metabolism	Fructose-bisphosphate aldolase 1	KPWALTFSYG R
↓	424	-4.2	2.0	1	3	gi 212701532 ; cell defense	DNA processing protein DprA	EDNVAIIGAR AADK
↑	17	-3.1	2.0	1	2	gi 47766078 ; unknown	hypothetical protein	GGJGIR
↑	442		2.0				No identifications	
‡	Up and down regulation of proteins in response to <b>Zn</b> stress relative to controls <b>are</b> indicated by an upward arrow, '↑' and a downward arrow, '↓' respectively							

## **Appendix E**

## Appendix E Proteins uniquely expressed at different CO<sub>2</sub> treatments in WT and QXR Sydney rock oysters

### Appendix E1 Proteins uniquely expressed in QXR oysters only

Identifier	Uni-prot AC	Protein name	BP category
gi 405953356	K1QHF0	40S ribosomal protein S27	translation
gi 405953750	K1QI77	ATP synthase lipid-binding protein, mitochondrial	
gi 405957058	K1Q350	Glyceraldehyde-3-phosphate dehydrogenase	carbohydrate metabolism
gi 405959695	K1PNR3	Clathrin heavy chain 1	Transport
gi 405962686	K1PVF6	Proteasome subunit beta type	protein metabolic processes
gi 405963233	K1QCC1	Phosphoglycerate kinase	carbohydrate metabolism
gi 405964580	K1Q821	Actin, cytoplasmic	Cy/P
gi 405964938	K1R8Q5	Coactosin-like protein	defense response
gi 405965637	K1QII6	Tubulin alpha-1C chain	Cy/P
gi 405966177	K1QK18	Cytochrome b5	Energy metabolic processes
gi 405967149	K1QML1	Cysteine and glycine-rich protein 3	
gi 405967288	K1QF01	40S ribosomal protein S4, X isoform	translation
gi 405967540	K1QFN1	60S ribosomal protein L23	translation
gi 405969330	K1RJ70	Cytosolic non-specific dipeptidase	protein metabolic processes
gi 405969654	K1R0L4	Sodium/potassium-transporting ATPase subunit alpha	energy metabolism
gi 405970320	K1R278	Tubulin beta chain	Cy/P
gi 405970598	K1RM80	Citrate synthase	carbohydrate metabolism
gi 405971602	K1QZ29	Uncharacterized protein	
gi 405971745	K1R5V4	GTP-binding nuclear protein Ran	signal transduction
gi 405972882	K1R294	T-complex protein 1 subunit beta	protein folding
gi 405975834	K1RZE2	Isocitrate dehydrogenase	carbohydrate metabolism
gi 405976318	K1RH70	6-phosphogluconate dehydrogenase, decarboxylating (EC 1.1.1.44)	carbohydrate metabolism
gi 405976915	K1R6F1	Proteasome subunit alpha type (EC 3.4.25.1)	protein metabolic processes
gi 405977575	K1R8C6	40S ribosomal protein S12	translation
gi 405978841	A5LGH1	Voltage-dependent anion channel	transport/ signal transduction

**Appendix E2 Proteins present only WT oysters**

Identifier	Uni-prot AC	Protein name	BP category
gi 405954824	K1PE57	Severin	Cy/P
gi 405971658	K1QS40	Calcium-regulated heat stable protein1	transcription
gi 405973684	K1RUK6	Cathepsin B	protein metabolic processes

**Appendix E3 Proteins present in both all WT and QXR oysters**

Identifier	Uni-prot AC	Protein names	BP category
gi 405950098	K1P9N7	14-3-3 protein zeta	signal transduction
gi 405952674	K1PFT9	Myophilin	Cy/P
gi 405962347	K1PUQ5	Histone H2B	nucleosome assembly
gi 405962351	K1R2N0	Histone H4	nucleosome assembly
gi 405963427	K1R4Z3	Malate dehydrogenase, mitochondrial	carbohydrate metabolism
gi 405964579	K1Q0U8	Actin	Cy/P
gi 405964948	K1R8R6	Fructose-bisphosphate aldolase	carbohydrate metabolism
gi 405965232	K1Q2L2	60S ribosomal protein L12	translation
gi 405970739	K1R3A7	Dynein light chain 2, cytoplasmic	transport
gi 405972993	K1QVS0	Ras-like GTP-binding protein Rho1	signal transduction
gi 405974790	K1RWW5	ATP synthase subunit beta	energy metabolism
gi 405974897	K1R7F8	Peroxiredoxin-5, mitochondrial	oxidation reduction process
gi 405978782	K1RHA5	Nucleoside diphosphate kinase	energy metabolism

#### Appendix E4 Proteins present only in WT oysters exposed to hypercapnia

Identifier	Uniprot AC	Protein names	BP category
gi 405950284	K1Q9Z5	Peptidyl-prolyl cis-trans isomerase (EC 5.2.1.8)	protein folding
gi 405950429	K1PHM8	14-3-3 protein zeta	signal transduction
gi 405950795	K1PBC0	Non-neuronal cytoplasmic intermediate filament protein	Cy/P
gi 405951454	K1PSE7	Outer dense fiber protein 3unknown	Unknown
gi 405957004	K1PNI6	Heterogeneous nuclear ribonucleoprotein A/B	transcription
gi 405957528	K1PIB2	Uncharacterized protein	unknown
gi 405959274	K1PMU4	Uncharacterized protein	unknown
gi 405959327	K1PUI4	Uncharacterized protein	protein folding
gi 405962295	K1PUJ1	Radixin	Cy/P
gi 405962350	K1QGW2	Histone H3	nucleosome assembly
gi 405963180	K1PWR0	Protein SET	nucleosome assembly
gi 405964146	K1Q6X5	Protein disulfide-isomerase	oxidation reduction processes
gi 405964694	K1Q122	Myosin regulatory light chain sqh	Cy/P
gi 405965392	K1QHY0	Actin-3	Cy/P
gi 405966986	K1QTC1	Paramyosin	Cy/P
gi 405967637	K1QNV6	Tropomyosin	Cy/P
gi 405968607	K1QIR8	78 kDa glucose-regulated protein	response to stress
gi 405969523	K1QTD6	Catalase	response to stress
gi 405970995	K1R3T3	Transcription factor BTF3-like protein 4	transcription
gi 405971092	K1QGF9	Rootletin	organelle organization
gi 405972362	K1R7I9	Heterogeneous nuclear ribonucleoprotein Q	transcription
gi 405973812	K1R4R1	Coiled-coil domain-containing protein 19, mitochondrial	unknown
gi 405975242	K1R1X5	Calponin-2	Cy/P
gi 405975469	K1QTB9	Tektin-3	Cy/P
gi 405977263	K1QXS6	Heterogeneous nuclear ribonucleoprotein A2-like protein 1	transcription
gi 405977799	K1R8W3	S-phase kinase-associated protein 1	protein metabolic processes

**Appendix E5 Present only in QXR oysters exposed to hypercapnia**

Identifier	Uniprot AC	Protein names	BP category
gi 405957760	Q70MT4	40S ribosomal protein S10	translation
gi 405960791	K1Q5Y4	Small nuclear ribonucleoprotein-associated protein B	transcription
gi 405961968	K1QFS4	Actin-related protein 2	Cy/P
gi 405962479	K1QH58	Succinyl-CoA ligase subunit alpha	carbohydrate metabolism
gi 405962800	K1Q3F4	Inorganic pyrophosphatase	energy metabolism
gi 405965040	K1Q948	glycogen phosphorylase	carbohydrate metabolism
gi 405965075	K1QNT7	Aldehyde dehydrogenase, mitochondrial	oxidation reduction processes
gi 405968311	K1Q9G3	Isocitrate dehydrogenase subunit alpha, mitochondrial	carbohydrate metabolism
gi 405969724	K1QCS6	Ankyrin-1	transport
gi 405969917	K1R150	Ras-related protein Rab-1A	transport
gi 405976470	K1S151	Rab GDP dissociation inhibitor beta	transport
gi 405978203	K1RA77	Ubiquitin	protein metabolic processes

## References

- [1] Devier, M. H., Augagneur, S., Budzinski, H., Le Menach, K., *et al.*, One-year monitoring survey of organic compounds (PAHs, PCBs, TBT), heavy metals and biomarkers in blue mussels from the Arcachon Bay, France. *J Environ Monit* 2005, 7, 224-240.
- [2] Steinert, S. A., Streib-Montee, R., Leather, J. M., Chadwick, D. B., DNA damage in mussels at sites in San Diego Bay. *Mutat Res* 1998, 399, 65-85.
- [3] Beiras, R., Fernandez, N., Bellas, J., Besada, V., *et al.*, Integrative assessment of marine pollution in Galician estuaries using sediment chemistry, mussel bioaccumulation, and embryo-larval toxicity bioassays. *Chemosphere* 2003, 52, 1209-1224.
- [4] Ye, F., Huang, X., Zhang, D., Tian, L., *et al.*, Distribution of heavy metals in sediments of the Pearl River Estuary, Southern China: Implications for sources and historical changes. *J Environ Sci (China)* 2012, 24, 579-588.
- [5] Birch, G., Rochford, L., Stormwater metal loading to a well-mixed/stratified estuary (Sydney Estuary, Australia) and management implications. *Environ Monit Assess* 2010, 169, 531-551.
- [6] Birch, G., Taylor, S., Possible biological significance of contaminated sediments in Port Jackson, Sydney, Australia. *Environ Monit Assess* 2002, 77, 179-190.
- [7] Birch, G. F., Taylor, S. E., Application of sediment quality guidelines in the assessment and management of contaminated surficial sediments in Port Jackson (Sydney harbour), Australia. *Environ Manage* 2002, 29, 860-870.
- [8] Birch, G. F., Taylor, S. E., Assessment of possible sediment toxicity of contaminated sediments in Port Jackson, Sydney, Australia. *Hydrobiologia* 2002, 472, 19-27.
- [9] Arai, T., Ikemoto, T., Hokura, A., Terada, Y., *et al.*, Chemical forms of mercury and cadmium accumulated in marine mammals and seabirds as determined by XAFS Analysis. *Environ Sci Technol.* 2004, 38, 6468-6474.
- [10] Zhu, J. Y., Huang, H. Q., Bao, X. D., Lin, Q. M., *et al.*, Acute toxicity profile of cadmium revealed by proteomics in brain tissue of *Paralichthys olivaceus*: Potential role of transferrin in cadmium toxicity. *Aquat Toxicol.* 2006, 78, 127-135.
- [11] Muralidharan, S., Thompson, E., Raftos, D., Birch, G., *et al.*, Quantitative proteomics of heavy metal stress responses in Sydney rock oysters. *Proteomics* 2012, 12, 906-921.
- [12] Ling, X.-P., Zhu, J.-Y., Huang, L., Huang, H.-Q., Proteomic changes in response to acute cadmium toxicity in gill tissue of *Paralichthys olivaceus*. *Environ Toxicol Pharmacol.* 2009, 27, 212-218.
- [13] Gomiero, A., Pampanin, D. M., Bjørnstad, A., Larsen, B. K., *et al.*, An ecotoxicoproteomic approach (SELDI-TOF mass spectrometry) to biomarker discovery in crab exposed to pollutants under laboratory conditions. *Aquat Toxicol* 2006, 78, Supplement, S34-S41.
- [14] Apraiz, I., Mi, J., Cristobal, S., Identification of proteomic signatures of exposure to marine pollutants in mussels (*Mytilus edulis*). *Mol Cell Proteomics* 2006, 5, 1274-1285.
- [15] Knigge, T., Monsinjon, T., Andersen, O.-K., Surface-enhanced laser desorption/ionization-time of flight-mass spectrometry approach to biomarker discovery in blue mussels (*Mytilus edulis*) exposed to polyaromatic hydrocarbons and heavy metals under field conditions. *Proteomics* 2004, 4, 2722-2727.
- [16] Nzoughet, J. K., Hamilton, J. T., Botting, C. H., Douglas, A., *et al.*, Proteomics identification of azaspiracid toxin biomarkers in blue mussels, *Mytilus edulis*. *Mol Cell Proteomics* 2009, 8, 1811-1822.
- [17] Gardeström, J., Elfving, T., Löf, M., Tedengren, M., *et al.*, The effect of thermal stress on protein composition in dogwhelks (*Nucella lapillus*) under normoxic and hyperoxic conditions. *Comp Biochem Physiol A Mol Integr Physiol* 2007, 148, 869-875.
- [18] Dowling, V., Hoarau, P. C., Romeo, M., O'Halloran, J., *et al.*, Protein carbonylation and heat shock response in *Ruditapes decussatus* following p,p'-dichlorodiphenyldichloroethylene (DDE) exposure: a proteomic approach reveals that DDE causes oxidative stress. *Aquat Toxicol* 2006, 77, 11-18.
- [19] Romero-Ruiz, A., Carrascal, M., Alhama, J., Gomez-Ariza, J. L., *et al.*, Utility of proteomics to assess pollutant response of clams from the Donana bank of Guadalquivir Estuary (SW Spain). *Proteomics* 2006, 6 Suppl 1, S245-255.
- [20] Lemos, M. F. L., Soares, A. M. V. M., Correia, A. C., Esteves, A. C., Proteins in ecotoxicology – How, why and why not? *Proteomics* 2010, 10, 873-887.
- [21] Neilson, K. A., Ali, N. A., Muralidharan, S., Mirzaei, M., *et al.*, Less label, more free: Approaches in label-free quantitative mass spectrometry. *Proteomics* 2011, 11, 535-553.
- [22] Ong, S. E., Blagoev, B., Kratchmarova, I., Kristensen, D. B., *et al.*, Stable isotope labeling by amino acids in cell culture, SILAC, as a simple and accurate approach to expression proteomics. *Mol Cell Proteomics* 2002, 1, 376-386.
- [23] Ong, S. E., Mann, M., Mass spectrometry-based proteomics turns quantitative. *Nat Chem Biol* 2005, 1, 252-262.
- [24] Steen, H., Pandey, A., Proteomics goes quantitative: measuring protein abundance. *Trends Biotechnol* 2002, 20, 361-364.
- [25] Ross, P. L., Huang, Y. N., Marchese, J. N., Williamson, B., *et al.*, Multiplexed protein quantitation in *Saccharomyces cerevisiae* using amine-reactive isobaric tagging reagents. *Mol Cell Proteomics* 2004, 3, 1154-1169.

- [26] Byers, H. L., Campbell, J., van Ulsen, P., Tommassen, J., *et al.*, Candidate verification of iron-regulated *Neisseria meningitidis* proteins using isotopic versions of tandem mass tags (TMT) and single reaction monitoring. *J Proteomics* 2009, 73, 231-239.
- [27] Gygi, S. P., Rist, B., Gerber, S. A., Turecek, F., *et al.*, Quantitative analysis of complex protein mixtures using isotope-coded affinity tags. *Nat Biotechnol* 1999, 17, 994-999.
- [28] Bondarenko, P. V., Chelius, D., Shaler, T. A., Identification and relative quantitation of protein mixtures by enzymatic digestion followed by capillary reversed-phase liquid chromatography-tandem mass spectrometry. *Anal Chem* 2002, 74, 4741-4749.
- [29] Chelius, D., Bondarenko, P. V., Quantitative profiling of proteins in complex mixtures using liquid chromatography and mass spectrometry. *J Proteome Res* 2002, 1, 317-323.
- [30] Liu, H., Sadygov, R. G., Yates, J. R., 3rd, A model for random sampling and estimation of relative protein abundance in shotgun proteomics. *Anal Chem* 2004, 76, 4193-4201.
- [31] Lundgren, D. H., Hwang, S.-I., Wu, L., Han, D. K., Role of spectral counting in quantitative proteomics. *Expert Rev Proteomics* 2010, 7, 39-53.
- [32] Florens, L., Carozza, M. J., Swanson, S. K., Fournier, M., *et al.*, Analyzing chromatin remodeling complexes using shotgun proteomics and normalized spectral abundance factors. *Methods* 2006, 40, 303-311.
- [33] Zybaylov, B., Mosley, A. L., Sardi, M. E., Coleman, M. K., *et al.*, Statistical analysis of membrane proteome expression changes in *Saccharomyces cerevisiae*. *J Proteome Res* 2006, 5, 2339-2347.
- [34] Zybaylov, B. L., Florens, L., Washburn, M. P., Quantitative shotgun proteomics using a protease with broad specificity and normalized spectral abundance factors. *Mol Biosyst* 2007, 3, 354-360.
- [35] Pavelka, N., Fournier, M. L., Swanson, S. K., Pelizzola, M., *et al.*, Statistical similarities between transcriptomics and quantitative shotgun proteomics data. *Mol Cell Proteomics* 2008, 7, 631-644.
- [36] Chick, J. M., Haynes, P. A., Bjellqvist, B., Baker, M. S., A Combination of Immobilised pH Gradients Improves Membrane Proteomics. *J Proteome Res* 2008, 7, 4974-4981.
- [37] Mosley, A. L., Florens, L., Wen, Z., Washburn, M. P., A label free quantitative proteomic analysis of the *Saccharomyces cerevisiae* nucleus. *J Proteomics* 2009, 72, 110-120.
- [38] Gammulla, C. G., Pascovici, D., Atwell, B. J., Haynes, P. A., Differential metabolic response of cultured rice (*Oryza sativa*) cells exposed to high- and low-temperature stress. *Proteomics* 2010, 10, 3001-3019.
- [39] Voelckel, C., Mirzaei, M., Reichelt, M., Luo, Z., *et al.*, Transcript and protein profiling identify candidate gene sets of potential adaptive significance in New Zealand Pachycladon. *BMC Evol Biol* 2010, 10, 151.
- [40] Zhao, Y., Denner, L., Haidacher, S. J., LeJeune, W. S., *et al.*, Comprehensive analysis of the mouse renal cortex using two-dimensional HPLC - tandem mass spectrometry. *Proteome Sci* 2008, 6, 15.
- [41] Eng, J., McCormack, A., Yates, J., An approach to correlate tandem mass spectral data of peptides with amino acid sequences in a protein database. *J Am Soc Mass Spectrom* 1994, 5, 976-989.
- [42] Craig, R., Beavis, R. C., TANDEM: matching proteins with tandem mass spectra. *Bioinformatics* 2004, 20, 1466-1467.
- [43] Geer, L. Y., Markey, S. P., Kowalak, J. A., Wagner, L., *et al.*, Open mass spectrometry search algorithm. *J Proteome Res* 2004, 3, 958-964.
- [44] Nesvizhskii, A. I., Vitek, O., Aebersold, R., Analysis and validation of proteomic data generated by tandem mass spectrometry. *Nat Methods* 2007, 4, 787-797.
- [45] Bantscheff, M., Schirle, M., Sweetman, G., Rick, J., *et al.*, Quantitative mass spectrometry in proteomics: a critical review. *Anal Bioanal Chem* 2007, 389, 1017-1031.
- [46] Oberg, A. L., Vitek, O., Statistical design of quantitative mass spectrometry-based proteomic experiments. *J Proteome Res* 2009, 8, 2144-2156.
- [47] Zhang, B., VerBerkmoes, N. C., Langston, M. A., Uberbacher, E., *et al.*, Detecting differential and correlated protein expression in label-free shotgun proteomics. *J Proteome Res* 2006, 5, 2909-2918.
- [48] Grossmann, J., Fischer, B., Baerenfaller, K., Oвити, J., *et al.*, A workflow to increase the detection rate of proteins from unsequenced organisms in high-throughput proteomics experiments. *Proteomics* 2007, 7, 4245-4254.
- [49] Denev, V. J., Shah, M. B., VerBerkmoes, N. C., Hettich, R. L., *et al.*, Implications of Strain- and Species-Level Sequence Divergence for Community and Isolate Shotgun Proteomic Analysis. *J Proteome Res* 2007, 6, 3152-3161.
- [50] Mirzaei, M., Pascovici, D., Keighley, T., George, I., *et al.*, Shotgun proteomic profiling of five species of New Zealand Pachycladon. *Proteomics* 2010, 11, 166-171.
- [51] Poliakov, A., Russell, C. W., Ponnala, L., Hoops, H. J., *et al.*, Large-scale label-free quantitative proteomics of the pea aphid-*Buchnera symbiosis*. *Mol Cell Proteomics* 2011.
- [52] Carpentier, S. C., Coemans, B., Podevin, N., Laukens, K., *et al.*, Functional genomics in a non-model crop: transcriptomics or proteomics? *Physiol Plant* 2008, 133, 117-130.
- [53] Nanduri, B., Lawrence, M. L., Vanguri, S., Burgess, S. C., Proteomic analysis using an unfinished bacterial genome: The effects of subminimum inhibitory concentrations of antibiotics on *Mannheimia haemolytica* virulence factor expression. *Proteomics* 2005, 5, 4852-4863.
- [54] Schneider, T., Schellenberg, M., Meyer, S., Keller, F., *et al.*, Quantitative detection of changes in the leaf-mesophyll tonoplast proteome in dependency of a cadmium exposure of barley (*Hordeum vulgare* L.) plants. *Proteomics* 2009, 9, 2668-2677.

- [55] Friso, G., Majeran, W., Huang, M., Sun, Q., *et al.*, Reconstruction of Metabolic Pathways, Protein Expression, and Homeostasis Machineries across Maize Bundle Sheath and Mesophyll Chloroplasts: Large-Scale Quantitative Proteomics Using the First Maize Genome Assembly. *Plant Physiol* 2010, 152, 1219-1250.
- [56] Shevchenko, A., Leal de Sousa, M. M., Waridel, P., Bittencourt, S. T., *et al.*, Sequence Similarity-Based Proteomics in Insects: a characterization of the larvae venom of the brazilian moth *Cerodirphia speciosa*. *J Proteome Res* 2005, 4, 862-869.
- [57] Shevchenko, A., Sunyaev, S., Loboda, A., Shevchenko, A., *et al.*, Charting the proteomes of organisms with unsequenced genomes by MALDI-quadrupole time-of-flight mass spectrometry and BLAST Homology Searching. *Anal Chem* 2001, 73, 1917-1926.
- [58] Sunyaev, S., Liska, A. J., Golod, A., Shevchenko, A., *et al.*, MultiTag: Multiple error-tolerant sequence tag search for the sequence-similarity identification of proteins by mass spectrometry. *Anal Chem* 2003, 75, 1307-1315.
- [59] Keller, A., Purvine, S., Nesvizhskii, A. I., Stolyar, S., *et al.*, Experimental protein mixture for validating tandem mass spectral analysis. *OMICS* 2002, 6, 207-212.
- [60] Nriagu, J. O., The global copper cycle. *Copper in the environment. Part 1: ecological cycling* 1979a, 1-17.
- [61] Nriagu, J. O. b., in: Nriagu, J. O. (Ed.), *Copper in the environment. Part 1: ecological cycling.*, John Wiley, New York 1979, pp. 45-75.
- [62] Ellenberger, S. A., Baumann, P. C., May, T. W., Evaluation of effects caused by high copper concentrations in Torch lake, Michigan, on reproduction of yellow perch. *J Great Lakes Res* 1994, 20, 531-536.
- [63] Sunda, W. G., Tester, P. A., Huntsman, S. A., Toxicity of trace metals to *Acartia tonsa* in the Elizabeth River and southern Chesapeake Bay. *Estuar Coast Shelf Sci* 1990, 30, 207-221.
- [64] Craig, P. M., Hogstrand, C., Wood, C. M., McClelland, G. B., Gene expression endpoints following chronic waterborne copper exposure in a genomic model organism, the zebrafish, *Danio rerio*. *Physiol Genomics* 2009, 40, 23-33.
- [65] Hodson, P. V., Borgmann, U., Shear, H., in: Nriagu, J. O. (Ed.), *Copper in the environment. Part2: health effects.*, John Wiley, New York 1979, pp. 307-372.
- [66] Rodney, E., Herrera, P., Luxama, J., Boykin, M., *et al.*, Bioaccumulation and tissue distribution of arsenic, cadmium, copper and zinc in *Crassostrea virginica* grown at two different depths in Jamaica Bay, New York. *In Vivo (Brooklyn)* 2007, 29, 16-27.
- [67] Weis, J. S., Weis, P., Effects of contaminants from chromated copper arsenate-treated lumber on benthos. *Arch Environ Contam Toxicol* 1994, 26, 103-109.
- [68] Rivera-Mancia, S., Perez-Neri, I., Rios, C., Tristan-Lopez, L., *et al.*, The transition metals copper and iron in neurodegenerative diseases. *Chem Biol Interact* 2010, 186, 184-199.
- [69] Schwarz, J. A., Mitchelmore, C. L., Jones, R., O'Dea, A., *et al.*, Exposure to copper induces oxidative and stress responses and DNA damage in the coral *Montastraea franksi*. *Comp Biochem Physiol C Toxicol Pharmacol* 2012, 157, 272-279.
- [70] Halliwell, B., Gutteridge, J. M., Role of free radicals and catalytic metal ions in human disease: an overview. *Methods Enzymol* 1990, 186, 1-85.
- [71] Jomova, K., Valko, M., Advances in metal-induced oxidative stress and human disease. *Toxicology* 2011, 283, 65-87.
- [72] Jarrup, L., Hazards of heavy metal contamination. *Br Med Bull.* 2003, 68, 167-182.
- [73] Linder, M. C., The relationship of copper to DNA damage and damage prevention in humans. *Mutat Res* 2012, 733, 83-91.
- [74] Wang, Y., Zi, X. Y., Su, J., Zhang, H. X., *et al.*, Cuprous oxide nanoparticles selectively induce apoptosis of tumor cells. *Int J Nanomedicine* 2012, 7, 2641-2652.
- [75] Jomova, K., Vondrakova, D., Lawson, M., Valko, M., Metals, oxidative stress and neurodegenerative disorders. *Mol Cell Biochem* 2010, 345, 91-104.
- [76] Apostoli, P., Catalani, S., Metal ions affecting reproduction and development. *Met Ions Life Sci* 2011, 8, 263-303.
- [77] Kao, W. C., Chen, Y. R., Yi, E. C., Lee, H., *et al.*, Quantitative proteomic analysis of metabolic regulation by copper ions in *Methylococcus capsulatus* (Bath). *J Biol Chem* 2004, 279, 51554-51560.
- [78] Liu, X., Shen, Y., Lou, L., Ding, C., *et al.*, Copper tolerance of the biomass crops Elephant grass (*Pennisetum purpureum* S.), Vetiver grass (*Vetiveria zizanioides*) and the upland reed (*Phragmites australis*) in soil culture. *Biotechnol Adv* 2009, 27, 633-640.
- [79] Maric, M., Antonijevic, M., Alagic, S., The investigation of the possibility for using some wild and cultivated plants as hyperaccumulators of heavy metals from contaminated soil. *Environ Sci Pollut Res Int* 2013, 20, 1181-1188.
- [80] Eisler, R., *Compendium of Trace Metals and Marine Biota: Volume 1: Plants and Invertebrates*, Elsevier Science 2009.
- [81] Ahmad, M. S., Ashraf, M., Tabassam, Q., Hussain, M., *et al.*, Lead (Pb)-induced regulation of growth, photosynthesis, and mineral nutrition in maize (*Zea mays* L.) plants at early growth stages. *Biol Trace Elem Res* 2011, 144, 1229-1239.
- [82] Fujimura, T., Matsui, T., Funaba, M., Regulatory responses to excess zinc ingestion in growing rats. *Br J Nutr* 2012, 107, 1655-1663.
- [83] Widmeyer, J. R., Bendell-Young, L. I., Heavy metal levels in suspended sediments, *Crassostrea gigas*, and the risk to humans. *Arch Environ Contam Toxicol* 2008, 55, 442-450.

- [84] Almeida, E. A., Bairy, A. C., Loureiro, A. P., Medeiros, M. H., *et al.*, DNA and lipid damage in the brown mussel *Perna perna* from a contaminated site. *Bull Environ Contam Toxicol* 2003, 71, 270-275.
- [85] Bolognesi, C., Frenzilli, G., Lasagna, C., Perrone, E., *et al.*, Genotoxicity biomarkers in *Mytilus galloprovincialis*: wild versus caged mussels. *Mutat Res* 2004, 552, 153-162.
- [86] Gabbianelli, R., Lupidi, G., Villarini, M., Falcioni, G., DNA damage induced by copper on erythrocytes of gilthead sea bream *Sparus aurata* and mollusk *Scapharca inaequivalvis*. *Arch Environ Contam Toxicol* 2003, 45, 350-356.
- [87] Rank, J., Lehtonen, K. K., Strand, J., Laursen, M., DNA damage, acetylcholinesterase activity and lysosomal stability in native and transplanted mussels (*Mytilus edulis*) in areas close to coastal chemical dumping sites in Denmark. *Aquat Toxicol* 2007, 84, 50-61.
- [88] Gomes, T., Araujo, O., Pereira, R., Almeida, A. C., *et al.*, Genotoxicity of copper oxide and silver nanoparticles in the mussel *Mytilus galloprovincialis*. *Mar Environ Res* 2013, 84, 51-59.
- [89] Mai, H., Cachot, J., Brune, J., Geffard, O., *et al.*, Embryotoxic and genotoxic effects of heavy metals and pesticides on early life stages of Pacific oyster (*Crassostrea gigas*). *Mar Pollut Bull* 2012, 64, 2663-2670.
- [90] Okocha, R. O., Adediji, O. B., *Rep Opinion*, Veterinary Public Health and Preventive Medicine University of Ibadan 2012, pp. 57-67.
- [91] Birge, W. J., and J. A. Black, in: Nriagu, J. O. (Ed.), *Copper in the environment. Part 2: health effects.*, John Wiley, New York 1979, pp. 373-399.
- [92] Aaseth J, N. T., *Copper*, Elsevier Science Publishers, New York, NY 1986.
- [93] Nesto, N., Romano, S., Moschino, V., Mauri, M., *et al.*, Bioaccumulation and biomarker responses of trace metals and micro-organic pollutants in mussels and fish from the Lagoon of Venice, Italy. *Mar Pollut Bull* 2007, 55, 469-484.
- [94] Sanders, D. E., Evaluating copper and zinc in dairy rations. *J Am Vet Med Assoc* 1991, 199, 1119-1120.
- [95] Hoare, K., Davenport, J., *et al.*, Effects of exposure and previous exposure to copper on growth of veliger larvae and survivorship of *Mytilus edulis* juveniles. *Mar Ecol Prog Ser* 1995, 120, 163-168.
- [96] (EPA), U. S. E. P. A., *U.S. Environmental Protection Agency Report* 1980, p. 158.
- [97] Han, B. C., Jeng, W. L., Hung, T. C., Wen, M. Y., Relationship between copper speciation in sediments and bioaccumulation by marine bivalves of Taiwan. *Environ Pollut* 1996, 91, 35-39.
- [98] Soria-Dengg, S., Ochavillo, D., Comparative toxicities of trace metals on embryos of the giant clam, *Tridacna derasa*. *Asian Marine Biol* 1990, 7, 161-166.
- [99] Betzer, S. B., and P. P. Yevich, Copper toxicity in *Busycon canaliculatum* L. *Biol Bul.* 1975, 148, 16-25.
- [100] Ebele, S., Oladimeji, A. A., Daramola, J. A., Molluscicidal and piscicidal properties of copper(II) tetraoxosulfate(VI) on *Bulinus globosus* (Morelet) and *Clarias anguillaris* (L.). *Aquat Toxicol* 1990, 17, 231-238.
- [101] Winger, P. V., Imlay, M. J., McMillan, W. E., Martin, T. W., *et al.*, Field and laboratory evaluation of the influence of copper-diquat on apple snails in Southern Florida. *Environ Toxicol Chem* 1984, 3, 409-424.
- [102] Hussein, M. A., Obuid-Allah, A. H., Mohammad, A. H., Scott-Fordsmand, J. J., *et al.*, Seasonal variation in heavy metal accumulation in subtropical population of the terrestrial isopod, *Porcellio laevis*. *Ecotoxicol Environ Saf* 2006, 63, 168-174.
- [103] Rao, S. N., Anjaneyulu, N., Effect of Copper Sulfate on Molt and Reproduction in Shrimp *Litopenaeus vannamei*. *Int. J Biol. Chem.* 2008, 2, 35-41.
- [104] Adeyemi, J. A., Klerks, P. L., Occurrence of copper acclimation in the least killifish *Heterandria formosa*, and associated biochemical and physiological mechanisms. *Aquat Toxicol* 2013, 130-131, 51-57.
- [105] Barwick, M., Maher, W., Biotransference and biomagnification of selenium copper, cadmium, zinc, arsenic and lead in a temperate seagrass ecosystem from Lake Macquarie Estuary, NSW, Australia. *Mar Environ Res* 2003, 56, 471-502.
- [106] Jones, M. A., Stauber, J., Apte, S., Simpson, S., *et al.*, A risk assessment approach to contaminants in Port Curtis, Queensland, Australia. *Mar Pollut Bull* 2005, 51, 448-458.
- [107] Bitzan, M., Bickford, B. B., Foster, G. H., Verotoxin (Shiga Toxin) sensitizes renal epithelial cells to increased heme toxicity: Possible implications for the hemolytic uremic syndrome. *Journal of the American Society of Nephrology* 2004, 15, 2334-2343.
- [108] Eisler, R., *Contaminant Hazard Reviews Report (USA)*, no. 26, U.S. Dept. of the Interior, Fish and Wildlife Service, Washington, DC (USA) 1993, pp. 126 p., tables.
- [109] Kim, J., Koo, T.-H., Acute and/or chronic contaminations of heavy metals in shorebirds from Korea. *Journal of Environmental Monitoring* 2010, 12, 1613-1618.
- [110] Hogstrand, C., Balesaria, S., Glover, C. N., Application of genomics and proteomics for study of the integrated response to zinc exposure in a non-model fish species, the rainbow trout. *Comp Biochem Physiol B Biochem Mol Biol* 2002, 133, 523-535.
- [111] Hilmy, A. M., el Domiaty, N. A., Daabees, A. Y., Abdel Latife, H. A., Some physiological and biochemical indices of zinc toxicity in two freshwater fishes, *Clarias lazera* and *Tilapia zilli*. *Comp Biochem Physiol C* 1987, 87, 297-301.
- [112] Taneja, S. K., Arya, P., Bains, U., Effects of ZnSO<sub>4</sub> toxicity on the skeletal muscles of the mosquitofish, *Gambusia affinis*. *Res. Bul. Panjab Univ. Sc.* 1988, 39, 207-211.
- [113] Garcia-Luque, E., DelValls, A. T., Forja, J. M., Gomez-Parra, A., Biological adverse effects on bivalves associated with trace metals under estuarine environments. *Environ Monit Assess* 2007, 131, 27-35.
- [114] Skidmore, J. F., Respiration and osmoregulation in rainbow trout with gills damaged by zinc sulphate. *J Exp Biol* 1970, 52, 481-494.

- [115] Hilmy, A. M., El Domiaty, N. A., Daabees, A. Y., Alsarha, A., The toxicity to *Clarias Lazera* of copper and zinc applied jointly. *Comp Biochem Physiol C Comp Pharmacol* 1987, 87, 309-314.
- [116] Elliott, N. G., Ritz, D. A., Swain, R., Interaction between copper and zinc accumulation in the barnacle *Elminius modestus* Darwin. *Mar Env Res* 1985, 17, 13-17.
- [117] Loro, V. L., Jorge, M. B., Silva, K. R., Wood, C. M., Oxidative stress parameters and antioxidant response to sublethal waterborne zinc in a euryhaline teleost *Fundulus heteroclitus*: protective effects of salinity. *Aquat Toxicol* 2012, 110-111, 187-193.
- [118] Chung, M. J., Walker, P. A., Brown, R. W., Hogstrand, C., ZINC-mediated gene expression offers protection against H<sub>2</sub>O<sub>2</sub>-induced cytotoxicity. *Toxicol Appl Pharmacol* 2005, 205, 225-236.
- [119] Fernandez, T. V., N. V. Jones. , Studies on the toxicity of zinc and copper applied singly and jointly to *Nereis diversicolor* at different salinities and temperatures. *Tropical Ecol* 1990, 31, 47-55.
- [120] Shuhaimi-Othman, M., Nur-Amalina, R., Nadzifah, Y., Toxicity of metals to a freshwater snail, *Melanoides tuberculata*. *Scientific World J* 2012, 2012, 125785.
- [121] Irato, P., Santovito, G., Cassini, A., Piccinni, E., et al., Metal accumulation and binding protein induction in *Mytilus galloprovincialis*, *Scapharca inaequivalvis*, and *Tapes philippinarum* from the Lagoon of Venice. *Arch Environ Contam Toxicol* 2003, 44, 476-484.
- [122] Mourgaud, Y., Martinez, E., Geffard, A., Andral, B., et al., Metallothionein concentration in the mussel *Mytilus galloprovincialis* as a biomarker of response to metal contamination: validation in the field. *Biomarkers* 2002, 7, 479-490.
- [123] Voets, J., Redeker, E. S., Blust, R., Bervoets, L., Differences in metal sequestration between zebra mussels from clean and polluted field locations. *Aquat Toxicol* 2009, 93, 53-60.
- [124] Spear, P. A., *National Research Council of Canada (NRCC) 17589*, National Research Council of Canada 1981, p. 145.
- [125] Brungs, W. A., Chronic Toxicity of Zinc to the Fathead Minnow, *Pimephales promelas* Rafinesque. *Trans Am Fish Soc* 1969, 98, 272-279.
- [126] Ward, D. J., Perez-Landa, V., Spadaro, D. A., Simpson, S. L., et al., An assessment of three harpacticoid copepod species for use in ecotoxicological testing. *Arch Environ Contam Toxicol* 2011, 61, 414-425.
- [127] Somasundaram, B., King, P. E., Shackley, S. E., The effect of zinc on the ultrastructure of the trunk muscle of the larva of *Clupea harengus* L. *Comp Biochem Physiol C* 1985, 79, 311-315.
- [128] Kraak, M. H. S., Wink, Y. A., Stuijzand, S. C., Buckert-de Jong, M. C., et al., Chronic ecotoxicity of Zn and Pb to the zebra mussel *Dreissena polymorpha*. *Aquat Toxicol* 1994, 30, 77-89.
- [129] (EPA), U. S. E. P. A., *U.S. Environmental Protection Agency Report* 1987, p. 207.
- [130] Brereton, A., Lord, H., Thornton, I., Webb, J. S., Effect of zinc on growth and development of larvae of the Pacific oyster *Crassostrea gigas*. *Mar Biol* 1973, 19, 96-101.
- [131] Eisler, R., in: Nriagu, J. O. (Ed.), *Zinc in the environment. Part II: health effects.* , John Wiley & Sons, Inc., New York 1980, pp. 259-351.
- [132] Hunt, J. W., Anderson, B. S., Sublethal effects of zinc and municipal effluents on larvae of the red abalone *Haliotis rufescens*. *Mar Biol* 1989, 101, 545-552.
- [133] McCready, S., Greely, C. R., Hyne, R. V., Birch, G. F., et al., Sensitivity of an indigenous amphipod (*Corophium colo*) to chemical contaminants in laboratory toxicity tests conducted with sediments from Sydney Harbor, Australia, and vicinity. *Environ Toxicol Chem* 2005, 24, 2545-2552.
- [134] Ciarelli, S., Vonck, W. A. P. M. A., van Straalen, N. M., Stronkhorst, J., Ecotoxicity Assessment of Contaminated Dredged Material with the Marine Amphipod *Corophium volutator*. *Arch Environ Contam Toxicol* 1998, 34, 350-356.
- [135] Díaz Rizo, O., Olivares Reumont, S., Viguri Fuente, J., Díaz Arado, O., et al., Copper, zinc and lead enrichments in sediments from Guacanayabo Gulf, Cuba, and its bioaccumulation in oysters, *Crassostrea rhizophorae*. *Bull Environ Contam Toxicol* 2010, 84, 136-140.
- [136] Bryan, G. W., Hummerstone, L. G., Ward, E., Zinc regulation in the lobster *Homarus Gammarus*: Importance of different pathways of absorption and excretion. *J Mar Biol Assoc U. K.* 2009, 66, 175-199.
- [137] Sterling, K. M., Roggenbeck, B., Ahearn, G. A., Dual control of cytosolic metals by lysosomal transporters in lobster hepatopancreas. *J Exp Biol* 2010, 213, 769-774.
- [138] Kelly, E. J., Quaife, C. J., Froelick, G. J., Palmiter, R. D., Metallothionein I and II protect against zinc deficiency and zinc toxicity in mice. *J Nutr.* 1996, 126, 1782-1790.
- [139] Mirenda, R. J., Acute toxicity and accumulation of zinc in the crayfish, *Orconectes virilis* (Hagen). *Bull Environ Contam Toxicol* 1986, 37, 387-394.
- [140] Guan, R., Kang, T., Lu, F., Zhang, Z., et al., Cytotoxicity, oxidative stress, and genotoxicity in human hepatocyte and embryonic kidney cells exposed to ZnO nanoparticles. *Nanoscale Res Lett* 2012, 7, 602.
- [141] Stahl, J. L., Greger, J. L., Cook, M. E., Zinc, copper and iron utilisation by chicks fed various concentrations of zinc. *Br Poult Sci* 1989, 30, 123-134.
- [142] Allen, J. G., Masters, H. G., Peet, R. L., Mullins, K. R., et al., Zinc toxicity in ruminants. *J Comp Pathol* 1983, 93, 363-377.
- [143] Blundell, R., Adam, F., Haemolytic anaemia and acute pancreatitis associated with zinc toxicosis in a dog. *Vet Rec* 2013, 172, 17.
- [144] Demayo, A., Taylor, M. C., Taylor, K. W., Hodson, P. V., et al., Toxic effects of lead and lead compounds on human health, aquatic life, wildlife plants, and livestock. *CRC Crit Rev Environ Control* 1982, 12, 257-305.

- [145] Eisler, R., Center, P. W. R., *Lead hazards to fish, wildlife, and invertebrates: a synoptic review*, U.S. Fish and Wildlife Service, Patuxent Wildlife Research Center 1988.
- [146] Anwer, J., Ali, S., Mehrotra, N. K., Antagonistic effect of zinc in lead treated developing chick embryos. *Drug Chem Toxicol* 1988, 11, 85-95.
- [147] Vido, K., Spector, D., Lagniel, G., Lopez, S., *et al.*, A Proteome Analysis of the Cadmium Response in *Saccharomyces cerevisiae*. *J Biol Chem* 2001, 276, 8469-8474.
- [148] Almeida, J. A., Diniz, Y. S., Marques, S. F. G., Faine, L. A., *et al.*, The use of the oxidative stress responses as biomarkers in Nile tilapia (*Oreochromis niloticus*) exposed to in vivo cadmium contamination. *Environ Int* 2002, 27, 673-679.
- [149] Oliva, M., Perales, J. A., Gravato, C., Guilhermino, L., *et al.*, Biomarkers responses in muscle of Senegal sole (*Solea senegalensis*) from a heavy metals and PAHs polluted estuary. *Mar Poll Bull* 2012.
- [150] Pretto, A., Loro, V., Morsch, V., Moraes, B., *et al.*, Acetylcholinesterase activity, lipid peroxidation, and bioaccumulation in silver catfish exposed to cadmium. *Arch Environ Contam Toxicol* 2010, 58, 1008-1014.
- [151] Fang, Z. Q., Cheung, R. Y., Wong, M. H., Heavy metals in oysters, mussels and clams collected from coastal sites along the Pearl River Delta, South China. *J Environ Sci* 2003, 15, 9-24.
- [152] Gifford, S., Dunstan, R. H., O'Connor, W., Roberts, T., *et al.*, Pearl aquaculture-profitable environmental remediation? *Sci Total Environ* 2004, 319, 27-37.
- [153] Ke, C., Wang, W. X., Bioaccumulation of Cd, Se, and Zn in an estuarine oyster (*Crassostrea rivularis*) and a coastal oyster (*Saccostrea glomerata*). *Aquat Toxicol* 2001, 56, 33-51.
- [154] de Carvalho, G. P., Cavalcante, P. R., de Castro, A. C., Rojas, M. O., Preliminary assessment of heavy metal levels in *Mytella falcata* (Bivalvia, Mytilidae) from Bacanga River estuary, Sao Luis, state of Maranhao, northeastern Brazil. *Rev Bras Biol* 2000, 60, 11-16.
- [155] Julshamn, K., Torpe, E. K., Bornes, C., Saethre, L. J., *et al.*, Cadmium, lead, copper and zinc in blue mussels (*Mytilus edulis*) sampled in the Hardangerfjord, Norway. *J Environ Monit* 2001, 3, 539-542.
- [156] Li, X., Li, J., Wang, Y., Fu, L., *et al.*, Kinetic study of the bioaccumulation of heavy metals (Cu, Pb, and Cd) in Chinese domestic oyster *Ostrea plicatula*. *J Environ Sci Health A Tox Hazard Subst Environ Eng* 2010, 45, 836-845.
- [157] Tanguy, A., Boutet, I., Bonhomme, F., Boudry, P., *et al.*, Polymorphism of metallothionein genes in the Pacific oyster *Crassostrea gigas* as a biomarker of response to metal exposure. *Biomarkers* 2002, 7, 439-450.
- [158] Geffard, O., Geffard, A., His, E., Budzinski, H., Assessment of the bioavailability and toxicity of sediment-associated polycyclic aromatic hydrocarbons and heavy metals applied to *Crassostrea gigas* embryos and larvae. *Mar Pollut Bull* 2003, 46, 481-490.
- [159] Jing, G., Li, Y., Xie, L., Zhang, R., Metal accumulation and enzyme activities in gills and digestive gland of pearl oyster (*Pinctada fucata*) exposed to copper. *Comp Biochem Physiol C Toxicol Pharmacol* 2006, 144, 184-190.
- [160] Sokolova, I. M., Ringwood, A. H., Johnson, C., Tissue-specific accumulation of cadmium in subcellular compartments of eastern oysters *Crassostrea virginica* Gmelin (Bivalvia: Ostreidae). *Aquat Toxicol* 2005, 74, 218-228.
- [161] Blackmore, G., Wang, W.-X., The transfer of cadmium, mercury, methylmercury, and zinc in an intertidal rocky shore food chain. *J Exp Mar Bio Ecol* 2004, 307, 91-110.
- [162] Apraiz, I., Cajaraville, M. P., Cristobal, S., Peroxisomal proteomics: biomonitoring in mussels after the Prestige's oil spill. *Mar Pollut Bull* 2009, 58, 1815-1826.
- [163] (ACIA), A. C. I. A., *Impacts of a Warming Arctic: Arctic Climate Impact Assessment*, Cambridge University Press 2004.
- [164] King, C. K., Gale, S. A., Hyne, R. V., Stauber, J. L., *et al.*, Sensitivities of Australian and New Zealand amphipods to copper and zinc in waters and metal-spiked sediments. *Chemosphere* 2006, 63, 1466-1476.
- [165] Bellan-Santini, D., Reish, D. J., Use of three species of crustacea as test animals for the toxicity of two salts of heavy metals. *C R Acad Sci Hebd Seances Acad Sci D* 1976, 282, 1325-1327.
- [166] Bryan, G. W., Langston, W. J., Bioavailability, accumulation and effects of heavy metals in sediments with special reference to United Kingdom estuaries: a review. *Environ Pollut* 1992, 76, 89-131.
- [167] de-la-Ossa-Carretero, J. A., Del-Pilar-Ruso, Y., Giménez-Casaldueiro, F., Sánchez-Lizaso, J. L., *et al.*, Sensitivity of amphipods to sewage pollution. *Estuar Coast Shelf Sci* 2012, 96, 129-138.
- [168] Boets, P., Lock, K., Goethals, P. L., Janssen, C. R., *et al.*, A comparison of the short-term toxicity of cadmium to indigenous and alien gammarid species. *Ecotoxicol* 2012, 21, 1135-1144.
- [169] Ippolito, A., Todeschini, R., Vighi, M., Sensitivity assessment of freshwater macroinvertebrates to pesticides using biological traits. *Ecotoxicol* 2012, 21, 336-352.
- [170] Annicchiarico, C., Biantolino, F., Cardellicchio, N., Di Leo, A., *et al.*, Predicting toxicity in marine sediment in Taranto Gulf (Ionian Sea, Southern Italy) using Sediment Quality Guidelines and a battery bioassay. *Ecotoxicol* 2007, 16, 239-246.
- [171] Costa, F. O., Neuparth, T., Correia, A. D., Costa, M. H., Multi-level assessment of chronic toxicity of estuarine sediments with the amphipod *Gammarus locusta*: II. Organism and population-level endpoints. *Mar Environ Res* 2005, 60, 93-110.
- [172] De Jonge, M., Van de Vijver, B., Blust, R., Bervoets, L., Responses of aquatic organisms to metal pollution in a lowland river in Flanders: a comparison of diatoms and macroinvertebrates. *Sci Total Environ* 2008, 407, 615-629.

- [173] De Lange, H. J., Sperber, V., Peeters, E. T., Avoidance of polycyclic aromatic hydrocarbon-contaminated sediments by the freshwater invertebrates *Gammarus pulex* and *Asellus aquaticus*. *Environ Toxicol Chem* 2006, 25, 452-457.
- [174] Prato, E., Biantolino, F., Scardicchio, C., Effects of temperature on the sensitivity of *Gammarus aequicauda* (Martynov, 1931) to cadmium. *Bull Environ Contam Toxicol* 2009, 83, 469-473.
- [175] Prato, E., Di Leo, A., Biantolino, F., Cardellicchio, N., Sediment toxicity tests using two species of marine amphipods: *Gammarus aequicauda* and *Corophium insidiosum*. *Bull Environ Contam Toxicol* 2006, 76, 629-636.
- [176] Roman, Y. E., De Schampelaere, K. A., Nguyen, L. T., Janssen, C. R., Chronic toxicity of copper to five benthic invertebrates in laboratory-formulated sediment: sensitivity comparison and preliminary risk assessment. *Sci Total Environ* 2007, 387, 128-140.
- [177] Vandegehuchte, M. B., Nguyen, L. T., De Laender, F., Muysen, B. T., *et al.*, Whole sediment toxicity tests for metal risk assessments: On the importance of equilibration and test design to increase ecological relevance. *Environ Toxicol Chem* 2013.
- [178] Dauvin, J.-C., Bellan, G., Bellan-Santini, D., Benthic indicators: From subjectivity to objectivity – Where is the line? *Marine Pollution Bulletin* 2010, 60, 947-953.
- [179] Cohen, T., Hee, S. S., Ambrose, R. F., Trace metals in fish and invertebrates of three California coastal Wetlands. *Mar Pollut Bull* 2001, 42, 224-232.
- [180] Fang, Z. Q., Cheung, R. Y., Wong, M. H., Heavy metal concentrations in edible bivalves and gastropods available in major markets of the Pearl River Delta. *J Environ Sci* 2001, 13, 210-217.
- [181] Monsinjon, T., Knigge, T., Proteomic applications in ecotoxicology. *Proteomics* 2007, 7, 2997-3009.
- [182] Yeh, H. C., Chen, I. M., Chen, P., Wang, W. H., Heavy metal concentrations of the soldier crab (*Mictyris brevidactylus*) along the inshore area of Changhua, Taiwan. *Environ Monit Assess* 2009, 153, 103-109.
- [183] Teh, S. J., Adams, S. M., Hinton, D. E., Histopathologic biomarkers in feral freshwater fish populations exposed to different types of contaminant stress. *Aquat Toxicol* 1997, 37, 51-70.
- [184] Ahsanullah, M., Mobley, M., Rankin, P., Individual and combined effects of zinc, cadmium and copper on the marine amphipod *Allorchestes compressa*. *Marine and Freshwater Research* 1988, 39, 33-37.
- [185] Ahsanullah, M., Williams, A. R., Sublethal effects and bioaccumulation of cadmium, chromium, copper and zinc in the marine amphipod *Allorchestes compressa*. *Mar Biol* 1991, 108, 59-65.
- [186] Bagshaw, J., Rafiee, P., Matthews, C., MacRae, T., Cadmium and zinc reversibly arrest development of *Artemia* larvae. *Bull Environ Contam Toxicol* 1986, 37, 289-296.
- [187] Johnson, I., Jones, M. B., Effects Of Zinc/Salinity Combinations on Zinc Regulation in *Gammarus Duebeni* from the Estuary and the Sewage Treatment Works at Looe, Cornwall. *J Mar Biol Assoc U. K.* 1989, 69, 249-260.
- [188] Spry, D. J., Wood, C. M., Acid-base, plasma ion and blood gas changes in rainbow trout during short term toxic zinc exposure. *J Comp Physiol B Biochem Environ* 1984, 154, 149-158.
- [189] Spry, D. J., Wood, C. M., Ion Flux Rates, Acid-Base Status, and Blood Gases in Rainbow Trout, *Salmo gairdneri*, Exposed to Toxic Zinc in Natural Soft Water. *Canadian Journal of Fisheries and Aquatic Sciences* 1985, 42, 1332-1341.
- [190] Hogstrand, C., Reid, S., Wood, C., Ca<sup>2+</sup> versus Zn<sup>2+</sup> transport in the gills of freshwater rainbow trout and the cost of adaptation to waterborne Zn<sup>2+</sup>. *Journal of Experimental Biology* 1995, 198, 337-348.
- [191] Hogstrand, C., Verbost, P. M., Bonga, S. E., Wood, C. M., Mechanisms of zinc uptake in gills of freshwater rainbow trout: interplay with calcium transport. *Am J Physiol Reg Integr Comp Physiol* 1996a, 270, R1141-R1147.
- [192] Hogstrand, C., Webb, N., Wood, C. M., Covariation in regulation of affinity for branchial zinc and calcium uptake in freshwater rainbow trout. *J Exp Biol* 1998, 201, 1809-1815.
- [193] Hogstrand, C., Wilson, R. W., Polgar, D., Wood, C. M., Effects of zinc on the kinetics of branchial calcium uptake in freshwater rainbow trout during adaptation to waterborne zinc. *J Exp Biol* 1994, 186, 55-73.
- [194] Spry, D. J., Wood, C. M., A Kinetic Method for the Measurement of Zinc Influx In Vivo in the Rainbow Trout, and the Effects of Waterborne Calcium on Flux Rates. *Journal of Experimental Biology* 1989, 142, 425-446.
- [195] Bradley, R. W., DuQuesnay, C., Sprague, J. B., Acclimation of rainbow trout, *Salmo gairdneri* Richardson, to zinc: kinetics and mechanism of enhanced tolerance induction. *J Fish Biol* 1985, 27, 367-379.
- [196] Thomas, D. G., Brown, M. W., Shurben, D., del G. Solbe, J. F., *et al.*, A comparison of the sequestration of cadmium and zinc in the tissues of rainbow trout (*salmo gairdneri*) following exposure to the metals singly or in combination. *Comp Biochem Physiol C Comp Pharm* 1985, 82, 55-62.
- [197] Hogstrand, C., Wood, C. M., Taylor, E. W., *The physiology and toxicology of zinc in fish toxicology of aquatic pollution*, Cambridge University Press 1996.
- [198] Hooper, D. U., Adair, E. C., Cardinale, B. J., Byrnes, J. E., *et al.*, A global synthesis reveals biodiversity loss as a major driver of ecosystem change. *Nature* 2012, 486, 105-108.
- [199] Randerson, J. T., Climate science: Global warming and tropical carbon. *Nature* 2013, 494, 319-320.
- [200] Rosner, H., Climate adaptation: Survival of the flexible. *Nature* 2013, 494, 22-23.
- [201] Shakun, J. D., Clark, P. U., He, F., Marcott, S. A., *et al.*, Global warming preceded by increasing carbon dioxide concentrations during the last deglaciation. *Nature* 2012, 484, 49-54.
- [202] Orr, J. C., Fabry, V. J., Aumont, O., Bopp, L., *et al.*, Anthropogenic ocean acidification over the twenty-first century and its impact on calcifying organisms. *Nature* 2005, 437, 681-686.

- [203] Doney, S. C., Fabry, V. J., Feely, R. A., Kleypas, J. A., Ocean Acidification: The Other CO<sub>2</sub> Problem. *Ann Rev Mar Sci* 2009, 1, 169-192.
- [204] Kleypas, J. A., Feely, R. A., Fabry, V. J., Langdon, C., *et al.*, 2006.
- [205] Smith, S. V., Buddemeier, R. W., Global Change and Coral Reef Ecosystems. *Ann Rev Ecol Syst* 1992, 23, 89-118.
- [206] Hönisch, B., Ridgwell, A., Schmidt, D. N., Thomas, E., *et al.*, The Geological Record of Ocean Acidification. *Science* 2012, 335, 1058-1063.
- [207] Weiss, R. F., Carbon dioxide in water and seawater: the solubility of a non-ideal gas. *Marine Chemistry* 1974, 2, 203-215.
- [208] acidification, O., Australia 2012.
- [209] Caldeira, K., Wickett, M. E., Oceanography: Anthropogenic carbon and ocean pH. *Nature* 2003, 425, 365-365.
- [210] Feely, R. A., Sabine, C. L., Hernandez-Ayon, J. M., Ianson, D., *et al.*, Evidence for Upwelling of Corrosive "Acidified" Water onto the Continental Shelf. *Science* 2008, 320, 1490-1492.
- [211] Orr, J. C., Fabry, V. J., Aumont, O., Bopp, L., *et al.*, Anthropogenic ocean acidification over the twenty-first century and its impact on calcifying organisms. *Nature* 2005, 437, 681-686.
- [212] Arnold, H. E., Kerrison, P., Steinke, M., Interacting effects of ocean acidification and warming on growth and DMS-production in the haptophyte coccolithophore *Emiliania huxleyi*. *Glob Chang Biol* 2013, 19, 1007-1016.
- [213] Li, W., Gao, K., Beardall, J., Interactive effects of ocean acidification and nitrogen-limitation on the diatom *Phaeodactylum tricornutum*. *PLoS One* 2012, 7, e51590.
- [214] Tomanek, L., Zuzow, M. J., Ivanina, A. V., Beniash, E., *et al.*, Proteomic response to elevated PCO<sub>2</sub> level in eastern oysters, *Crassostrea virginica*: evidence for oxidative stress. *J Exp Biol* 2011, 214, 1836-1844.
- [215] Anthony, K. R. N., Kline, D. I., Diaz-Pulido, G., Dove, S., *et al.*, Ocean acidification causes bleaching and productivity loss in coral reef builders. *Proc Nat Acad Sci U. S. A.* 2008, 105, 17442-17446.
- [216] Glas, M. S., Fabricius, K. E., de Beer, D., Uthicke, S., The O<sub>2</sub>, pH and Ca<sup>2+</sup> microenvironment of benthic foraminifera in a high CO<sub>2</sub> world. *PLoS One* 2012, 7, e50010.
- [217] Raymond, C. E., Lloyd, A., Kline, D. I., Dove, S. G., *et al.*, Decline in growth of foraminifer *Marginopora rossi* under eutrophication and ocean acidification scenarios. *Glob Chang Biol* 2013, 19, 291-302.
- [218] Webster, N. S., Uthicke, S., Botte, E. S., Flores, F., *et al.*, Ocean acidification reduces induction of coral settlement by crustose coralline algae. *Glob Chang Biol* 2013, 19, 303-315.
- [219] Shaw, E. C., McNeil, B. I., Tilbrook, B., Matear, R., *et al.*, Anthropogenic changes to seawater buffer capacity combined with natural reef metabolism induce extreme future coral reef CO conditions. *Glob Chang Biol* 2013.
- [220] Markert, S., Arndt, C., Felbeck, H., Becher, D., *et al.*, Physiological proteomics of the uncultured endosymbiont of *Riftia pachyptila*. *Science* 2007, 315, 247-250.
- [221] Koch, M., Bowes, G., Ross, C., Zhang, X. H., Climate change and ocean acidification effects on seagrasses and marine macroalgae. *Glob Chang Biol* 2013, 19, 103-132.
- [222] Saba, G. K., Schofield, O., Torres, J. J., Ombres, E. H., *et al.*, Increased feeding and nutrient excretion of adult Antarctic krill, *Euphausia superba*, exposed to enhanced carbon dioxide (CO<sub>2</sub>). *PLoS One* 2012, 7, e52224.
- [223] Ries, J. B., Cohen, A. L., McCorkle, D. C., Marine calcifiers exhibit mixed responses to CO<sub>2</sub>-induced ocean acidification. *Geology* 2009, 37, 1131-1134.
- [224] Gazeau, F., Gattuso, J. P., Greaves, M., Elderfield, H., *et al.*, Effect of carbonate chemistry alteration on the early embryonic development of the Pacific oyster (*Crassostrea gigas*). *PLoS One* 2011, 6, e23010.
- [225] Grossman, E., *Yale Environment 360* Yale School of Forestry & Environmental Studies.
- [226] Matoo, O. B., Ivanina, A. V., Ullstad, C., Beniash, E., *et al.*, Interactive effects of elevated temperature and CO<sub>2</sub> levels on metabolism and oxidative stress in two common marine bivalves (*Crassostrea virginica* and *Mercenaria mercenaria*). *Comp Biochem Physiol A Mol Integr Physiol* 2013, 164, 545-553.
- [227] Miller, A. W., Reynolds, A. C., Sobrino, C., Riedel, G. F., Shellfish face uncertain future in high CO<sub>2</sub> world: influence of acidification on oyster larvae calcification and growth in estuaries. *PLoS One* 2009, 4, e5661.
- [228] Dineshram, R., Wong, K. K., Xiao, S., Yu, Z., *et al.*, Analysis of Pacific oyster larval proteome and its response to high-CO<sub>2</sub>. *Mar Pollut Bull* 2012, 64, 2160-2167.
- [229] Wong, K. K. W., Lane, A. C., Leung, P. T. Y., Thiagarajan, V., Response of larval barnacle proteome to CO<sub>2</sub>-driven seawater acidification. *Comp Biochem Physiol D Genomics and Prot* 2011, 6, 310-321.
- [230] Breci, L., Hattrup, E., Keeler, M., Letarte, J., *et al.*, Comprehensive proteomics in yeast using chromatographic fractionation, gas phase fractionation, protein gel electrophoresis, and isoelectric focusing. *Proteomics* 2005, 5, 2018-2028.
- [231] Craig, R., Beavis, R. C., TANDEM: matching proteins with tandem mass spectra. *Bioinformatics* 2004, 20, 1466-1467.
- [232] Neilson, K. A., Keighley, T., Pascovici, D., Cooke, B., *et al.*, Label-free quantitative shotgun proteomics using normalized spectral abundance factors. *Methods Mol Biol* 2013, 1002, 205-222.
- [233] Zybaylov, B., Mosley, A. L., Sardi, M. E., Coleman, M. K., *et al.*, Statistical Analysis of Membrane Proteome Expression Changes in *Saccharomyces cerevisiae*. *J Proteome Res* 2006, 5, 2339-2347.

- [234] Neilson, K. A., George, I. S., Emery, S. J., Muralidharan, S., *et al.*, Analysis of rice proteins using SDS-PAGE shotgun proteomics. *Methods Mol Biol* 2014, **1072**, 289-302.
- [235] Neilson, K. A., Mariani, M., Haynes, P. A., Quantitative proteomic analysis of cold-responsive proteins in rice. *Proteomics* 2011, **11**, 1696-1706.
- [236] Altschul, S. F., Gish, W., Miller, W., Myers, E. W., *et al.*, Basic local alignment search tool. *J Mol Biol* 1990, **215**, 403-410.
- [237] Peng, J., Elias, J. E., Thoreen, C. C., Licklider, L. J., *et al.*, Evaluation of Multidimensional Chromatography Coupled with Tandem Mass Spectrometry (LC/LC-MS/MS) for Large-Scale Protein Analysis: The Yeast Proteome. *J Proteome Res* 2002, **2**, 43-50.
- [238] Taris, N., Lang, R., Camara, M., Sequence polymorphism can produce serious artefacts in real-time PCR assays: hard lessons from Pacific oysters. *BMC Genomics* 2008, **9**, 234.
- [239] Gestal, C., Costa, M., Figueras, A., Novoa, B., Analysis of differentially expressed genes in response to bacterial stimulation in hemocytes of the carpet-shell clam *Ruditapes decussatus*: Identification of new antimicrobial peptides. *Gene* 2007, **406**, 134-143.
- [240] Green, T. J., Dixon, T. J., Devic, E., Adlard, R. D., *et al.*, Differential expression of genes encoding antioxidant enzymes in Sydney rock oysters, *Saccostrea glomerata* (Gould) selected for disease resistance. *Fish Shellfish Immunol* 2009, **26**, 799-810.
- [241] Hernroth, B., Lothigius, Å., Bölin, I., Factors influencing survival of enterotoxigenic *Escherichia coli*, *Salmonella enterica* (serovar Typhimurium) and *Vibrio parahaemolyticus* in marine environments. *FEMS Microbiol Ecol* 2010, **71**, 272-280.
- [242] Labreuche, Y., Lambert, C., Soudant, P., Boulo, V., *et al.*, Cellular and molecular hemocyte responses of the Pacific oyster, *Crassostrea gigas*, following bacterial infection with *Vibrio aestuarianus* strain 01/32. *Microbes Infect* 2006, **8**, 2715-2724.
- [243] Saulnier, D., De Decker, S., Haffner, P., Cobret, L., *et al.*, A large-scale epidemiological study to identify bacteria pathogenic to Pacific oyster *Crassostrea gigas* and correlation between virulence and metalloprotease-like activity. *Microb Ecol* 2010, **59**, 787-798.
- [244] Simonian, M., Nair, S. V., O'Connor, W. A., Raftos, D. A., Protein markers of *Marteilia sydneyi* infection in Sydney rock oysters, *Saccostrea glomerata*. *J Fish Dis* 2009, **32**, 367-375.
- [245] Williams, H. R., Macey, B. M., Burnett, L. E., Burnett, K. G., Differential localization and bacteriostasis of *Vibrio campbellii* among tissues of the Eastern oyster, *Crassostrea virginica*. *Dev Comp Immunol* 2009, **33**, 592-600.
- [246] Zapata, M., Tanguy, A., David, E., Moraga, D., *et al.*, Transcriptomic response of *Argopecten purpuratus* post-larvae to copper exposure under experimental conditions. *Gene* 2009, **442**, 37-46.
- [247] Wang, Q., Liu, B., Yang, H., Wang, X., *et al.*, Toxicity of lead, cadmium and mercury on embryogenesis, survival, growth and metamorphosis of *Meretrix meretrix* larvae. *Ecotoxicology* 2009, **18**, 829-837.
- [248] Bebianno, M. J., Company, R., Serafim, A., Camus, L., *et al.*, Antioxidant systems and lipid peroxidation in *Bathymodiolus azoricus* from Mid-Atlantic Ridge hydrothermal vent fields. *Aquat Toxicol* 2005, **75**, 354-373.
- [249] Cantu-Medellin, N., Olguin-Monroy, N. O., Mendez-Rodriguez, L. C., Zenteno-Savin, T., Antioxidant enzymes and heavy metal levels in tissues of the black chocolate clam *Megapitaria squalida* in Bahia de La Paz, Mexico. *Arch Environ Contam Toxicol* 2009, **56**, 60-66.
- [250] Geret, F., Serafim, A., Bebianno, M. J., Antioxidant enzyme activities, metallothioneins and lipid peroxidation as biomarkers in *Ruditapes decussatus*? *Ecotoxicology* 2003, **12**, 417-426.
- [251] Niyogi, S., Biswas, S., Sarker, S., Datta, A. G., Antioxidant enzymes in brackishwater oyster, *Saccostrea cucullata* as potential biomarkers of polyaromatic hydrocarbon pollution in Hooghly Estuary (India): seasonality and its consequences. *Sci Total Environ* 2001, **281**, 237-246.
- [252] Perez, E., Blasco, J., Sole, M., Biomarker responses to pollution in two invertebrate species: *Scrobicularia plana* and *Nereis diversicolor* from the Cadiz bay (SW Spain). *Mar Environ Res* 2004, **58**, 275-279.
- [253] Abe, M., Takahashi, K., Hiwada, K., *J Biochem* 1990, pp. 835-838.
- [254] Lewis, W. G., Smillie, L. B., The amino acid sequence of rabbit cardiac tropomyosin. *J Biol Chem* 1980, **255**, 6854-6859.
- [255] MacLeod, A. R., Genetic origin of diversity of human cytoskeletal tropomyosins. *Bioessays* 1987, **6**, 208-212.
- [256] Wolska, B. M., Wieczorek, D. M. F., The role of tropomyosin in the regulation of myocardial contraction and relaxation. *Pflugers Arch* 2003, **446**, 1-8.
- [257] Chora, S., Starita-Geribaldi, M., Guignonis, J. M., Samson, M., *et al.*, Effect of cadmium in the clam *Ruditapes decussatus* assessed by proteomic analysis. *Aquat Toxicol* 2009, **94**, 300-308.
- [258] Stillitano, F., Mugelli, A., Cerbai, E., Vanucci, S., Quantification of midkine gene expression in *Patella caerulea* (Mollusca, Gastropoda) exposed to cadmium. *Estuar Coast Shelf Sci* 2007, **75**, 120-124.
- [259] Tanguy, A., Boutet, I., Laroche, J., Moraga, D., Molecular identification and expression study of differentially regulated genes in the Pacific oyster *Crassostrea gigas* in response to pesticide exposure. *FEBS J* 2005, **272**, 390-403.
- [260] Chandra Sanyal, S., Liljas, A., The end of the beginning: structural studies of ribosomal proteins. *Curr Opin Struct Biol* 2000, **10**, 633-636.
- [261] Maguire, B. A., Zimmermann, R. A., The Ribosome in Focus. *Cell* 2001, **104**, 813-816.
- [262] Chan, Y.-L., Olvera, J., Paz, V., Wool, I. G., The Primary Structures of Rat Ribosomal Proteins S3a (The V-Fos Transformation Effector) and of S3b. *Biochem Biophys Res Commun* 1996, **228**, 141-147.

- [263] Gauthier-Clerc, S., Pellerin, J., Blaise, C., Gagné, F., Delayed gametogenesis of *Mya arenaria* in the Saguenay fjord (Canada): a consequence of endocrine disruptors? *Comp Biochem Physiol C Toxicol Pharmacol* 2002, 131, 457-467.
- [264] Murphy, M. P., How mitochondria produce reactive oxygen species. *Biochem J* 2009, 417, 1-13.
- [265] Remacle, C., Barbieri, M., Cardol, P., Hamel, P., Eukaryotic complex I: functional diversity and experimental systems to unravel the assembly process. *Mol Genet Genomics* 2008, 280, 93-110.
- [266] Cruz-Rodriguez, L. A., Chu, F. L., Heat-shock protein (HSP70) response in the eastern oyster, *Crassostrea virginica*, exposed to PAHs sorbed to suspended artificial clay particles and to suspended field contaminated sediments. *Aquat Toxicol* 2002, 60, 157-168.
- [267] Zhang, G., Fang, X., Guo, X., Li, L., *et al.*, The oyster genome reveals stress adaptation and complexity of shell formation. *Nature* 2012, 490, 49-54.
- [268] Moorthy, S., Chen, L., Bennett, V., *Caenorhabditis elegans* beta-G spectrin is dispensable for establishment of epithelial polarity, but essential for muscular and neuronal function. *J Cell Biol* 2000, 149, 915-930.
- [269] Jaffe, A. B., Hall, A., Rho GTPases: biochemistry and biology. *Annu Rev Cell Dev Biol* 2005, 21, 247-269.
- [270] Thompson, E. L., Taylor, D. A., Nair, S. V., Birch, G., *et al.*, A proteomic analysis of the effects of metal contamination on Sydney Rock Oyster (*Saccostrea glomerata*) haemolymph. *Aquat Toxicol* 2011, 103, 241-249.
- [271] Casselli, T., Lynch, T., Southward, C. M., Jones, B. W., *et al.*, *Vibrio parahaemolyticus* inhibition of rho family gtpase activation requires a functional chromosome i type iii secretion system. *Infect Immun* 2008, 76, 2202-2211.
- [272] Zoroddu, M. A., Kowalik-Jankowska, T., Kozłowski, H., Molinari, H., *et al.*, Interaction of Ni(II) and Cu(II) with a metal binding sequence of histone H4: AKRHRK, a model of the H4 tail. *Biochim Biophys Acta* 2000, 1475, 163-168.
- [273] Seo, J. K., Stephenson, J., Crawford, J. M., Stone, K. L., *et al.*, American oyster, *Crassostrea virginica*, expresses a potent antibacterial histone H2B protein. *Mar Biotechnol (NY)* 2010, 12, 543-551.
- [274] Terranova, R., Pujol, N., Fasano, L., Djabali, M., Characterisation of set-1, a conserved PR/SET domain gene in *Caenorhabditis elegans*. *Gene* 2002, 292, 33-41.
- [275] Collin, H., Meistertzheim, A.-L., David, E., Moraga, D., *et al.*, Response of the Pacific oyster *Crassostrea gigas*, Thunberg 1793, to pesticide exposure under experimental conditions. *J Exp Biol* 2010, 213, 4010-4017.
- [276] Harvey, K., Tapon, N., The Salvador-Warts-Hippo pathway - an emerging tumour-suppressor network. *Nat Rev Cancer* 2007, 7, 182-191.
- [277] Huang, J., Wu, S., Barrera, J., Matthews, K., *et al.*, The Hippo signaling pathway coordinately regulates cell proliferation and apoptosis by inactivating Yorkie, the Drosophila Homolog of YAP. *Cell* 2005, 122, 421-434.
- [278] Dong, J., Feldmann, G., Huang, J., Wu, S., *et al.*, Elucidation of a Universal Size-Control Mechanism in Drosophila and Mammals. *Cell* 2007, 130, 1120-1133.
- [279] Park, S., Park, S. Y., Choi, S., Zheng, Z., *et al.*, Toxicological biomarkers of 2,3,4,7,8-pentachlorodibenzofuran in proteins secreted by HepG2 cells. *Biochim Biophys Acta* 2012, 1824, 656-666.
- [280] Mizuno, T., Hisamoto, N., Terada, T., Kondo, T., *et al.*, The *Caenorhabditis elegans* MAPK phosphatase VHP-1 mediates a novel JNK-like signaling pathway in stress response. *EMBO J* 2004, 23, 2226-2234.
- [281] Sokolova, I. M., Evans, S., Hughes, F. M., Cadmium-induced apoptosis in oyster hemocytes involves disturbance of cellular energy balance but no mitochondrial permeability transition. *J Exp Biol* 2004, 207, 3369-3380.
- [282] Reutelingsperger, C. P., Dumont, E., Thimister, P. W., van Genderen, H., *et al.*, Visualization of cell death in vivo with the annexin A5 imaging protocol. *J Immunol Methods* 2002, 265, 123-132.
- [283] Lewis, S., Keller, S., Identification of copper-responsive genes in an early life stage of the fathead minnow *Pimephales promelas*. *Ecotoxicol* 2009, 18, 281-292.
- [284] Chen, S. J., Wu, Y. H., Huang, H. Y., Wang, C. C., *Saccharomyces cerevisiae* possesses a stress-inducible glycyl-tRNA synthetase gene. *PLoS One* 2012, 7, e33363.
- [285] Nandakumar, R., Espirito Santo, C., Madayiputhiya, N., Grass, G., Quantitative proteomic profiling of the *Escherichia coli* response to metallic copper surfaces. *Biometals* 2011, 24, 429-444.
- [286] Komatsubara, A. T., Asano, T., Tsumoto, H., Shimizu, K., *et al.*, Proteomic analysis of S-nitrosylation induced by 1-methyl-4-phenylpyridinium (MPP+). *Proteome Sci* 2012, 10, 74.
- [287] Bhaskar, Kumari, N., Goyal, N., Cloning, characterization and sub-cellular localization of gamma subunit of T-complex protein-1 (chaperonin) from *Leishmania donovani*. *Biochem Biophys Res Commun* 2012, 429, 70-74.
- [288] Usami, M., Nakajima, M., Mitsunaga, K., Miyajima, A., *et al.*, Proteomic analysis of indium embryotoxicity in cultured postimplantation rat embryos. *Reprod Toxicol* 2009, 28, 477-488.
- [289] Zhang, L., Li, L., Zhu, Y., Zhang, G., *et al.*, Transcriptome analysis reveals a rich gene set related to innate immunity in the eastern oyster (*Crassostrea virginica*). *Mar Biotechnol* 2013, 1-17.
- [290] Beatham, J., Romero, R., Townsend, S. K., Hacker, T., *et al.*, Filamin C interacts with the muscular dystrophy KY protein and is abnormally distributed in mouse KY deficient muscle fibres. *Hum Mol Genet* 2004, 13, 2863-2874.

- [291] Lee, K. H., Marshall, R. S., Slivicke, L. M., Vierstra, R. D., Genetic analyses of the Arabidopsis 26S proteasome regulatory particle reveal its importance during light stress and a specific role for the N-terminus of RPT2 in development. *Plant Signal Behav* 2012, 7, 973-978.
- [292] Tomanek, L., Zuzow, M. J., The proteomic response of the mussel congeners *Mytilus galloprovincialis* and *M. trossulus* to acute heat stress: implications for thermal tolerance limits and metabolic costs of thermal stress. *J Exp Biol* 2010, 213, 3559-3574.
- [293] Li, J., Powell, S. R., Wang, X., Enhancement of proteasome function by PA28 $\alpha$ ; overexpression protects against oxidative stress. *FASEB J* 2011, 25, 883-893.
- [294] Satchell, M. A., Zhang, X., Kochanek, P. M., Dixon, C. E., *et al.*, A dual role for poly-ADP-ribosylation in spatial memory acquisition after traumatic brain injury in mice involving NAD<sup>+</sup> depletion and ribosylation of 14-3-3 $\gamma$ . *J Neurochem* 2003, 85, 697-708.
- [295] Saba, J. A., McComb, M. E., Potts, D. L., Costello, C. E., *et al.*, Proteomic mapping of stimulus-specific signaling pathways involved in THP-1 cells exposed to *Porphyrromonas gingivalis* or its purified components. *J Proteome Res* 2007, 6, 2211-2221.
- [296] van der Heyden, M. A., van Kempen, M. J., Tsuji, Y., Rook, M. B., *et al.*, P19 embryonal carcinoma cells: a suitable model system for cardiac electrophysiological differentiation at the molecular and functional level. *Cardiovasc Res* 2003, 58, 410-422.
- [297] Ilies, I., Zupanc, M. M., Zupanc, G. K. H., Proteome analysis reveals protein candidates involved in early stages of brain regeneration of teleost fish. *Neuroscience* 2012, 219, 302-313.
- [298] Jin, K. S., Park, C. M., Lee, Y. W., Identification of differentially expressed genes by 2,3,7,8-tetrachlorodibenzo-p-dioxin in human bronchial epithelial cells. *Hum Exp Toxicol* 2012, 31, 107-112.
- [299] Xu, K. Y., Zweier, J. L., Becker, L. C., Functional coupling between glycolysis and sarcoplasmic reticulum Ca<sup>2+</sup> transport. *Circ Res* 1995, 77, 88-97.
- [300] Geiger, B., Avnur, Z., Rinnerthaler, G., Hinssen, H., *et al.*, Microfilament-organizing centers in areas of cell contact: cytoskeletal interactions during cell attachment and locomotion. *J Cell Biol* 1984, 99, 83s-91s.
- [301] Hund, T. J., Koval, O. M., Li, J., Wright, P. J., *et al.*, A beta(IV)-spectrin/CaMKII signaling complex is essential for membrane excitability in mice. *J Clin Invest* 2010, 120, 3508-3519.
- [302] Balastik, M., Ferraguti, F., Pires-da Silva, A., Lee, T. H., *et al.*, Deficiency in ubiquitin ligase TRIM2 causes accumulation of neurofilament light chain and neurodegeneration. *Proc Natl Acad Sci U S A* 2008, 105, 12016-12021.
- [303] Yamazaki, T., Walchli, S., Fujita, T., Ryser, S., *et al.*, Splice variants of enigma homolog, differentially expressed during heart development, promote or prevent hypertrophy. *Cardiovasc Res* 2010, 86, 374-382.
- [304] Dicken, B. J., Graham, K., Hamilton, S. M., Andrews, S., *et al.*, Lymphovascular invasion is associated with poor survival in gastric cancer: an application of gene-expression and tissue array techniques. *Ann Surg* 2006, 243, 64-73.
- [305] Fields, J. H. A., Hochachka, P. W., Purification and Properties of Alanopine Dehydrogenase from the Adductor Muscle of the Oyster, *Crassostrea gigas* (Mollusca, Bivalvia). *Eu J Biochem* 1981, 114, 615-621.
- [306] Fields, J. H. A., Eng, A. K., Ramsden, W. D., Hochachka, P. W., *et al.*, Alanopine and strombine are novel imino acids produced by a dehydrogenase found in the adductor muscle of the oyster, *Crassostrea gigas*. *Arch Biochem Biophys* 1980, 201, 110-114.
- [307] De Zwaan, A., Zandee, D. I., The utilization of glycogen and accumulation of some intermediates during anaerobiosis in *Mytilus edulis* L. *Comp Biochem Physiol B Biochem* 1972, 43, 47-54.
- [308] Stokes, T. M., Awapara, J., Alanine and succinate as end-products of glucose degradation in the clam *Rangia cuneata*. *Comp Biochem Physiol* 1968, 25, 883-892.
- [309] Simpson, J. W., Awapara, J., The pathway of glucose degradation in some invertebrates. *Comp Biochem Physiol* 1966, 18, 537-548.
- [310] Mustafa, T., Hochachka, P. W., Catalytic and regulatory properties of pyruvate kinases in tissues of a marine bivalve. *J Biol Chem* 1971, 246, 3196-3203.
- [311] Mustafa, T., Hochachka, P. W., Enzymes in facultative anaerobiosis of molluscs. 3. Phosphoenolpyruvate carboxykinase and its role in aerobic-anaerobic transition. *Comp Biochem Physiol B* 1973, 45, 657-667.
- [312] Mustafa, T., Hochachka, P. W., Enzymes in facultative anaerobiosis of molluscs. II. Basic catalytic properties of phosphoenolpyruvate carboxykinase in oyster adductor muscle. *Comp Biochem Physiol B* 1973, 45, 639-655.
- [313] Collicutt, J., Hochachka, P., The anaerobic oyster heart: Coupling of glucose and aspartate fermentation. *J comp physiol* 1977, 115, 147-157.
- [314] Patrick, S., Faury, N., Gouletquer, P., Seasonal changes in carbohydrate metabolism and its relationship with summer mortality of Pacific oyster *Crassostrea gigas* (Thunberg) in Marennes-Oléron bay (France). *Aquaculture* 2006, 252, 328-338.
- [315] Ciacci, C., Barmo, C., Gallo, G., Maisano, M., *et al.*, Effects of sublethal, environmentally relevant concentrations of hexavalent chromium in the gills of *Mytilus galloprovincialis*. *Aquat Toxicol* 2012, 120-121, 109-118.
- [316] Dondero, F., Banni, M., Negri, A., Boatti, L., *et al.*, Interactions of a pesticide/heavy metal mixture in marine bivalves: a transcriptomic assessment. *BMC Genomics* 2011, 12, 195.
- [317] Canesi, L., Ciacci, C., Betti, M., Gallo, G., Growth factor-mediated signal transduction and redox balance in isolated digestive gland cells from *Mytilus galloprovincialis* Lam. *Comp Biochem Physiol C Toxicol Pharmacol* 2000, 125, 355-363.

- [318] Fando, J. J., Garcia-Fernandez, M. C., Candela, J. L., Glycogen metabolism in *Ostrea edulis* (L.)--factors affecting glycogen synthesis. *Comp Biochem Physiol B* 1972, 43, 807-814.
- [319] Uma Devi, V., Bioaccumulation and metabolic effects of cadmium on marine fouling dressinid bivalve, *Mytilopsis sallei* (Recluz). *Arch Environ Contam Toxicol* 1996, 31, 47-53.
- [320] Krumova, E., Stoitsova, S. R., Paunova-Krasteva, T. S., Pashova, S. B., *et al.*, Copper stress and filamentous fungus *Humicola lutea* 103 - ultrastructural changes and activities of key metabolic enzymes. *Can J Microbiol* 2012, 58, 1335-1343.
- [321] Satyaparameshwar, K., Reddy, T. R., Kumar, N. V., Effect of chromium on protein metabolism of fresh water mussel, *Lamellidens marginalis*. *J Environ Biol* 2006, 27, 401-403.
- [322] Chakravarti, B., Chattopadhyay, N., Brown, E. M., Signaling through the extracellular calcium-sensing receptor (CaSR). *Adv Exp Med Biol* 2012, 740, 103-142.
- [323] Kim, H., Sengupta, A., Glogauer, M., McCulloch, C. A., Filamin A regulates cell spreading and survival via beta1 integrins. *Exp Cell Res* 2008, 314, 834-846.
- [324] Kovacevic, I., Orozco, J. M., Cram, E. J., Filamin and phospholipase C-epsilon are required for calcium signaling in the *Caenorhabditis elegans* spermatheca. *PLoS Genet* 2013, 9, e1003510.
- [325] Morga, B., Arzul, I., Faury, N., Segarra, A., *et al.*, Molecular responses of *Ostrea edulis* haemocytes to an in vitro infection with *Bonamia ostreae*. *Dev Comp Immunol* 2011, 35, 323-333.
- [326] Gomes, T., Pereira, C. G., Cardoso, C., Bebianno, M. J., Differential protein expression in mussels *Mytilus galloprovincialis* exposed to nano and ionic Ag. *Aquat Toxicol* 2013, 136-137, 79-90.
- [327] Trinick, J., Tskhovrebova, L., Titin: a molecular control freak. *Trends in cell biology* 1999, 9, 377-380.
- [328] Miller, G., Musa, H., Gautel, M., Peckham, M., A targeted deletion of the C-terminal end of titin, including the titin kinase domain, impairs myofibrillogenesis. *J Cell Sci* 2003, 116, 4811-4819.
- [329] Vainzof, M., Moreira, E. S., Suzuki, O. T., Faulkner, G., *et al.*, Telethonin protein expression in neuromuscular disorders. *Biochim Biophys Acta* 2002, 1588, 33-40.
- [330] Heineke, J., Kempf, T., Kraft, T., Hilfiker, A., *et al.*, Downregulation of cytoskeletal muscle LIM protein by nitric oxide: impact on cardiac myocyte hypertrophy. *Circulation* 2003, 107, 1424-1432.
- [331] Xun, Z., Sowell, R. A., Kaufman, T. C., Clemmer, D. E., Quantitative proteomics of a presymptomatic A53T alpha-synuclein *Drosophila* model of Parkinson disease. *Mol Cell Proteomics* 2008, 7, 1191-1203.
- [332] Papalouka, V., Arvanitis, D. A., Vafiadaki, E., Mavroidis, M., *et al.*, Muscle LIM protein interacts with cofilin 2 and regulates F-actin dynamics in cardiac and skeletal muscle. *Mol Cell Biol* 2009, 29, 6046-6058.
- [333] Himmel, D. M., Mui, S., O'Neill-Hennessey, E., Szent-Gyorgyi, A. G., *et al.*, The on-off switch in regulated myosins: different triggers but related mechanisms. *J Mol Biol* 2009, 394, 496-505.
- [334] Guo, N., Krutzsch, H. C., Inman, J. K., Roberts, D. D., Thrombospondin 1 and type I repeat peptides of thrombospondin 1 specifically induce apoptosis of endothelial cells. *Cancer Res* 1997, 57, 1735-1742.
- [335] Iruela-Arispe, M. L., Lombardo, M., Krutzsch, H. C., Lawler, J., *et al.*, Inhibition of angiogenesis by thrombospondin-1 is mediated by 2 independent regions within the type 1 repeats. *Circulation* 1999, 100, 1423-1431.
- [336] Thingholm, T. E., Bak, S., Beck-Nielsen, H., Jensen, O. N., *et al.*, Characterization of human myotubes from type 2 diabetic and nondiabetic subjects using complementary quantitative mass spectrometric methods. *Mol Cell Proteomics* 2011, 10, M110 006650.
- [337] McAlister, G. C., Huttlin, E. L., Haas, W., Ting, L., *et al.*, Increasing the multiplexing capacity of TMTs using reporter ion isotopologues with isobaric masses. *Anal Chem* 2012, 84, 7469-7478.
- [338] Ting, L., Rad, R., Gygi, S., Haas, W., MS3 eliminates ratio distortion in isobaric multiplexed quantitative proteomics. *Nat Meth* 2011, 8, 937-940.
- [339] Thompson, E. L., Taylor, D. A., Nair, S. V., Birch, G., *et al.*, Proteomic analysis of Sydney Rock oysters (*Saccostrea glomerata*) exposed to metal contamination in the field. *Environ Pollut* 2012, 170, 102-112.
- [340] Gale, S. A., King, C. K., Hyne, R. V., Chronic sublethal sediment toxicity testing using the estuarine amphipod, *Melita plumulosa* (Zeidler): evaluation using metal-spiked and field-contaminated sediments. *Environ Toxicol Chem* 2006, 25, 1887-1898.
- [341] Mann, R. M., Hyne, R. V., Spadaro, D. A., Simpson, S. L., Development and application of a rapid amphipod reproduction test for sediment-quality assessment. *Environ Toxicol Chem* 2009, 28, 1244-1254.
- [342] Simpson SL, B. G., Chariton AA, Stauber JL, King CK, Chapman JC, Hyne RV, Gale SA, Roach AC, Maher WA, *Handbook for Sediment Quality Assessment*, Commonwealth Scientific and Industrial Research Organisation (CSIRO), Bangor, NSW, Australia 2005.
- [343] Batley, G. E., The development and application of ANZECC and ARMCANZ sediment-quality guidelines. *Australasian journal of ecotoxicology* 2001, 7, 81-92.
- [344] King, C. K., Short-term accumulation of Cd and Cu from water, sediment and algae by the amphipod *Melita plumulosa* and the bivalve *Tellina deltoidalis*. *Mar ecol* 2005, 287, 177-188.
- [345] Mann, R. M., Hyne, R. V., Embryological Development of the Australian Amphipod, *Melita Plumulosa* Zeidler, 1989 (Amphipoda, Gammaridea, Melitidae). *Crustaceana* 2008, 81, 57-66.
- [346] Simpson, S. L., Spadaro, D. A., Performance and sensitivity of rapid sublethal sediment toxicity tests with the amphipod *Melita plumulosa* and copepod *Nitocra spinipes*. *Environ Toxicol Chem* 2011, 30, 2326-2334.
- [347] Mann, R. M., Hyne, R. V., Ascheri, L. M., Foraging, feeding, and reproduction on silica substrate: Increased waterborne zinc toxicity to the estuarine epibenthic amphipod *Melita plumulosa*. *Environ Toxicol Chem* 2011, 30, 1649-1658.

- [348] Khan, F. R., Irving, J. R., Bury, N. R., Hogstrand, C., Differential tolerance of two *Gammarus pulex* populations transplanted from different metallogenic regions to a polymetal gradient. *Aquat Toxicol* 2011, 102, 95-103.
- [349] Mouneyrac, C., Amiard, J. C., Amiard-Triquet, C., Cottier, A., *et al.*, Partitioning of accumulated trace metals in the talitrid amphipod crustacean *Orchestia gammarellus*: a cautionary tale on the use of metallothionein-like proteins as biomarkers. *Aquat Toxicol* 2002, 57, 225-242.
- [350] Shu, Y., Zhang, G., Wang, J., Response of the common cutworm *Spodoptera litura* to zinc stress: Zn accumulation, metallothionein and cell ultrastructure of the midgut. *Sci Total Environ* 2012, 438, 210-217.
- [351] Hop, C. E. C. A., Bakhtiar, R., An introduction to electrospray ionization and matrix-assisted laser desorption/ionization mass spectrometry: Essential tools in a modern biotechnology environment. *Biospectroscopy* 1997, 3, 259-280.
- [352] Wilm, M., Shevchenko, A., Houthaeve, T., Breit, S., *et al.*, Femtomole sequencing of proteins from polyacrylamide gels by nano-electrospray mass spectrometry. *Nature* 1996, 379, 466-469.
- [353] Shevchenko, A., Jensen, O. N., Podtelejnikov, A. V., Sagliocco, F., *et al.*, Linking genome and proteome by mass spectrometry: Large-scale identification of yeast proteins from two dimensional gels. *Proc Natl Acad Sci U S A* 1996, 93, 14440-14445.
- [354] Medzihradszky, K., Leffler, H., Baldwin, M., Burlingame, A. L., Protein identification by in-gel digestion, high-performance liquid chromatography, and mass spectrometry: Peptide analysis by complementary ionization techniques. *J Am Soc Mass Spectrom* 2001, 12, 215-221.
- [355] Lim, H., Eng, J., Yates, J. R., 3rd, Tollaksen, S. L., *et al.*, Identification of 2D-gel proteins: a comparison of MALDI/TOF peptide mass mapping to mu LC-ESI tandem mass spectrometry. *J Am Soc Mass Spectrom* 2003, 14, 957-970.
- [356] Hyne, R. V., Gale, S. A., King, C. K., Laboratory culture and life-cycle experiments with the benthic amphipod *Melita plumulosa* (Zeidler). *Environ Toxicol Chem* 2005, 24, 2065-2073.
- [357] Atkinson, C. A., Jolley, D. F., Simpson, S. L., Effect of overlying water pH, dissolved oxygen, salinity and sediment disturbances on metal release and sequestration from metal contaminated marine sediments. *Chemosphere* 2007, 69, 1428-1437.
- [358] Spadaro, D. A., Micevska, T., Simpson, S. L., Effect of nutrition on toxicity of contaminants to the epibenthic amphipod *Melita plumulosa*. *Arch Environ Contam Toxicol* 2008, 55, 593-602.
- [359] Hyne, R. V., Mann, R. M., Dillon, C. T., de Jonge, M. D., *et al.*, Secondary vitellogenesis persists despite disrupted fecundity in amphipods maintained on metal-contaminated sediment: X-ray fluorescence assessment of oocyte metal content. *Ecotoxicol Environ Saf* 2013, 93, 31-38.
- [360] Hyne, R. V., Sanchez-Bayo, F., Bryan, A. D., Johnston, E. L., *et al.*, Fatty acid composition of the estuarine amphipod, *Melita plumulosa* (Zeidler): link between diet and fecundity. *Environ Toxicol Chem* 2009, 28, 123-132.
- [361] Hook, S. E., Osborn, H. L., Spadaro, D. A., Simpson, S. L., Assessing mechanisms of toxicant response in the amphipod *Melita plumulosa* through transcriptomic profiling. *Aquat Toxicol* 2014, 146, 247-257.
- [362] Anumanthan, G., Halder, S. K., Friedman, D. B., Datta, P. K., Oncogenic serine-threonine kinase receptor-associated protein modulates the function of Ewing sarcoma protein through a novel mechanism. *Cancer Res* 2006, 66, 10824-10832.
- [363] Halder, S. K., Anumanthan, G., Maddula, R., Mann, J., *et al.*, Oncogenic function of a novel WD-domain protein, STRAP, in human carcinogenesis. *Cancer Res* 2006, 66, 6156-6166.
- [364] Kim, C. J., Choi, B. J., Song, J. H., Park, Y. K., *et al.*, Overexpression of serine-threonine receptor kinase-associated protein in colorectal cancers. *Pathol Int* 2007, 57, 178-182.
- [365] Fischer, U., Liu, Q., Dreyfuss, G., The SMN-SIP1 complex has an essential role in spliceosomal snRNP biogenesis. *Cell* 1997, 90, 1023-1029.
- [366] He, Y., Yang, F., Wang, F., Song, S. X., *et al.*, The upregulation of expressed proteins in HepG2 cells transfected by the recombinant plasmid-containing HBx gene. *Scand J Immunol* 2007, 65, 249-256.
- [367] Bayer, T. S., Booth, L. N., Knudsen, S. M., Ellington, A. D., Arginine-rich motifs present multiple interfaces for specific binding by RNA. *RNA* 2005, 11, 1848-1857.
- [368] Petroski, M. D., Deshaies, R. J., Function and regulation of cullin-RING ubiquitin ligases. *Nat Rev Mol Cell Biol* 2005, 6, 9-20.
- [369] Huang, R., Xing, Z., Luan, Z., Wu, T., *et al.*, A specific splicing variant of SVH, a novel human armadillo repeat protein, is up-regulated in hepatocellular carcinomas. *Cancer Res* 2003, 63, 3775-3782.
- [370] Tanner, N. K., Linder, P., DExD/H box RNA helicases: from generic motors to specific dissociation functions. *Mol Cell* 2001, 8, 251-262.
- [371] Guan, Q., Wu, J., Zhang, Y., Jiang, C., *et al.*, A DEAD box RNA helicase is critical for pre-mRNA splicing, cold-responsive gene regulation, and cold tolerance in Arabidopsis. *Plant Cell* 2013, 25, 342-356.
- [372] Macovei, A., Tuteja, N., microRNAs targeting DEAD-box helicases are involved in salinity stress response in rice (*Oryza sativa* L.). *BMC Plant Biol* 2012, 12, 1-12.
- [373] Umate, P., Tuteja, N., microRNA access to the target helicases from rice. *Plant Signal Behav* 2010, 5, 1171-1175.
- [374] Mishra, M., Sharma, A., Shukla, A. K., Pragya, P., *et al.*, Transcriptomic analysis provides insights on hexavalent chromium induced DNA double strand breaks and their possible repair in midgut cells of *Drosophila melanogaster* larvae. *Mutat Res* 2013, 747-748, 28-39.
- [375] Zheng, J., Zhang, X. X., Yu, H., Taggart, J. E., *et al.*, Zinc at cytotoxic concentrations affects posttranscriptional events of gene expression in cancer cells. *Cell Physiol Biochem* 2012, 29, 181-188.

- [376] Wolska, B. M., Wieczorek, D. M., The role of tropomyosin in the regulation of myocardial contraction and relaxation. *Pflugers Arch* 2003, **446**, 1-8.
- [377] Drees, B., Brown, C., Barrell, B. G., Bretscher, A., Tropomyosin is essential in yeast, yet the TPM1 and TPM2 products perform distinct functions. *J Cell Biol* 1995, **128**, 383-392.
- [378] Thompson, E. L., Taylor, D. A., Nair, S. V., Birch, G., *et al.*, A proteomic analysis of the effects of metal contamination on Sydney Rock Oyster (*Saccostrea glomerata*) haemolymph. *Aquat Toxicol* 2011, (in press accepted manuscript).
- [379] Yamada, A., Yoshio, M., Oiwa, K., Nyitray, L., Catchin, a novel protein in molluscan catch muscles, is produced by alternative splicing from the myosin heavy chain gene. *J Mol Biol* 2000, **295**, 169-178.
- [380] Jeffery, C. J., Moonlighting proteins: old proteins learning new tricks. *Trends Genet* 2003, **19**, 415-417.
- [381] Baxi, M. D., Vishwanatha, J. K., Uracil DNA-glycosylase/glyceraldehyde-3-phosphate dehydrogenase is an Ap4A binding protein. *Biochemistry* 1995, **34**, 9700-9707.
- [382] Chuang, D. M., Hough, C., Senatorov, V. V., Glyceraldehyde-3-phosphate dehydrogenase, apoptosis, and neurodegenerative diseases. *Annu Rev Pharmacol Toxicol* 2005, **45**, 269-290.
- [383] Ishitani, R., Tanaka, M., Sunaga, K., Katsube, N., *et al.*, Nuclear localization of overexpressed glyceraldehyde-3-phosphate dehydrogenase in cultured cerebellar neurons undergoing apoptosis. *Mol Pharmacol* 1998, **53**, 701-707.
- [384] Sundararaj, K. P., Wood, R. E., Ponnusamy, S., Salas, A. M., *et al.*, Rapid shortening of telomere length in response to ceramide involves the inhibition of telomere binding activity of nuclear glyceraldehyde-3-phosphate dehydrogenase. *J Biol Chem* 2004, **279**, 6152-6162.
- [385] Mansur, N. R., Meyer-Siegler, K., Wurzer, J. C., Sirover, M. A., Cell cycle regulation of the glyceraldehyde-3-phosphate dehydrogenase/uracil DNA glycosylase gene in normal human cells. *Nucleic Acids Res* 1993, **21**, 993-998.
- [386] Hara, M. R., Agrawal, N., Kim, S. F., Cascio, M. B., *et al.*, S-nitrosylated GAPDH initiates apoptotic cell death by nuclear translocation following Siah1 binding. *Nat Cell Biol* 2005, **7**, 665-674.
- [387] Sheline, C. T., Wang, H., Cai, A. L., Dawson, V. L., *et al.*, Involvement of poly ADP ribosyl polymerase-1 in acute but not chronic zinc toxicity. *Eur J Neurosci* 2003, **18**, 1402-1409.
- [388] Sheline, C. T., Behrens, M. M., Choi, D. W., Zinc-induced cortical neuronal death: contribution of energy failure attributable to loss of NAD(+) and inhibition of glycolysis. *J Neurosci* 2000, **20**, 3139-3146.
- [389] Schinzel, R., Nidetzky, B., Bacterial alpha-glucan phosphorylases. *FEMS Microbiol Lett* 1999, **171**, 73-79.
- [390] Haynes, P. A., Ferguson, M. A., Cross, G. A., Structural characterization of novel oligosaccharides of cell-surface glycoproteins of *Trypanosoma cruzi*. *Glycobiology* 1996, **6**, 869-878.
- [391] Satterlee, J., Hsu, R. Y., Duck liver malic enzyme: sequence of a tryptic peptide containing the cysteine residue labeled by the substrate analog bromopyruvate. *Biochim Biophys Acta* 1991, **1079**, 247-252.
- [392] Hyne, R. V., Review of the reproductive biology of amphipods and their endocrine regulation: identification of mechanistic pathways for reproductive toxicants. *Environ Toxicol Chem* 2011, **30**, 2647-2657.
- [393] Marsh, J. J., Lebherz, H. G., Fructose-bisphosphate aldolases: an evolutionary history. *Trends Biochem Sci* 1992, **17**, 110-113.
- [394] Macomber, L., Elsey, S. P., Hausinger, R. P., Fructose-1,6-bisphosphate aldolase (class II) is the primary site of nickel toxicity in *Escherichia coli*. *Mol Microbiol* 2011, **82**, 1291-1300.
- [395] Cheng, Y., Zhou, W., El sheery, N. I., Peters, C., *et al.*, Characterization of the Arabidopsis glycerophosphodiester phosphodiesterase (GDPD) family reveals a role of the plastid-localized AtGDPD1 in maintaining cellular phosphate homeostasis under phosphate starvation. *Plant J* 2011, **66**, 781-795.
- [396] Bacon, R. M., Pilgard, M. A., Johnson, B. J., Raffel, S. J., *et al.*, Glycerophosphodiester phosphodiesterase gene (glpQ) of *Borrelia lonestari* identified as a target for differentiating *Borrelia* species associated with hard ticks (Acari:Ixodidae). *J Clin Microbiol* 2004, **42**, 2326-2328.
- [397] Yepiskoposyan, H., Egli, D., Fergestad, T., Selvaraj, A., *et al.*, Transcriptome response to heavy metal stress in *Drosophila* reveals a new zinc transporter that confers resistance to zinc. *Nucleic Acids Res* 2006, **34**, 4866-4877.
- [398] Philippsen, P., Kleine, K., Pohlmann, R., Dusterhoft, A., *et al.*, The nucleotide sequence of *Saccharomyces cerevisiae* chromosome XIV and its evolutionary implications. *Nature* 1997, **387**, 93-98.
- [399] Zheng, J. L., Luo, Z., Liu, C. X., Chen, Q. L., *et al.*, Differential effects of acute and chronic zinc (Zn) exposure on hepatic lipid deposition and metabolism in yellow catfish *Pelteobagrus fulvidraco*. *Aquat Toxicol* 2013, **132-133**, 173-181.
- [400] Zheng, J. L., Hu, W., Luo, Z., Zhao, Y. H., *et al.*, Comparative study on the kinetic behaviour of carnitine palmitoyltransferase I between Javelin goby *Synechogobius hasta* (carnivorous) and grass carp *Ctenopharyngodon idella* (herbivorous). *Aquaculture Nutrition* 2013, **19**, 665-676.
- [401] Doseff, A. I., Arndt, K. T., LAS1 is an essential nuclear protein involved in cell morphogenesis and cell surface growth. *Genetics* 1995, **141**, 857-871.
- [402] Lee, I., Berdis, A. J., Suzuki, C. K., Recent developments in the mechanistic enzymology of the ATP-dependent Lon protease from *Escherichia coli*: highlights from kinetic studies. *Mol Biosyst* 2006, **2**, 477-483.
- [403] Ivanina, A. V., Sokolov, E. P., Sokolova, I. M., Effects of cadmium on anaerobic energy metabolism and mRNA expression during air exposure and recovery of an intertidal mollusk *Crassostrea virginica*. *Aquat Toxicol* 2010, **99**, 330-342.
- [404] Preininger, A. M., Hamm, H. E., G protein signaling: insights from new structures. *Sci* 2004, re3.

- [405] Roberts, D. J., Waelbroeck, M., G protein activation by G protein coupled receptors: ternary complex formation or catalyzed reaction? *Biochem Pharmacol* 2004, 68, 799-806.
- [406] Albert, P. R., Robillard, L., G protein specificity: traffic direction required. *Cell Signal* 2002, 14, 407-418.
- [407] Hildebrandt, J. D., Role of subunit diversity in signaling by heterotrimeric G proteins. *Biochem Pharmacol* 1997, 54, 325-339.
- [408] Whitehead, K., Versalovic, J., Roos, S., Britton, R. A., Genomic and Genetic Characterization of the Bile Stress Response of Probiotic *Lactobacillus reuteri* ATCC 55730. *Appl Environ Microbiol* 2008, 74, 1812-1819.
- [409] Moons, A., Ospdr9, which encodes a PDR-type ABC transporter, is induced by heavy metals, hypoxic stress and redox perturbations in rice roots. *FEBS Lett* 2003, 553, 370-376.
- [410] Potter, A. J., Trappetti, C., Paton, J. C., Streptococcus pneumoniae uses glutathione to defend against oxidative stress and metal ion toxicity. *J Bacteriol* 2012, 194, 6248-6254.
- [411] Peuser, V., Remes, B., Klug, G., Role of the Irr protein in the regulation of iron metabolism in Rhodobacter sphaeroides. *PLoS One* 2012, 7, e42231.
- [412] Moussian, B., Recent advances in understanding mechanisms of insect cuticle differentiation. *Insect Biochem Mol Biol* 2010, 40, 363-375.
- [413] Chaudhari, S. S., Arakane, Y., Specht, C. A., Moussian, B., et al., Knickkopf protein protects and organizes chitin in the newly synthesized insect exoskeleton. *Proc Natl Acad Sci USA* 2011, 108, 17028-17033.
- [414] McCarthy, M. P., Carroll, D. L., Ringwood, A. H., Tissue specific responses of oysters, Crassostrea virginica, to silver nanoparticles. *Aquat Toxicol* 2013, 138-139, 123-128.
- [415] Wood, H. L., Spicer, J. I., Widdicombe, S., Ocean acidification may increase calcification rates, but at a cost. *Proceedings of the Royal Society B: Biological Sciences* 2008, 275, 1767-1773.
- [416] Feely, R. A., Sabine, C. L., Lee, K., Berelson, W., et al., Impact of anthropogenic CO<sub>2</sub> on the CaCO<sub>3</sub> system in the oceans. *Science* 2004, 305, 362-366.
- [417] Kleypas, J. A., Buddemeier, R. W., Archer, D., Gattuso, J.-P., et al., Geochemical Consequences of Increased Atmospheric Carbon Dioxide on Coral Reefs. *Science* 1999, 284, 118-120.
- [418] Todgham, A. E., Hofmann, G. E., Transcriptomic response of sea urchin larvae *Strongylocentrotus purpuratus* to CO<sub>2</sub>-driven seawater acidification. *J Exp Biol* 2009, 212, 2579-2594.
- [419] Dineshram, R., Wong, K. K. W., Xiao, S., Yu, Z., et al., Analysis of pacific oyster larval proteome and its response to high-CO<sub>2</sub>. *Mar Poll Bull* 2012, 64, 2160-2167.
- [420] Bezemer, B., Butt, D., Nell, J., Adlard, R., et al., Breeding for QX disease resistance negatively selects one form of the defensive enzyme, phenoloxidase, in Sydney rock oysters. *Fish Shellfish Immunol* 2006, 20, 627-636.
- [421] Haskin, H. H., Ford, S. E., Development of resistance to *Minchinia nelsoni* (MSX) mortality in laboratory-reared and native oyster stocks in Delaware Bay. *Marine Fisheries Rev* 1979, 41, 54-63.
- [422] Culloty, S. C., Cronin, M. A., Mulcahy, M. F., Potential resistance of a number of populations of the oyster *Ostrea edulis* to the parasite *Bonamia ostreae*. *Aquaculture* 2004, 237, 41-58.
- [423] Lapegue, S., Bedier, F., Goyard, E., Degremont, L., et al., Apport d'un programme de gé&#x0301;ne&#x0301;tique a&#x0300; une filie&#x0300;re de production aquacole: L'exemple de l'ostre&#x0301;iculture. *Actes Colloq. IFREMER No. 38* 2004, 38, 113-121.
- [424] Simonian, M., Nair, S. V., Nell, J. A., Raftos, D. A., Proteomic clues to the identification of QX disease-resistance biomarkers in selectively bred Sydney rock oysters, *Saccostrea glomerata*. *J Proteomics* 2009, 73, 209-217.
- [425] Harrang, E., Lapegue, S., Morga, B., Bierre, N., A high load of non-neutral amino-acid polymorphisms explains high protein diversity despite moderate effective population size in a marine bivalve with sweepstakes reproduction. *G3 (Bethesda)* 2013, 3, 333-341.
- [426] Jones, D. B., Jerry, D. R., Foret, S., Kononov, D. A., et al., Genome-wide SNP validation and mantle tissue transcriptome analysis in the silver-lipped pearl oyster, *Pinctada maxima*. *Mar Biotechnol (NY)* 2013.
- [427] Marie, B., Joubert, C., Tayale, A., Zanella-Cleon, I., et al., Different secretory repertoires control the biomineralization processes of prism and nacre deposition of the pearl oyster shell. *Proc Natl Acad Sci U S A* 2012, 109, 20986-20991.
- [428] Lodish H, B. A., Matsudaira P, Kaiser CA, Krieger M, Scott MP, Zipursky SL, Darnell J, *Folding, Modification, and Degradation of Proteins*, W.H. Freeman and CO. , New York 2004.
- [429] Leroux, M. R., Candido, E. P., Characterization of four new tcp-1-related cct genes from the nematode *Caenorhabditis elegans*. *DNA Cell Biol* 1995, 14, 951-960.
- [430] Krebs HA, W. P., *Krebs' citric acid cycle: half a century and still turning.* , Biochemical Society, London 1987.
- [431] Lay, A. J., Jiang, X. M., Kisker, O., Flynn, E., et al., Phosphoglycerate kinase acts in tumour angiogenesis as a disulphide reductase. *Nature* 2000, 408, 869-873.
- [432] Zieker, D., Königsrainer, I., Tritschler, I., Löffler, M., et al., Phosphoglycerate kinase 1 a promoting enzyme for peritoneal dissemination in gastric cancer. *Int J Cancer Suppl* 2010, 126, 1513-1520.
- [433] Kruger, N. J., von Schaewen, A., The oxidative pentose phosphate pathway: structure and organisation. *Curr Opin Plant Biol* 2003, 6, 236-246.
- [434] Buchanan, B. B., Arnon, D. I., A reverse KREBS cycle in photosynthesis: consensus at last. *Photosynth Res* 1990, 24, 47-53.

- [435] Davis, W. L., Jones, R. G., Farmer, G. R., Dickerson, T., *et al.*, Identification of glyoxylate cycle enzymes in chick liver--the effect of vitamin D3: cytochemistry and biochemistry. *Anat Rec* 1990, 227, 271-284.
- [436] Davis, W. L., Jones, R. G., Farmer, G. R., Cortinas, E., *et al.*, The glyoxylate cycle in rat epiphyseal cartilage: the effect of vitamin-D3 on the activity of the enzymes isocitrate lyase and malate synthase. *Bone* 1989, 10, 201-206.
- [437] Davis, W. L., Goodman, D. B., Crawford, L. A., Cooper, O. J., *et al.*, Hibernation activates glyoxylate cycle and gluconeogenesis in black bear brown adipose tissue. *Biochim Biophys Acta* 1990, 1051, 276-278.
- [438] Schafer, F. Q., Buettner, G. R., Redox environment of the cell as viewed through the redox state of the glutathione disulfide/glutathione couple. *Free Radic Biol Med* 2001, 30, 1191-1212.
- [439] Zheng, L., Roeder, R. G., Luo, Y., S phase activation of the histone H2B promoter by OCA-S, a coactivator complex that contains GAPDH as a key component. *Cell* 2003, 114, 255-266.
- [440] Ma, J., Zhang, D., Jiang, J., Cui, S., *et al.*, Molecular characterization and expression analysis of cathepsin L1 cysteine protease from pearl oyster *Pinctada fucata*. *Fish Shellfish Immunol* 2010, 29, 501-507.
- [441] Morga, B., Renault, T., Faury, N., Arzul, I., New insights in flat oyster *Ostrea edulis* resistance against the parasite *Bonamia ostreae*. *Fish Shellfish Immunol* 2012, 32, 958-968.
- [442] Tian, R., Vogel, P., Lassen, N. A., Mulvany, M. J., *et al.*, Role of Extracellular and Intracellular Acidosis for Hypercapnia-Induced Inhibition of Tension of Isolated Rat Cerebral Arteries. *Circulation Res* 1995, 76, 269-275.
- [443] Williamson, J. R., Safer, B., Rich, T., Schaffer, S., *et al.*, Effects of acidosis on myocardial contractility and metabolism\*. *Acta Med Scand* 1976, 199, 95-112.
- [444] Burnett, L. E., The Challenges of Living in Hypoxic and Hypercapnic Aquatic Environments. *Am Zool* 1997, 37, 633-640.
- [445] Gazeau, F., Quiblier, C., Jansen, J. M., Gattuso, J.-P., *et al.*, Impact of elevated CO<sub>2</sub> on shellfish calcification. *Geophys Res Lett* 2007, 34, L07603.
- [446] Michaelidis, B., Vavoulidou, D., Rousou, J., Portner, H. O., The potential role of CO<sub>2</sub> in initiation and maintenance of estivation in the land snail *Helix lucorum*. *Physiol Biochem Zool* 2007, 80, 113-124.
- [447] Bhui, T., Roy, J. K., Rab11 is required for cell adhesion, maintenance of cell shape and actin-cytoskeleton organization during Drosophila wing development. *Int J Dev Biol* 2011, 55, 269-279.
- [448] Oehlke, O., Martin, H. W., Osterberg, N., Roussa, E., Rab11b and its effector Rip11 regulate the acidosis-induced traffic of V-ATPase in salivary ducts. *J Cell Physiol* 2011, 226, 638-651.
- [449] Warrick, H. M., De Lozanne, A., Leinwand, L. A., Spudich, J. A., Conserved protein domains in a myosin heavy chain gene from *Dictyostelium discoideum*. *Proc Natl Acad Sci USA* 1986, 83, 9433-9437.
- [450] Matsuno, A., Kannda, M., Okuda, M., Ultrastructural studies on paramyosin core filaments from native thick filaments in catch muscles. *Tissue Cell* 1996, 28, 501-505.
- [451] Collin, H., Meistertzheim, A. L., David, E., Moraga, D., *et al.*, Response of the Pacific oyster *Crassostrea gigas*, Thunberg 1793, to pesticide exposure under experimental conditions. *J Exp Biol* 2010, 213, 4010-4017.
- [452] Yu, Y., Ji, H., Doudna, J. A., Leary, J. A., Mass spectrometric analysis of the human 40S ribosomal subunit: native and HCV IRES-bound complexes. *Protein Sci* 2005, 14, 1438-1446.
- [453] Xiong, X., Feng, Q., Xie, L., Zhang, R., Cloning and Characterization of a Heterogeneous Nuclear Ribonucleoprotein Homolog from Pearl Oyster, *Pinctada fucata*. *Acta Biochim Biophys Sin* 2007, 39, 955-963.
- [454] Galas, M.-C., Dourlen, P., Bégard, S., Ando, K., *et al.*, The Peptidylprolyl cis/trans-Isomerase Pin1 Modulates Stress-induced Dephosphorylation of Tau in Neurons: Implication in a pathological mechanism related to alzheimer disease. *J Biol Chem* 2006, 281, 19296-19304.
- [455] Wang, J. Z., Li, S. R., Li, Y. L., Zhang, Y. Z., *et al.*, Could Pin1 help us conquer essential hypertension at an earlier stage? A promising early-diagnostic biomarker and its therapeutic implications for the disease. *Med Hypotheses* 2013, 81, 931-935.